University of the Highlands and Islands
Oilthigh na Gàidhealtachd agus nan Eilean

INTRODUCTION TO WELLBORE POSITIONING

An ISCWSA initiative

PUBLISHED THROUGH THE RESEARCH OFFICE OF UHI

Copyright notice

Revisions

The authors of this publication are fully aware the nature of the subject matter covered will develop over time as new techniques arise or current practices and technologies are updated. It is, therefore, the intension of the authors to regularly revise this eBook to reflect these changes and keep this publication current and as complete as possible.

Anyone who has expertise, techniques or updates they wish to submit to the author for assessment for inclusion in the next revision should email the data in the first instance to:

RO@uhi.ac.uk

This version is V01.7.12

This eBook and all subsequent revisions will be hosted at:
http://www.uhi.ac.uk/en/research-enterprise/energy/wellbore-positioning-download

Acknowledgements

Chapter contributors

Although Professor Angus Jamieson is the main author of this publication with overall responsibility for its content, thanks are given to the following people who contributed to certain chapters;

- Andy McGregor who contributed the write up of the 'Error model' chapters
- Jonathan Stigant who contributed the first chapter on 'Geodesy'
- John Weston of Gyrodata chapter 10 – 'Basic Gyro Theory'
- Steve Grindrod who contributed to the chapter on 'Magnetic spacing'
- David McRobbie who contributed on 'Gyro surveying'

This book was compiled by members of the Industry Steering Committee for Wellbore Survey Accuracy (ISCWSA), a Society of Petroleum Engineers (SPE) Technical Section for Wellbore Positioning.
The main author was Angus Jamieson.

Sponsors

Thanks go to the sponsors of this publication, who contributed funding to the project to bring all this knowledge together into one publication, with the aim of creating a guidebook for the industry without restriction;

ExxonMobil ConocoPhillips Chevron devon gyrodata Schlumberger

University of the Highlands and Islands (UHI) Research Office who helped initiate this project in 2009 and then provided the editing, publishing and web developing expertise to shape this eBook into its published form, with the subsequent provision of web space to make this guide freely available across the world.

University of the Highlands and Islands
Oilthigh na Gàidhealtachd agus nan Eilean

HIE Highlands and Islands Enterprise Iomairt na Gàidhealtachd 's nan Eilean
EUROPE & SCOTLAND
European Regional Development Fund Investing in your Future

This eBook has been edited, images and diagrams re-created, converted to its different formats and published to the UHI website by Stuart Knight of the UHI Research Office, Inverness. Funding for the editing was provided to UHI by HIE and EU ERDF structural funds via the Energy Research Group.

All comments on this publication, submissions or amendments should be directed to:
RO@uhi.ac.uk

Introduction to Wellbore Positioning

Summary Contents

(Turn on navigation for easy section skipping – view/show/navigation – full index at the end of this publication)

List of figures - images, tables and diagrams

All images, tables and diagrams have been created for this publication unless otherwise credited on the figure.

Introduction

AJ Consulting Ltd

University of the Highlands and Islands
Oilthigh na Gàidhealtachd agus nan Eilean

The subject of Borehole Surveying has frequently been dealt with in best practice manuals, guidelines and check sheets but this book will attempt to capture in one document the main points of interest for public access through the UHI and SPE websites. The author would like to thank the sponsors for their generous support in the compilation of this book and their willingness to release all restrictions on the intellectual property so that the industry at large can have free access and copying rights.

After matters of health and spirit, Borehole Surveying is, of course, the single most important subject of human interest. We live on a planet of limited resources supporting a growing population. At the time of writing, the efficient extraction of fossil fuels is crucial to the sustainable supply of the energy and materials we need. Whilst renewable energies are an exciting emerging market, we will still be dependent on our oil and gas reserves for many years to come.

As an industry we have not given the accuracy and management of survey data the attention it deserves. Much better data quality and survey accuracy has been available at very little additional cost but the industry has frequently regarded accuracy as an expensive luxury. Simple corrections to our surveys such as correcting for the stretch of the drill pipe or even sag correction and IFR (see later) have been seen as belonging to the 'high tech' end of the market and we have, unlike nearly all other survey disciplines, thrown good data away, when 'better' data becomes available.

The advent of the ISCWSA, The Industry Steering Committee for Wellbore Survey Accuracy, brought in a new era in survey practice. Not only was work done on improving the realism of error models, but a bi-annual forum was provided to allow industry experts to share ideas and experiences. This project has emerged out of a recognised need for better educational materials to support the understanding of borehole surveying issues. The contents of this e-book are free to use and distribute. Any additional chapters will be welcome for assessment and potential inclusion in the book so this is the first draft of a work in progress.

My thanks also go to the many participants in this effort who have contributed from their knowledge in specialist areas. In particular to Andy McGregor who contributed the write up of the error model, Jonathan Stigant who contributed the first chapter on geodesy and John Weston, Steve Grindrod and David McRobbie who contributed other chapters on gyro surveying and magnetic spacing.

Prof Angus Jamieson BSc FRICS
University of the Highlands & Islands
Inverness
Scotland

Introduction to Wellbore Surveying

Compiled and co-written by

Angus Jamieson

1. Coordinate Systems and Geodesy

1.1 The Origin – Reference Surfaces and Elevations in Mapping

There are three basic surfaces that are pertinent to good mapping, shown here, these are:

***Terrain**: The topographic surface of the ground or seabed*

***Geoid**: An equipotential surface that is irregular and approximates to Mean Sea Level (MSL)*

***Ellipsoid**: A regular model surface that approximates the geoid, created by rotating an ellipse about the polar axis. Used to simplify the computational complexity of the Geoid*

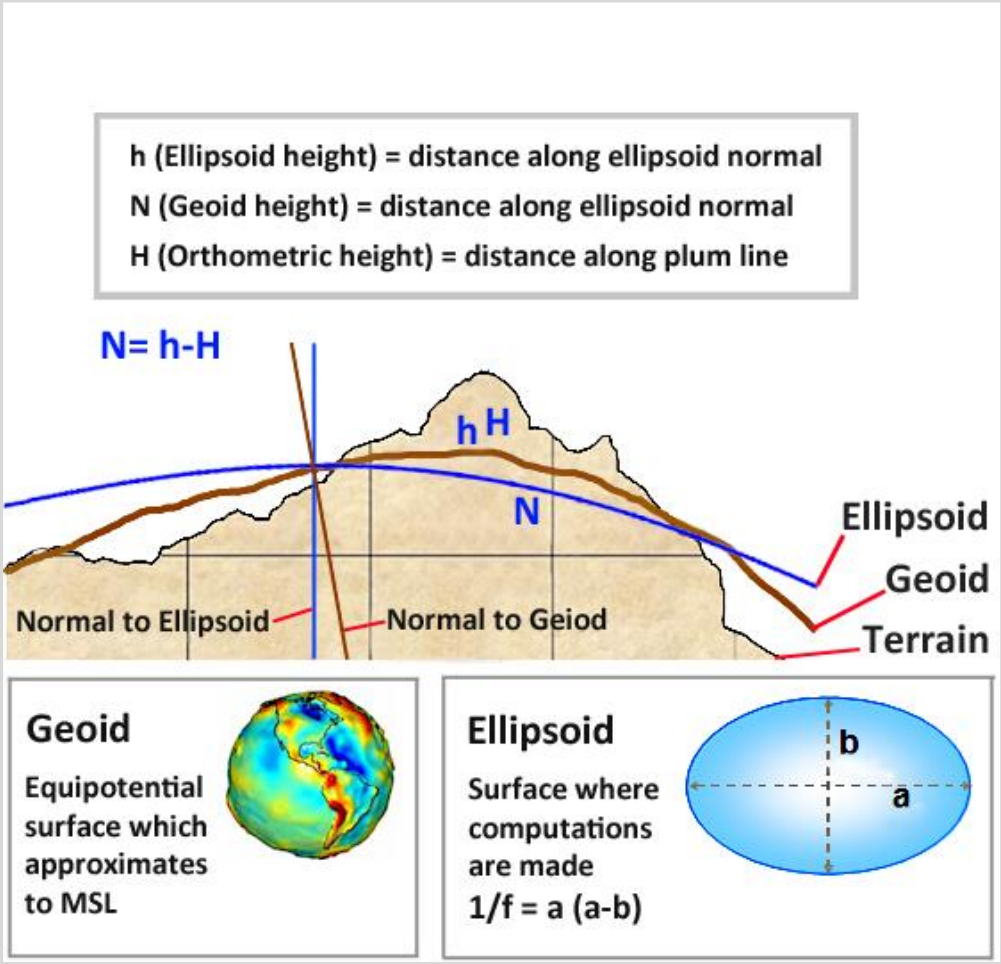

Figure 1: The three reference surfaces in geodesy.

Terrain: The terrain is the surface we walk on or the seabed. This surface is irregular. It is the surface we have to set up our survey measuring devices, such as a 'total station' or a GPS receiver. The nature of the surface will dictate the direction of gravity at a point. In mountainous terrain, the vertical will deflect in towards the main 'centre of mass' of the mountains.

The Geoid: The equipotential surface of the Earth's gravity field which best fits, in a least squares sense, global mean sea level (MSL). An equipotential surface is a one where gravity is an equal force everywhere, acting normal to the surface.The geoid is an irregular surface that is too complex for calculation of coordinates.

The Ellipsoid: The ellipsoid is a 'model' of the Earth that permits relatively simple calculations of survey observations into coordinates. The ellipsoid provides the mathematical basis of geodesy. Note that the Geoid is an 'actual physical surface like the terrain, but the ellipsoid is a 'theoretical' surface that is designed to 'match' the geoid as closely as possible in the area of operations. Note also that the normal to the geoid (which is 'vertical') is not the same as the normal to the ellipsoid.

An ellipsoid is created when an ellipse is rotated around its polar axis. The 'mathematical' properties of an ellipse are shown in figure 2. 'a' is assigned to represent the semi-major axis or equatorial radius and 'b' the semi-minor or polar axis. The flattening, 'f', equals the ratio of the difference in 'a' and 'b' over 'a'.

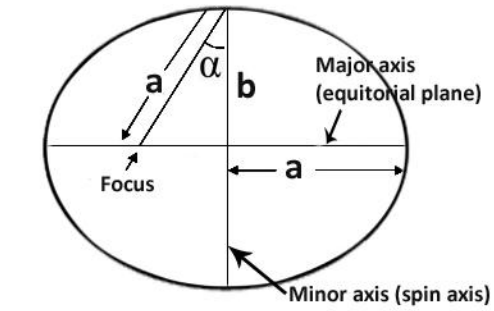

a is semi-major axis
b is semi-minor axis
f is flattening = (a-b)/a
e is first eccentricity = $[(a^2-b^2)/a^2]^{½} = (2f-f^2)^{½}$

e' is second eccentricity = $[(a^2-b^2)/b^2]^{½}$

$ae = \sqrt{(a^2-b^2)}$
$e = \sqrt{(a^2-b^2)}/a$
$\sin\alpha = e$
α is angular eccentricity

Figure 2: Mathematical properties of an ellipse.

1.1.1 MSL, Elevation and Height

Mean Sea Level is established by measuring the rise and fall of the tides. This is another 'inexact' science. The tides are affected by the juxtaposition of 'celestial' objects, most notably the moon but also the planets to varying degrees. A well-established MSL reference datum is one where tidal movement has been observed for over 18 years at what is called a 'Primary port'. The majority of countries with a coastline today have established these primary ports along that coastline and the predicted level of tides is reported by the US National Oceanographic and Atmospheric Administration (NOAA) and the UK Hydrographic Office tide tables.

LINKS NOAA tide tables UKHO tide tables

In order to tie MSL to both onshore elevations and offshore depths, these observations are tied to a physical benchmark usually in a nearby building wall or some other place unlikely to be inundated by the sea. This benchmark is quoted as a certain height above mean sea level. Sometimes MSL is used also as chart datum for the reduction of depth measurements to a common reference. Sometimes chart datum is established as the lowest level of low water, in order to provide mariners with the least possible depth at a point (i.e. the worst case). Onshore selected benchmarks represent an origin or starting point that can be used to provide the starting point for levelling across the whole country and continent.

The references for North America are the 'Sea Level Datum of 1929' - later renamed to the 'National Geodetic Vertical Datum' (NGVD 29) - and recently adjusted 'North American Vertical Datum of 1988' (NAVD 88).

Figure 1 shows the difference between heights (h) above the reference ellipsoid and the height above the geoid (H) also known as 'orthometric' height. A more general picture of this relationship with the definitions is in figure 3. The caution is that the GPS system provides 'height' above the ellipsoid, not MSL elevation. These heights have to be adjusted to make sure they match elevations from other datasets.

h (Ellipsoid height) = distance along ellipsoid normal (Q to P)
N (Geoid height) = distance along ellipsoid normal (Q to P_0)
H (Orthometric height) = distance along plum line (P_0 to P)

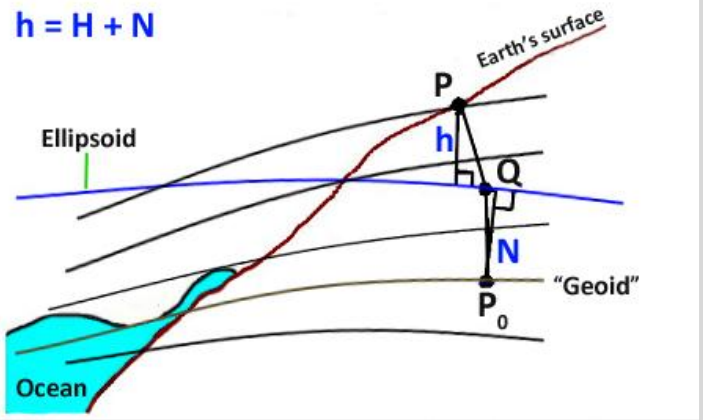

Figure 3: Shows the relationship between surfaces.

1.1.2 Coordinate Systems

There are three fundamental types of coordinate systems that are used to define locations on the Earth:
'Geocentric' coordinates measuring X, Y, Z from the centre of an ellipsoid, 'Geographical' - latitude and longitude and height (figure 4) and 'Projection' - easting and northing and elevation. Various subsets of these can also be used as '2D' consisting of only latitude and longitude or easting and northing.

1.1.3 Geographical coordinates

These are derived from an ellipsoid and the origin of the coordinates is the centre of the ellipsoid.

They are usually referenced to the 'Greenwich' meridian that runs through the Greenwich observatory just east of London in the UK. Meridians increase from 0° at Greenwich to 180° east and west of Greenwich. The 'International Date Line' runs through the Pacific and is nominally at 180° east or west of Greenwich. However, different island groups in the Pacific decide to be one side or the other of the Date Line, and the line is drawn at various longitudes to defer to national boundaries. On older maps the '0'° meridian is not always Greenwich. There are several other reference meridians, mainly in Europe. A list of these can be found in the EPSG parameter database.

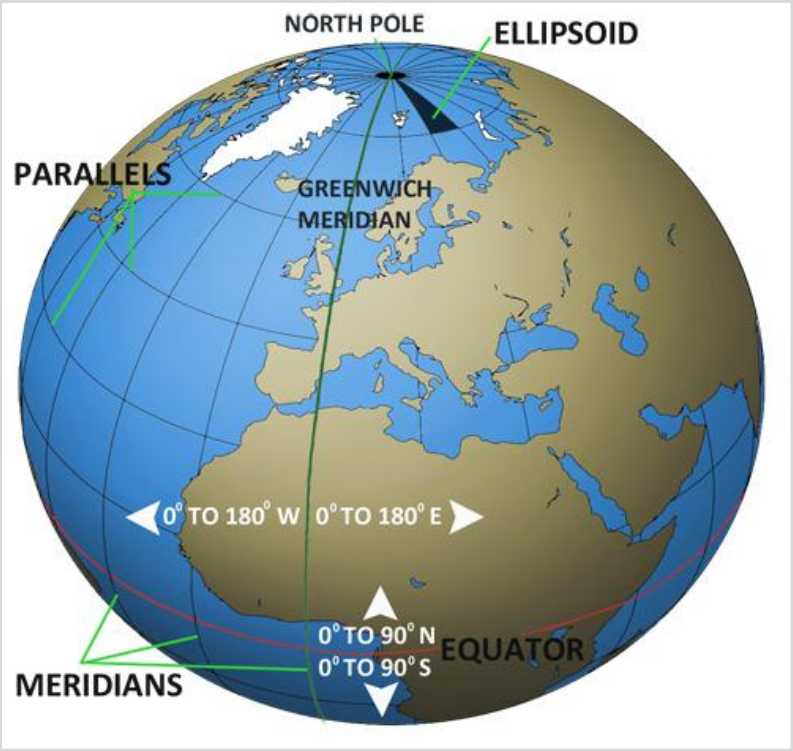

Figure 4: Geographic coordinate system.

In order to facilitate loading of data in some software applications, the convention is that North and East are 'positive' and South and West are negative. However the reader should beware that local applications that do not apply outside their 'quadrant', may not obey this convention.

Projection coordinates are usually called eastings and northings. Sometimes they are referred to as 'x' and 'y'. However, this can be confusing as in about 50% of the world, easting is represented by 'y' and northing by 'x'. Caution is advised!

More information about how these two types of coordinate system relate will be discussed in the following chapters.

✧

CONTENTS

1.2 Principles of Geodesy – The forgotten Earth science!

Why "The Forgotten Earth Science"? Because there is a pervading ignorance of this science, but an illusion that it is inherently understood! (Daniel Boorstin)

1.2.1 Geodesy

Geophysics and Geology – is a study of the Earth. We use models as the other two disciplines do, and make adjustments for distortion and errors in those models.

Geodesy provides the 'frame of reference' for all good maps. It is the means by which we can put together all sorts of different data attributes and ensure that they are correctly juxtaposed. So while we are interested in the relative position of one piece of data to another, the means by which this is achieved is through providing an 'absolute' framework or set of rules that ensures that we can do this correctly. Geodesy is rightly then to be considered the underlying and immutable doctrine required to ensure that maps (the cartographers 'art') properly represent the real world they are designed to portray.

Geodesy is defined as the study of:

- the exact size and shape of the Earth
- the science of exact positioning of points on the Earth (geometrical geodesy)
- the impact of gravity on the measurements used in the science (physical geodesy)
- Satellite geodesy, a unique combination of both geometrical and physical geodesy, which uses satellite data to determine the shape of the Earth's geoid and the positioning of points.

Let us return to the ellipsoid that we studied in the previous section (figure 5). This time, I have 'cut away' a quadrant of the ellipsoid so we can see the centre. On this diagram we can see two coordinate systems. One is the Latitude, Longitude and Height of a point 'P' in space above the ellipsoid surface (it could just as well be below). The other is a three dimensional Cartesian coordinate system where X is in the direction of the Greenwich meridian in the equatorial plane, Y is orthogonal to the Greenwich meridian and Z is parallel to the polar axis (orthogonal to the other two axes). The Cartesian system is directly referenced to the ellipsoid centre, the geographic system is directly referenced to the ellipsoid surface and indirectly to the ellipsoid centre. However, both systems are valid and both describe in different 'numbers' the coordinates of the point 'P'.

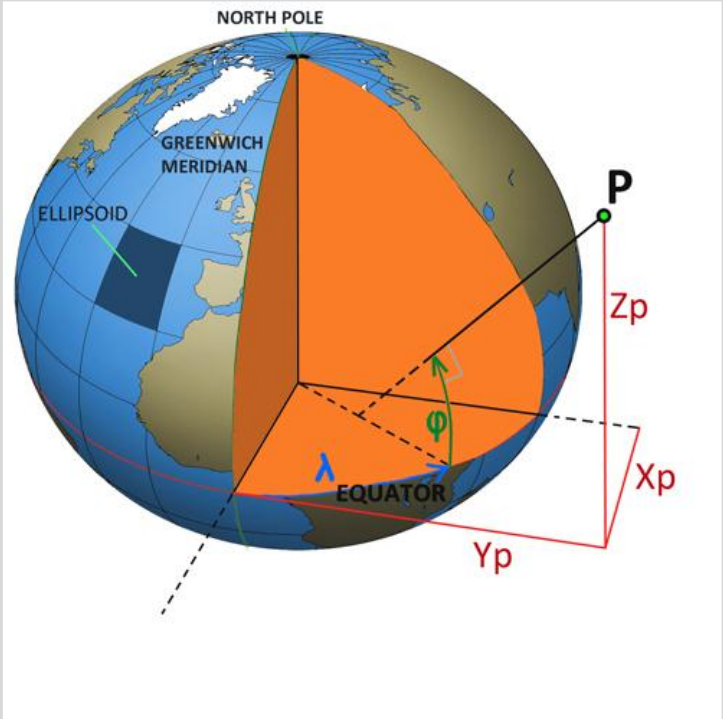

Figure 5: Ellipsoid coordinate reference systems.

The relationship between the two systems is per the

following algorithms:

$X = (v + h) * \cos \phi * \cos \lambda$
$Y = (v + h) * \cos \phi * \sin \lambda$
$Z = [(b2 * v/a2) + h] * \sin \phi$

(where 'v' is the radius of the ellipsoid at P).

1.2.2 Geodetic Datum

One of the most important lessons in geodesy is the next step. How do we tie the ellipsoid to the real world? Now that the model is set up, we have to attach it to the real world. Here is the definition of a 'Geodetic Reference Datum':

A Geodetic Datum is an ellipsoid of revolution attached to the Earth at some point. There are two types:

- *Astro-Geodetic (Regional usage)*
- *Global (Global application)*

We move from simply an ellipsoid, 'floating' in space to a 'geodetic reference datum'. There are two valid ways to do this, the historic, astro-geodetic (regional), pre-navigation satellite days method and the global method using satellite orbits.

Figure 6 shows how an astro-geodetic datum is established. Astro-geodetic means the geodetic system is set up by direct observation of the stars using very specialized survey instruments. The surface origin is the place where the survey instrument is set up.

The ellipsoid is attached at the observation point and several 'alignments' have to take place mathematically:

The equatorial plane of the ellipsoid has to align with the physical equatorial plane

The Polar Axis of the ellipsoid has to be parallel to the physical polar axis of the Earth

The ellipsoid surface has to be positioned so that it matches as closely as possible to the Geoid over the area of interest

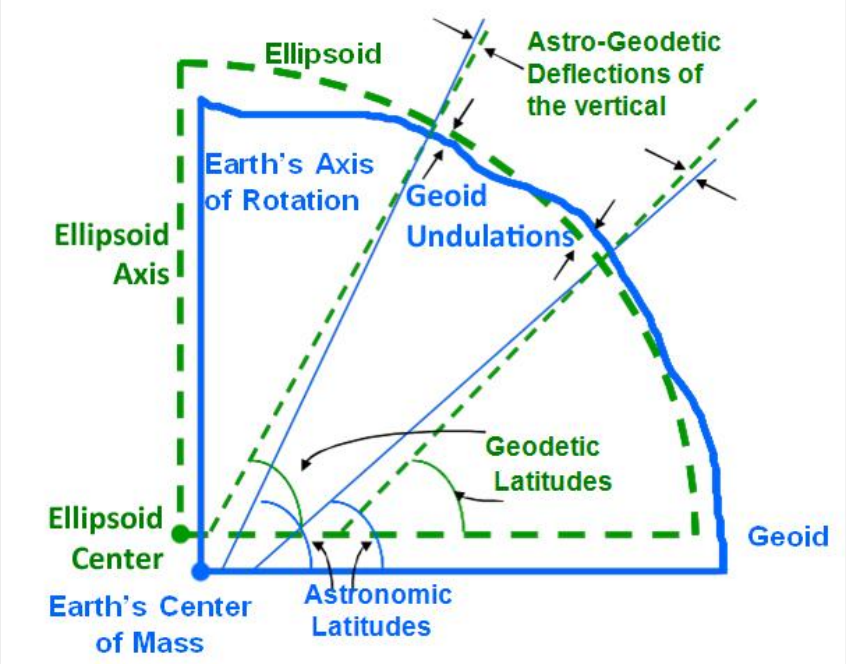

Figure 6: Establishing an Astro-geodetic Datum.

In figure 6, note three significant issues:

1. Astro-geodetic (geoid referenced) latitudes are not quite the same as geodetic (ellipsoid referenced) latitudes. This due to the slight difference in the normal to the respective surfaces. This is the model 'distortion' due to using an ellipsoid. If the region covered is a continent like the USA or Russia, then as the datum network is spread across the land then least squares corrections called 'Laplace' corrections have to be made to minimize the distortion.
2. They take much time to observe under demanding accuracy conditions which can be affected by the weather.
3. They are subject to the observation idiosyncrasies of the observer. Relative accuracy between datums established in the same place by different observers can be several hundred meters.

The drawback of the astro-geodetic method is that it is only useful over a specified region, and in general cannot be carried across large expanses of impenetrable terrain or water, since inter-visibility is required. Thus in archipelagos, like Indonesia, this can result in a large number of small regional datums none of which quite match with the others. Political boundaries can also mean a multiplicity of datums even in contiguous land masses; West Africa is a good example, where each country has its own unique astro-geodetic datum. Figure 7 shows a global view of continental regional datum 'blocks'. Eight datums to cover the world does not seem so difficult, but in fact there are well over 100 unique astro-geodetic datums. Figure 8 shows the proliferation of datums in SE Asia.

Figure 7: The World's Major Datum Blocks.

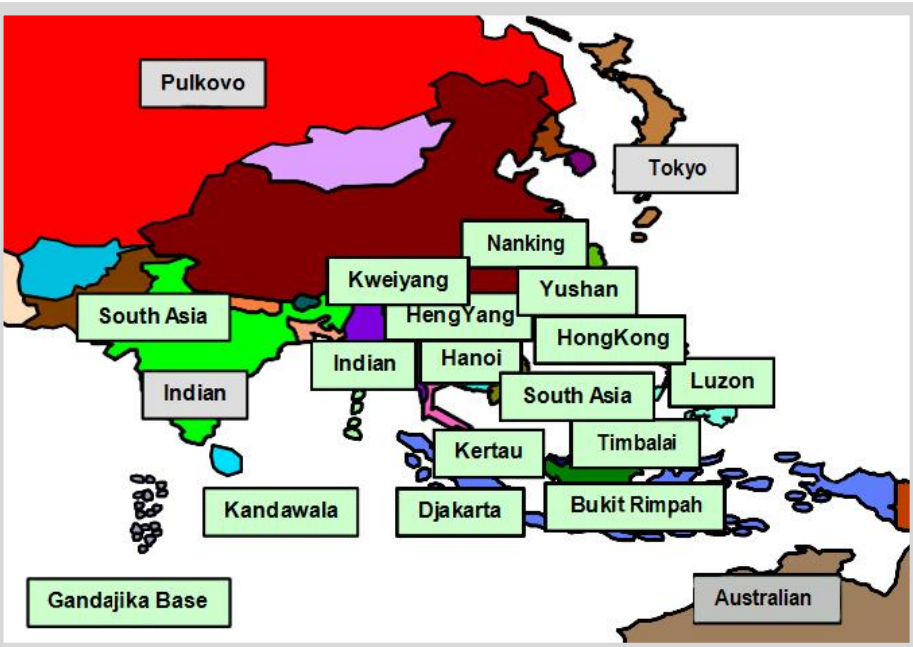

Figure 8: Shows the multiplicity of Astro-geodetic datums in the Indonesian Archipelago.

A global datum is a datum that is established to model the entire global geoid as closely as possible; something an astro- geodetic datum cannot do. A global is datum is established by observing the orbit of navigation satellites, calculating the Earth's centre of mass based on the orbits and then adjusting the ellipsoid by harmonic analysis to fit the global geoid. There have been several variants, but the two primary ones are WGS 72 and WGS 84. WGS stands for World Geodetic System. The WGS 72 datum was established for the 'Transit Doppler' satellite system, WGS 84 was established for the GPS system. The 'connection' point or origin for the global datums is the Earth's centre of mass. Due to iterative improvement of the gravitational analysis, the centre of mass is slightly different for WGS 72 and WGS 84.

Figures 9a through 9d *show, in cartoon form, the juxtaposition of two astro- geodetic datums with the geoid and a global datum. In figure 9a we see the geoid. There is an outline for representation in the other figures. In figure 9b red and green astro-geodetic datums are shown connected to the surface at two different points. The differences are exaggerated for effect. Figure 9c shows the geoid and the global datum. Figure 9d shows all three ellipsoids juxtaposed with the center of the ellipsoids clearly shown in three different places (again exaggerated for effect). Since latitude and longitude are referenced to the centre of the respective ellipsoid, it is clear that a latitude and longitude on one datum will not be compatible with a latitude and longitude on another datum unless some sort of transform takes place to adjust the one to match the other.*

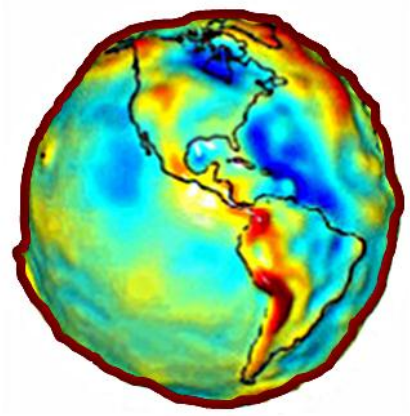

Figure 9a: The Geoid and an outline of the geoid

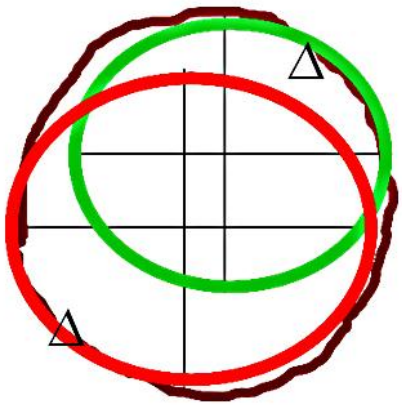

Figure 9b: Shows the red and green ellipsoid attached to the earth in two different places

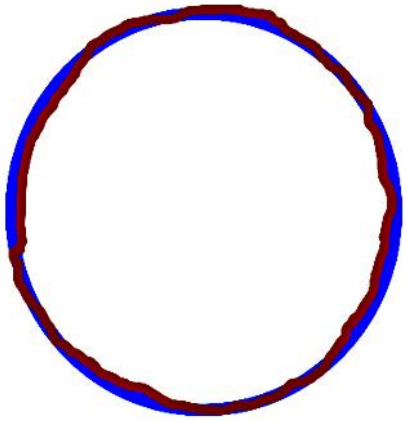

Figure 9c: Shows a blue 'global' ellipsoid attached to the earth's center of mass

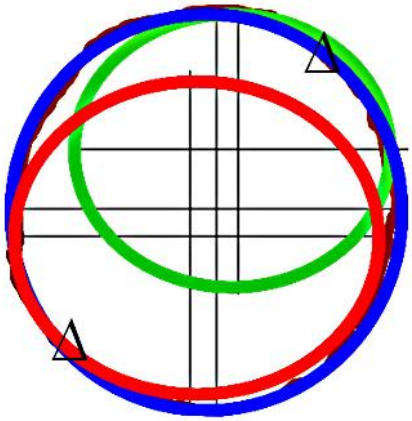

Figure 9d: Shows all three datums ellipsoids attched to the earth, with ellipsoid centers located differently

Reference Datum Transformation: Figure 10 shows a global (blue) and an astro-geodetic or regional datum (green), with the offset of the two centres. In order for a coordinate on the blue datum to be transformed to the green datum, the latitude and longitude have to be converted to x,y,z Cartesian coordinates on the blue datum. The dx, dy, dz have to be applied giving the x,y,z on the green datum. This can then be converted back to latitude and longitude on the green datum.

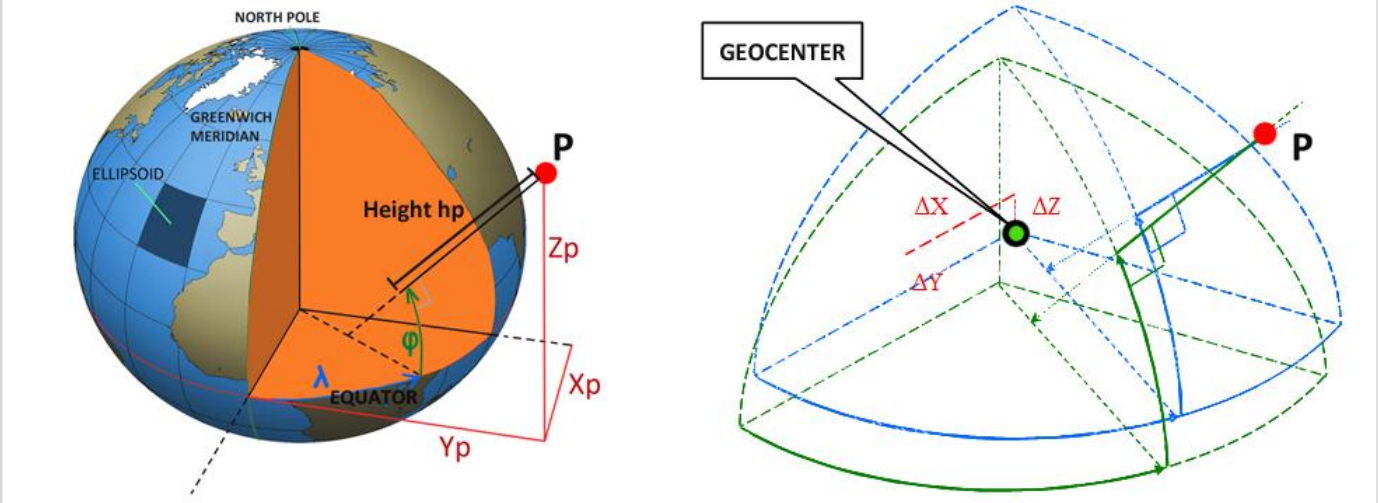

Figure 10: Showing a global datum (blue) and a regional/astro-geodetic datum (green) and the application of the geocentric transformation. The point P has not moved. It is just described by different coordinates.

Numerically these two sets of coordinates will be different but they will continue to represent the same physical point in space, as can be seen in figures 10 and 11. The corollary is that coordinates referenced to one datum that are mapped in a different datum will appear in the wrong place! The reader should note that in some of the larger regional datums, there are a variety of 3 parameter datum transformation sets depending on where in the region the operator is working (figure 12).

Datum	Latitude	Longitude	Local to WGS84	Local to Local
Aratu	20° 36' 13.2757"N	38° 56' 56.3341"W	236.7 meters	220.56 meters
SAD69	20° 36' 17.4283"N	38° 56' 50.1240"W	65.12 meters	
WGS84	20° 36' 19.2794"N	38° 56' 51.2166"W		

Figure 11: Shows three latitude and longitude locations referenced to different geodetic datums that all represent the same point. The differences in the right-hand two columns shows the error in mapped location if the datums are confused.

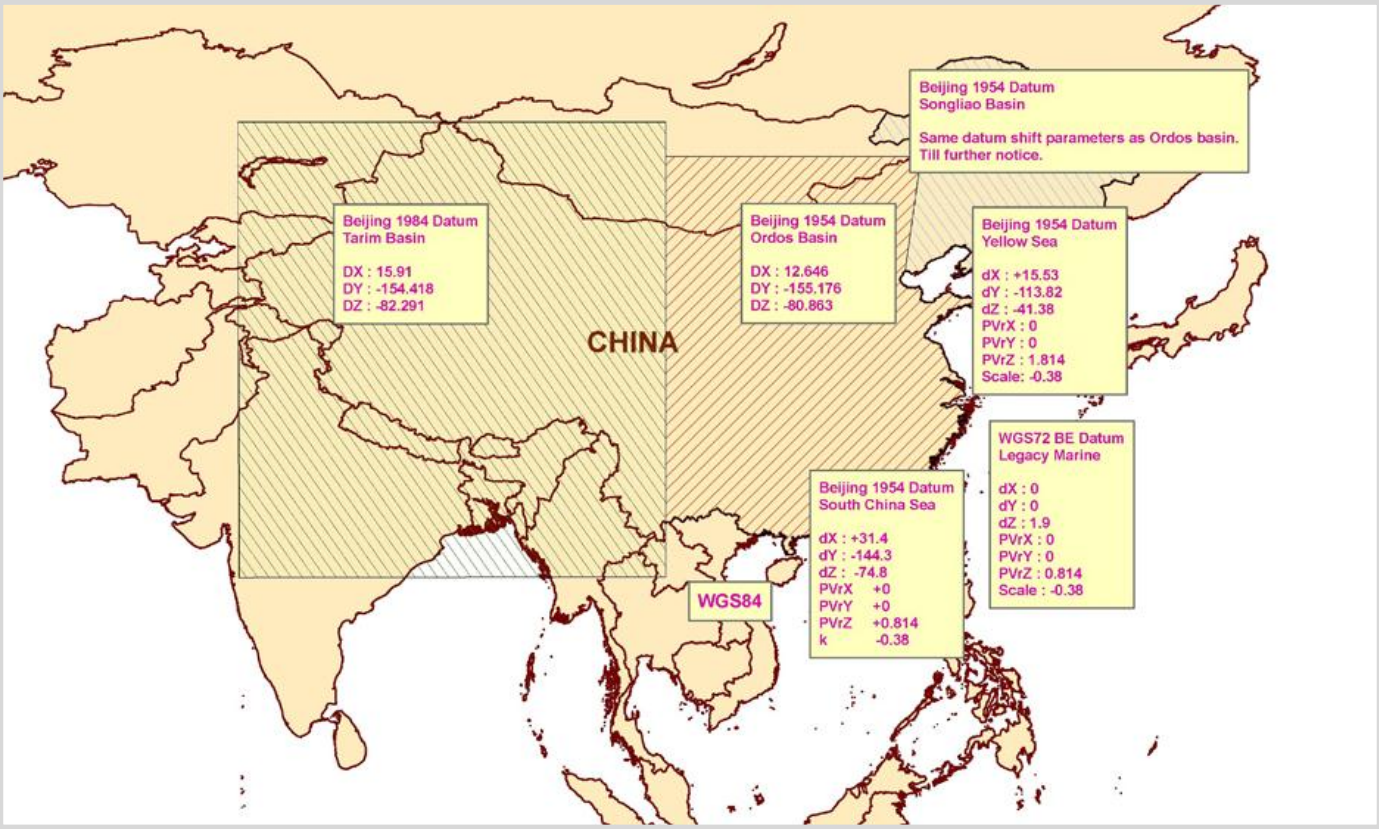

Figure 12: Shows various datum transformation parameters in China as they relate to WGS 84. Datums in China are WGS 84, WGS 72 BE, Beijing 1954 and Xian 1980. Note the difference in the parameters for the Beijing datum in the Ordos and Tarim basin, both three parameter transformations and the difference between the South China Sea and the Yellow Sea seven parameter transformations.

These are captured in the EPSG parameter database. Note also there are more sophisticated methods of calculating the datum transformation which may appear in various applications. These include parameters that not only translate but also allow for rotation and scaling differences between the two datums. The EPSG parameter database also contains many of these. Care should be taken when applying such parameters, and it is best to obtain the services of a specialist when using them or coding them into software. For most applications in the E&P domain, a three parameter shift will provide the necessary accuracy. In some countries more elaborate parameters are required by law.

LINK EPSG parameter database

1.2.3 Distortions in the Ellipsoidal Model

As the reader will have surmised, the ellipsoidal model is not an exact fit. The larger the area covered by a datum, the more distortion there is.

Height and Elevation – the elevation above MSL is not the same generally as the height above the ellipsoid. Corrections must be made to GPS or other satellite derived 'heights' to adjust them to mean sea level. Measurements made and adjusted to mean sea level by the surveyor may be assumed to lie on the ellipsoid as long as the separation between the two surfaces is relatively small.

Related to the previous one, the direction of the local vertical is not the same as the normal to the ellipsoid. This difference is known as the 'deflection in the vertical' and has to be minimized especially across larger regional and continental datums. This is done using Laplace corrections at regular intervals across the area of interest. Since these corrections vary in a non-regular and non-linear manner, the datum transformation between two datums may vary significantly across larger datums. The EPSG database is a means of identifying where a particular set of parameters should be used.

Radius of curvature adjustment (Figure 13) – The ellipsoid has a radius of curvature at a point (varies across the ellipsoid). When measuring distances at heights above or below the ellipsoid of more than about 5000 ft, the distances need to be adjusted to allow for the change in radius of curvature, so that they 'map' correctly onto the ellipsoid. Measurements made above the ellipsoid need to be reduced and measurements made below the ellipsoid need to be increased respectively, so that a map of the area (computed at the 'true' ellipsoid radius) map correctly onto the map in relation to other features. The calculation can be made with the following equation:

Ellipsoidal length = d[1 –(h/(R + h))] where
d = measured length
h = mean height above mean sea level (negative if below)
R = mean radius of curvature along the measured line

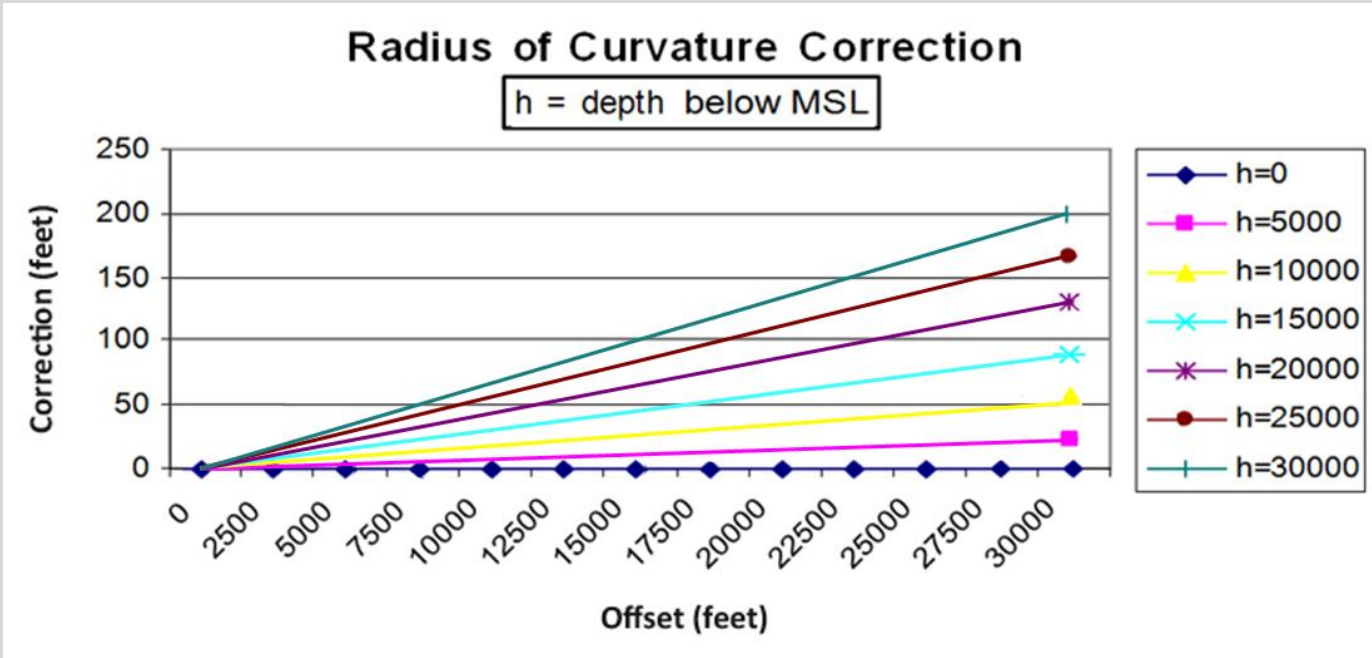

Figure 13: Shows the increase in offset correction with depth and offset distance.

Section summary

The most important lessons:

The most important lesson from all this is that a latitude and longitude coordinate do not uniquely define a point in space unless the datum name is included as part of the description! Please also note that knowing the name of the ellipsoid is not enough. An ellipsoid is a shape in space and the same ellipsoid can be attached to the Earth at an infinite number of places. Each time an ellipsoid is attached to another place it represents a different datum. Particular examples occur in West Africa, where many countries use the Clarke 1880 ellipsoid but set up as a different astro-geodetic datum in each case, and in Brazil where three datums use the International ellipsoid of 1924.

Ten Things to Remember about Geodesy and References:

1. Latitude and Longitude are not unique unless qualified with a Datum name.
2. Heights/Elevations are not unique unless qualified with an height/elevation reference.
3. Units are not unique unless qualified with unit reference.
4. Orientations are not unique unless qualified with a heading reference.
5. Most field data of all types are acquired in WGS 84 using GPS.
6. Every time data are sent somewhere there is a chance someone will misinterpret the references.
7. Most datasets have an incomplete set of metadata describing the references.
8. All software applications are not created equal with respect to tracking and maintaining metadata.
9. Data can be obtained by anyone from anywhere – that doesn't make it right!
10. Most people do not understand geodesy - if you are in doubt – check with someone who knows!

CONTENTS

1.3 Principles of Cartography – It's a 'Square World'! Or is it?

Figure 14:

Shows the hierarchy of mapping.

The foundation is the datum. Geographic coordinates (latitude and longitude) describe points in the datum. These are then converted into Projection coordinates.

Without knowledge of the datum, projection coordinates are not unique and can easily be wrongly mapped.

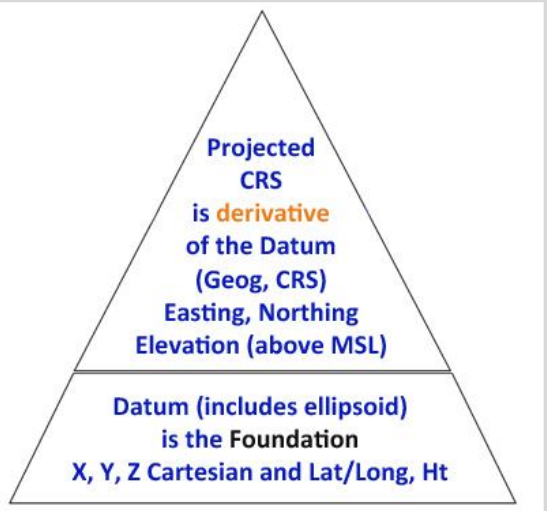

Why is it necessary to project geographic coordinates? We do this for three primary reasons:

- Ease of communication
- Ease of computation
- Presentation and Planning

1.3.1 Projection Categories

Figure 14 shows the various surfaces and orientation of the surfaces with respect to the ellipsoid axes. The three surfaces for projecting the ellipsoid are a cylinder, a cone and a plane. The main projection types used in E&P are *Transverse Mercator* and *Lambert Conformal Conic*.

Other projection types that occur less frequently are: *Mercator, Oblique Mercator (Alaska) Oblique Stereographic (Syria), Albers Equal Area*. The majority of the standard projections in use in E&P are listed with parameters in the EPSG database.

There are many 'standard' projection parameter definitions, but a project projection can be custom designed for specific purposes if needed. In general, one or two of the following criteria can be preserved when designing a projection:

Shape
Area
Scale
Azimuth

The majority of the projections we use are conformal. This means that scale at a point is the same in all directions, angular relationships are preserved (but not necessarily north reference) and small shapes and areas are preserved.

They are also generally computational.

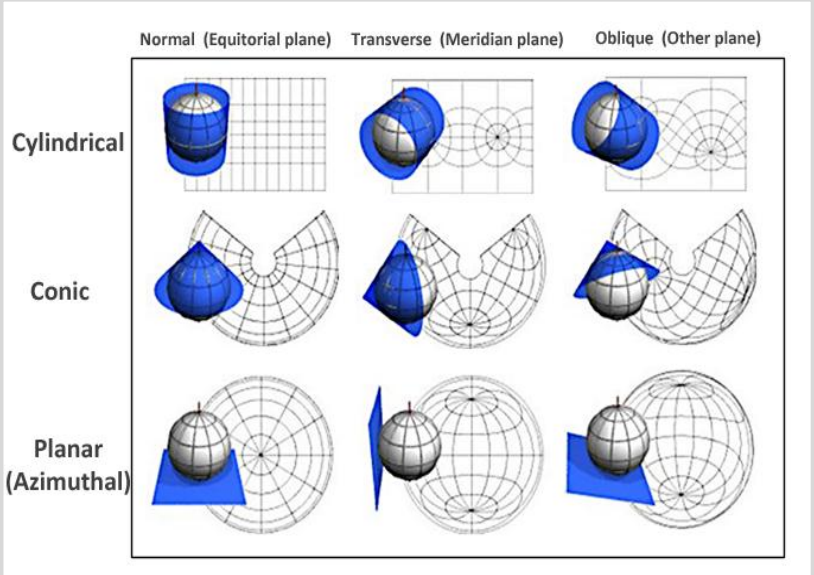

Figure 15: Shows the various types of projection based on various plane surfaces and the orientation of the surface with respect to the ellipsoid.

Figure 17 shows that making the plane surface secant to the ellipsoid allows for a greater area to be covered with an equivalent scale distortion.

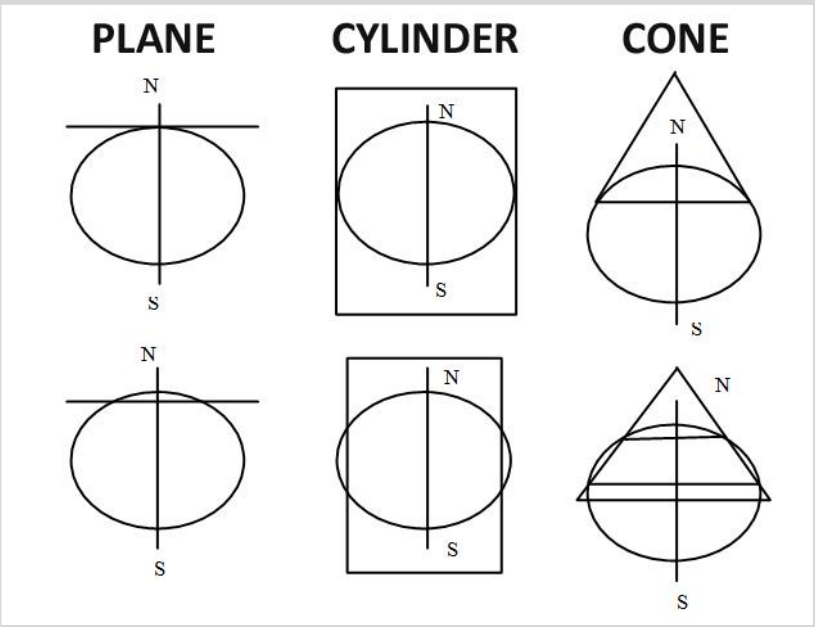

Figure 17: The plane surface can be tangent or secant to the ellipsoid. Secant permits the scale distortion to be distributed more evenly and therefore a larger area to be covered per unit distortion.

LINK EPSG parameter database

1.3.2 Mapping Parameters

A projection requires a set of parameters that are used to convert between latitude and longitude and easting and northing. These parameters can be found in the EPSG geodetic parameter database.

For a Transverse Mercator projection and a Lambert Conformal Conic projection these are respectively:

Datum	*e.g. NAD83*
Projection Type	*e.g. Transverse Mercator*
Projection Name	*e.g. Mississippi State Plane Coordinate System*
Zone Name	*e.g. West*
Central Meridian	*e.g. 90°20' W*
Latitude of Origin	*e.g. 29°30' N*
Central Scale Factor	*e.g. 0.99975*
False Easting	*e.g. 2,296,583.333 (NB = 700,000 meters)*
False Northing	*e.g. 0*
Units	*e.g. US Survey feet*

Datum	*e.g. NAD27*
Projection Type	*e.g. Lambert Conformal Conic*
Projection Name	*e.g. Texas State Plane Coordinate System*
Zone	*e.g. South Central*
Central Meridian	*e.g. 99°00' W*
Latitude of Origin	*e.g. 27°50' N*
****North Standard Parallel***	*e.g. 30°17' N*
****South Standard Parallel***	*e.g. 28°23' N*
False Easting	*e.g. 2,000,000*
False Northing	*e.g. 0*
Units	*e.g. US Survey feet*

The geographic origin is the intersection of the central meridian with the latitude of the origin. The projection origin values at that point are the false easting and false northing. The reason for the high positive values for these parameters where applicable, is to avoid negative values. In both cases above this is for the easting but is not necessary for the northings which are both '0', as the projection is not intended for use south of the origin.

There are several other types of projection, most of which are of more interest to cartographers than having any application in E&P.

1.3.3 Distortions in Mapping

We have already seen in the Geodesy section above, that by modelling the Geoid using an ellipsoid, we have already introduced some distortion in the way that the Earth is represented. Without adjustment, that distortion increases as we proceed further from the point of origin where the datum was established. However, with a well-established datum, these distortions can be minimized. When we make calculations from the Earth's surface to a flat (projection) surface, we introduce an additional set of distortions. These are in area, shape, scale and azimuth.

These distortions:

- Can be calculated and understood, but without proper care and well educated workforce, it is easy to make mistakes.
- Are non-linear; that is to say, the size of the distortion varies across the projected area are very important component in mapping wellbores.

The most important and potentially destructive distortions when projecting geospatial data to a map are scale and orientation, particularly when mapping wellbore positions. Figure 18 shows a 'macro' level example of scale and azimuth distortion. This effect happens even at short distances but not so obviously to the eye. The orientation or azimuth change is what is called convergence. Its value can be calculated and applied to 'real world' measurements to adjust them to projection north referenced value. Similarly scale distortion can be applied to survey measurements to represent a scaled distance on the map.

1.3.4 Azimuth Distortion

A key point to remember is that the projection central meridian is truly a meridian - there is no azimuth distortion. As one moves away from the central meridian east or west, the other meridians plot on the projection as curved lines that curve towards the nearest pole, whereas grid north lines are parallel to the central meridian. At any given point, the difference in azimuth between the grid north lines and the meridian lines is the convergence angle. On the equator, convergence is generally zero also, and increases as one moves north.
Figure 18 shows a 'global' cartoon view of the concept.

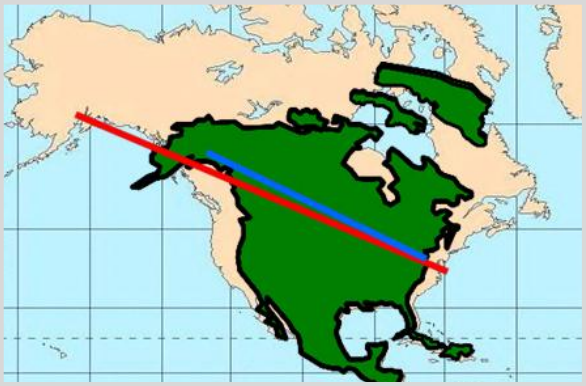

Figure 18: The plane surface can be tangent or secant to the ellipsoid. Secant permits the scale distortion to be distributed more evenly and therefore a larger area to be covered per unit distortion.

Figure 19 shows a simple way to verify that the value derived is correct (i.e. that the sign of convergence has been correctly applied). It is important when dealing with convergence to do a couple of 'sanity' checks:

- Always draw a diagram (Figure 19)
- Always check that the software application is applying the correct value, correctly
- Always have someone else check that the results agree with supplied results of wellbore location
- If you are not sure – find a specialist

The formal algorithm is *Grid azimuth = True Azimuth – Convergence* but many applications do not observe the correct sign. It is better to use *True Azimuth = Grid Azimuth ± Convergence α* where (per figure 19), α -ve West of CM, and α +ve East of CM in Northern hemisphere and the opposite in Southern hemisphere.

In the equation above, use the sign in the diagram, not the sign you get with the software, because some applications use the opposite convention.

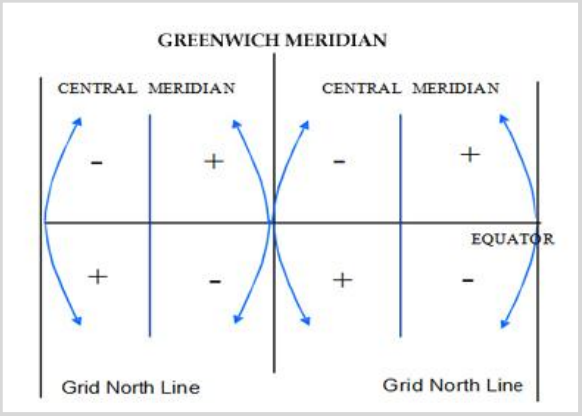

Figure 19: Shows two projection zones with Central Meridians, as well as non-central meridians plotted on the projection (curved lines) that converge towards the nearest pole. Two additional grid north lines are shown to the right and left of the figure. Grid north lines are parallel on the projection, creating a grid. Convergence and scale sign distortion vary in a non-linear fashion across the projection, but can be calculated for any given point.

1.3.5 Scale Distortion

Referring back to figure 18, it is clear from the example that a projection will distort the distance between two points. Clearly the true (Earth surface measured) distance between anchorage and Washington DC has not changed, but the length on the map can change depending on the projection. Most projections we use have a sub unity 'central scale factor'. In the example above the Mississippi West state plane projection has a central scale factor of 0.99975. This means that on the central meridian a 1,000 meter line measured on the ground will be represented by a line 999.75 meters at the scale of the map. If the map has a scale of 1:10,000, then the line on the map will be represented by a line 9.9975 cms long. If you plotted the same line on the central meridian of a UTM projection with a central scale factor of 0.9996, then the line on the map would be represented by a line 9.996 cms long.

CONTENTS

2. Changing from One Map System to Another

2.1 Ellipsoids and datums

This is covered in more detail in the Geodesy section above but here are some basic guidelines.

The Earth is elliptical in cross section due to the fact that the planet is mainly molten rock and the rotation of the Earth causes a slight 'flattening' as the centrifugal force throws the mass of liquid away from the centre of spin.

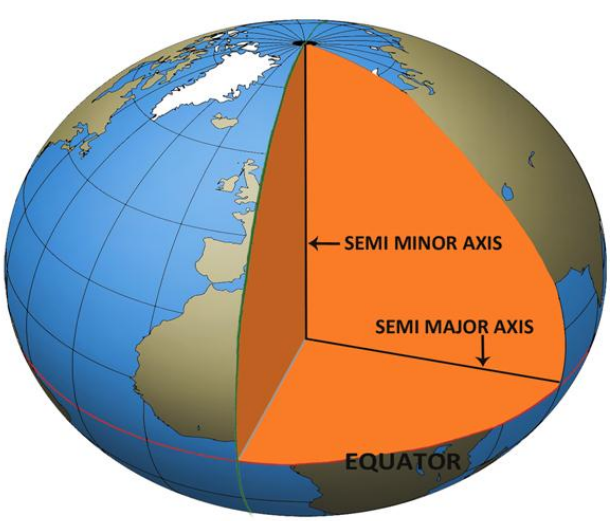

Figure 20a: Earths elliptical cross section.

A datum by definition is an ellipsoidal model of the Earth and a centre point. Historically we have estimated the dimensions of the ellipsoid and its centre from surface observations and the best fit datum has naturally varied from region to region around the world. For example, in the USA, an elliptical model and centre point was chosen in 1927 and is referred to as the NAD 27 datum.

It uses the Clarke 1866 Ellipsoid (named after Alexander Ross Clarke a British Geodesist 1828 - 1914 with dimensions as follows:

Semi-Major Axis: 6378206.4 metres
Semi-Minor Axis: 6356583.8 metres

Whereas in 1983 the datum was updated to NAD 83 which uses a spheroid as follows:

Semi-Major Axis: 6378137 metres
Semi-Minor Axis: 6356752.3 metres

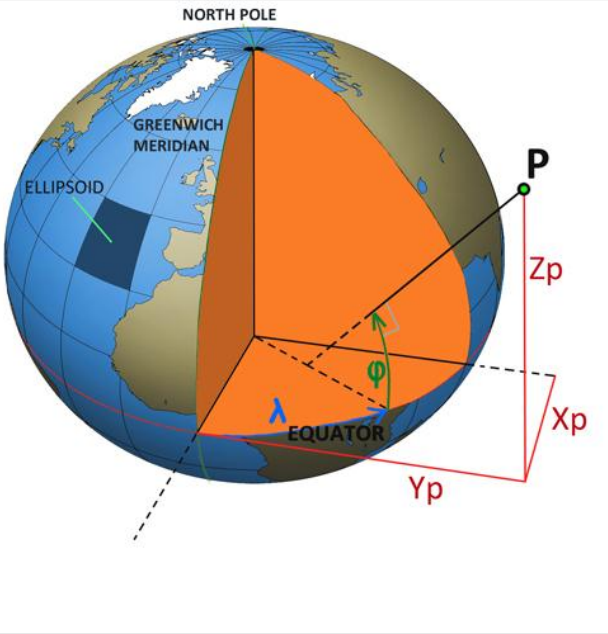

Figure 20b: Geo Centric XYZ coordinates.

Not only did the shape update but the centre point shifted by several hundred feet. In order to correctly convert from one system to another, the latitude and longitude have to be converted to an XYZ coordinate from the estimated centre of the Earth (Geo Centric Coordinates). After that a shift in the coordinates to allow for the shift between the centre estimates is applied. Then the coordinates can be converted back to a vertical angle (latitude) and horizontal angle (longitude) from the new centre on the new ellipsoid. In some cases there may be a scale change and even a small rotation around the three axes so it is not recommended that a home-made calculation is done for such a critical and sensitive conversion.

Latitude and Longitude for a point are NOT UNIQUE. They depend on the centre point and spheroid in use.

It is worth checking out the EPSG web site. This is the internet domain of the European Petroleum Survey Group which maintains an accurate database of geodetic parameters and provides on line software for doing such conversions.

LINK EPSG website

Here, for example is the conversion of a point at 30 degrees North latitude and 70 degrees West Longitude from NAD 27 to NAD 83.

	Latitude	Longitude
NAD 27 datum values:	30 00 0.00000	70 00 0.00000
NAD 83 datum values:	30 00 1.15126	69 59 57.30532
NAD 83 - NAD 27 shift values:	1.15126 (secs)	-2.69468(secs)
	35.450 (meters)	-72.222(meters)
Magnitude of total shift:	80.453(meters)	

The main consideration here is that it is essential that when positioning a well, the geoscientists, the operator and the drilling contractor are all working on the same map system on the same datum as the shift in position can be enormous and frequently far bigger than the well target tolerance.

CONTENTS

3. True North, Grid North, Convergence Summary & Exercises

3.1 Map projections

For any point on the Earth's surface True North is towards the Geographic North Pole (The Earth's axis of revolution).

This fact is independent of any map system, datum or spheroid. However, when a map projection surface is introduced, it is impossible to maintain a parallel map North that still meets at a single point.

In this example a vertically wrapped cylinder such as those used in Transverse Mercator map projections includes the North Pole but the straight blue line on the globe will become slightly curved on the surface of the cylinder. The black line in the diagram shows the direction of Map North (Grid North) and clearly they are not the same.

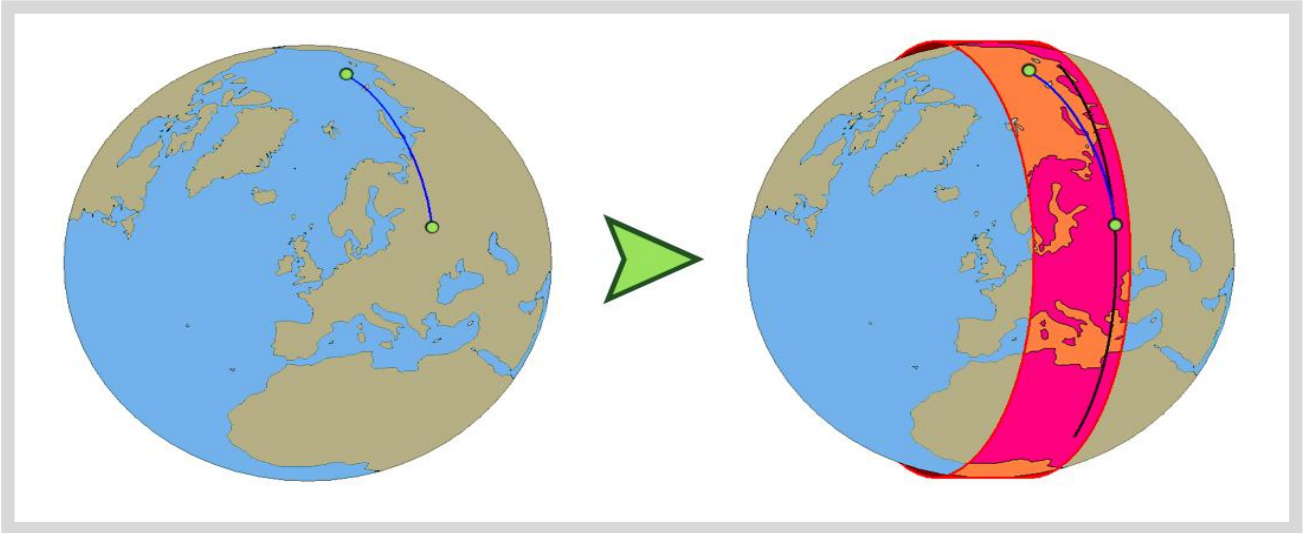

Figure 21: Map projection surface exercise showing it is impossible to maintain a parallel map North.

When the cylinder is unwrapped, the two lines look like figure 22a.

Because all True North lines converge to a single point, the angle from True to Grid North is referred to as the 'Convergence' Angle.

Convergence is the True Direction of Map North.

In the case of the Universal Transverse Mercator Projection, the convergence within one map zone can vary from -3 degrees to + 3 degrees.

When correcting a true North Azimuth to Grid, this convergence angle must be subtracted from the original azimuth. It is essential that a North Arrow is drawn in order to correctly visualize the relative references.

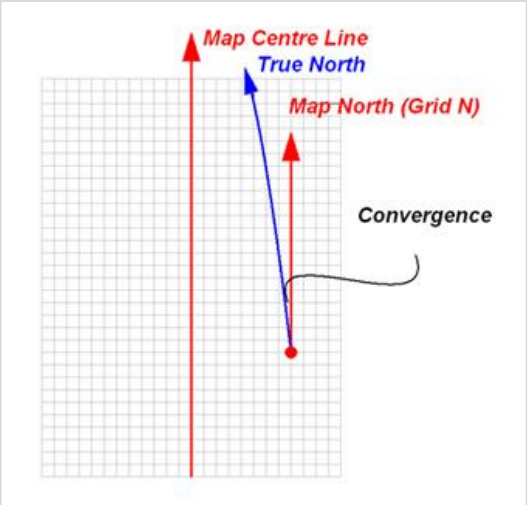

Figure 22a: The 'Convergence' Angle.

When magnetic north is included (see next chapter) we have three different North References to contend with.

These can be in any order with several degrees of variation between them so a clear North Arrow is essential on all well plans and spider maps.

When correcting from one reference to the other it is common practice to set the company reference North straight upwards and plot the others around it. In figure 22a & 22b, Grid North is the preferred company reference, so all quoted azimuths would be referenced to Grid and the North arrow is centred on Grid North.

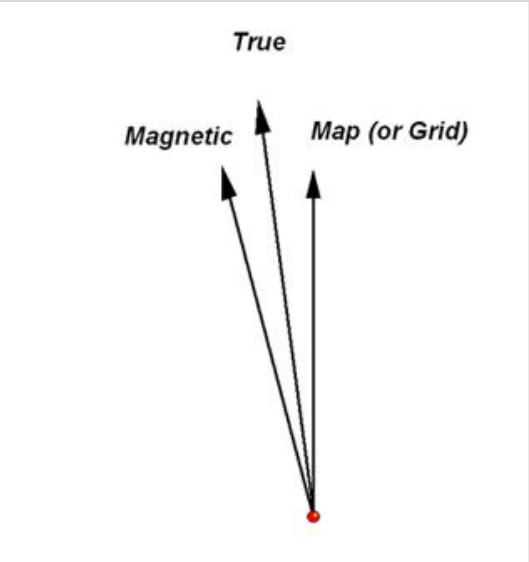

Figure 22b: The three north references.

In this example the well is heading 60° Grid with magnetic North at 6° west of True and Grid North 2° East of True - figure 22c. Depending on which reference we use, the azimuth can be expressed three different ways. It is easy to see how confusion can occur.

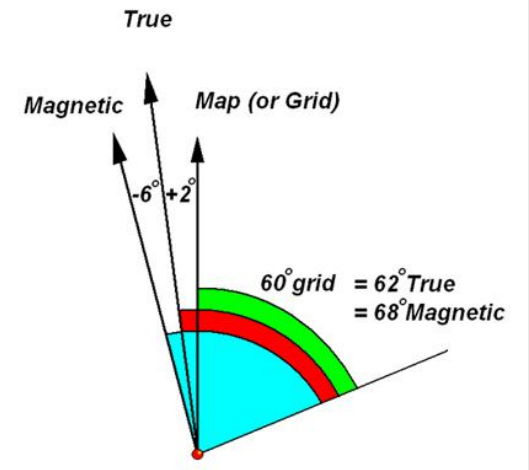

Figure 22c: The Convergence angle calculation.

Worked examples follow on the next pages…..

✧

CONTENTS

Some simple worked examples:

Example 1

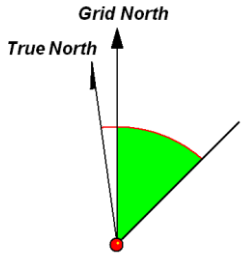

Grid Convergence is +2.5

True Direction is 47.5

What is the Grid Direction

It's 45 degrees

Example 2

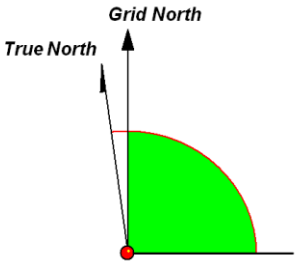

Grid Convergence is +1.8 degrees

True Direction is 91.8 degrees

What is the Grid Direction

It's 90 degrees

Example 3

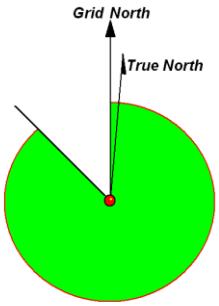

Grid Convergence is - 0.7 degrees

True Direction is 312.4 degrees

What is the Grid Direction

It's 313.1 degrees

Example 4

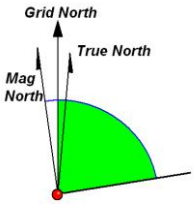

Magnetic Declination is - 8 degrees

Magnetic Direction is 88 degrees

What is the True Direction

It's 80 degrees

And if the Convergence was +2

What would be the Grid Direction

It's 82 Degrees

Example 5

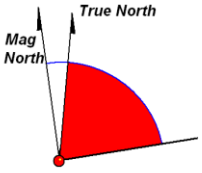

Magnetic Declination is - 8 degrees

Magnetic Direction is 88 degrees

What is the True Direction

It's 80 degrees

Extended example 1

Convergence is the True Direction of Grid North ***(West is Negative East is Positive)***
Declination is the True Direction of Magnetic North ***(West is Negative East is Positive)***

True Bearing = Magnetic Bearing + Declination
Grid Bearing = True Bearing - Convergence
Grid Bearing = Magnetic Bearing + (Declination - Convergence)

(Declination - Convergence) is known as the Grid Correction

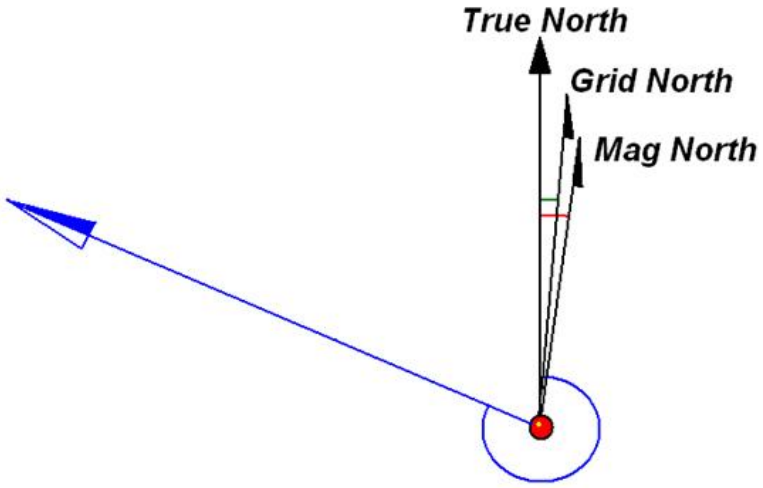

Example Convergence = +3
Declination = +6

Grid Correction = 6 - 3 = 3

Magnetic Bearing = 295
Grid Bearing = 298
True Bearing = 301

Extended example 2

Convergence is the True Direction of Grid North ***(West is Negative East is Positive)***
Declination is the True Direction of Magnetic North ***(West is Negative East is Positive)***

True Bearing = Magnetic Bearing + Declination
Grid Bearing = True Bearing - Convergence
Grid Bearing = Magnetic Bearing + (Declination - Convergence)

(Declination - Convergence) is known as the Grid Correction

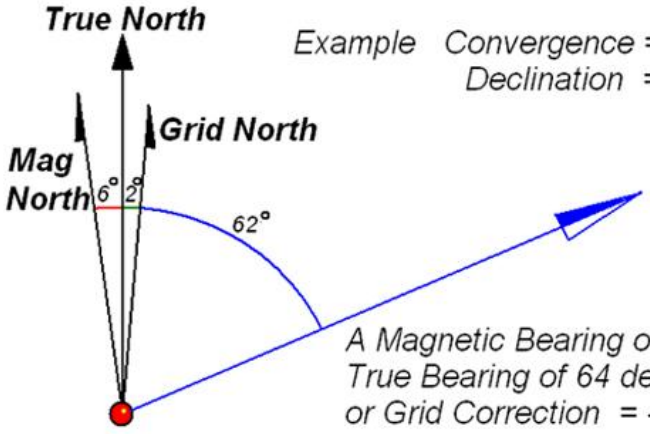

Example Convergence = +2 degs
Declination = -6 degs

A Magnetic Bearing of 70 degs = True Bearing of 64 degs
True Bearing of 64 degs = Grid Bearing of 62 degs
or Grid Correction = -6-2 = -8 so Grid Bearing = 70 + (-8) = 62

4 The Earth's Magnetic Field

4.1 Basic Outline

At the heart of the planet is an enormous magnetic core that gives the Earth's navigators a useful reference. The lines of magnetic force run from south to north and these provide a reference for our compasses.

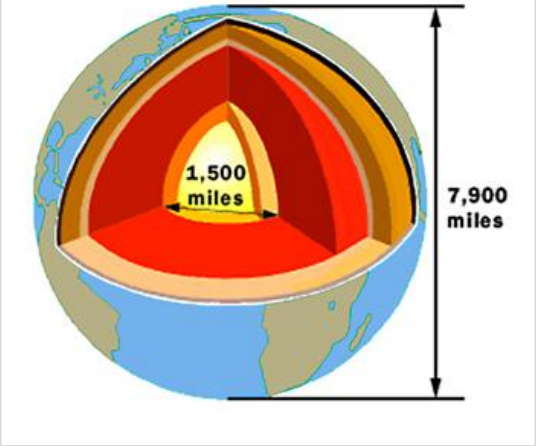

Figure 25: Basic Earth internal layers.

To fully define the Earth's Magnetic Field at any location, we need three components of a vector. The Field Strength, usually measured in nano Teslas or micro Teslas, the Declination Angle defined as the True Direction of Magnetic North and the Dip Angle defined as the vertical dip of the Earth vector below horizontal. For computing reasons, this vector is often defined as three orthogonal magnetic field components pointing towards True North, East, and vertical referred to as Bn, Be and Bv. A fundamental law of physics relating magnetic field strength to electric current is known as the Biot-Savart Law and this is our best explanation for why B is used to denote magnetic field strength. If you know better, please contact the author - details at the front of this publication.

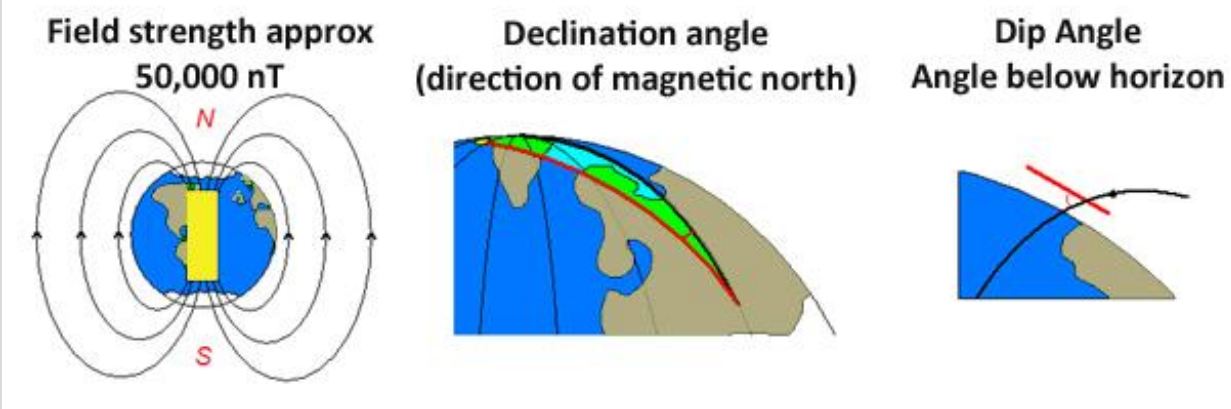

Figure 26: Elements of the magnetic field vector.

4.2 Variations in the Earth's Magnetic Field

One problem with the Earth's Magnetic Field is that it will not stand still. Over the course of history, the magnetic core of the Earth has been turbulent with the result that the magnetic vector is constantly changing. In geological time scales this change is very rapid. It is referred to as the 'Secular' variation.

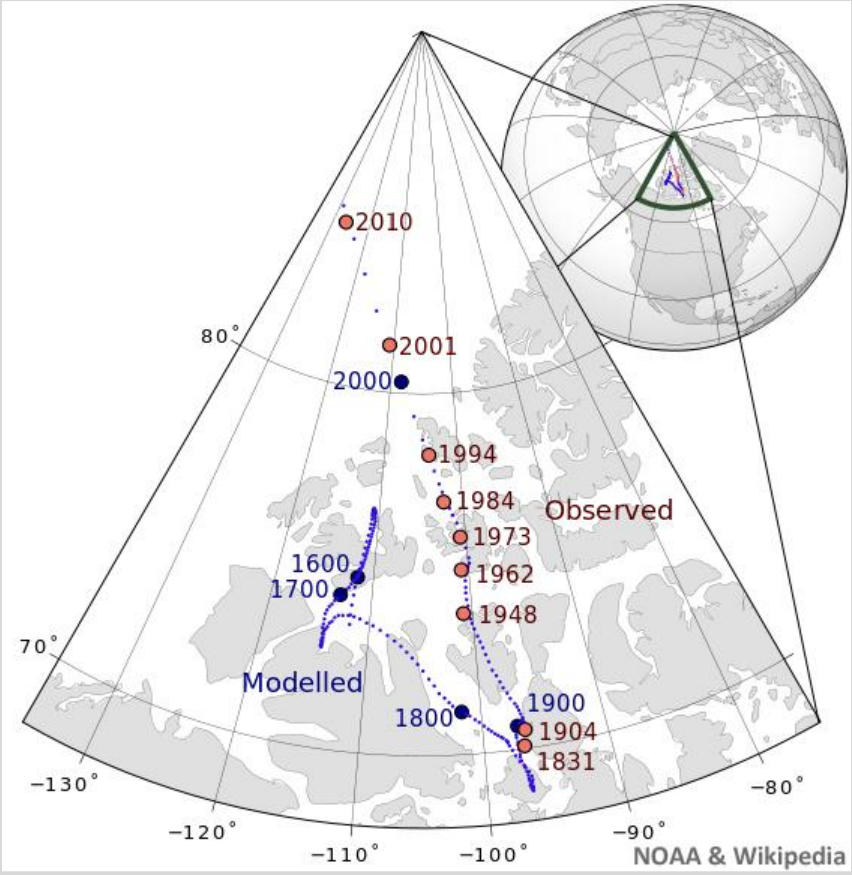

Figure 27: Tracking the magnetic North Pole.

In order to keep track of this movement, several global magnetic models are maintained to provide prediction models. For example, an international organization called INTERMAGNET collates data from observatories scattered throughout the world to model the intensity and attitude of the Earth's magnetic field. Every year, the data is sent to the British Geological Survey in Edinburgh where it is distilled to a computer model called the British Global Geomagnetic Model (BGGM). Historically this has been the most commonly used model for magnetic field prediction for the drilling industry but there are others. The United States National Oceanic and Atmospheric Administration (NOAA) also produce a model known as the High Definition Geomagnetic Model from their National Geophysical Data Centre in Boulder Colorado. This takes account of more localized crustal effects by using a higher order function to model the observed variations in the Earth field. In practice, when higher accuracy MWD is required, it is increasingly popular to measure the local field using IFR (see chapter 6) and to map the local anomalies as corrections to one of the global models. In this way, the global model takes care of the secular variation over time and the local effects are not dependent on a mathematical best fit over long wavelengths.

LINKS BGGM NOAA

The model in figure 28 below is a combined effort between NOAA and the BGS called the World Magnetic Model which is updated every 5 years. This is a lower order model, as is the International Geomagnetic Reference Field produced by IAGA but these are freely accessible over the internet whereas the higher order models require an annual license.

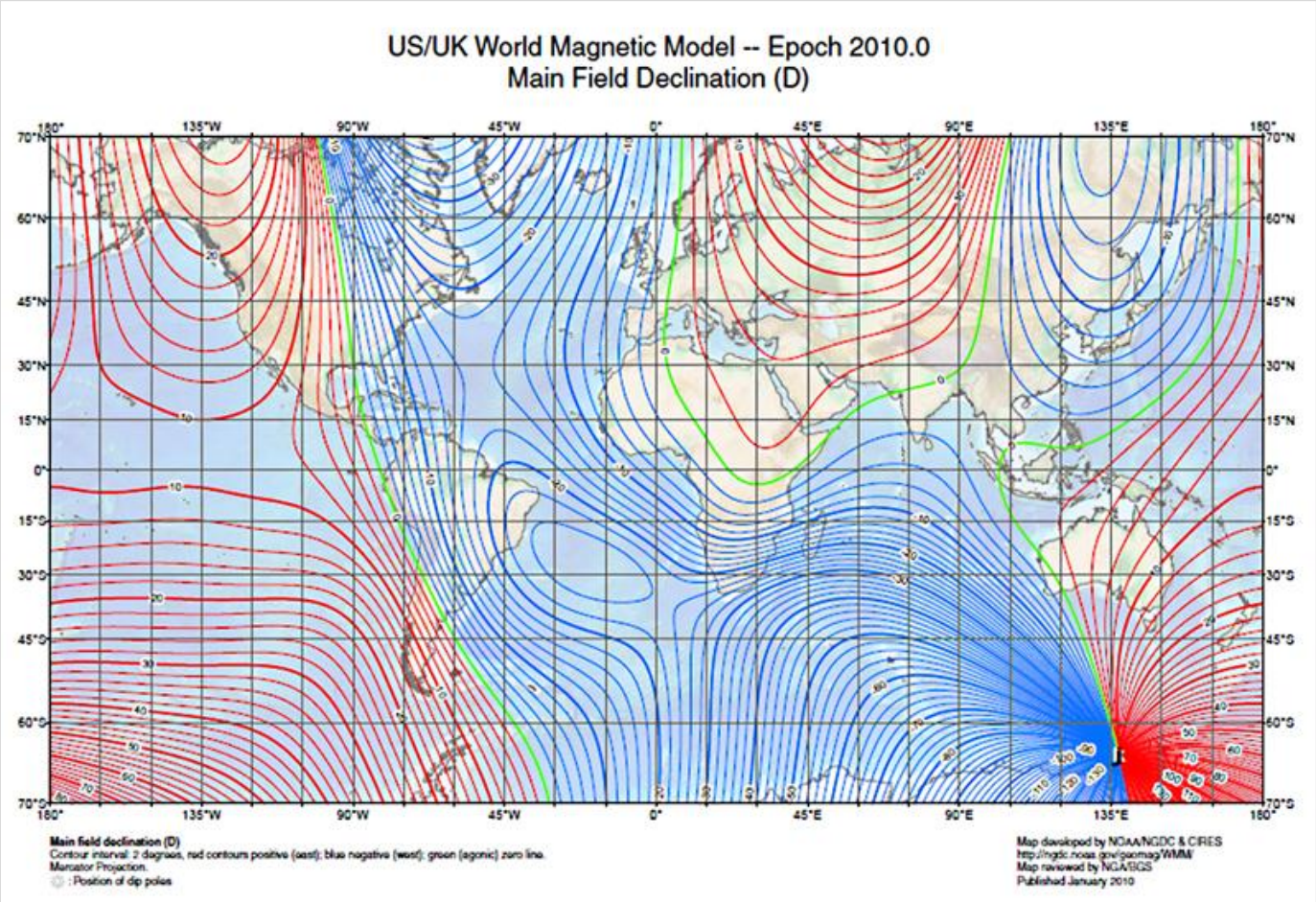

Figure 28: Main field declination Jan 2010.

The higher order world models (BGGM and HDGM) are considered to be better than 1 degree (99% confidence) at most latitudes. This may be less true at higher latitudes above 60^0 but at these latitudes, IFR techniques are frequently used.

Figure 29: Typical magnetic observatories.

4.3 Magnetic Observatory Distribution

It should be noted that the global models such as BGGM and even HDGM, can only measure longer wave length effects of the Earth's magnetic field distribution and cannot be expected to take account of very localised crustal effects caused by magnetic minerals, typically found in deep basement formations in the vicinity of drilling. See chapter 6 for a discussion of In Field Referencing (IFR), a technique for measuring the local field to a higher accuracy.

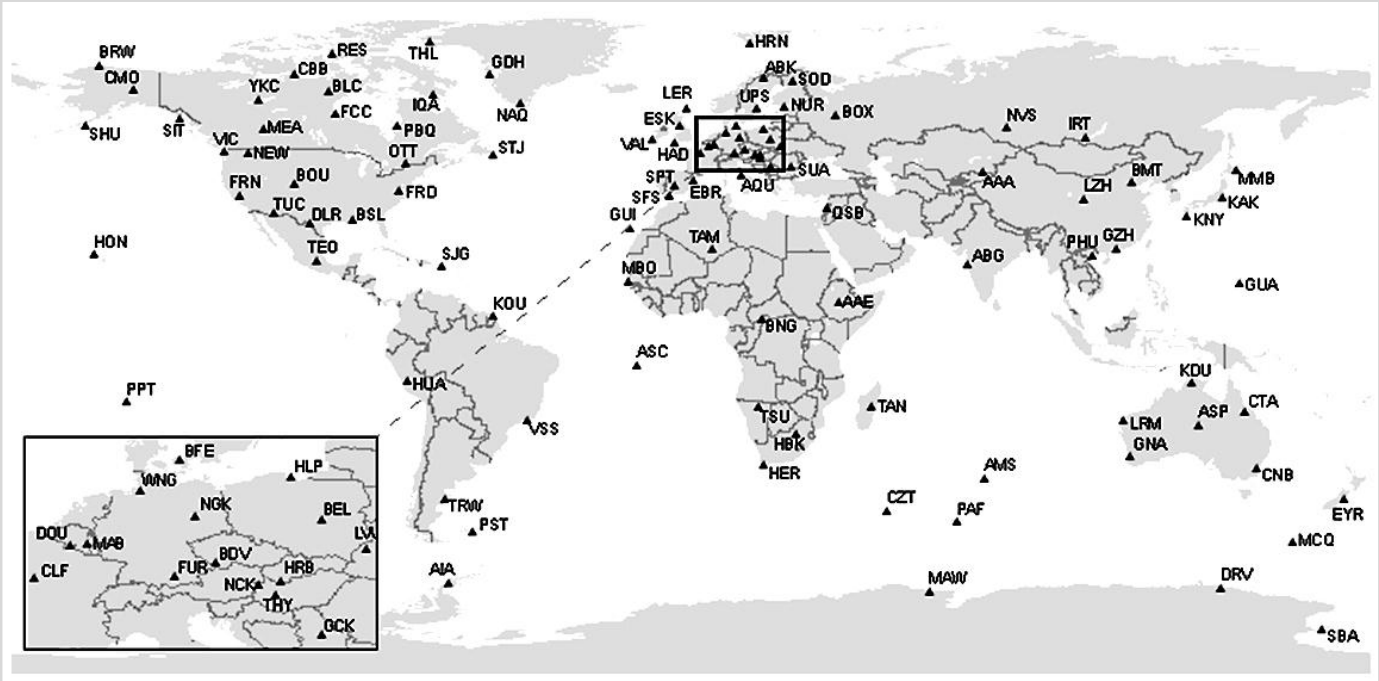

Figure 30: Magnetic Observatory distribution.

4.4 Diurnal Variation

The term Diurnal simply means 'daily' and for many centuries it has been noticed that the magnetic field seems to follow a rough sine wave during the course of the day. Here is a graph of field strength observations taken in Colorado over a 2 day period.

It can be seen that the field strength is following a 24 hour period sine wave.
See chapter 7 for a discussion of 'Interpolated In Field Referencing', a method of correcting for diurnal variation in the field.

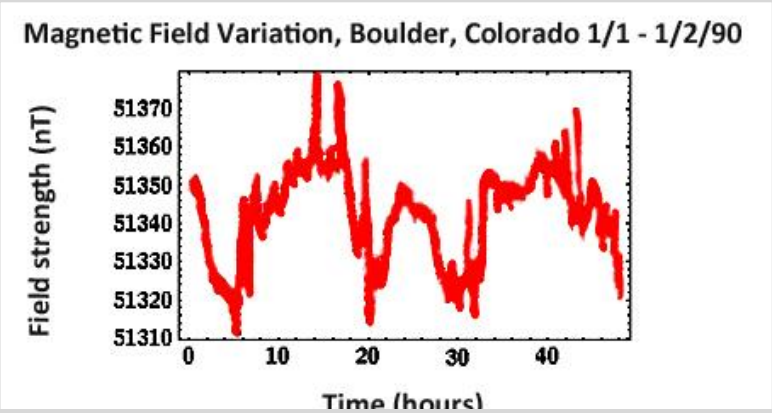

Figure 31: Diurnal field variation.

These variations may be small but for high accuracy MWD work especially at high latitudes, they may need to be corrected for. We now know that this effect is due to the rotation of the Earth and a varying exposure to the solar wind. The sun is constantly emitting ionized plasma in huge quantities across the solar system. These winds intensify during magnetic storms and the material can be seen on a clear night at high or low latitudes, being concentrated at the magnetic poles and forming the 'Aurora Borealis' and the 'Aurora Australis'.

During such storms the measurements taken from magnetometers and compasses are unlikely to be reliable but even in quiet times, the diurnal variation is always present.

✧

CONTENTS

5. Principles of MWD and Magnetic Spacing

5.1 Measurement While Drilling (MWD)

Figure 33: A non-magnetic drill collar.

MWD usually consists of a non-magnetic drill collar as in figure 33, containing a survey instrument in which are mounted 3 accelerometers, 3 magnetometers and some method of sending the data from these to surface.

Accelerometers measure the strength of the Earth's gravity field component along their axis. Magnetometers measure the strength of the Earth's magnetic field along their axis. With three accels mounted orthogonally, it is always possible to work out which way is 'down' and with three magnetometers it is always possible to work out which way is North (Magnetic). The following equations can be used to convert from three orthogonal accelerations, Gx, Gy and Gz (sometimes called Ax, Ay and Az) and three orthogonal magnetic field measurements, Bx, By and Bz (sometimes called Hx,Hy and Hz), to the inclination and direction (Magnetic).

$$I = \cos^{-1}\left(\frac{Gz}{\sqrt{Gx^2 + Gy^2 + Gz^2}}\right)$$

$$A = \tan^{-1}\left(\frac{(GxBy - GyBx)\ \sqrt{Gx^2 + Gy^2 + Gz^2}}{Bz(Gx^2 + Gy^2) - Gz(GxBx + GyBy)}\right)$$

In these equations the z axis is considered to point down hole and x and y are the cross axial axes. Some tools are arranged with the x axis downhole and y and z form the cross axial components so care should be taken when reading raw data files and identifying the axes. Similarly there is no consistency in units in that some systems output accelerations in gs, others in mg and some in analogue counts. Similarly the magnetometer outputs can be in counts, nano Teslas or micro Teslas.

The magnetometers are of various types but usually consist either of a coil with alternating current used to fully magnetise a core alternating with or against the Earth field component, or a small electro magnet used to cancel the Earth's magnetic field component.

The accelerometers are simply tiny weighing machines, measuring the weight of a small proof weight suspended between two electromagnets. Held vertically they will measure the local gravity field and held horizontally they will measure zero. In theory we could measure inclination with only one accelerometer but a z axis accelerometer is very insensitive to near vertical movement due to the cosine of small angles being so close to unity. Besides we also require the instrument to tell us the toolface (rotation angle in the hole).

If we want the toolface as an angle from magnetic north corrected to our chosen reference (grid or true) we use the x and y magnetometers and resolve tan-1(Bx/By) and if we want the angle from the high side of the hole we resolve tan-1(Gx/Gy). For practical reasons, most MWD systems switch from a magnetic toolface to a high side toolface once the inclination exceeds a preset threshold typically set between 3 and 8 degrees.

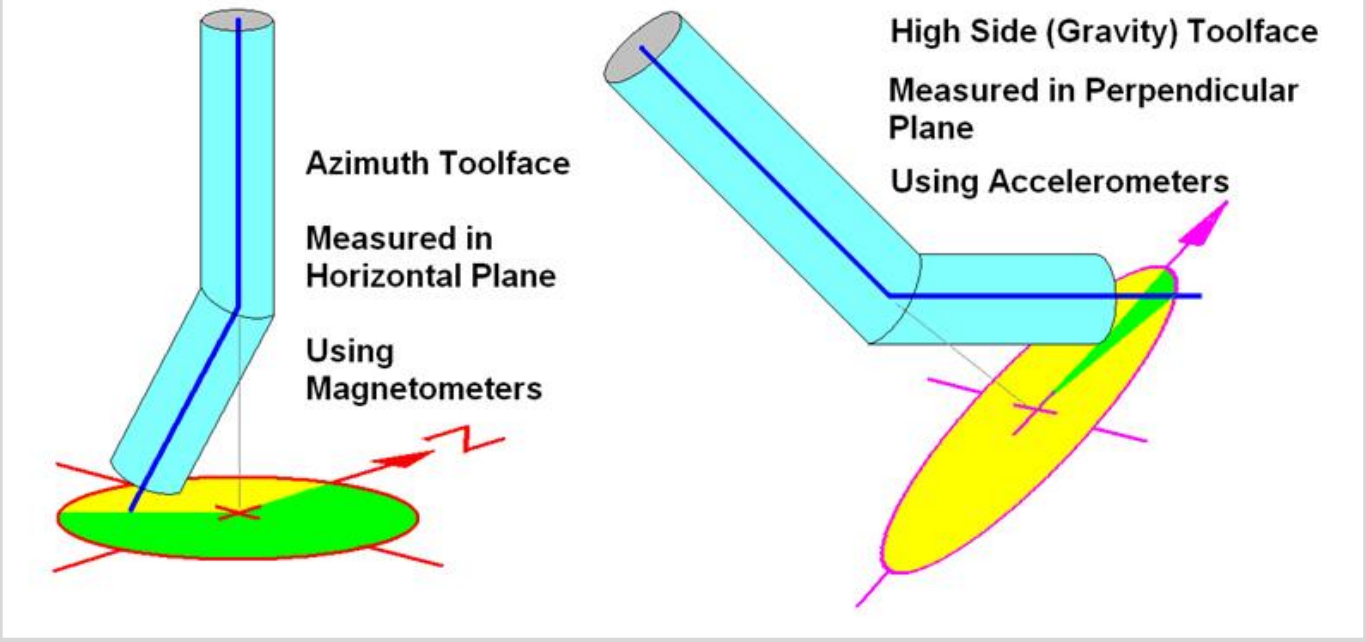

Figure 34: Graphical representation of two types of toolface.

5.1 Data Recovery

Most commonly, the technique used currently is to encode the data as a series of pressure pulses in the drilling fluid using poppet valves that will restrict the fluid flow to represent a one and release to represent a zero. This is known as positive mud pulse telemetry.

There are other systems which will open a small hole to the annulus to allow the pressure to drop for a 1 and recover for a zero. This is known as negative mud pulse telemetry. A third method is to generate a sinusoidal continuous pressure cycle onto which a phase modulation can be super-imposed to create a decipherable message signal. This is known as continuous wave telemetry.

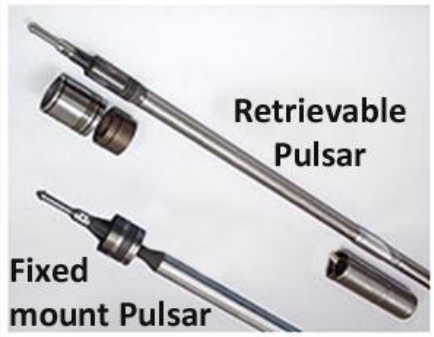

Figure 35: Pulse equipment.

The data is interpreted at surface and displayed in a surface display unit. Direction is measured from Magnetic North initially but usually corrected to either grid or true. Inclination is measured up from vertical and toolface, as mentioned, can be measured either as an Azimuth Toolface or a High Side toolface. In the picture below, the drilling tool is currently oriented on a gravity of toolface of 136^{O} right of high side.

Figure 36: Typical toolface display.

5.2 MWD Magnetic Spacing

Clearly, if we are to make use of magnetic sensors in an MWD tool, we need to ensure that there is sufficient magnetic isolation to avoid significant magnetic influences from the other drilling equipment.

The following explanation is included courtesy of Dr Steve Grindrod of Copsegrove Developments Ltd.

NON-MAGNETIC DRILL COLLAR LENGTH REQUIREMENTS

This section describes the theoretical background to drillstring magnetic interference, explains the origin of NMDC charts and makes recommendations on NMDC usage and inspection. This is based on [Reference CUR 252] (SPE 11382 by S.J. Grindrod and C.J.M. Wolff on Calculating NMDC length).

5.2.1 Drill String Magnetic Interference

The drillstring is a long slender metallic body, which can locally disturb the Earth's magnetic field. Rotation of the string and its shape causes the magnetisation to be aligned along the drillstring axis.
The magnetised drillstring locally corrupts the horizontal component of the Earth's magnetic field and hence accurate measurement of magnetic azimuth is difficult. For sensible magnetic azimuth measurement, the magnetic effect of the drillstring has to be reduced and this is done by the insertion of non-magnetic drill collars (NMDC) into the drillstring.

Non-magnetic drill collars only reduce the effect of magnetic interference from the drillstring – they do not remove it completely. An acceptable azimuth error of 0.25° was chosen based on Wolff and de Wardt (References CUR 443 and CUR 86) as this was the limit for 'Good Magnetic' surveys in their systematic error model. It should be noted that more recent work has suggested that magnetic interference azimuth error is likely to be of the order of 0.25 + 0.6 x sin (Inc) x sin(azimuth) so these values can be exaggerated at high angle heading east west.

By making assumptions about the magnetic poles in the steel above and below the NMDC, the expected optimum compass spacing to minimise azimuth error and the magnitude of the expected azimuth error can be calculated.

5.2.2 Pole Strength Values

Field measurements by Shell (Reference CUR 252) have been made of pole strengths for typical Bottom Hole Assemblies. These values are for North Sea area in Northern Hemisphere; these should be reversed for Southern Hemisphere. However, it should be noted that the polarity and intensity of magnetic interference is not easily predictable. In many cases the interference is mainly caused by the use of magnetic NDT techniques which of course have nothing to do with geographic location. The numbers suggested here are merely a guide and certainly not an upper limit.

Upper Pole
Drill collars up to + 900 µWb.

Lower Pole
Stabilisers and bit up to -90 µWb.
10m drill collar below NMDC up to -300 µWb
Turbines up to -1000, µWb

5.2.3 Azimuth Error

Drillstring magnetisation affects the observed horizontal component of the local magnetic field. A magnetic compass detects the horizontal component of the Earth's magnetic field. The drillstring induced error, ΔBz acts along the drillstring axis and this affects the east/west component of the observed field in proportion to (Sine Inclination x Sine Azimuth). This means that the compass error increases with inclination and with increased easterly or westerly azimuth of the wellbore.

5.2.4 NMDC Length Selection Charts

Using the formulae from SPE 11382 by S.J. Grindrod and C.J.M. Wolff, NMDC charts can be constructed for various well inclinations and azimuths and for a maximum acceptable azimuth error. The latter is taken as 0.25 degrees as the limit for good magnetic surveying practice. By varying the DIP and B for local conditions, charts can be prepared for various areas of the world.

An example chart for a bit and stabiliser BHA is given in figure 37:

The charts can be used in two ways.

1. To estimate the recommended length of NMDC for a particular situation.
2. If a different length was used, an estimate of the possible azimuth error can be obtained.

To find the recommended length of NMDC for a particular BHA, the azimuth from North or South and the inclination are used to arrive at a point on the selection chart. For example a section of a well being drilled at 60° inclination and 35° azimuth requires 24 m of NMDC.

This is demonstrated on the example chart above, with the 24 m being found by visually interpolating between the 20 m and 30 m length lines.

Where inadequate lengths of NMDC are used, (or when reviewing past surveys where insufficient NMDC was used) it is possible to estimate the resulting compass error: -

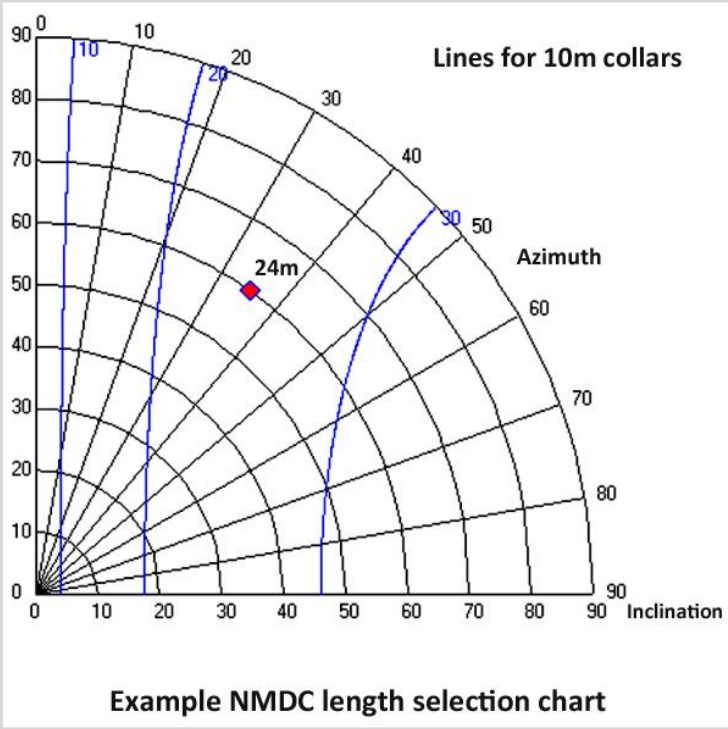

Figure 37: An example NMDC selection chart.

Possible Azimuth Error for length of NMDC used = Acceptable Azimuth Error x (Length required)^2 / (Length used)^2

Example:

If only 2 NMDC's with a total length of 18.9 m (62 ft) were used instead of the recommended NMDC total length of 24 m (69 ft) we have: -

Estimated possible azimuth error = 0.25 x (24)2 / (18.9)2 = 0.4 deg

Note that it is not valid to deliberately cut back on NMDC usage and plan to theoretically correct a survey by the above formulae. This is because the formula assumes pole strengths for the BHA components and actual pole strengths are not generally measured in the field.

CONTENTS

6. In-Field Referencing

6.1 Measuring Crustal Anomalies using In-field Referencing

The biggest source of error in MWD is usually the crustal variation. The global models such as the BGGM and HDGM can only take into account the longer wave length variations in the Earth Field and cannot be expected to allow for the localised effects of magnetic rock in the basement formations. In order to correct for these effects, the magnetic field has to be measured on site. From these local measurements, a series of corrections from a global model can be mapped out for the field so that in future years, the more permanent effect of local geology can be added to the secular effects for an up to date local field model.

IFR is a technique that measures the strength (Field Strength), direction (Declination) and vertical angle (Dip Angle) in the vicinity of the drilling activity to give the MWD contractor a more accurate reference to work to.

To accurately measure the magnetic field locally we can take direct measurements from the land, the sea or the air. On land, a non-magnetic theodolite with a fluxgate magnetometer aligned on its viewing axis, is used to measure the orientation of the magnetic field against a true north, horizontal reference from which accurate maps can be made. A proton or Caesium magnetometer is used to accurately the local field strength. In the air, only the field strength variations can be measured but if a wide enough area is measured at high resolution, the field strength data can be used to derive the effects on the compass and good estimates of the declination and dip angle can then be mapped. At sea, specialist non-magnetic equipment can be towed behind a vessel or carried on board a non-magnetic survey vessel with very accurate attitude sensors and magnetometers that output their data at high frequency and the motion effects are taken out in the processing.

6.1.1 IFR Survey Maps

Once the measurements have been taken, contoured maps are produced to allow the MWD contractor to interpolate suitable magnetic field values for use on his well.

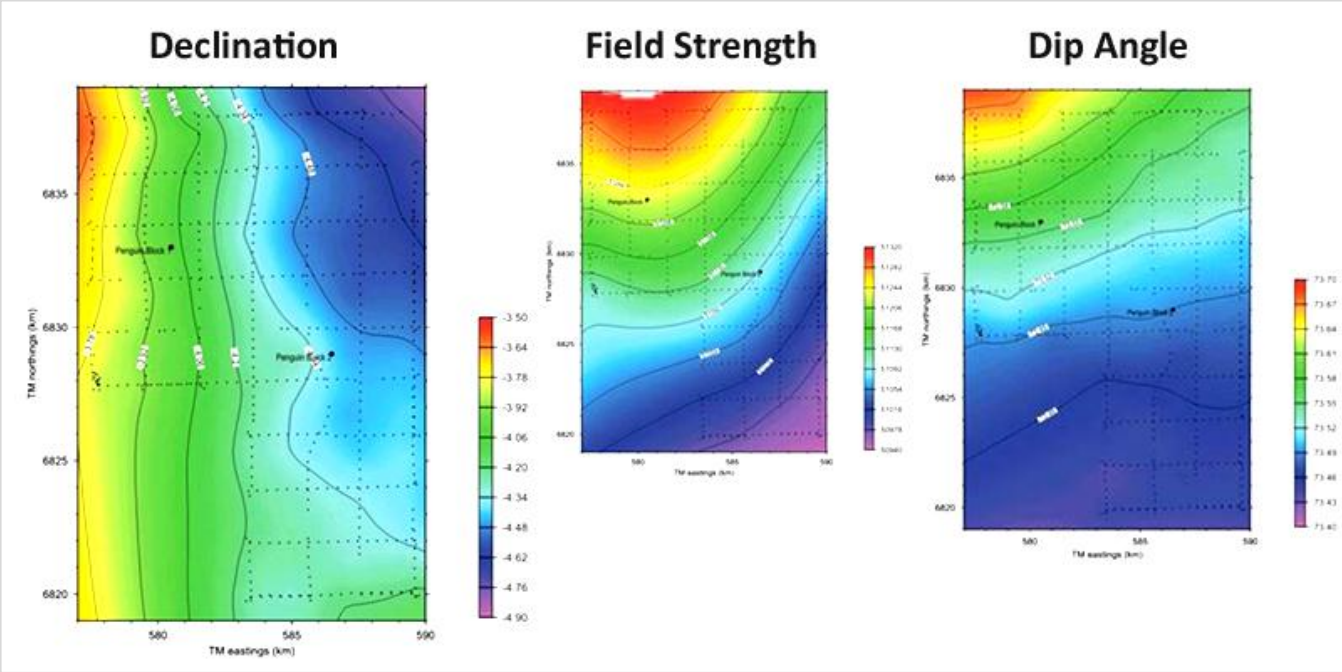

Figure 39: Examples of IFR survey results.

The IFR survey results are usually provided as digital data files which can be viewed with the supplied computer program. This allows the contractor to view the data and determine magnetic field values at any point within the oilfield.

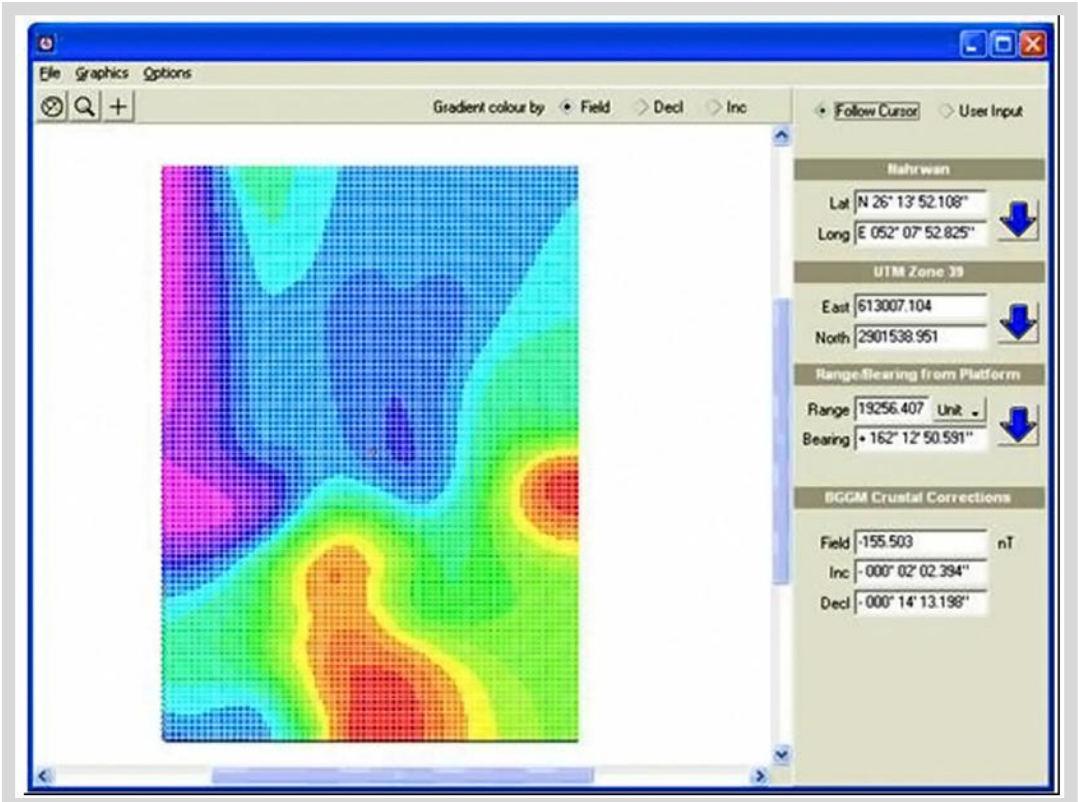

Figure 40: Typical software display of an IFR survey.

Two versions of the field maps are supplied. The first shows the absolute values of the total field, declination and dip angles, observed at the time of the IFR survey. The second set of maps shows how these values differed from the predictions of the BGGM model, due to the magnetic effects of Earth's crust in the oilfield. It is these crustal corrections which are used by MWD contractors.

The crustal corrections vary only on geological timescales and therefore can be considered to be fixed over the lifetime of the field. The BGGM model does a very good job of tracking the time variation in the overall magnetic field. By combining the BGGM model and the IFR crustal corrections, the MWD contractor obtains the best estimate of the magnetic field at the rig.

First, we use the BGGM model to get an estimate of the total field, dip and declination.
Then the IFR correction values for the background magnetic field are applied by adding the BGGM values and the corrections. i.e.

Total Field	**Tf = TfBGGM + TfCrustal Correction**
Declination	**Dec = DecBGGM + DecCrustal Correction**
Dip Angle	**Dip = DipBGGM + DipCrustal Correction**

In most cases, this just involves selecting the location of the rig and choosing a single set of crustal corrections. In some cases, when the magnetic gradients are strong, the MWD contractor may chose a different declination for each hole section along the wellbore. If the declination or dip value varied by more than 0.1 degrees, or the field strength varied by more than 50nT along the wellbore, it would be recommended to derive values for each hole section.

Note on Use of Error Models – see from chapter 17

Once IFR has been applied to an MWD survey, the contractor can change the error model applied to the survey to determine the uncertainty on its position. The Industry Steering Committee for Wellbore Survey Accuracy (ISCWSA) maintain industry standard error models for MWD that allow software to determine the positional uncertainty of the wellpath.

Normal MWD for example would have a declination error component of 0.36 degrees at 1 standard deviation but with IFR this is reduced to 0.15 degrees.

The effect of all this is to significantly reduce the uncertainty of the well position with all the benefits of the improved accuracy for collision risk, target sizing, close proximity drilling, log positional accuracy, relief well planning and so on.

Figure 41: Calibrating a marine observation frame on land & using a non-magnetic vessel for marine surveying.

6.2 Interpolated In-field Referencing

One solution to diurnal variations is to use a reference station on surface. In this way, the observed variations observed at surface can be applied to the Downhole Data which will experience similar variation. This is not always practical and requires a magnetically clean site with power supply nearby and some method of transmitting the data in real time from the temporary observatory. The other issue is establishing the baseline from which these variations are occurring in order to correct to the right background field values.

In a combined research project between Sperry Sun and the British Geological Survey, it was discovered that the diurnal and other time variant disturbances experienced by observatories, even a long way apart follow similar trends. The researchers compared observations made at a fixed observatory with derived observations interpolated from those taken at other observatories some distance away. The match was very encouraging and a new technique for diurnal correction was established called Interpolated In-Field Referencing or IIFR (not be confused with IFR discussed below). This technique is a patented method of correcting for time variant disturbances in the Earth's magnetic field but is widely used under licence from the inventors. The readings observed at the nearby stations are effectively weighted by the proximity to the drill site and the time stamped combined corrections applied to the Downhole observations either in real time or retrospectively.

LINK BGS - GeoMagnetic

✧

CONTENTS

7. Survey Calculation Methods

7.1 Examples of current methods

Over the years there have been several methods of calculating survey positions from the raw observations of measure depth, inclination and direction. At the simplest level if a straight line model is used over a length dM with inclination I and Azimuth A, we can derive a shift in coordinates as in figure 42.

This simple technique is often referred to as the Tangential Method and is relatively easy to hand calculate. However, the assumption that the inclination and direction remain unchanged for the interval can cause significant errors to accumulate along the wellpath.

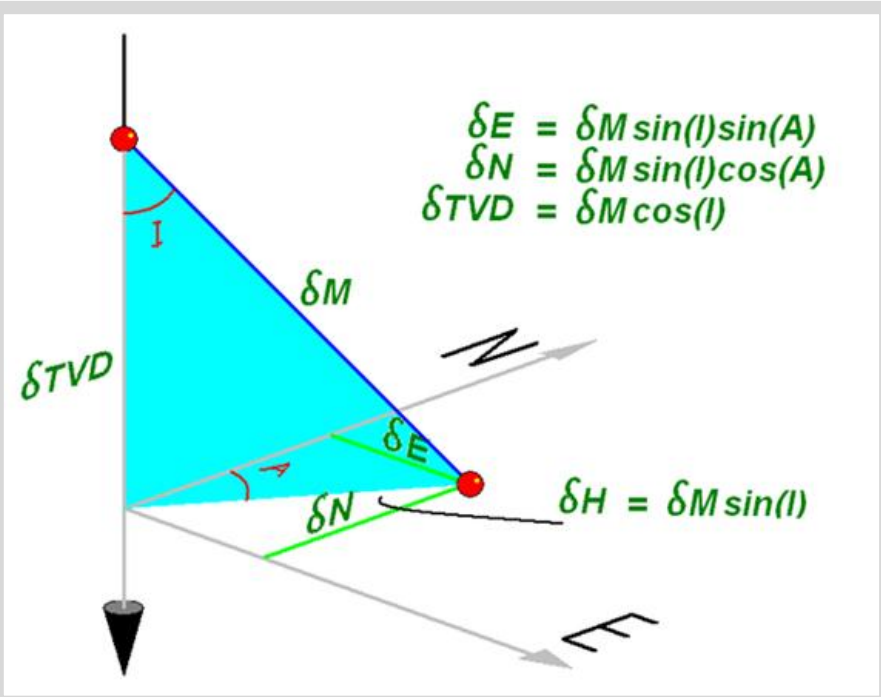

Figure 42: Tangential method to derive a shift in coordinates.

An improvement to this was the 'Average Angle Method' where the azimuth and inclination used in the above formulas was simply the average of the values at the start and end of the interval.

$$I = \frac{Inc1 + Inc2}{2} \qquad A = \frac{Azi1 + Azi2}{2}$$

$$\delta E = \delta M \sin(I)\sin(A)$$
$$\delta N = \delta M \sin(I)\cos(A)$$
$$\delta TVD = \delta M \cos(I)$$

Average Angle Example

- Md1 = 1000 Inc1 = 28 Azi1 = 54
- Md2 = 1100 Inc2 = 32 Azi2 = 57
- Delta MD = 100
- Average Inc = 30
- Average Azi = 55.5
- Delta East = 100 sin(30) sin(55.5) = 41.2
- Delta North = 100 sin(30) cos(55.5) = 28.3
- Delta TVD = 100 cos(30) = 86.6

A further improvement was the Balanced Tangential Method whereby the angle observed at a survey station are applied half way back into the previous interval and half way forward into the next.

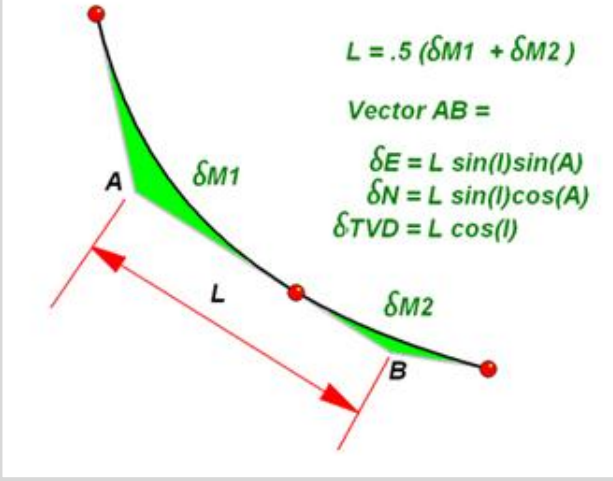

Figure 43: Balanced Tangential Method

These techniques all suffer from the weakness that the wellpath is modelled as a straight line. More recently, the computational ability of computers has allowed a more sophisticated approach. In the summary slide figure 44 we see two curved models.

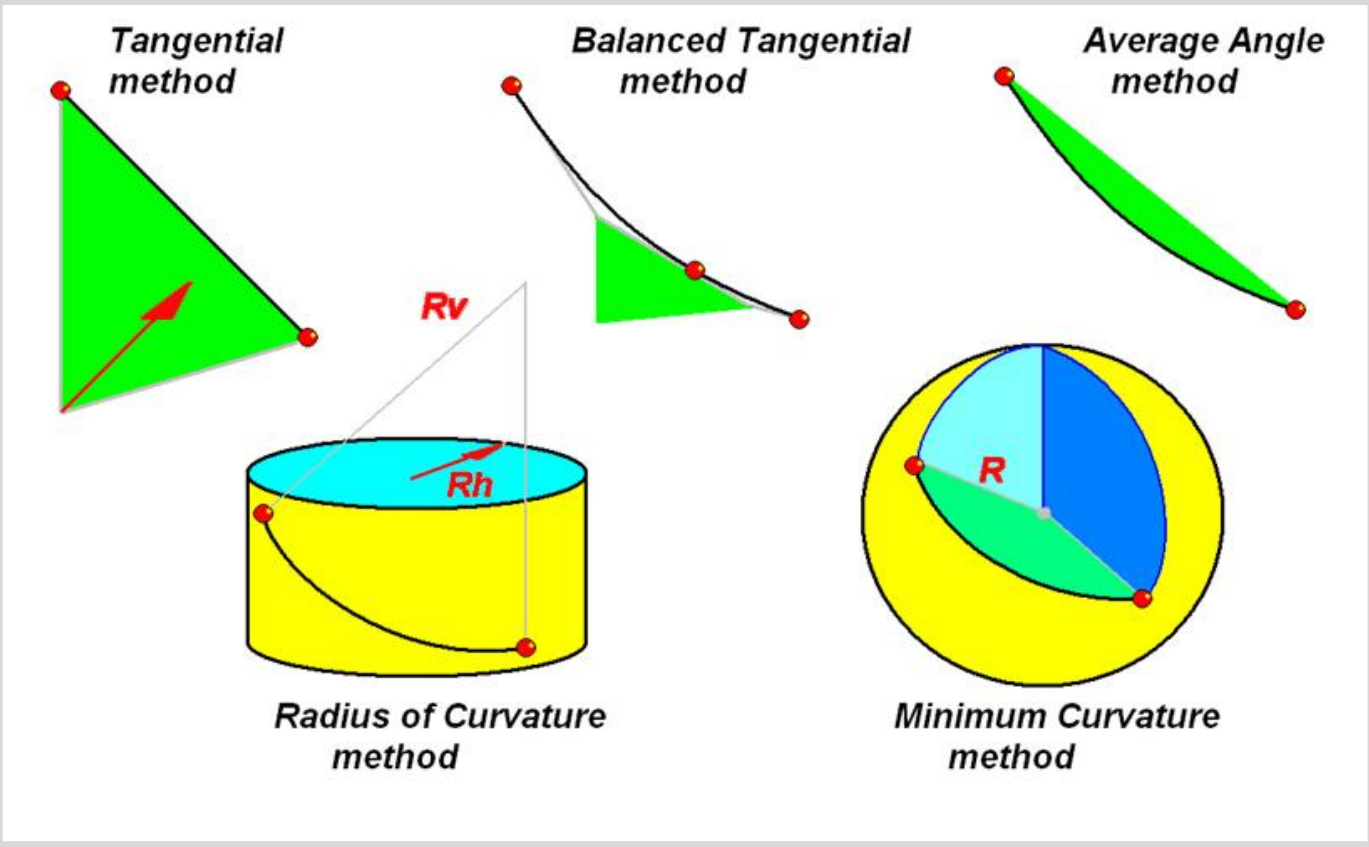

Figure 44: Methods of dealing with curvature.

The one on the left assumes that the wellpath fits on the surface of a cylinder and therefore can have a horizontal and vertical radius. The one on the right assumes the wellpath fits on the surface of a sphere and simply has one radius in a 3D plane that minimizes the curvature required to fit the angular observations. This method, known as the 'Minimum Curvature' method, is now effectively the industry standard.

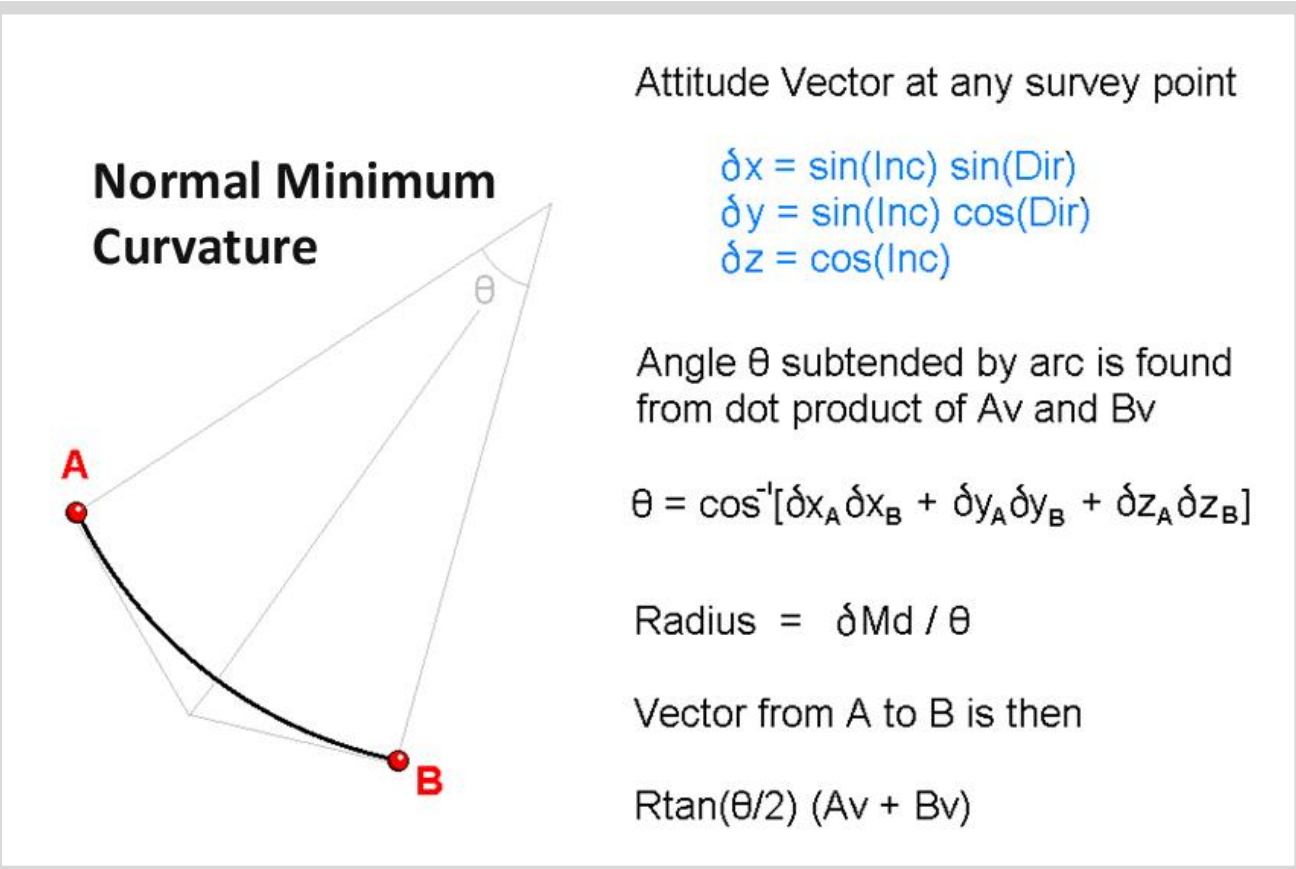

Figure 45: Minimum curvature method.

Imagine a unit vector tangential to a survey point. Its shift in x, y and z would be as shown above. The angle between any two unit vectors can be derived from inverse cosine of the vector dot product of the two vectors. This angle is the angle subtended at the centre of the arc and is assumed to have occurred over the observed change in measured depth. From this the radius can be derived and a simple kite formed in 3D space whose smaller arm length follows vector A then vector B to arrive at position B.

Notice however that the method assumes a constant arc from one station to the next and particularly when using mud motors, this is unlikely to be the case.

✧

CONTENTS

8. Survey Frequency

8.1 Determining TVD

Consider two possible procedures for drilling from A to B - both of these trajectories start and end with the same attitude and have the same measured depth difference.

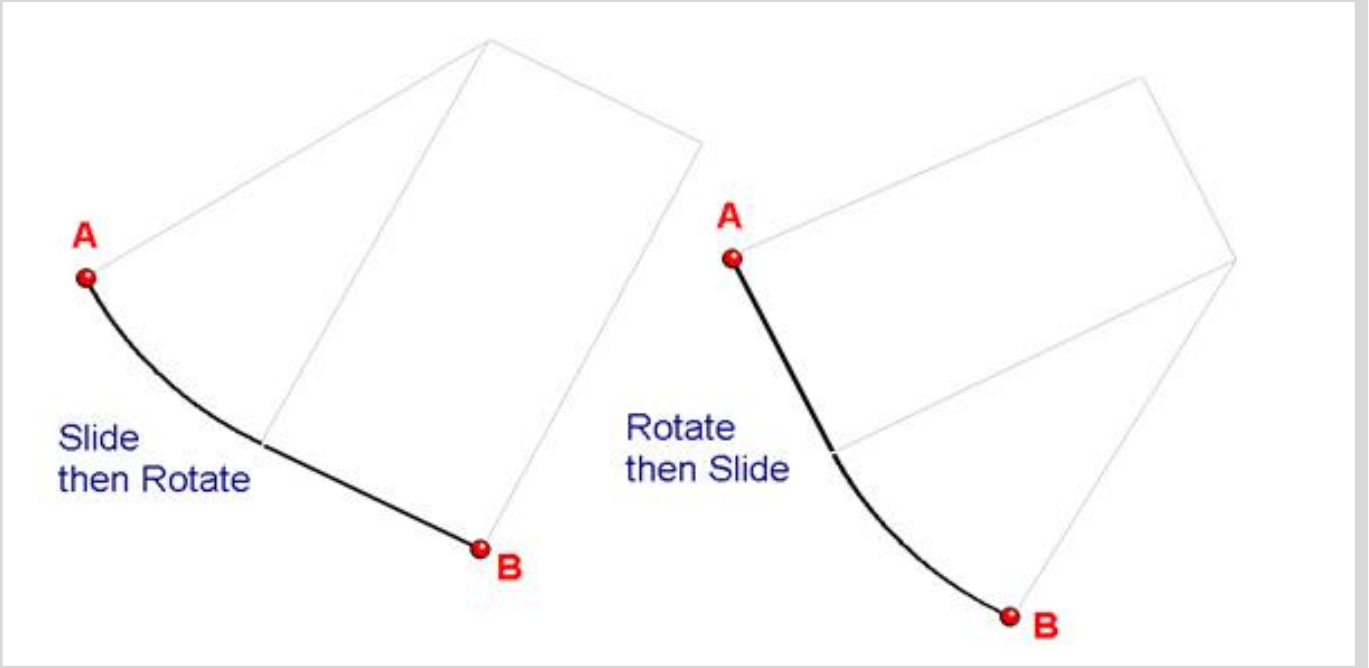

Figure 46: Example drilling trajectories.

Suppose we were at 50 degrees inclination at A and built to 60 degrees inclination at B. In the case on the left the curve comes first followed by a straight and vice versa on the right. Clearly the wellpaths are different but the surveys would be identical since the measured depths are the same, the azimuth has not changed and the inclinations have risen by 10 degrees. Because a single arc is applied, there is a potential for significant TVD error to accumulate along the wellpath if the changes in geometry are not sufficiently observed.

For this reason it is often recommended that when building angle faster than 3 degrees per 100 ft (or 30 m) it is best to survey every pipe joint rather than every stand to ensure adequate observations to truly represent the well path. In the next chapter it will be seen that a rate gyro can observe at very short intervals indeed with no additional survey time and in general these are better at determining TVD than MWD. Normally however, gyro surveys are interpolated at 10 or 20 ft intervals or equivalent just for ease of handling and processing the data.

Sometimes when a well is misplaced in TVD, it is necessary to re-analyse the MWD survey to obtain a better estimate of TVD. This is done by including the slide sheet information. The technique can only be used as a rough guide to the likely TVD adjustment required but has often explained poor production results or severe disagreement between gyro and MWD depths.

Using the slide sheet in figure 47 as an example:

BHA	Survey Depth	Incl. Degree	Azimuth Degree	Depth From	Depth To	Feet	Drill O/R	Tool Face / RPM	Drill Hrs.	WOB 1000#	PU,SO & ROT WT	Pump SPM	Flow Rate	Pressure OFF/ON	Comments Date	Bit to Survey
6	11519	82.8	177.3	11537	11559	22	R	50	1.25	10	165,155	94	230	3000/3120	28-Nov	40
6				11559	11573	14	o	10R	1.75	10	165,155	94	230	3000/3120	28-Nov	40
6	11551	82.2	176	11573	11591	18	r	50	1.50	10	165,155	94	230	3000/3120	28-Nov	40
6				11591	11615	24	o	15L	4.50	20	165,155	94	230	3000/3120	28-Nov	40
6	11581	83.7	175.7	11615	11621	6	r	45	0.75	5	165,155	94	230	3000/3120	28-Nov	40
6				11621	11639	18	o	hs	1.75	20	165,155	94	230	3000/3120	28-Nov	40
6				11639	11649	10	o	hs	1.25	20	165,155	94	230	3000/3120	29-Nov	40
6	11613	86.1	173.9	11649	11653	4	r	45	0.25	8	165,155	94	230	3000/3120	29-Nov	40
6				11653	11665	12	o	15R	1.25	20	165,155	94	230	3000/3120	29-Nov	40
6	11644	88.3	175.6	11665	11684	19	r	45	1.00	8	165,155	94	230	3000/3120	29-Nov	40
6				11684	11699	15	o	hs	3.25	20	165,155	94	230	3000/3120	29-Nov	40
6	11676	89.9	176.1	11699	11716	17	r	45	1.50	8	165,155	94	230	3000/3120	29-Nov	40
6	11707	90.4	176.2	11716	11747	31	r	45	3.00	8	165,155	94	230	3000/3120	29-Nov	40
6	11739	90.5	175.3	11747	11779	32	r	45	2.75	8	165,155	94	230	3000/3120	29-Nov	40
6				11779	11785	6	o	70R	1.00	8	165,155	94	230	3000/3120	29-Nov	40
6	11771	90.5	175	11785	11811	26	r	45	2.75	8	165,155	94	230	3000/3120	29-Nov	40
6				11811	11843	32	r	45	3.50	8	165,155	94	230	3000/3120	29-Nov	40
6				11843	11851	8	o	50R	2.00	8	165,155	94	230	3000/3120	30-Nov	40
6				11851	11872	21	r	45	1.75	8	165,155	94	230	3000/3120	30-Nov	40
				11872	11390	-482				8	165,155	94	230	3000/3120	30-Nov	43
8				11390	11402	12	o	65L	12.50	8	165,155	94	230	3000/3120	12-Dec	37
8				11402	11421	19	o	45L	9.00	8	165,155	94	230	3000/3120	13-Dec	37
9				11421	11426	5	o	65L	2.00	8	165,155	90	230	3000/3120	15-Dec	37

Figure 47: Typical slide sheet.

Looking at the data for BHA 6, we can see a few points where surveys were taken and several changes from rotating to oriented (sliding) mode. The lengths and toolfaces are listed for each slide. Whilst these values will only be approximate it is possible to then estimate the wellbore attitude at the points where the slides began and ended.

Firstly if we take the total curvature generated over the BHA run by measuring the angle changes between surveys (see minimum curvature described above in chapter 7) we can work out the dogleg severity capability of this assembly. If we then apply that curvature on the toolfaces quoted, it is possible to determine a fill in survey at the beginning and end of each slide by using the approximation that the inclination change will be:

DLS x length x cos(Toolface) and the azimuth change will be the DLS x length x sin(Toolface) / sin(Inclination)

- where DLS means dogleg severity in degrees per unit length. This allows us to complete surveys at the start and end of each slide and minimum curvature will then be more valid when joining the points.

This assumes that:

1. The DLS is unchanged during the run
2. The curvature all happens when sliding
3. The toolface was constant during the slide

These assumptions are very simplistic but the analysis will generally give a better idea of TVD than the assumption that the sparse surveys can be safely joined with 3D constant arcs.

✧

CONTENTS

9. Gyro Surveying

9.1 Background and History of Gyros

What is a Gyro?

A Gyroscope is a device which enables us to measure or maintain an orientation in free space and rotor gyros specifically, operate on the principle of the conservation of angular momentum. The first gyros were built early in the 19th century as spinning spheres or disks (rotors), with designs incorporating one, two or three gimbals, providing the rotor spin axis with up to three degrees of freedom. These early systems were predominantly used within the academic community, to study gyroscopic effects as rotor speeds (angular momentum) could not be sustained for long periods, due to bearing friction effects. The development of the electric motor overcame this rotation decay problem and lead to the first designs of prototype gyrocompasses during the 1860's.

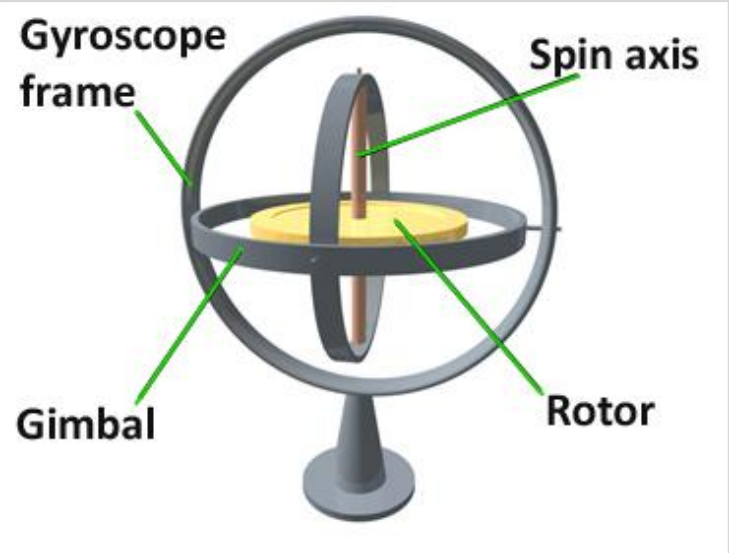

Figure 48: Representation of a basic gyrocompass.

As with most scientific and technology advances, continued development and refinement was propagated and accelerated to address military applications and by the early 1900's gyros were being used in many attitude control, orientation and navigation applications. Rotor gyros are still by far the most common system used by the oil industry.

During the second half of the 20th century several additional technologies were developed and exploited providing gyroscopic capabilities. These included:

- Vibrating Gyros
- Hemispherical Resonator Gyros
- Quartz Rate Sensors
- MHD Sensor
- Fibre Optic Gyros
- Laser Gyros
- MEMS Gyros

The systems currently considered to have the most potential for the oil industry are the Laser and MEMS systems. Indeed, *Inteq* developed and successfully marketed and operated the highly accurate RIGS (Ring-Laser Inertial Gyro Surveyor) for many years servicing the North Sea. The current performance capability of the MEMS unit is still less than desired but is regarded as having potential for the future.

9.2 Oilfield Applications – A Brief History

In the early years of oil well drilling the process of drilling the borehole was more of an art than a science. The general principals of geology and exploration were understood and followed but the effects of formation changes and dip on bit deflection and hence borehole trajectory were not clearly understood and largely ignored. This perpetuated state of ignorance lead to many unresolved lease disputes, where wells drilled and brought on stream, close to an adjacent lease, would often result in diminished production rates on the adjacent lease wells. However, as now, wells already in production were cased and the magnetic compass based survey instruments available, could not provide post completion trajectory data. Throughout this time, many inclination-only devices were developed, later versions of which were accurate to 1 or 2 degrees throughout their operating range.

In 1928 Alexander Anderson published a study of Borehole Survey Inclination Data obtained from a significant population of wells from various locations. Anderson had developed a Pendulum Instrument, the position of which was recorded on film as the tool was lowered in the borehole. This publication, illustrating universal and significant wellbore deviation, brought focus on the extent of the problem within the industry. As a direct result of Andersons study, J. N. Pew, then the Vice President of Sun Oil Co. instructed a team of Engineers working out of the Sun Research Laboratory in Dallas, to design and develop instruments which would provide the Inclination of the borehole and the Direction of that Inclination within casing. The 5.5" SURWEL Gyro Instrument incorporated a Gyro Compass Face superimposed over a Bubble Level Unit with the permanent record obtained with a Camera.

The Sperry Gyroscope Co. was chosen as the Gyro supplier and with each company holding a 50 per cent stake in the new company, the Sperry-Sun Well Surveying Company was formed and gyro referenced borehole surveying became a reality on 9th October 1929.

9.3 Chronology of gyro development

1920's: Several designs of Inclinometers and very basic Magnetic Compasses are in use. Companies of note operating Directional Survey Services are H. John Eastman, Hewitt Kuster and Alexander Anderson.

1929: First Gyro Survey Tool designed and built by Sperry-Sun Well Surveying Company, a joint venture between Sun Oil and Sperry Gyroscope Co. The gyro had a DC Rotor speed of 14,000 RPM and was 5.5"Dia.

1930: Gyro Survey Tool Data used in settlement of many Lease Line violation cases in East Texas and California. In-Run and Out-Run Data were recorded.

1936: Gyro Tool Intercardinal Error and Drift Curve Corrections, refined to improve accuracy of survey data in inclined boreholes.
Survey Tool True Centre Correction methodology developed using a two dimensional Polar Coordinate System Calculation.

1939: 1st K Monel Non Magnetic Drill Collar designed (Not a gyro but notable)

1945: Humphrey (Gyro) provides Instrumentation to Directional Service Companies for the first time (Post WW11 manufacturing surplus)

1947: Transistors developed but not yet used by industry.
Sperry-Sun buys out Sperry Gyroscopes interest in Sperry-Sun Well Surveying Company.

1950's: By late 1940's wellbores get deeper and smaller with 5" Casing frequently used necessitating a requirement for smaller Gyro Tools.

1960: East Texas Railroad Commission Scandals again encourage tool development. Many wellbores are small diameter (5" Casing) and some have > 65 deg Inclination.

1961: Use of Solid State Electronics for first time in Instrument Timers and Solenoids for Film Advance mechanisms. Computers used for Survey Calculations at the Office. Field Data continued to be hand calculated until mid-seventies.

1961: Atomic Energy Commission (AEC) in the USA uses Gyro Survey Tools in 4" – 144" Dia. Test Holes, drilled 800 – 6000 ft deep, in Nevada and Alaska. Project ends in 1976.

1962: 3" Dia. Surwell Gyro built utilizing 40,000 rpm AC Rotor.

1964: Counter Claims made against Gyro Survey accuracy related to numerous Law Suits. A Test Pipe is laid down the Hurricane Messa in Utah. Over 2000ft of Aluminium Irrigation Pipe is fixed down the hillside on a continuously irregular course. The first 200ft was near vertical with sections of the pipe path reaching 60-70 degs of inclination. Multiple surveys were performed with both Gyro and Magnetic tools, with surveys taken

at 25 ft intervals. In the final analysis the accuracy of both Survey Systems were proven and the East Texas Claims Issues finally settled.

1.75" Gyro Tools developed using 26,000 rpm AC Rotors. Specifically designed for Directional Drilling Tool Orientation and surveying of Production wells in Tubing.

1971: Atomic Energy Commission Test Bore intersected at 6000 ft TD with Bottom Hole location land surveyed in at < 5 ft variance/error.

1974: Multi-well Platform drilling is prevalent. Level Rotor Gyro System developed with glass file Mercury Switch used to control the inner gimbal horizontal position to +/- 1-2degs but system is sensitive to gimbal/switch attitude, resulting in azimuth error propagation.

1977: Introduction of Surface Recording Gyros (SRG's - 3" and 1.75" versions), transmitting data to surface via Wireline. Inner gimbal position now monitored and controlled by electronic resolver to +/- 0.01 degs resulting in significantly reduced error propagation.

1978: Ferranti Full Inertial System introduced into the North Sea as reconfigured Harrier Jump Jet IN System, developed for Shell, Mobil, BNOC (BP) and marketed by Eastman Christiansen (Inteq). Proven Accuracy < 1/1000 ft potentially at all attitudes.

9.4 Improving Performance and Service Capability

As outlined above, Gyro Survey Tools were initially and primarily introduced into the industry, to provide a means of obtaining or checking borehole attitude, when the wellbore was already cased, negating the application or repeated use of magnetic based tools (Lease Scandals). Similar conditions were to foster the requirement for reduced diameter tools when later legal argument ensued over deeper smaller diameter wells. However, the primary motivation for technology advancement has been the requirement to survey ever deeper, higher angle boreholes (beyond horizontal), with significant azimuthal change at greater latitudes.

The first gyros used by the industry had no means of inner gimbal/spin axis control but the surveyor could determine its approximate position from the film record at each survey station. These gyros were originally intended for use up to 20 – 30 degs inclination. However, as borehole inclinations increased, hardware improvements were made and operational techniques were developed which enabled these tools to be used successfully beyond 60 degs inclination. As noted above, Gimbal Tilt control and Drift Curve correction methods were refined to better account for the increasingly difficult operating conditions encountered and its interactive effects on gyro stability and data quality at a relatively early stage.

9.5 The Gyro Survey Process

9.5.1 Surface Reference Orientation

Prior to the use of North Seeking Gyros the gyro had to be 'Referenced' and set to a known bearing at surface (On the rig floor) before entering the borehole. On land, this was a relatively simple process involving the establishment of a Sight Mark or Back Sight (Reverse Sight), from a distant mark clearly visible from the rig floor through the Sighting Scope oriented and attached to the Survey Tool in line with the internal Gyro Compass Reference. This Land Sight Mark was on occasion provided by the client, using the land survey company responsible for locating the rig but was often determined by the well survey company, using conventional land survey techniques and a Magnetic Brunton Compass. For low angle wells the gyro reference was then set to the Grid or True North orientation (dependent on the client requirements).

For offshore locations this observed and required Sight Reference had either to be pre-established (for each Slot Position) relative to Platform Centre or calculated using distant installations or features visible from the rig floor rotary. If/when no feature was visible from the rig floor the Sight Orientation Reference would be transferred from a position external to the rig floor (e.g. Helideck).

These techniques were also applicable to semi-submersible (floating) installations, with the added complication that the sight reference value might be subject to small but constant change. As a last resort the rigs Ships Compass Heading value would be used. This mobile condition had implications for both the start and end reference for the survey and its effect on Drift Curve closure and survey reference accuracy.

When setting the Gyro Orientation Reference for higher inclination surveys the gyro would be set with the spin axis perpendicular (oriented across) to the wellbore path, with due account taken of the expected gyro drift rate and any change in the wellbore azimuth trajectory. Setting the spin axis in this attitude, provides the most stable orientation for gyro operation as the gimbals tilt with inclination and reduces the potential for Gimbal Lock (System Bearing Jam) and subsequent gyro spin out and survey miss-run. The offset reference orientation value (relative to True or Grid North) applied in this technique was accounted and corrected for by applying a baseline shift to the calculated Drift Curve.

9.5.2 Gyro Drift – Precession Correction

The vast majority of gyro surveying performed for the industry, even today, still utilises rotor systems. A spinning gyro rotor tends to keep its axis pointing in the same direction. This is called Gyro Rigidity. If a force is applied which tends to change the direction of the spin axis, the axis will move at right angles to the direction of the applied force. If the spin axis is horizontal and you try to tilt it, the axis will turn. If the axis is horizontal and you try to turn it, the spin axis will tilt. This second characteristic of a gyro is called Precession.

In normal operational use, conditions such as bearing wear, Temperature Coefficients of Expansion (Inertial Mass Distribution – C of G) and System Attitude Change (related to a given well profile) all interact to generate a net force which acting on the Gyro Spin Axis cause the gyro to precess (drift from its initial orientation reference).

The gyro precession experienced during a survey has historically been corrected with a Drift Curve constructed with drift data samples recorded during the in-run and outrun survey. The frequency and duration of drift checks has tended to change over time but the basic premise has always been to take samples related to time, attitude change and temperature (particularly for deeper, hotter surveys). Drift checks were normally taken at least every 15 minutes, for a sample duration of 5 minutes with film systems. However, with the introduction of later Vernier scale readings, SRG and digital data, sampling criteria tended to change to 10 minute intervals with 3 minute sample duration.

Drift Checks during the survey were no longer relevant or required with the advent of earlier discreet sampling North Seeking Systems (more later). However, they are beneficial and recommended when operating the current North Seeking Systems in continuous Dynamic Mode where the individual or calculated survey sample stations are not determined by discreet north seek sensing.

The drift correction data is then either applied on its own or as a super set to the Gyro Calibration Model (current systems). The calculated real-time drift correction curve is tied and closed to the start and end reference data, be it a sight observation or north seek reference as in current technology systems.

9.5.3 True Centre Correction (or Offset Centre Correction)

From an early stage it was recognised that a gyro survey tool had inherent misalignments associated with the modular structure of the Instrument Stack and more particularly the vane type centralization (Weatherford) which was universally adopted for running in both open and cased hole. These centralizers were not a precision piece of manufactured equipment and variants of this centralizer design, all be it with improved centralization capability, continue to be used today for some applications. These misalignments result in small errors in both the inclination and azimuth values calculated and recorded for each survey point.

In 1936 the Sperry-Sun Well Surveying Company developed a ‘True Centre Correction’ methodology which still forms the basis of current applications. The ‘true centre’ and ‘corrected values’ are calculated using a Polar Coordinate Method by representing each Station data set as a radial and angular coordinate. Provided sufficient tool rotation has taken place between the in-run and out-run samples, the common intercept of each sample vector pair denotes the True Centre Correction Value which can then be applied to each individual survey sample. True Centre Correction is particularly important in shallow, low angle, multi-well applications where small errors in Inclination can seriously misrepresent current well position and hence adjacent well displacement.

9.5.4 Tool Centralization

Gyro Tool Centralization or Decentralization within the cased borehole remains a fundamental and important aspect of all gyro surveys performed. This applies equally to the limited number of surveys still carried out using older technologies as well as those performed with the latest systems inclusive of full inertial applications.
As noted above, earlier forms of Spring Bow (Weatherford Type) centralizers could contribute significantly to errors in true borehole axis representation. Early attempts at offset calculation and correction did provide a partial solution but this improvement was also dependent on the centralizer integrity with respect to uniform vane wear and varying borehole inclination. As now, the main dilemma was to use centralization which adequately supported the tool in the central axis whilst allowing the system to smoothly progress down hole, keeping in mind the loss of effective mass (α Cos incl.) in the borehole axis to aid transport and the simultaneous increasing mass supported by the centralizers.

Ultimately, the most effective and practical solution was to run full centralization until the tool could be guaranteed to run low-side. However, dependent on the casing/survey program deployed, this procedure could require a minimum of two separate runs in hole in which the second run was performed with very stiff (rigid) under gage centralization which basically operated as skids and supported the tool at a fixed constant distance from the contact low-side and hence parallel to the borehole axis.

As wellbore inclination increased, various forms of Sinker Bar were used to aid tool transport but these too could generate off-axis problems where the Sinker Bar is screwed directly to the survey tool but not adequately supported (centralized), with a tendency to bias the overall tool alignment. Ideally, Sinker Bar should be attached to the survey tool using a universal joint or more preferably a connecting rod with universal joints at each end. This hook-up predominantly isolates any off-axis interaction between tool and weight bar.

These basic criteria still hold true today where the use of Centrollers (Precision Wheeled Centralizers) and Roller Bearing De-centralizers are used with North Seeking and full Inertial Gyro Tools in cased boreholes up to ≈ 70° inclination.

Ideally the use of De-centralizers should be avoided where possible, in large surface casings near vertical as tool alignment can be disturbed by the effects of off-axis cable tension. Similar problems can exist in the early build or high dogleg sections within smaller casings.

9.6 ERD and Horizontal Transit

With the prevalence of ERD and Horizontal Well Profiles, gyro surveying became even more difficult to perform by conventional wireline operations. Various techniques were adopted with improvements made relative to technology advances in both assisted tool transport and survey tool development.

Side-Entry Sub:– The Side-Entry Sub was first used with the Magnetic W/L Steering Tool Systems (Pre MWD) in order that drilling could proceed during deeper drilling operations without the requirement to trip out the W/L – Steering Tool from the drill pipe to make a connection (Add Pipe). Using this system enabled W/L Gyro Surveys to be performed in extended reach horizontal wells, with the survey tool latched within the BHA and surveys recorded at each planned depth interval.

The Side Entry Sub consisted of a sub with a side wall orifice with associated clamp and stuffing gland arrangement which allowed the cable to pass through the sub wall with the clamp and gland seal applied as required. The BHA/drill pipe would be tripped in hole to the high angle survey start depth. The W/L and survey tool would then be run to bottom within the pipe entering via the side wall sub connected to the drill pipe at surface. The survey would then commence by tripping in hole to TD with pipe added as normal. The assembly was then tripped out (with outrun data also recorded) to retrieve the Sub at surface with the W/L Tool then pulled out of hole. The system was subsequently applied to W/L FE logging prior to equivalent MWD sensor development.

9.7 Ring Laser Gyro

Ring Laser Gyros (RLGs) are a form of optical rotation sensor and unlike the preceding mechanical rotor systems, contain no moving parts, in their simplest form. Within the sensor, containing a machined quartz block, two laser beams are formed, one moving clockwise and the other anti-clockwise around an enclosed polygonal optical path loop of three, four or more sides with mirrors at the vertices. These laser beams interfere with each other, creating a standing wave(s) diffraction pattern observed by a photo-detector located at one of the vertex mirrors. This is a little like dropping two stones into a still pond, where the waves from each stone meet and form a pattern of waves with even higher peaks and lower troughs where they cancel out.

If the device is rotated, one beam experiences a shift up in frequency, whilst the other experiences a shift down, causing the interference pattern to move. As the device rotates the vertex photo-detector counts the fringes and hence measures the rotation of the sensor. This relativistic phenomenon, is known as the Sagnac effect after G. Sagnac (Frenchman) demonstrated and recognised the condition whilst conducting experiments to detect “the effect of the relative motion of the ether” (1913). Related experiments were also conducted by F. Harress in 1911 but his results were misdiagnosed at the time and attributed to “unexpected bias”.

Typically, a RLG consists of a triangular block of low-expansion quartz. The laser cavity is machined into the glass and filled with He & Ne creating an HeNe laser. A high voltage is applied across areas of this cavity to create the lasing action. At two points of the triangle, very high quality mirrors are placed and at the third vertice the beams are combined in a prism to produce the interference pattern which is detected by a photodiode array. Typically RLG size is around 8cm on a side.

The sensitivity of a Ring Laser Gyro is proportional to the area enclosed by the laser beams and the scale factor of the instrument depends on the ratio of the enclosed area to the path length. RLGs can be extremely accurate devices and can measure a range of rotations from as low as 0.01 deg/hr to more than 360 deg/s. This gives them an enormous dynamic range, of as much as 109. They have excellent scale-factor stability and linearity over this range. Gyros performance is typically quantified in terms of bias stability and random walk. RLG can have bias levels of 0.01 deg/hr and random walks of 0.005 deg/rt (hr).

To ensure good sensor performance and bias stability the devices must be built in a high standard cleanroom, since any contaminants in the laser cavity will degrade performance. They must be machined from glass blocks with very low coefficient of thermal expansion to ensure that performance is maintained over a wide thermal range. The use of thermal shielding is essential for deeper oilfield applications.

RLGs suffer from a problem known as ‘lock-in’ where back scatter from the laser beams at a mirror causes the interference fringes to ‘lock’ together, giving the sensor a dead band, with no output at very low rotation rates. To minimise lock-in, extremely high quality mirrors are used. Also, typically the sensors are mechanically ‘dithered’, that is, vibrated rapidly and precisely through the dead band. It is small remaining periods in the dead band which causes the random walk performance of the sensor to deteriorate.

Ring laser gyros are very commonly used in inertial navigation systems in both civil and military aircraft, rocket launchers, tanks, artillery and high accuracy attitude systems, such as those used for geophysical surveys from the air.

RLG’s have only been utilised in one borehole survey system within the oil industry to-date. The RIGS Tool was developed by Sundstrand for Eastman Whipstock (Later to become part of Eastman Christiansen, Eastman Teleco and then Baker Hughes INTEQ). The Inertial Measurement Unit for a second generation RIGS was manufactured by Honeywell. The Tool was 5 ¼” in diameter, 14 ft long in standard configuration with a temperature rating of 100°C. A thermal shield allowed RIGS to survey to TD in wells with bottom hole temperatures of up to 150°C. The RIGS Tool demonstrated consistent lateral accuracy performance of 1-2 /1000 MD (2 sigma) at all attitudes. However, the tool was only ever operated within the North Sea Region. It was in commercial service from 1990 to 2006.

The main drawback of currently available RLGs is their relatively large size, which limits their use to >5” dia. Sonde Tools operating within >7” casings. The sensors commercially available have a temperature limitation of around 90 deg C. RLG technology is also currently covered by international arms trafficking laws and associated import and

export restrictions which severely restricts product placement, R&M and Tool Utilization for any potential global operation by a service company.

9.8 Fibre Optic Gyro

Fibre Optic Gyros (FOGs) consist of a coil of fibre optic cable in which two light beams travel through the entire cable length in opposite directions and are then combined. The development of low loss, single mode, optical fibre in the early 1970's, enabled Sagnac effect fibre optic gyros to be developed. The sensor operates on a similar principle to the RLG, where the interference pattern created from the counter-propagating light waves, after travelling through the fibre, is a measure of the angular rotation of the device. However, they differ in that an incoherent broadband light source is used.

Fibre optic gyros tend to be packaged in cylindrical containers, for example 10cm diameter by 2.0cm deep. A sensor may contain as much as 5 kilometres of fibre. FOG sensitivity is a function of coil radius (enclosed area) and optical path length, so once again larger sensors tend to be more accurate sensors.

FOG performance in general, is similar to but not quite as good as RLG. Bias stabilities of 0.1 deg/hr or better and random walks of 0.005 deg/rt(hr) would be typical. RLG has inherently better scale factor stability.

Outside of the oilfield, FOG sensors tend to be used for similar applications to RLGs, but for those applications where environmental conditions and accuracy is less important and where cost is a factor. Although experimental devises have been developed, no FOG system has been commercially marketed within the oilfield. Once again sensor size and temperature concerns are limiting factors. In general FOG performance is more sensitive than RLGs to environmental conditions such as shock, vibration and temperature gradients.

Large diameter, high accuracy systems have been developed and are in use in space and submarine applications, where size restrictions are secondary.

9.9 Vibrating Structure Gyroscope

Coriolis Effect

The Coriolis Effect is an inertial force first described by the 19th century French engineer-mathematician Gustave-Gaspard Coriolis in 1835. Coriolis showed that if the ordinary Newtonian laws of motion of bodies are to be used in a rotating frame of reference, an inertial force – acting to the right of the direction of body motion for counter clockwise rotation of the reference frame or to the left for clockwise rotation – must be included in the equations of motion.

The effect of the Coriolis force is an apparent deflection of the path of an object that moves within a rotating coordinate system. The object does not actually deviate from its path, but it appears to do so because of the motion of the coordinate system. A simple demonstration example of the effect is a ball rolling across the surface of a rotating merry-go-round.

9.10 Coriolis Vibratory Gyros (CVG)

A Coriolis Vibratory Gyro (CVG) operates on the principal that a vibrating object (mass) tends to keep vibrating in the same plane as its support is rotated in space. This type of device is known as a Coriolis Vibratory Gyro where the plane of oscillation of a proof mass is rotated, the orthogonal response resulting from the Coriolis term in the equations of motion, is detected by a pickoff transducer.

CVGs have been produced in various forms, including the original Foucault pendulum (1851), vibrating beams, tuning forks, vibrating plates and vibrating shells. In the Foucault pendulum (non-commercial), the swing path of the pendulum rotates a fraction of the Earth's rotation, dependent on the location latitude. Due to friction effects in the mounting fixture, some of the energy is transposed into quadrature effects, so that the pendular path becomes

elliptical and theoretically, ultimately circular, negating the angular measuring capability of the system. This unwanted quadrature effect is present in the majority of CVG designs and necessitates quadrature suppression control loop electronics, signal processing and compensation.
Two CVG systems show potential [Tuning Fork Gyro (TFG) and the Hemispherical Resonator Gyro (HRG)] and these sensor developments are continuously kept under observation by the industry.

9.10.1 Micro electro mechanical System (MEMS) – Tuning Fork Gyro

A typical MEMS-TFG incorporates a single or dual (contra – mass-balanced) tuning fork (Proof Mass) arrangement, integrated on a silicon chip. Capacitive measurements are made between the fork tines (Proof Mass) as they contort relative to device rotation (Coriolis Effect). Current fabrication and manufacturing techniques enables the production of very small sensor devices with proof mass size typically only 1-5 mm. However, even the best commercially available MEMS gyro struggles to reach a bias performance of 1 deg/hr, with units in associated defence developments approaching 0.3 deg/hr. Oilfield applications requires the sensor have a performance capability within the range 0.1-0.01 deg/hr.

MEMS Gyros have to-date found a wide market in low performance applications. They are used in cars, smartphones, gaming systems etc. In the navigation world they are used to assist GPS acquisition in artillery shells, but have not yet been used for any form of unaided inertial navigation.

The small size and mass of current sensors results in lower performance and resolution with poorer signal to noise characteristics. Their size does however lend the device to thermal shield encapsulation providing the necessary thermal operating stability. Improved performance is expected to follow as the industry succeeds in developing techniques and production methods to produce thicker and larger component parts including the proof mass. This should result in improved stability and signal to noise characteristics and hence improved performance. These developments will hopefully lead to low volume, high accuracy, high value applications and the Holy Grail for down-hole surveying in small, rugged, robust, vibration insensitive, accurate inertial navigation systems which can operate throughout all phases of the drilling process.

9.10.2 Hemispherical Resonator Gyro (HRG)

The HRG is often referred to as the Wineglass gyro as the CVG properties for a wineglass were first discovered and noted by Bryan in 1891. Due to Coriolis Forces, a vibration standing wave pattern induced on a hemispherical, cylindrical, or similarly shaped resonating cavity, rotates relative to the gyro case by a fraction of the rotation angle experienced about the angle of symmetry. The wave rotation scale factor is a function of resonator geometry but for a hemisphere is ≈ 0.3.

High quality Hemispherical Resonators are commonly machined from quartz, due to its excellent mechanical properties and it is the dimensional accuracy of the precision ground and polished unit which determines its accuracy. Temperature effects remain critical in this respect producing quadrature non-uniform mass distribution.

The system is robust, with almost no moving parts and can be very accurate, under strictly controlled temperature environments. Litton, now part of Northrop Grumman, produces a unit with < 0.01°/hr performance which is used by the military and for space flight in which it has recorded millions of operating hours without failure. This system has potential for oilfield use but is expensive, requires significant temperature stabilization which results in size implications. The system is also covered by the international arms trafficking laws with all the implications and restrictions applicable as noted above for RLG.

CONTENTS

10. Basic Gyro Theory

The purpose of this chapter is to explain the principles of gyroscopes and how such sensors are used specifically in *Gyrodata* gyro survey tools to determine borehole azimuth. This section was donated to the book by John Weston of *Gyrodata*, but the operating principles are largely applicable to any commercial rate gyros.

10.1 Fundamental principles

Gyroscopes are used in various applications to sense either the angle turned through by a body (displacement gyroscopes) or, more commonly, its angular rate of turn about some defined axis (rate gyroscopes).

The most basic and the original form of gyroscopes make use of the inertial properties of a wheel or rotor spinning at high speed. Many people are familiar with the child's toy which has a heavy metal rotor supported by a pair of gimbals. When the rotor is spun at high speed, the rotor axis continues to point in the same direction despite the gimbals being rotated. This is a crude example of a mechanical, or conventional, displacement gyroscope.

The operation of a conventional spinning mass gyroscopes depend the following phenomena:

- gyroscopic inertia
- angular momentum
- precession.

10.1.1 Gyroscopic inertia

This is fundamental to the operation of all spinning mass gyroscopes, as it defines a direction in space that remains fixed. The establishment of a fixed direction enables rotation to be detected, by making reference to this fixed direction. The rotation of an inertial element generates an angular momentum vector which is coincident with the axis of spin of the rotor or 'wheel'. It is the direction of this vector which remains fixed in space, given perfection in the construction of the gyroscope.

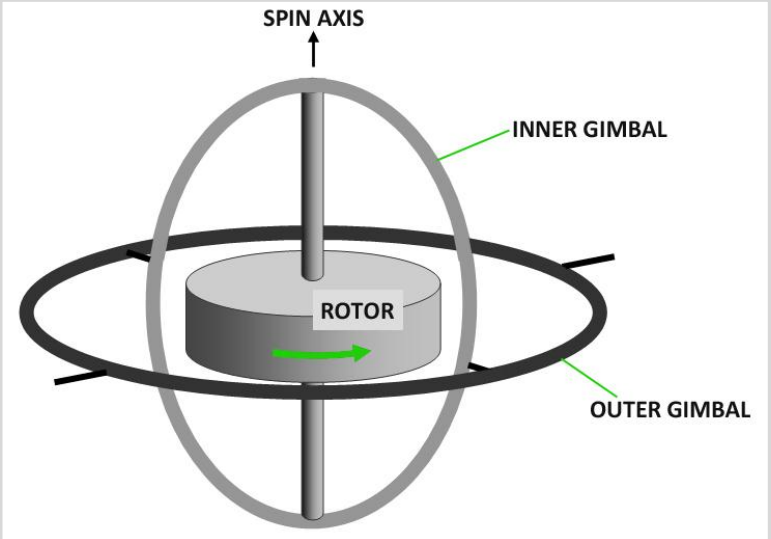

Figure 49: Schematic representation of a two axis gyroscope.

A practical reference instrument may be designed by having the rotor supported in a set of frames or gimbals which are free to rotate with respect to one another about orthogonal axes as shown in Figure 49. The orientation of the case of the instrument with respect to the direction of the spin axis may be measured with angle pick-off devices mounted on the gimbals.

10.1.2 Angular momentum

The angular momentum of a rotating body is the product of its moment of inertia and its angular velocity. The angular momentum is chosen to be very high, so that the effects of undesired torques that can act on a rotor and cause errors are small. This results in a gyroscope with little movement of the direction of the spin axis. Any undesired movement of the direction of the spin axis is usually referred to as 'drift'.

10.1.3 Precession

The tilting or turning of the gyro axis as a result of applied forces. When a deflective force is applied to the rim of a stationary gyro rotor the rotor moves in the direction of the force. However when the rotor is spinning, the same force causes the rotor to move in a different direction, as though the force had been applied to a point 90^0 around the rim in the direction of rotation.

A gyro will resist any force that attempts to change the direction of its spin axis. However, it will move (precess) in response to such force; NOT in the direction of the applied force, but at right angles to it, as illustrated in Figure 50. The figure shows the application of a force which gives rise to a couple about the torque axis. The resulting turning movement about the axis of precession causes the rotor to move to a new plane of rotation, as the spin axis attempts to align itself with the axis about which the torque is applied.

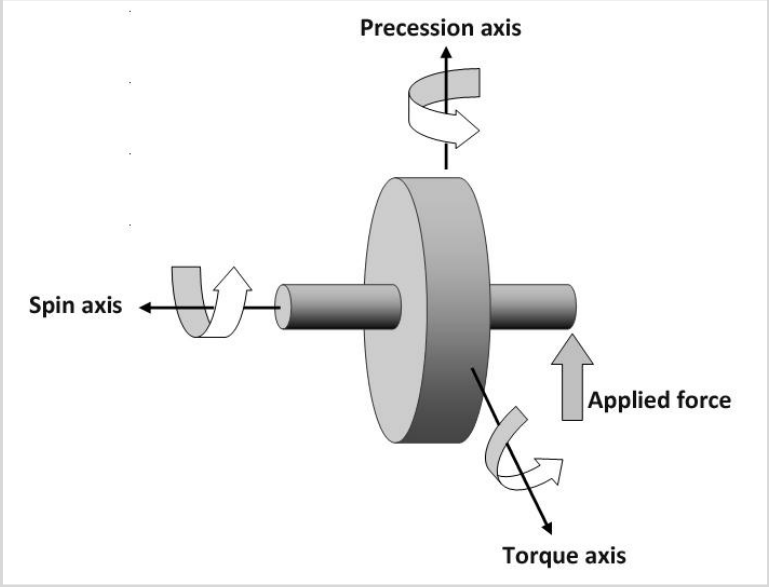

Figure 50: Illustration of gyroscopic precession.

These rules apply to all spinning gyros:

1. A gyro rotor will always precess about an axis at right angles to both the torque axis and the spin axis.
2. A gyro rotor always precesses in a direction so as to align itself in the same direction as the axis about which the torque is applied.
3. Only those forces tending to rotate the gyro rotor itself will cause precession.
4. Precession continues while torque is applied and remains constant under constant torque.
5. Precession ceases when the torque is removed or when the spin axis is in line with the torque axis (the axis about which the force is applied).

10.1.4 The application of the precession principle

The principle of precession can be exploited to provide a very accurate measure of angular rotation or rotation rate. Since a spinning wheel, or rotor, will only precess if a torque is applied to it, a rotor suspended in an instrument case by gimbals will maintain its spin axis in a constant direction in space. Changes in the angles of the gimbals will then reflect any changes in orientation of the case with reference to the spin axis direction.

Alternatively, if controlled torques are applied to the rotor to keep its spin axis aligned with a direction defined by the case of the instrument, then the measurement of these torques will provide measurements of the angular velocity of the instrument, and hence of the angular velocity of any body to which the instrument is attached.
Various sensor configurations have been developed over the years based on the principles described above. Attention is focused here on the dual-axis gyroscope, the type of sensor used in *Gyrodata* survey tools.

10.2 *Gyrodata* Rate Gyro

The gyroscope used in *Gyrodata* tools is known as a dynamically tuned or tuned rotor gyroscope. It has two input axes (denoted x and y) which are mutually orthogonal and which lie in a plane which is perpendicular to the spin (z) axis of the gyroscope. The rotor is connected to the drive shaft by pairs of flexure hinges to an inner gimbal ring. This inner 'gimbal' is also connected to the drive shaft by a pair of flexure hinges, the two axes of freedom being mutually orthogonal. This is often called a Hooke's joint and allows torsional flexibility in two directions (it is noted that this mechanical arrangement constitutes an internal type of gimbal and is far more compact than the external gimbal structure shown in Figure 51). At the other end of the drive shaft is a synchronous motor. The gyro derives its name from the rotor suspension mechanism which theoretically allows the rotor to become decoupled from the drive shaft at a certain tuned speed; typically in excess of 12,000 rpm. The rotor contains permanent magnets which set up a radial magnetic field within the assembly.

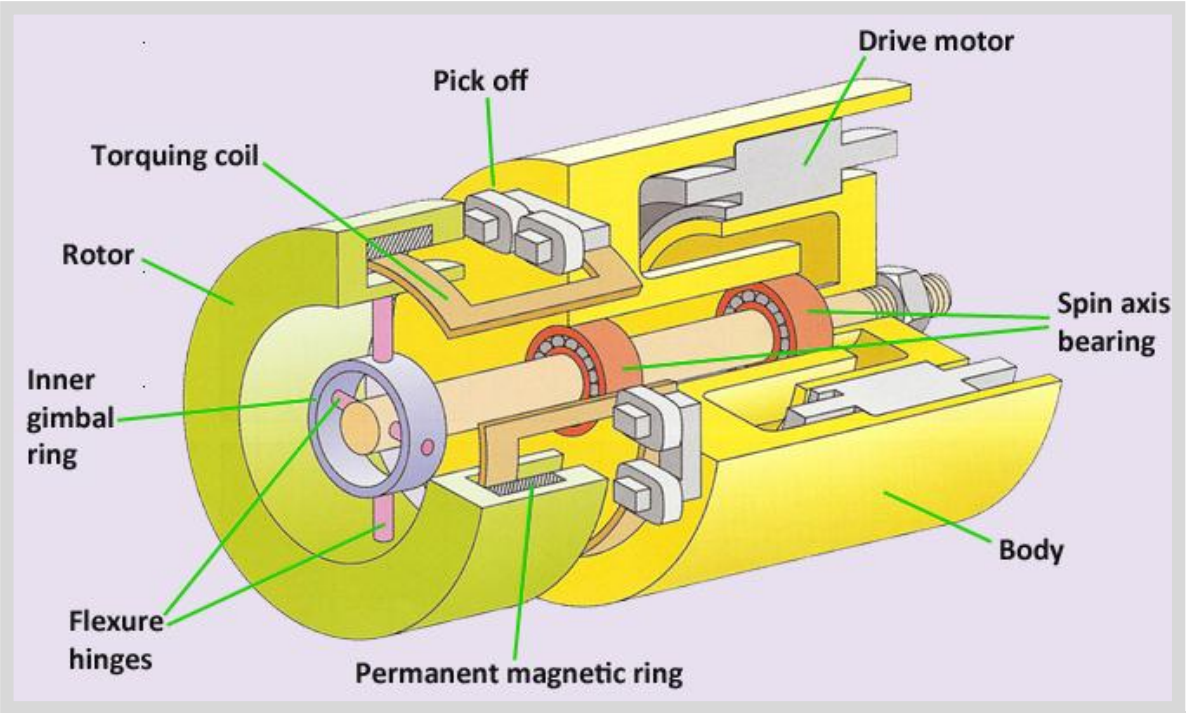

Figure 51: Dynamically tuned gyroscope.

In the presence of an applied turn rate which causes a displacement of the rotor with respect to the case of the gyro, the spin axis of a rotor is made to precess back to the 'null' position by the application of a suitable torque. A very accurate angular measurement can be made, provided that the torque required to null the deflection can be generated and measured. The mechanism by which this is achieved is outlined below.

The angular position of the rotor is sensed by pick-offs attached to the case of the gyroscope. When rotor deflection occurs, the resulting pick-off signals are sent to the gyro servo electronics which in turn drives currents through the torquer coils. The interaction of the magnetic field generated by these currents with the field produced by the rotor magnets produces forces on the rotor which cause it to precess and so drive its deflection to zero. When the system is 'balanced', the currents in the torquer coils provide a direct measure of the angular rate to which the gyro is subjected.

This application of the precession principle enables very accurate measurements to be made of the rate of turn of the case of the gyroscope. The torque re-balance technique described is fundamental to the application of inertial measurement systems in which the sensors are attached rigidly to the survey tool (often referred to as strapdown systems) as employed in *Gyrodata* tools. The application of a rate gyroscope to determine the azimuth of a borehole relies on measurement of the Earth's rate of turn, which forms the subject of the following section.

10.3 Earth's rate of Rotation

The Earth rotates about its polar (north-south) axis in 24 hours, rotating from West to East at a rate of approximately 15^0/hour. The duration of a solar day is 24 hours, the time taken for an Earth fixed object to point directly at the Sun. The time taken for the Earth to rotate to the same orientation in space, known as the Sidereal day, is 23 hours 56 min 4.1 seconds. The Earth rotates through one geometric revolution each Sidereal day, not in 24 hours, which accounts for the slightly strange value of Earth's rate; **15.041067^0/hour.**

Any point on the Earth's surface is moving in a circular arc because the Earth is spinning on its axis at this rate. The direction of the spin vector at any point on the Earth is parallel to the axis of rotation, i.e. the Earth's polar axis defined by the geographic North and South poles.

At any point on the Earth's surface, the Earth rate can be resolved into horizontal and vertical components as illustrated below.

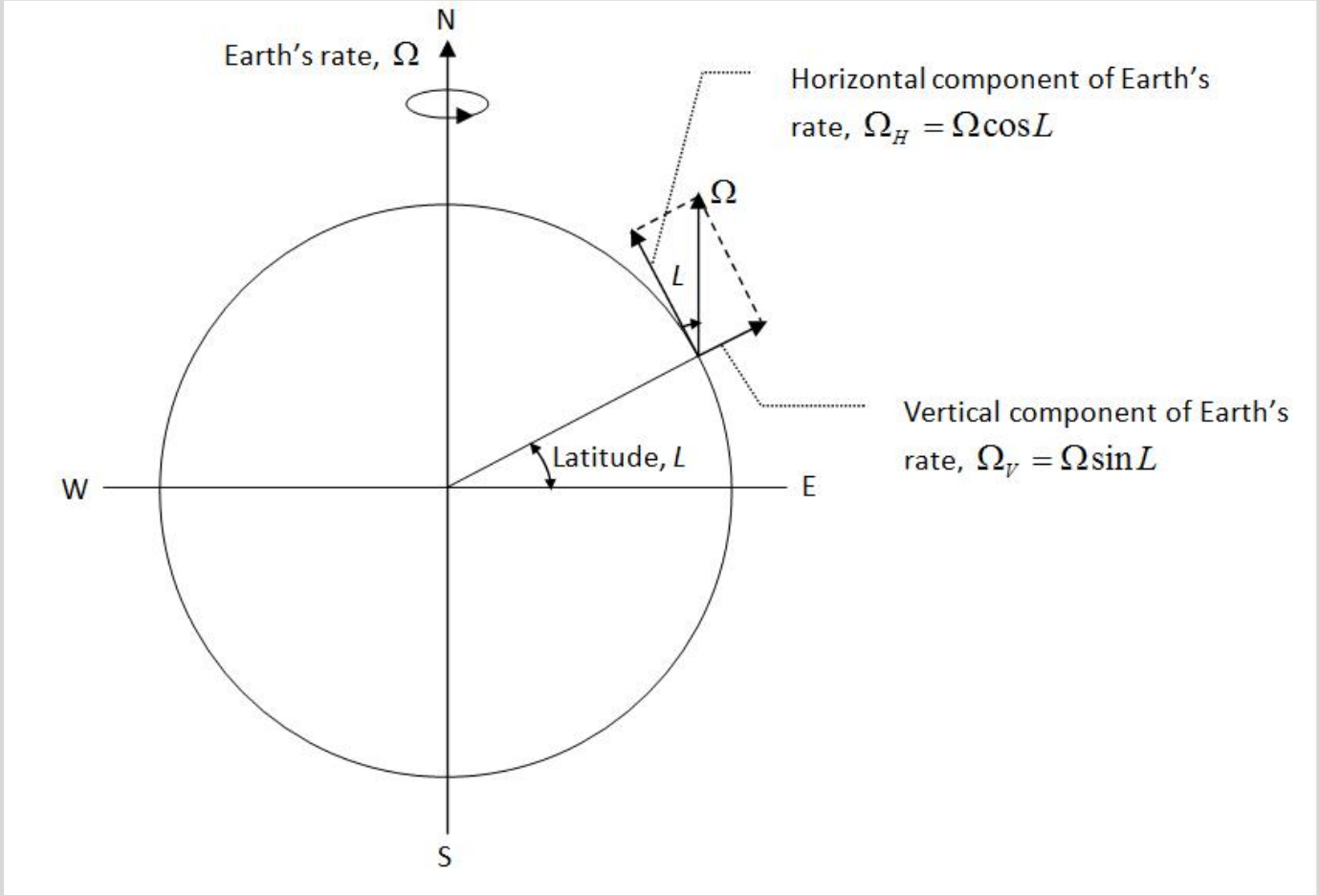

Figure 52: Calculating the Earth's rate of rotation.

The horizontal component of Earth's rate always points towards the geographic North Pole and defines a reference direction to which the orientation of the survey tool can be measured using a gyroscope.

10.4 How to Measure Azimuth

So how does the ability to measure rates of rotation help us to determine borehole azimuth? For ease of explanation and understanding of the methods used in a gyro survey system, consider first the simple case in which a dual-axis gyro is mounted with its spin axis vertical so that its input axes measure the horizontal component of Earth's rate as depicted in Figure 53.

Calculate the gyro measurement about the axes -
x-axis; $\mathbf{G_x = \Omega_H \sin \alpha}$
y-axis; $\mathbf{G_y = \Omega_H \cos \alpha}$.

It can be seen that the ratio of the x-axis measurement to the y-axis measurement defines the tangent of the direction (α) in which the y axis points with respect to the true north.

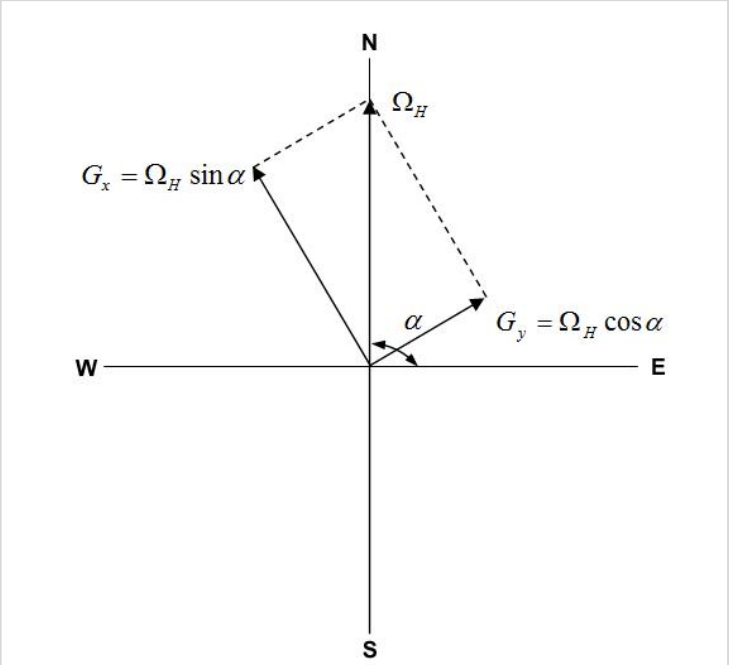

Figure 53: Measuring azimuth.

In most practical constructions of rate gyro survey tools, sensors are attached rigidly to the tool with the result that the input axis of the rate gyro takes measurements in the plane perpendicular to the tool axis; not in the local horizontal plane. Therefore, direct measurements of the horizontal components of Earth's rate are only generated when the tool is vertical.

In general, the output from the gyro measures components of Earth's rate which include both vertical and horizontal components.

In order to define the azimuth direction of a bore-hole in which the tool is located, it is necessary to have knowledge of the direction in which the gyro input axes are pointing with respect to the horizontal Earth's rate vector. This may be specified in terms of the inclination of the well and the orientation of the gyro input axes with respect to the high-side of the borehole. This information can be determined using accelerometers installed in the tool with their input axes aligned parallel to the axes of the gyro as shown schematically in figure 54.

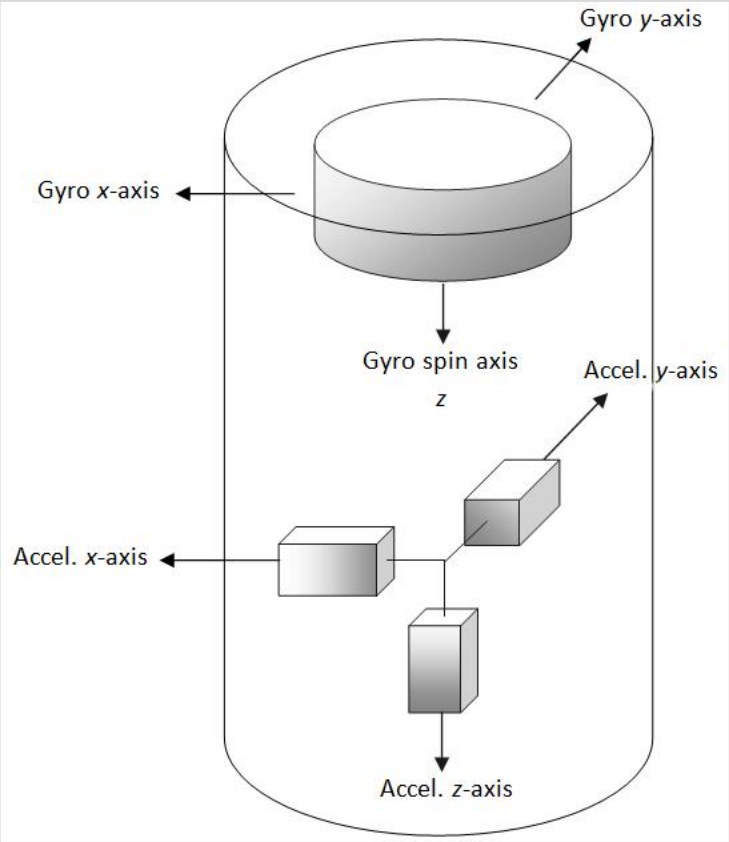

Figure 54: Instrument configuration with accelerometers.

The accelerometers provide measurements of the xyz-components of the specific force acting on the tool due to gravity (Ax Ay Az). The outputs from the accelerometer allow the inclination (I) to be calculated in accordance with the following equation.

$$I = \arctan\left[\frac{\sqrt{A_x^2 + A_y^2}}{A_z}\right]$$

The accelerometer outputs are also used to determine the relation between the input axis of the rate gyro at each measurement position and the high-side of the hole, often referred to as the high-side tool-face angle (TF), as follows.

$$TF = \arctan\left[\frac{-A_x}{-A_y}\right]$$

Given this information, the azimuth angle (*A*) can be computed as a function of the gyro measurements, the inclination and tool-face angles and the vertical component of Earth's rate using the following equation.

$$A = \arctan\left[\frac{\left(G_x \cos TF - G_y \sin TF\right)\cos I}{G_x \sin TF + G_y \cos TF + \Omega_V \sin I}\right]$$

Summary: The rate gyro survey tool uses accelerometers to measure components of the specific force due to gravity; these data are used to compute borehole inclination and to determine the position of all the sensors axes with respect to the high-side of the hole. The rate gyro is used to sense and accurately measure components of the Earth's spin rate from which the azimuth can be calculated. The horizontal component of Earth's rate always points to TRUE NORTH.

10.5 Sensor Errors

All gyroscopic sensors are subject to errors which limit the accuracy to which the angle of rotation or applied turn rate can be measured. Spurious and undesired torques (caused by design limitations and constructional deficiencies) act on the rotors of all mechanical gyroscopes. These imperfections give rise to precession of the rotor, which manifests itself as a 'drift' in the reference direction defined by the spin axis of the rotor. For a restrained gyroscope, i.e. one operating in a nulling or rebalance loop mode to provide a measure of angular rate as described in Section 3, any unwanted torques act to produce a 'bias' on the measurement of angular rate.

Major sources of error which arise in mechanical gyroscopes include the following:

1. Fixed bias – a sensor output which is present even in the absence of an applied input rotation;
2. Acceleration-dependent (g-dependent) bias – biases in the sensor outputs proportional to the magnitude of the applied acceleration. In this context, mass-unbalance effects are of particular concern, and are discussed further below
3. Anisoelastic (g2-dependent) bias – bias proportional to the product of accelerations applied along orthogonal axes of the sensor;
4. Scale factor errors – errors in the ratio relating the change in the output signal to a change in the input rate which is to be measured;
5. Cross-coupling/misalignment errors – errors arising because of gyroscope sensitivity to turn rates about axes perpendicular to the input axes, or is mounted in a position that is physically misaligned with respect to the required measurement axis.

Each of these errors will, in general, include some or all of the following components:

- fixed or repeatable terms
- temperature induced variations
- switch-on to switch-on variations
- in-run variations

For instance, the measurement of angular rate provided by a gyroscope will include:

- a bias component which is predictable and is present each time the sensor is switched on and can therefore be corrected following calibration
- a temperature dependent bias component which can be corrected with suitable calibration
- a random bias which varies from gyroscope switch-on to switch-on but is constant for any one run
- an in-run random bias which varies throughout a run; the precise form of this error varies from one type of sensor to another.

The fixed components of error, and to a large extent the temperature induced variations, can be corrected to leave residual errors attributable to switch-on to switch-on variation and in-run effects, i.e. the random effects caused by instabilities within the gyroscope. It is mainly the switch-on to switch-on and in-run variations which influence the performance of the survey system in which the sensors are installed.

Gyro mass unbalance

The performance of a mechanical gyroscope is extremely sensitive to mass unbalance in the rotor suspension, i.e. non-coincidence of the rotor centre of gravity and the centre of the suspension mechanism. Minute mechanical changes sufficient to affect gyro performance can arise as a result of shock and vibration to which the survey tool may be subjected; either down-hole or at surface as a result of knocks sustained during transport and surface handling. Movements of the rotor centre of gravity with respect to the suspension mechanism of a few nano-metres will produce changes is mass unbalance that are sufficient to give rise to significant changes in measurement accuracy.

Summary: Variations in the residual systematic bias components and the g-dependent bias caused by changes in mass-unbalance present the major concern in survey systems incorporating mechanical gyroscopes. Survey correction techniques are implemented, either during or after a survey operation, in order to compensate for survey inaccuracies resulting from the effects of these particular gyro errors.

10.6 Survey Tool Calibration

The purpose of calibration is to evaluate the coefficients for the various 'error' terms described above. Having established the performance figures or 'characterised' each sensor, any systematic errors may be compensated thus enhancing its accuracy.

To achieve this, the survey tool is placed on a calibration stand which allows the tool to be rotated between a series of known fixed orientations with respect to the local geographic axis set defined by the directions of true north and the local gravity vector. At each position, the turn rates and accelerations to which the sensors will be subjected in each controlled position are very accurately known. The series of positions are selected to excite each error contribution and so allow each error term to be identified separately and evaluated.

Figure 55: Typical calibration stand.

The highly accurate, custom made calibration stands used for this purpose were designed and developed by *Gyrodata*. Each calibration stand comprises a stabilised gimbal system with precisely controlled and instrumented gimbal angles. The stands are mounted on a plinth of granite that has its own foundations separate from, and vibrationally isolated from, the laboratory. The stands are aligned to true north within 0.001 degrees and are able to rotate the tool to any angle of inclination, azimuth or tool-face to an accuracy of 5 arc seconds (5/3600 degrees).

10.7 Survey Tool Operating Modes

Gyrodata gyroscopic survey tools contain up to three accelerometers and up to two dual-axis gyroscopes installed in various configurations within the survey tool. Systems designed to operate at all attitudes generally require a full complement of gyroscopes and accelerometers in order to provide measurements of both angular rate and acceleration about three orthogonal axes; essential for all attitude operation.

Some systems operate by taking sensor measurements at discrete intervals of depth along the well path trajectory when the survey tool is stationary, in what is described as gyro-compassing mode. Such systems provide estimates of inclination, high-side tool-face and azimuth angle as described above. Other systems can be operated in a continuous measurement mode. Given knowledge of the survey tool orientation at the start of a period of continuous surveying, changes in attitude that occur thereafter can be tracked by effectively integrating the subsequent gyro measurements of turn rate as the survey tool traverses the well path.

10.7.1 Gyro-compassing mode

Gyro biases, which have an unpredictable behaviour, are measured and corrected for directly at each gyro-compassing station though a process of indexing the gyro. This involves mounting the gyro on a rotatable platform and driving it between two positions that are 180^0 apart. Measurements of turn rate are taken when the gyro is stationary at each index position. Whilst the turn rate to which the gyro is subjected is reversed between the two index positions, any bias which is present in the measurements remains fixed. Hence, an estimate of the measurement bias can be obtained by summing the two measurements and dividing the result by two. Any residual bias which remains can still be significant and must therefore be estimated in the field.

Gyro mass unbalance is stable when the gyro is at rest. However, as discussed earlier, it may change significantly if the gyro is exposed to a mechanical impact, as can occur during transportation or surface handing. The average mass unbalance for the entire survey should therefore me estimated and corrected in the field.

Accelerometer calibrations are usually very stable, but they can change over time or as a result of temperature exposure. It is therefore important that the performance of the accelerometer pack is always verified for every recorded measurement and for the survey as a whole.

Gyrodata has developed a method for field calibration while surveying known as Multi-Station Correction (MSC). It is impossible to determine accurately all of the calibration terms in the field, the goal of MSC is therefore to correct those terms that are more likely to change, namely gyro fixed biases and mass unbalance, whist at the same time minimising the effect of residual errors in other terms. In addition, a MSC accelerometer test has also been included, to check the accelerometer measurements throughout the survey; only applicable for survey tools containing three accelerometers. MSC is a very powerful tool that updates the calibration values of residual biases and direct mass unbalance for the gyro and checks the performance of the accelerometer package. Additionally, since MSC is based on a least-squares adjustment technique, the standard deviations of the x and y gyro biases and mass unbalance are generated. This information is checked against the tolerance defined by the gyro error model and forms an essential part of the quality control (QC) procedure that is implemented each time a survey tool is run.

10.7.2 Continuous mode

Attitude data derived using continuous gyro survey systems have a tendency to drift exponentially with time. In many gyro systems, it is common practice to compensate for this effect by forming estimates of the drift at regular intervals during the survey. This is achieved by holding the tool stationary for short periods of time, and subtracting the estimated components of Earth's rate so which the tool is subjected a the current location. The drift estimates generated by this process are the accumulated effect of all physical errors at the given interval, and are used to implement a real-time re-calibration of the tool. The quality and effectiveness of this re-calibration are dependent on many factors that are difficult to predict, including the change in tool-face. It is almost impossible to keep track of what happens to the different physical sources of error when drift compensation is applied.

Studies of field data, where comparisons of in-run and out-run surveys have been made, indicated that accumulated azimuth error in most continuous surveys can be estimated using four simple empirical parameters. The four empirical parameters are:

- the error of the initial reference
- a term proportional to measured time (gyro drift)
- a term proportional to the square root of measured time (random walk)
- a random error which is irrelevant for position error calculations.

Whilst the use of empirical error sources is a departure from the usual form of error model linked to physical uncertainties, it does allow realistic uncertainty estimates to be produced. *Gyrodata* has developed a new method for final calculation of continuous surveys called Continuous Drift Correction (CDC). It is logically equivalent to averaging in-run and out-run surveys, but adopts a more complex approach which facilitates the estimation of error model terms, including the linear drift and random walk components.

CDC also checks for tool misalignments provided that the in-run and out-run high-side tool-faces are not the same throughout the survey. The misalignment correction compensates for systematic misalignment for the whole survey and provides additional quality control to the data. The use of CDC provides several benefits compared to a simple in-run/out-run comparison. It corrects for linear drift and systematic misalignment and allows QC checks to be implemented by providing estimates of residual errors that can be checked against the tool error model.

10.7.3 Summary

Stationary gyro-compassing and continuous survey methods have been outlined along with procedures developed by *Gyrodata* for quality control of the resulting surveys. The powerful MSC and CDC methods provide comprehensive quality control, for stationary and continuous surveys respectively, and tool performance characteristics linked directly to the respective tool error models.

11. When to run Gyros

Running gyro surveys is nearly always a benefit to survey accuracy and provide verification of the MWD surveys, but clearly the benefit has to be worth the cost. There are certain circumstances however, where running gyros are the only option for a safe an adequately accurate survey. Please note that in most of these scenarios apart from a) below, the assumption is that the gyro used is of sufficient accuracy to exceed the accuracy of the MWD. That is not always the case depending on the type of gyro and the expected performance of the gyro must be ascertained by suitable QC to ensure adequate accuracy.

a) When magnetic interference from nearby steel preclude the use of MWD.
   These circumstances include the following;
   - Measuring inside casing
   - Measuring close to casing shoe
   - Measuring close to adjacent wells
   - Measuring close to surface or shallow beneath the rig
   - Measuring close to a fish or when side-tracking close to original casing.

   This would naturally, include conductor surveys after conductors have been driven. This often neglected practice ensures that the collision risk assessment is based on the actual as built positions of the conductors and not an assumption that they landed vertically and parallel. It is not unknown for driven conductors to cross two rows of slots from their original surface position so the slot/ target allocation often has to be reviewed in the light of the conductor survey. When the casing of the nearest well is 50ft or more away it is usually considered to have negligible effect on MWD azimuth accuracy but the effect rises rapidly with proximity so gyros are often prescribed when separation from casing drops to 30ft or so.
b) When TVD accuracy is required less than 3/1000 on step out. This is very difficult to achieve with MWD in open hole and whilst the accelerometers may be just as accurate as the gyro sensors in the vertical plane, the hole quality and the measurement environment cannot deliver this level of accuracy with confidence.
c) When the MWD is surveyed every 90 ft but with dogleg severities exceeding 6^{o}/100ft the MWD survey interval will not adequately represent the wellpath. Here the gyro provides a higher resolution survey and can be requested at very small intervals although 25 ft is common.
d) When the target dimensions are less than 2% of the step out (1% if IFR is employed). This size of target will not leave sufficient room for the directional driller to steer successfully without the reduction in uncertainty afforded by a high accuracy gyro survey for at least part of the well bore.
e) Anywhere, where the separation factor requirements cannot be met using MWD alone.
f) In side-tracks where the original hole contains a fish, or casing and the accuracy requirements demand an adequate survey during the side-track section close to the original hole.
g) When drilling close to leaselines, geo hazards, fault blocks or other ‘hard line’ boundaries where MWD uncertainty wastes too much pay.

✧

CONTENTS

12. Correcting for Sag

Figure 56:

The BHAs used in directional drilling are designed to be flexible enough to drill round curves. Inevitably this leads to deflections in the BHA centreline which is unlikely to remain parallel to the wellbore. As a result the inclination observed may need to be corrected for the misalignment between the MWD sensor and the wellbore centreline.

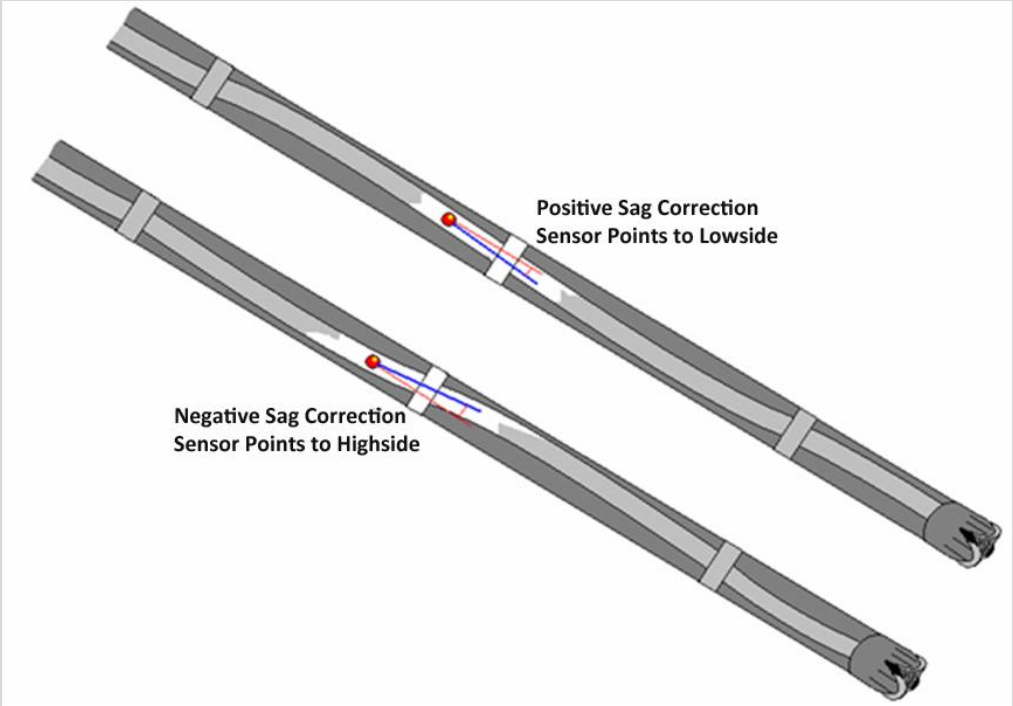

Sag Correction Software

Since finite element software or mechanical beam theory techniques are used anyway to model the side forces and stresses on a BHA as part of its performance design, the same software calculates the deflected shape of the BHA and can predict in advance the corrections needed to apply to the observed inclination. This is often the most important correction required for high angle drilling accuracy for good TVD placement. In the above example, there is also a mechanical bend in the BHA at the bent housing so the sag correction may not be just inclination dependent but may also be toolface dependent if the assembly has a bend that can be oriented.

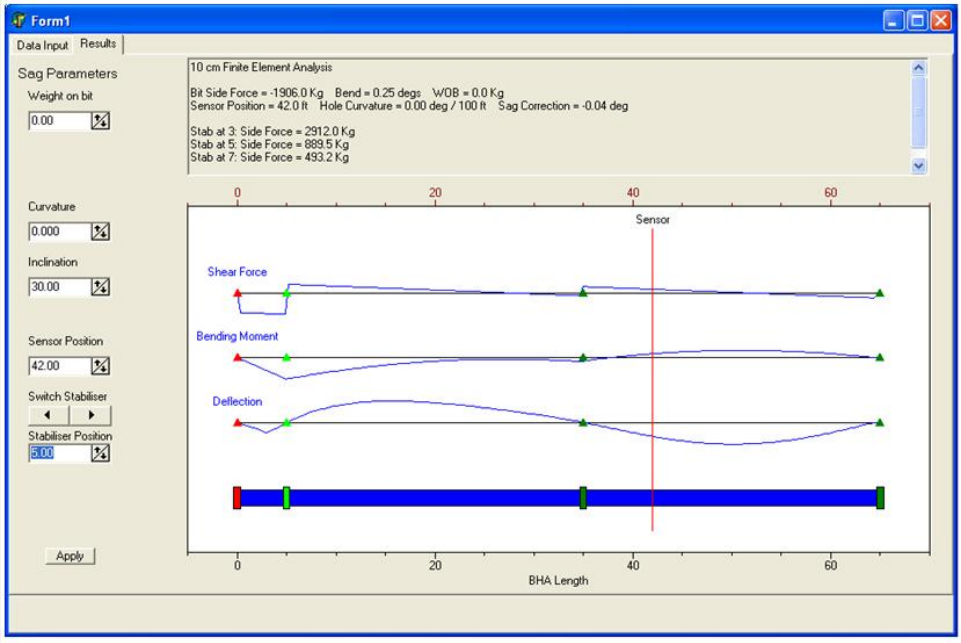

Figure 57: Typical sag correction software output.

Generally at low inclinations sag will be minimal but as it is mainly due to gravity effects, the magnitude is likely to increase with the sine of the inclination. Here is a typical sag sheet with corrections over a range of inclinations.

Sag Sheet

Sensor Position = 55.43 ft

Inc	Sag (deg)	Inc	Sag (deg)
0.0	0.000	60.0	0.177
5.0	0.018	65.0	0.186
10.0	0.036	70.0	0.193
15.0	0.053	75.0	0.198
20.0	0.070	80.0	0.202
25.0	0.087	85.0	0.201
30.0	0.102	90.0	0.201
35.0	0.118	95.0	0.201
40.0	0.132	100.0	0.202
45.0	0.145	105.0	0.198
50.0	0.157	110.0	0.193
55.0	0.168	115.0	0.186
60.0	0.177	120.0	0.177

Care should be taken when using bent housings in the BHA since the sag correction will then be toolface dependent. In such cases, the sag should be calculated on site using software which can include the bend in the finite element analysis when applied at any toolface.

It is recommended that any well that build above 45 degrees at any point should be sag corrected as a matter of course. This is a service that most drilling contractors can easily include and the effect on TVD accuracy is often dramatic.

If we use the approximate rule of thumb that 1 degree of angle produces 2% of distance as an error in position, even a small inclination error like 0.25 degrees will produce 0.5% of step out as an error in TVD. For example, if the step out to a reservoir entry point was 3000 ft, the TVD error would be + or – 15 ft for only a quarter of 1 degree of sag.

In the analysis of misplaced wells identified by poor production or a poor match with expected geological formation depths, the lack of sag correction is the most common cause. The cost of carrying out sag correction is far outweighed by its benefits in terms well positioning particularly at the entry point to the reservoir.

CONTENTS

13. Correcting for Magnetic Interference

13.1 Drilling magnetisation

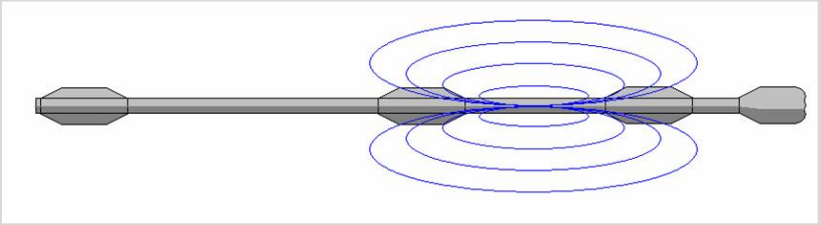

Figure 59: Drillstring magnetisation.

It is well known that the MWD sensors in themselves are extremely accurate but the weak link in the system is the accuracy of the magnetic field in which the azimuth readings are taken. We discussed earlier the effects of local crustal anomalies on the accuracy of our background reference vector but in this section we will look at the effects of the drillstring magnetisation which is always present to some degree. It should be noted however that since the sensor pack is always set inside non-magnetic material, the major interference component is likely to be either from below or above the sensor in the drillstring and therefore the z axis interference is usually the major influence on azimuth accuracy.

In the 1990s, Dr Robin Hartman of Shell International developed SUCOP (Survey Correction Program) to implement a technique for measuring and removing the magnetic influence of the drillstring.

If a magnetometer is placed in a magnetic field it will measure the component of the field along its own axis. A good analogy is if a tube with a small flow meter was inserted in stream, the flow through the tube will be the component of flow along the axis of the tube. Clearly if the tube is held perpendicular to the flow there will be no flow in the tube and if it is in line with the flow it will experience the full flow rate of the stream. At any other angle it will experience the flow vector x cosine of the angle of incidence. This value is often referred to as the vector dot product. This can be defined as the product of two vector lengths x cosine of the angle between them.

In figure 60 the magnetic field is represented by the green arrows and the magnetometers will only measure the component of that field along their own axis.

Now imagine two magnetometers facing in opposite directions at some angle to the magnetic field. Clearly they will read the same magnitude of field but with opposite signs. Hartman realized that if an MWD sensor pack was rotated around the z axis, the x and y magnetometer readings would follow a sine wave which should have an average of zero. If the average was anything else, there must be a component of the observation which is permanent. This will be some combination of a sensor bias or a magnetic field component which is rotating with the sensors and is never going away.

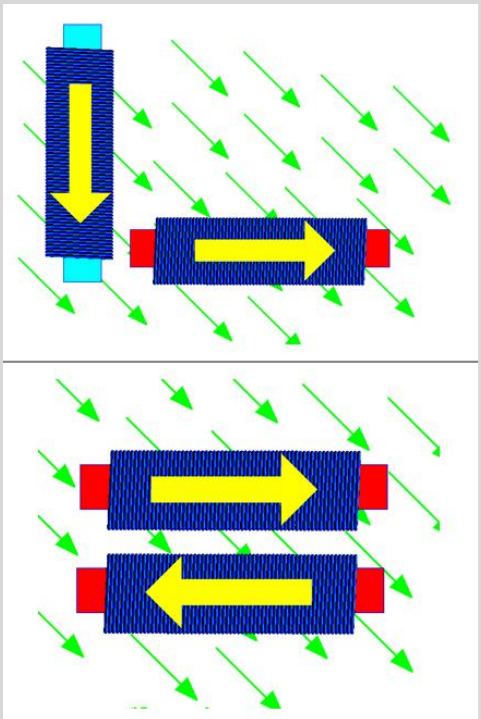

Figure 60: Axis components of magnetometers.

Figure 61: Straight plot of sensor readings.

In the field, the driller could observe raw sensor readings at several toolfaces (a rotational shot or cluster shot) and record the values on the x and y axes.

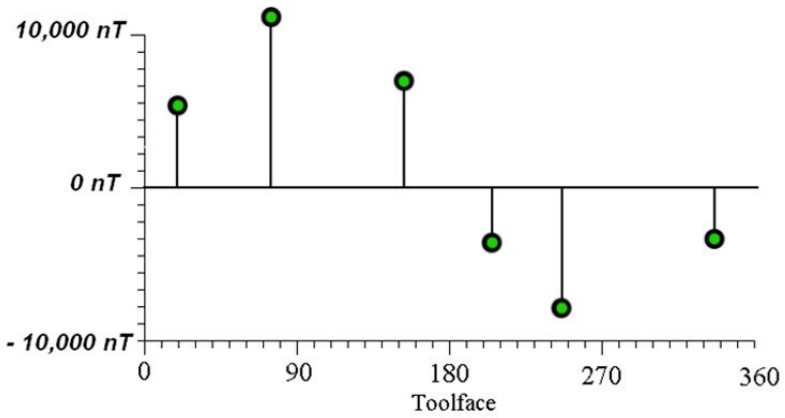

Figure 62: Adding a mathematical sine wave to the sensor readings.

If a mathematical sine wave was then made to fit this variation, the average value could then be derived as if the readings had been taken evenly around the clock.

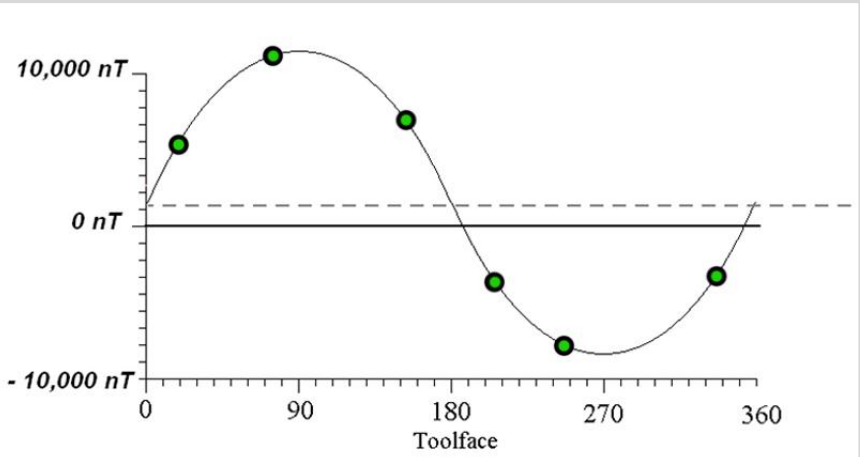

In this example, the magnetometer is clearly carrying a positive magnetic field value that is not going away.

This rotational data can then be used to correct the x and y magnetometer values for this bias. This still leaves the potential for a further magnetic field bias on the z axis. In practice the z axis is often the most significant direction of influence since the significant magnetic material in the drill string is always above or below the MWD sensors. Clearly it is not possible to flip the z axis so the clean z axis is derived from the following formula:

$$Clean\ Bz = \sqrt{Bt^2 - Clean\ Bx^2 - Clean\ By^2}$$

In this formula, Bt means the total background magnetic field strength and Bx By and Bz mean the sensor axes readings from the magnetometer. This formula relies on the accuracy of Bt and ideally should have an IFR survey to accurately measure Bt. This simple technique allows the surveyor to calculate bias values for all three axes and remove the majority of the magnetic interference from the subsequent observations.

One caveat that should be kept in mind is the stability of the calculation. The value for Bz is very sensitive to azimuth and inclination.

The formula is identical to a Pythagoras formula for calculating one side of a right angled triangle where Bt would be the hypotenuse and the base would be the cross axial field as follows.

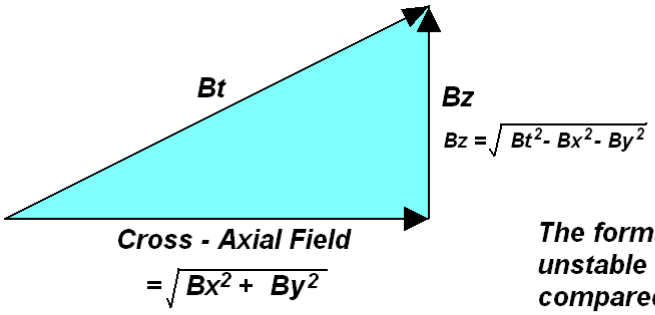

The formula for Bz becomes unstable when Bz is small compared with Bt. The result can also be positive or negative.

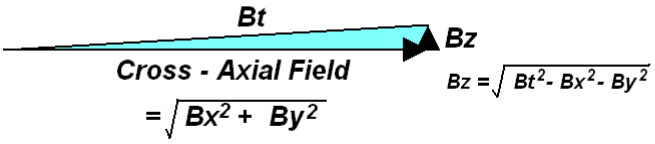

If the value of Bz is very small, which will happen when drilling at high angle heading East or West, the resolution of clean Bz will be extremely sensitive to the accuracy of the other two sides. The slightest error in Bt can produce a very exaggerated effect on Bz and, in many cases, produce a value in Bz more erroneous than the magnetic error. In other words, this technique should not be used in such geometries in case the correction is more erroneous than the original reading.

eg Bt = 50,000 nT

$$Bx^2 + By^2 = 49800\ nT$$

$$Bz = \sqrt{Bt^2 - Bx^2 - By^2} = 4467\ nT$$

suppose error in Bt is 100nT and Bt appears as 49900

$$Bz = \sqrt{Bt^2 - Bx^2 - By^2} = 3157$$

So 100 nT on Bt causes 1300nT in Bz !!

For this reason and because the Bz value can be positive or negative it is not recommended that this technique be employed in the following '**no go zones**' - above 70 degrees inclination within 20 degrees of East / West (magnetic).

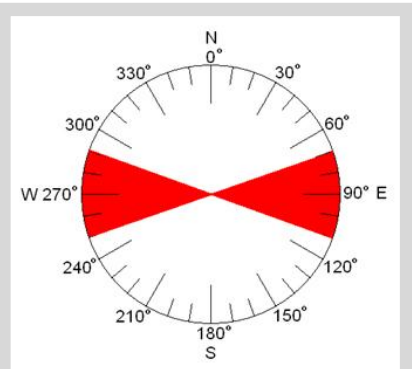

Figure 64: 'No go zone' for axial correction.

✧

CONTENTS

14. Multi Station Analysis

14.1 Calculation and background

A more recent development on the principle of magnetic interference correction is the use of Multi Station Analysis.

This technique is similar to the rotational shot technique described above but makes use of all available MWD data so far collected to 'best estimate' corrections to apply retrospectively. This is heavy on computing time but with modern computers allows a great deal more flexibility in what we analyse for. In the section following the mathematics will be set out but for now, the principles and process steps are as follows.

Earlier we discovered that a magnetometer will read a magnetic field value along its own axis. It is therefore possible to calculate a theoretical value if we know the background field vector and the 'attitude' (Inclination and Direction) of the sensor axis. If we gather a lot of raw data from multiple survey stations (with the same BHA), we can examine the consistency of the data versus the theoretical values and try to find corrections on each sensor that make for the least error.

This is known as Multi Station Analysis and since it is using all the raw data over several stations, in theory, there is no need to carry out a cluster shot since there will be variations in attitude anyway between each survey station. It should be said however, that cluster shots are strongly recommended at the start of the BHA run to produce a strong estimate of corrections before drilling much further on what could be a wrong azimuth.

The steps are as follows:

1. Over several readings observe Bx, By, Bz, Gx, Gy and Gz
2. Calculate inclination, direction and toolface as normal
3. Calculate the unit vectors that describe the attitude of each magnetic sensor
4. Calculate the theoretical value that should have been read
5. Record the errors (residuals) on each sensor
6. Calculate the sum of the squares of these residuals
7. Try variations of scale and bias corrections on each sensor until the result of step 6 is minimised
8. Apply these best fit biases and scale factors over the whole survey

The next section may help the mathematicians amongst you understand the steps more clearly, and for the rest, may offer an alternative to counting sheep.

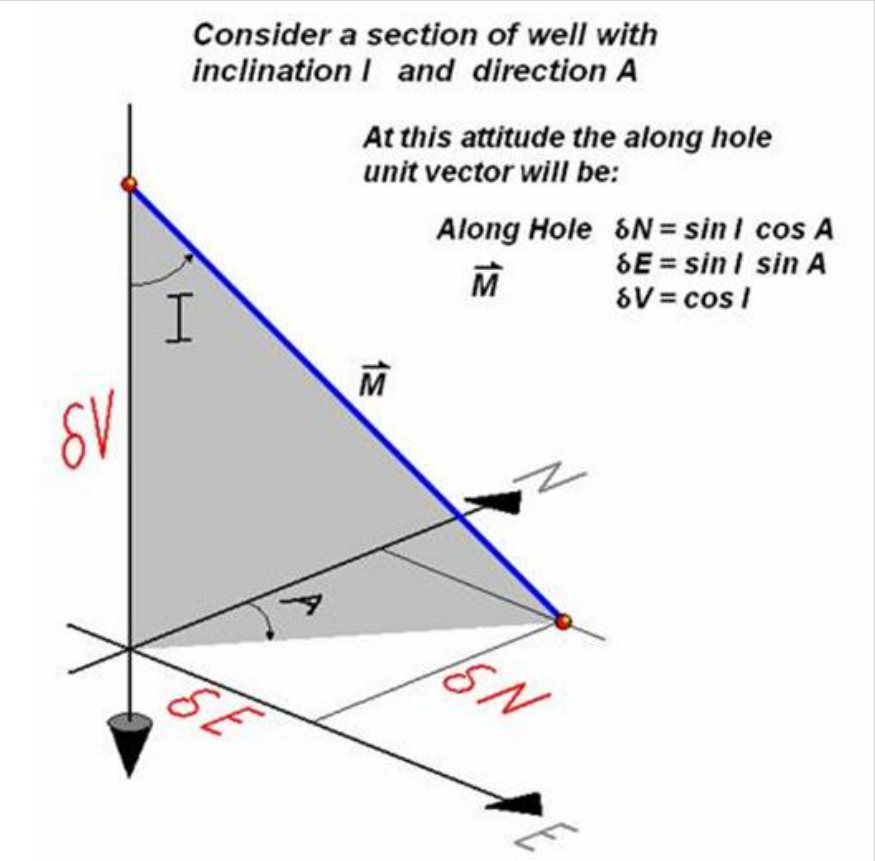

Figure 65: First we need to establish the unit vectors for each sensor axis.

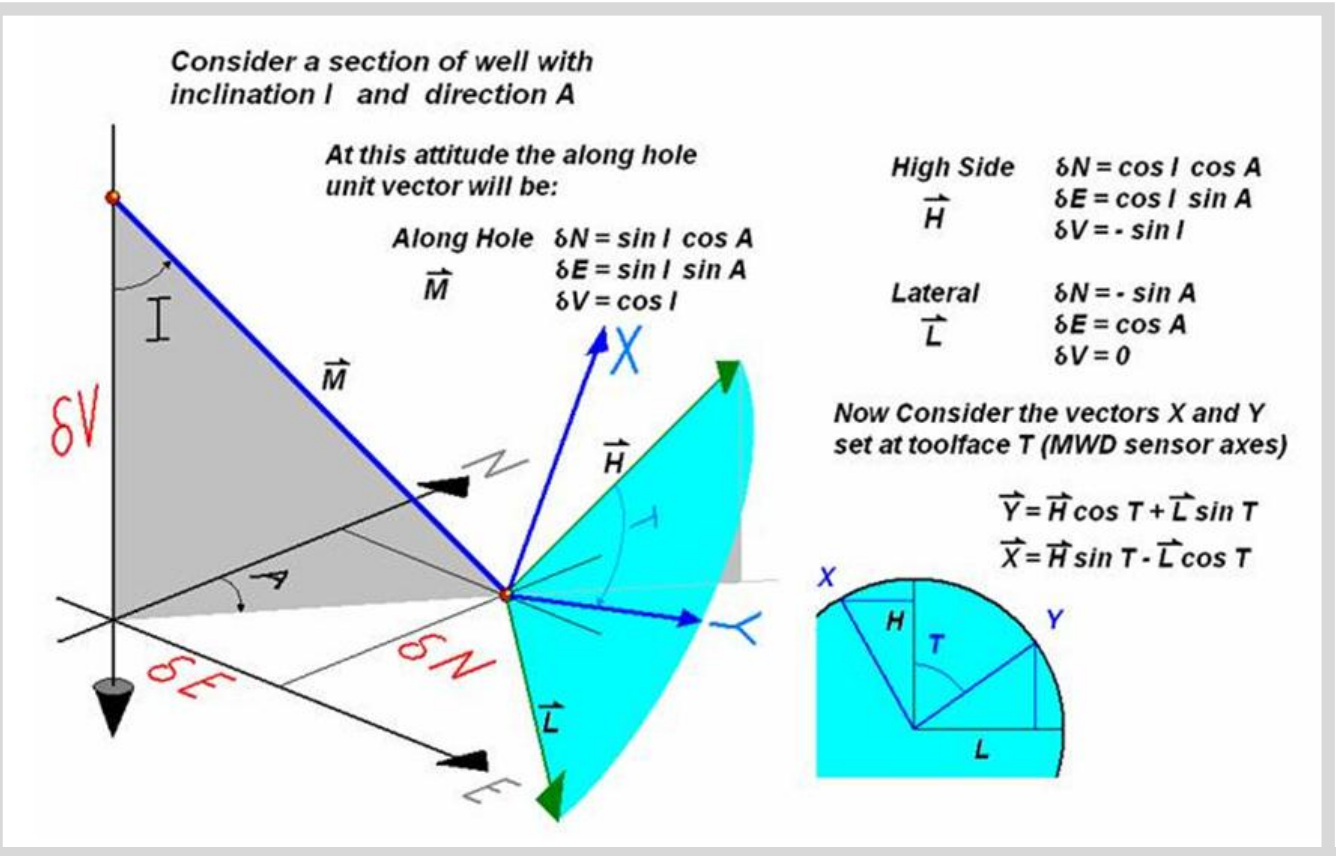

Figure 66: This vector is then the unit vector for the z axis.

These formulae describe the high side unit vector and the lateral unit vector from which we can derive the axes vectors when sitting at any given toolface from high side;

In summary, at Inclination I, Azimuth A and Toolface T

The unit vectors of the MWD sensor axes are as follows:

$$
\begin{aligned}
\textit{Y axis}\quad \delta Ny &= \cos I \cos A \cos T - \sin A \sin T \\
\delta Ey &= \cos I \sin A \cos T + \cos A \sin T \\
\delta Vy &= -\sin I \cos T \\
\\
\textit{X axis}\quad \delta Nx &= \cos I \cos A \sin T + \sin A \cos T \\
\delta Ex &= \cos I \sin A \sin T - \cos A \cos T \\
\delta Vx &= -\sin I \sin T \\
\\
\textit{Z axis}\quad \delta Nz &= \sin I \cos A \\
\delta Ez &= \sin I \sin A \\
\delta Vz &= \cos I
\end{aligned}
$$

If we describe the Earth vector in terms of a north, east and vertical component we can calculate theoretical readings for each axis using the vector dot product. If the Earth's magnetic Field Vector os Mag N, Mag E, Mag V and the Earth's Gravity Field Vector is Gn, Ge an Gv we would expect each sensor to read the vector dot products as follows;

Y axis

$$
By = \begin{bmatrix} \cos I \cos A \cos T - \sin A \sin T \\ \cos I \sin A \cos T + \cos A \sin T \\ -\sin I \cos T \end{bmatrix}^T \begin{bmatrix} Magn \\ Mage \\ Magv \end{bmatrix} \qquad Gy = \begin{bmatrix} \cos I \cos A \cos T - \sin A \sin T \\ \cos I \sin A \cos T + \cos A \sin T \\ -\sin I \cos T \end{bmatrix}^T \begin{bmatrix} Gn \\ Ge \\ Gv \end{bmatrix}
$$

X axis

$$
Bx = \begin{bmatrix} \cos I \cos A \sin T + \sin A \cos T \\ \cos I \sin A \sin T - \cos A \cos T \\ -\sin I \sin T \end{bmatrix}^T \begin{bmatrix} Magn \\ Mage \\ Magv \end{bmatrix} \qquad Gx = \begin{bmatrix} \cos I \cos A \sin T + \sin A \cos T \\ \cos I \sin A \sin T - \cos A \cos T \\ -\sin I \sin T \end{bmatrix}^T \begin{bmatrix} Gn \\ Ge \\ Gv \end{bmatrix}
$$

Z axis

$$
Bz = \begin{bmatrix} \sin I \cos A \\ \sin I \sin A \\ \cos I \end{bmatrix}^T \begin{bmatrix} Magn \\ Mage \\ Magv \end{bmatrix} \qquad Gz = \begin{bmatrix} \sin I \cos A \\ \sin I \sin A \\ \cos I \end{bmatrix}^T \begin{bmatrix} Gn \\ Ge \\ Gv \end{bmatrix}
$$

In practice we usually ignore any Gn and Ge components and assume that Gv is the Gravity Gt;

$$Gx = -\sin I \cos T \, Gt$$
$$Gy = -\sin I \sin T \, Gt$$
$$Gz = \cos I \, Gt$$

From these very much simpler formulae we can easily derive the inclination and the toolface

$$\sin I = \sqrt{(Gx^2 + Gy^2)} \,/\, Gt$$

$$\cos I = Gz / Gt \qquad I = \tan^{-1}(\sin I / \cos I) \text{ resolved } 0 - 180$$

$$\sin T = Gy / (-\sin I \, Gt)$$

$$\cos T = Gx / (-\sin I \, Gt) \qquad T = \tan^{-1}(\sin T / \cos T) \text{ resolved } 0 - 360$$

Returning to our magnetic equations, the red numbers are now known;

Y axis

$$By = \begin{bmatrix} \cos I \cos A \cos T - \sin A \sin T \\ \cos I \sin A \cos T + \cos A \sin T \\ -\sin I \cos T \end{bmatrix}^T \begin{bmatrix} Magn \\ Mage \\ Magv \end{bmatrix}$$

X axis

$$Bx = \begin{bmatrix} \cos I \cos A \sin T + \sin A \cos T \\ \cos I \sin A \sin T - \cos A \cos T \\ -\sin I \sin T \end{bmatrix}^T \begin{bmatrix} Magn \\ Mage \\ Magv \end{bmatrix}$$

Z axis

$$Bz = \begin{bmatrix} \sin I \cos A \\ \sin I \sin A \\ \cos I \end{bmatrix}^T \begin{bmatrix} Magn \\ Mage \\ Magv \end{bmatrix}$$

Each sensor observation provides one equation;

$$(Magn \cos I \cos T + Mage \sin T) \cos A + (Mage \cos I \cos T - Magn \sin T) \sin A = (By + Magv \sin I \cos T)$$

$$(Magn \cos I \sin T - Mage \cos T) \cos A + (Mage \cos I \sin T + Magn \cos T) \sin A = (Bx + Magv \sin I \sin T)$$

$$(Magn \sin I) \cos A + (Mage \sin I) \sin A = (Bz - Magv \cos I)$$

We can now reduce the bracketed terms to a simple matrix form:

$$\begin{bmatrix} m11 & m12 \\ m21 & m22 \\ m31 & m32 \end{bmatrix} \begin{bmatrix} \sin A \\ \cos A \end{bmatrix} = \begin{bmatrix} B1 \\ B2 \\ B3 \end{bmatrix}$$

These are now a set of oversubscribed simultaneous equations in sinA and cosA which can be solved by least squares as follows:

$$\begin{bmatrix} m11 & m12 \\ m21 & m22 \\ m31 & m32 \end{bmatrix}^T \begin{bmatrix} m11 & m12 \\ m21 & m22 \\ m31 & m32 \end{bmatrix} \begin{bmatrix} \sin A \\ \cos A \end{bmatrix} = \begin{bmatrix} m11 & m12 \\ m21 & m22 \\ m31 & m32 \end{bmatrix}^T \begin{bmatrix} B1 \\ B2 \\ B3 \end{bmatrix}$$

These equations can be used to solve for sin A and cos A and thus an unambiguous best fit azimuth can be derived from the observations. The unit vectors can be calculated and the theoretical readings subtracted from the observed readings to produce residuals for each observation and each axis.

A 'Monte Carlo' analysis is then run for variations in scale factor and bias for each sensor until the sum of the residuals squared is minimized. In the following graphs for all 6 corrections, a clear minimum sum squared occurs at the best value for each correction:

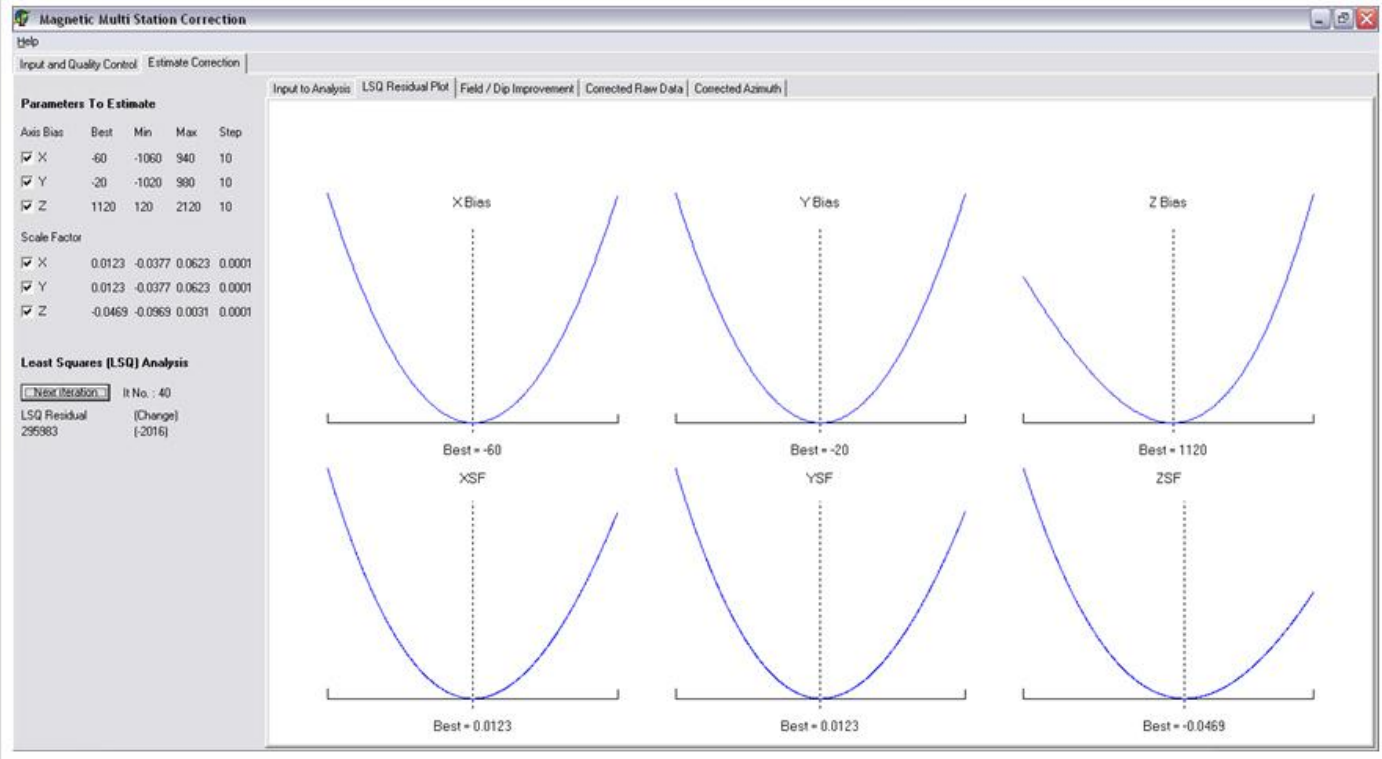

Figure 67: Correcting magnetic station observations.

All previous raw surveys up to that point are then corrected with this latest estimate and the azimuths recalculated as if there was no magnetic interference present.

In practice the data will be noisy and often requires some filtering before it can be used. Any bad readings are either weighted low in the least squares calculation or they are removed altogether.

✧

CONTENTS

15. Correcting for Pipe and Wireline Stretch

15.1 Forces on the drillpipe

It has not been routinely included in survey procedures to estimate and remove the mechanical or thermal expansion of the drillpipe and yet clearly the weight of the BHA itself and the drillpipe suspended below any section of pipe will stretch it, as will any increase in downhole temperature from that observed at surface where the drillpipe length is measured before deployment.

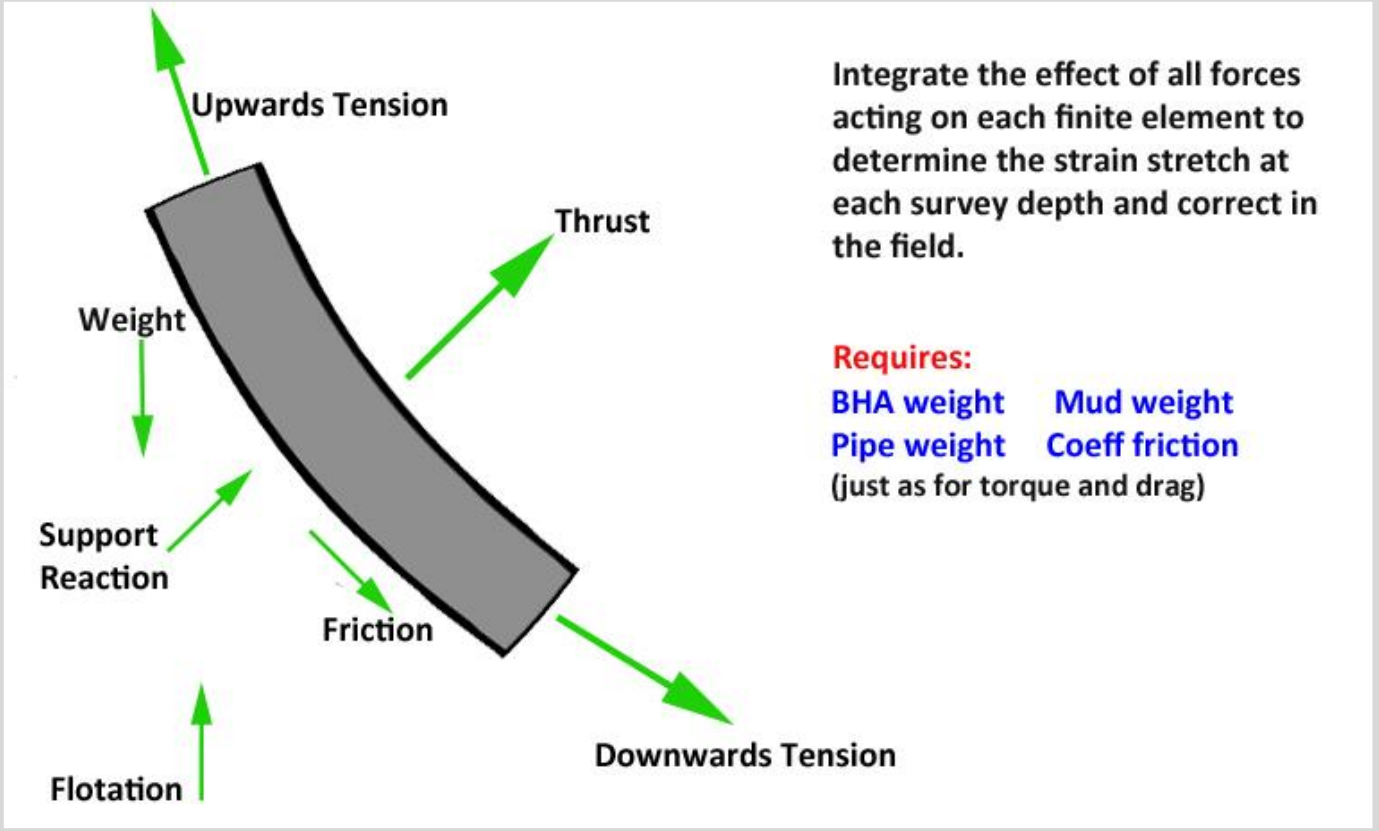

Figure 68: Forces acting on a finite element of drillpipe.

This diagram represents a finite element of drillpipe with all the forces likely to be acting on the element. There is an upward tension on the pipe as it is supported by the pipe above and a downward tension as it carries the drillstring below. These tensions will not be in alignment in curved hole producing a 'Thrust' force perpendicular to the wellbore, usually upwards in a build section and downwards in a drop section. There is also the weight of the pipe, countered to some degree by the flotation effect of the drilling fluid, a support reaction and corresponding friction force. If we estimate the coefficients of friction and assume that the survey models the shape of the pipe, we can estimate the mechanical stretch by integrating the axial components of the forces on the pipe and their local strain effects on each element.

E = Youngs Modulus = stress / strain *so the strain* = stress / Youngs Modulus

This calculation is most useful for high accuracy, absolute TVD measurement. It may seem sensitive to our estimate of the coefficient of friction but in practice this proves to be less than you might anticipate. This is because when the stress most affects TVD, the well is close to vertical and the friction component is small but when friction becomes very significant (i.e. at high angle), the stretch effect in measured depth does not translate to much of an error in TVD.

15.2 Thermal Effects

The thermal coefficient of expansion for steel is approximately 1.3 m / 1000 for every 100° C of warming so it is also possible to estimate from an approximate temperature profile, how much additional depth we will gain from thermal expansion. In the following example of a fairly typical well, there is 2 m of mechanical extension plus 5 m of thermal expansion giving a total of 7 m of additional drillpipe you never knew you had!

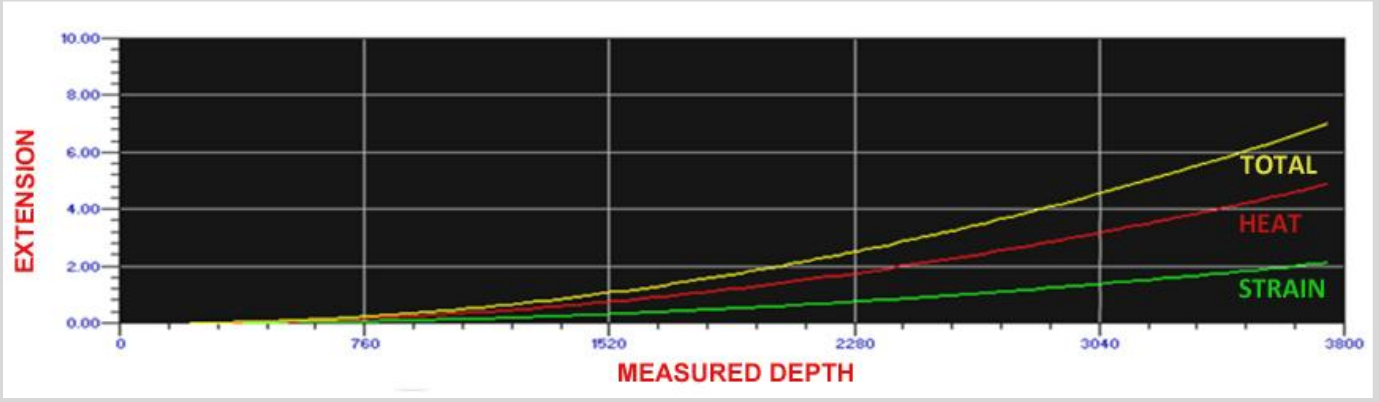

Figure 69: Measuring thermal expansion of a typical drillpipe.

This is one of the reasons that wireline measurements and drillpipe conveyed measurements seldom agree. The wireline will stretch much more than steel and when warmed up, oddly, becomes shorter rather than longer due to the lateral expansion of the elastomer within the reinforced sheathing. As a result, wireline is usually corrected for stretch whereas drillpipe almost never is (at the time of writing).

Great care should be taken when using drillpipe depths as they will usually be significantly less than actual depth. One common mistaken assumption is that if we fail to correct for drillpipe stretch in a vertical pilot well, we'll be able to land a horizontal target at the same depth if also ignore the stretch in that. However, in a vertical well the BHA is supported by the pipe whereas the horizontal wellbore will support the BHA on the low side producing a very different stretch profile.

✧

CONTENTS

16. Human Error v Measurement Uncertainty

When surveyors refer to error models they are usually referring to the inaccuracies of instruments or measurement systems. Clearly these cannot compensate for bad practice and human error such as using grid North instead of True or GPS on the wrong datum. The instrument inaccuracies are often referred to as modellable errors whereas the practical mistakes are referred to as unmodellable errors. Great care has to be taken when using industry standard error models to ensure that best practice has been adopted before assuming that the calculated uncertainties are representative. The following section points out a few common mistakes.

16.1 Common Human errors

Common Pitfalls
The following common well planning pitfalls are listed to raise awareness. Past experience has shown that these are likely errors that can be overlooked. Best policy is to review this list after producing a new well plan.

Missing Data
The most frequent reason for collision is not poor surveying but rather that the object well came as a "surprise". It is essential that the well planner ensures that he has all the data needed to plan a safe well path. Always check a list of wells with the client to ensure that nothing was lost in migration.

Using Gyro Error Models for Undrilled Sections
It may well be that a gyro survey is planned in for example, 9 5/8 casing. But prior to this gyro survey "confirming or more accurately describing" the well path of the well, this section will usually be a 12 ¼ inch hole which will be drilled with MWD. It is important during well planning that the anticipated survey program as each well section is drilled, is used. The updated or most accurate survey and error model should be entered and used for anti-collision purposes right before a new section is drilled. But during the initial planning the as drilled error models should be used to the total depth of the well to confirm the entire well can be drilled conforming to required separation factor rules.

16.2 Misapplication of Uncertainty in Top Hole

There are two common problems in applying uncertainty in the top-hole section.

Top-hole uncertainty must include the radius dimension of the well. This is unlike deep sections where the measurement uncertainty dimension is so great that the radius dimension component of the uncertainty is a very small percentage. In the top hole when measurement uncertainty is just beginning to accumulate, the well radius dimension is a significant component in anti-collision.

If the area being scanned includes multiple sites (platforms or surface locations from which wells have been drilled) then the uncertainty as to the actual coordinates of the surface site must be determined and included in the calculations. Refer to Section 3.2.1 for aid in determining the uncertainty of the sites' surface locations.

Caging
"Caging" is the term for the condition where a new well can no longer be drilled due to the poor positioning of previously drilled wells. This usually happens later in the development cycle of pad or platform drilling. It is useful to include all future planned wells in the collision scanning at the planning stage and during drilling operations so that, whilst not safety critical, sensible avoiding action can be taken so that the potential for future caging is minimized.

Overly Conservative Targets
Small targets cost a large amount of money to drill as the directional driller in the field will not be afforded much flexibility from the planned trajectory and will have to spend more rig time steering to the "line".

Curved Section Close Approaches
Interpolating at long intervals when scanning can completely miss a close approach to approach another well.
It is recommended to always perform a 3D visualization run down the planned well to visually sense the effects all close approaches.
Initial numerical scan reports should always be run at 100 ft or 30 m intervals. Then refine localized zones with searches using 15 ft or 5 m intervals to better characterize the near close approaches.

Long Parallels
It is almost impossible to keep a well straight, so the situation of having two wells with long parallel vertical sections before very deep kick offs should be avoided. (Even if it were possible to maintain a straight well, the survey uncertainty will be growing and with it the risk of collision). Where this happens the planner should include a 'nudge' to raise the inclination to around 5 degrees and return to vertical once enough separation had been achieved to compensate for the uncertainty at the deep kick off point.

CONTENTS

17. Understanding Error Models

17.1 Error Models and Instrument Performance Models

Historically four error models have been commonly used in the industry (including one special model developed by Shell for internal use only). These error models define how various error sources affect the observations in the well and thus the positional uncertainty along the wellbore. The mathematical relationship between for example, a bias error on the y axis accelerometer and the positional error at a given survey point is a complicated formula but easily established by these error models. The key to their ability to successfully represent the positional uncertainty is not usually the mathematics but rather the coefficients used to define the numerical accuracies for various tools and how they improve with corrections such as sag, IFR, stretch, interference corrections and so on.

The error models are:

The Cone of Uncertainty Model
The Wolff and De Wardt Error Model
The SESTEM Error Model
The ISCWSA Error Model

A brief explanation of each follows.

The Cone of Uncertainty was a simple model applied in the early versions of COMPASS introduced by Angus Jamieson in the early 1980s. It consisted of a simple ratio with measured depth that applied over a range of inclinations. For example, an MWD survey might provide uncertainty of 7ft/1000ft at up to 15° of inclination, then 10ft/1000ft at up to 30° degrees of inclination and so on. This model was widely used but is very conservative and probably not suitable for close drilling situations.

The Wolff and De Wardt Error Model was published in 1981 and used 5 separate sources of error. These are: a compass reference error; a drillstring magnetization error; an inclination error; a misalignment error; and a relative depth error. All tools were classified as either “gyro” or “magnetic” and either “good” or “poor” quality. A set of values (coefficients) were chosen for each tool and the mathematical model produced an ellipse of uncertainty around the wellbore that could be used for anti-collision calculations. These coefficients were only meant to be used for North Sea operations and were reference to the quality of tools available at the time.

In 1987 the **Shell Extended Systematic Tool Error Model (SESTEM)** was developed in The Hague by Robin Hartman. It provided a significant improvement on the earlier models. This model considers the equipment running conditions, the location of the well, the background magnetic field accuracy, and considers the measurement error sources at their individual component levels.

Around the same time, a group of industry wellbore surveying experts formed the **Industry Steering Committee for Wellbore Survey Accuracy or ISCWSA** under the leadership of Hugh Williamson. Under the auspices of ISCWSA a sophisticated model recognized as the industry standard has been developed.

An ‘IPM’ is an ‘Instrument Performance Model’ and describes the error sources, their magnitudes and how they propagate. It is these IPMs that determine how big the uncertainty envelope will be. The temptation is often to use IPMs that are overly optimistic. That is not a best practice. A good guideline is that the IPM values should be a realistic representation of the errors in the entire system and be able to be demonstrated by good quality control in the field or in the calibration process. In all cases the error models and IPMs should be agreed with the client during the well planning stage in order that subsequent changes do not render a planned well undrillable.

17.2 Modelling Uncertainty

Uncertainty modelling provides a method of determining how far out we might be when we estimate something. This can be very useful in all sorts of fields. If for example I were to take a bet on the height of the next person to walk down the street, I would want to know, first of all, what was the normal range of heights for people and even then I would not bet on the average. I would be much safer to bet that they fall between say 0.2 – 3.0 meters high so that I am confident that my bet is 'safe'.

In order to establish a 'safe' bet I need to know both the average and the range of the measurement I am trying to estimate. The German mathematician, Gauss described the 'Normal Distribution' of naturally occurring measurements (of which our heights are one). In this graph the x axis is height and the y axis describes the number of people in a given sample that might fall in a given height range.

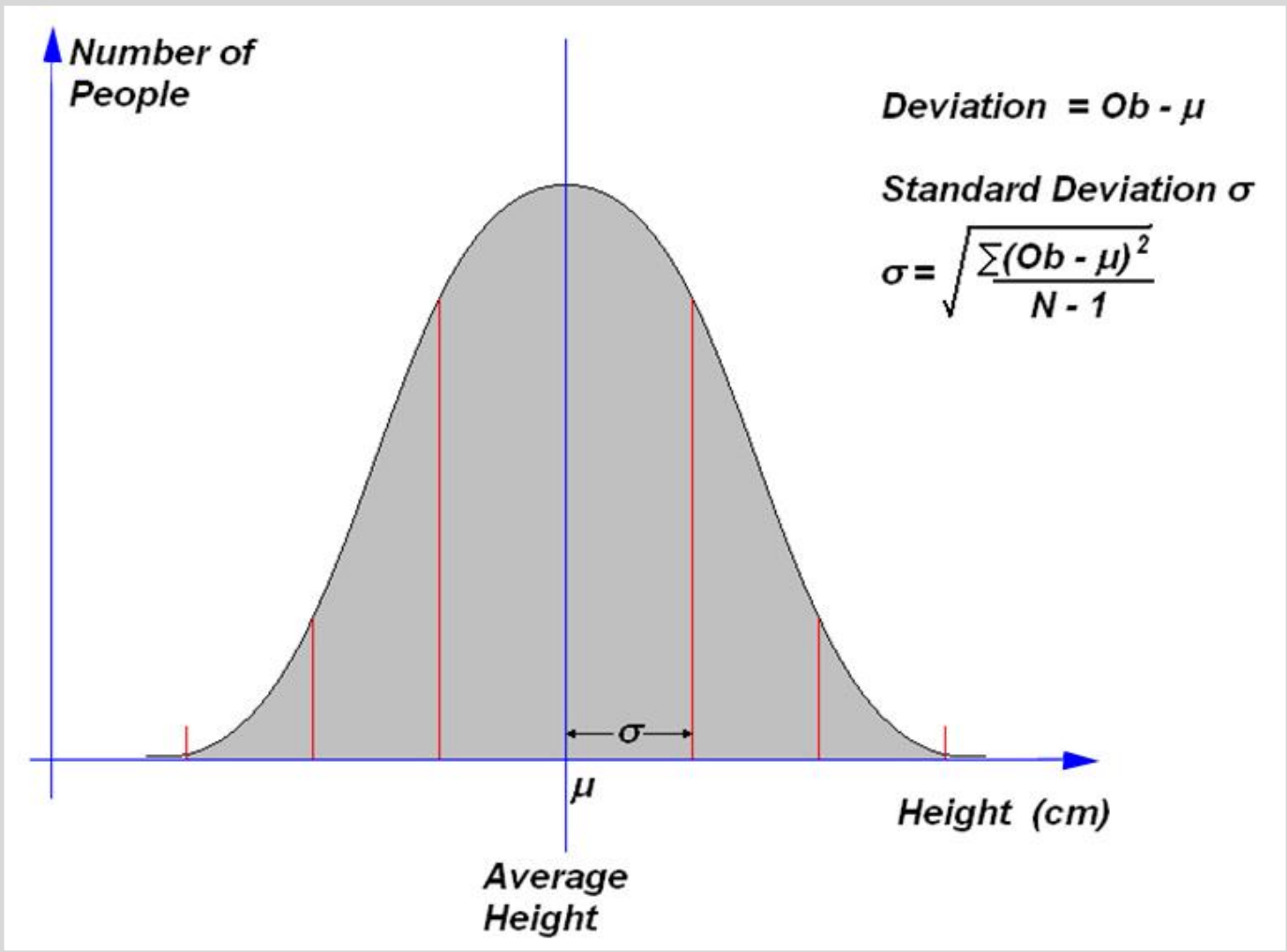

Figure 70: Modelling deviation graphically.

In this diagram the average height is in the centre and it can be seen that most people fall close to the average. The deviation of any observation is just how far it is from the average. For example if I am 1.80m tall and the average is 1.50m, my height "deviation" would be 0.3m. Notice that the greater the deviation from the average, the fewer people there will be.

The formula shows a useful parameter, the "standard deviation" which is the square root of the sum of all the deviations squared, divided by N-1 where N is the number of the sample. This number is used a great deal in uncertainty modelling and serves as a measure of the distribution around the average.

We usually use the Greek letter sigma (σ) for standard deviation.

For naturally occurring measurements Gauss showed that about 67% of observations will fall within 1 sigma, 95% within 2 sigma and 99.7% within 3 sigma. So if sigma is 0.2m and the average was 1.50m, I could bet on the next person to be between 1.3 and 1.7m and my "confidence" would be 67%. I am a Scotsman, not known for being overly generous so I may decide to bet at 2 standard deviations and say that the next person will be between 1.1m and 1.9m. Now my "confidence" goes up to 95%. If I am still worried, I could bet between 0.9m and 2.1m and now I would only be wrong 3 times in 1000 or 99.7% confident. Clearly with a critical estimate we would want a confident result. In theory it is not possible to obtain 100% confidence with the Gaussian model so we have set the limits somewhere. This is often referred to as "setting the sigma levels" and the higher the sigma levels, the lower the risk.

It should be noted that in nature nothing follows the Gaussian Model exactly. For example, we know that there are no people 3m high in the world so very low risk values are often ignored.

17.3 Probability in two dimensions

Something interesting happens when we try to guess two parameters at the same time and still need to be confident of our estimates. Let's say we now guess the person's height and their intelligence. First, it is important that we understand that these parameters are not "correlated". In other words, despite what your taller friends might like to think, there is no relationship between height and intelligence. If we were measuring height and weight, we might expect some "correlation" since taller people are probably going to be heavier than shorter people in general.

Watch what happens when we plot the normal distribution curves for the two parameters at once. In this diagram I have drawn the distribution curves on IQ for two height groups on either side of average height. Note that the average IQ for the small group is the same as the average IQ for the tall group.

This demonstrates no correlation between height and intelligence. The average intelligence of all height groups remains the same.

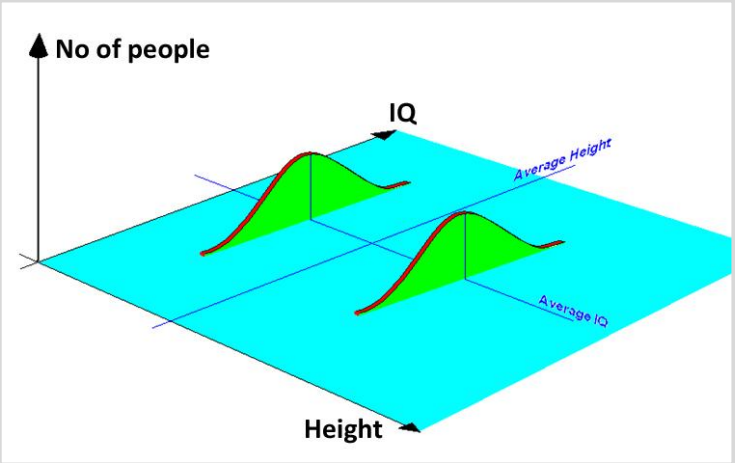

Figure 71: Plotting two normal distribution curves at once.

Now we shall plot all the normal distributions for all the height groups.

This normal distribution "mountain" describes the probabilities of two parameters whose ranges are not the same. Any probability "contour" on the slopes of this mountain will therefore be elliptical in shape since the IQ range and the height range have different values.

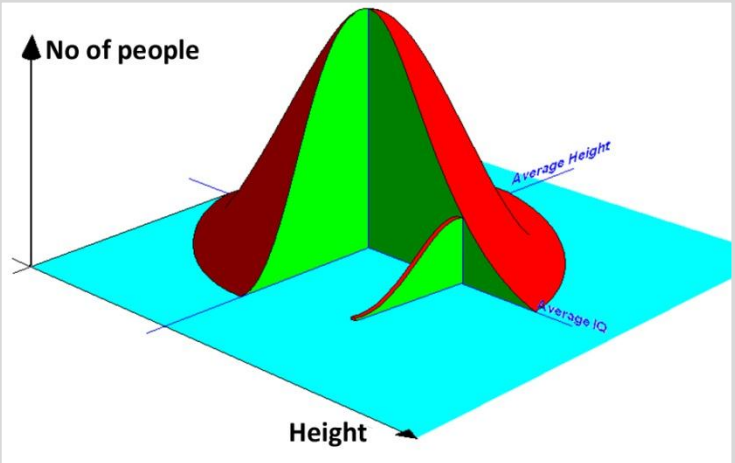

Figure 72: Plotting where ranges are not the same

Now we shall apply this to a section of wellbore. Let us imagine that the well section is straight and has an inclination "I" and an azimuth "A" but both are potentially in error.

An ellipse of uncertainty is formed around the wellbore where the lateral dimension is proportional to the azimuth error and the high side dimension is proportional to the inclination error. If the azimuth was more accurate than the inclination, the ellipse would be thinner across the wellbore. This example is more typical with the azimuth less certain than the inclination, creating an ellipse with a larger lateral dimension. The final shape is like an almond, elliptical in all three orthogonal planes.

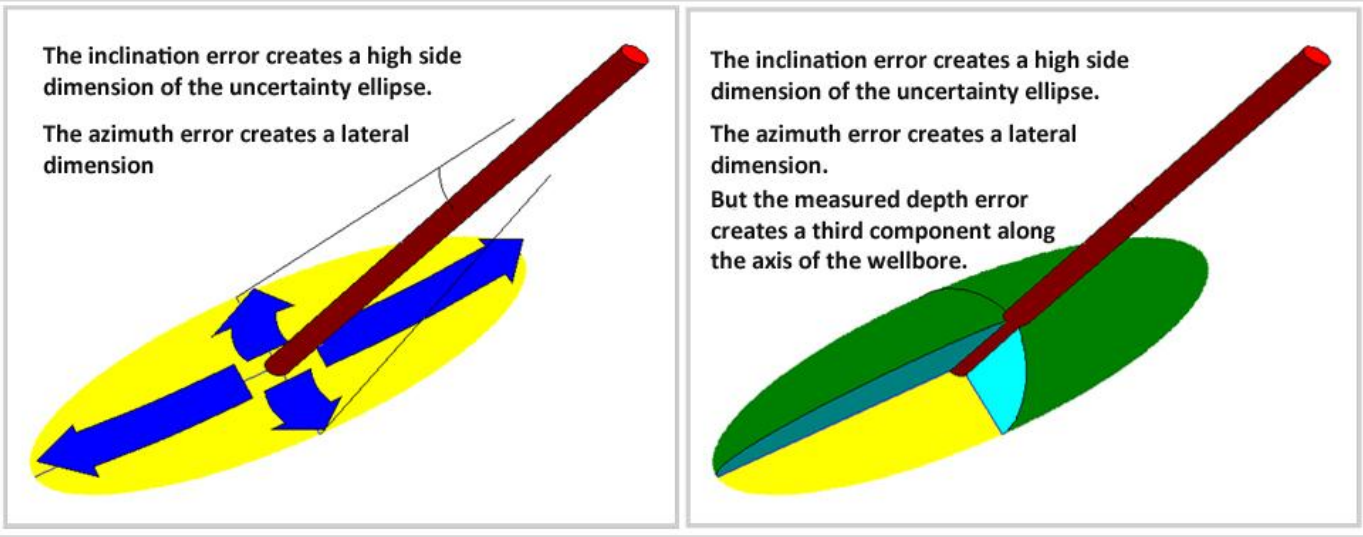

Figure 73: Applying normal distribution modelling to a section of the wellbore.

17.4 How can we determine the size and shape?

In reality this is a complex calculation best left to computer software but a very simple rule of thumb can estimate spatial error from an angular error as follows:

1 degree in angle creates about 2% in distance.

For example; if a line of 1000 m was measured on a bearing of 90 degrees plus or minus 1 degree, the final point would be in error by approximately +/- 2 0m.

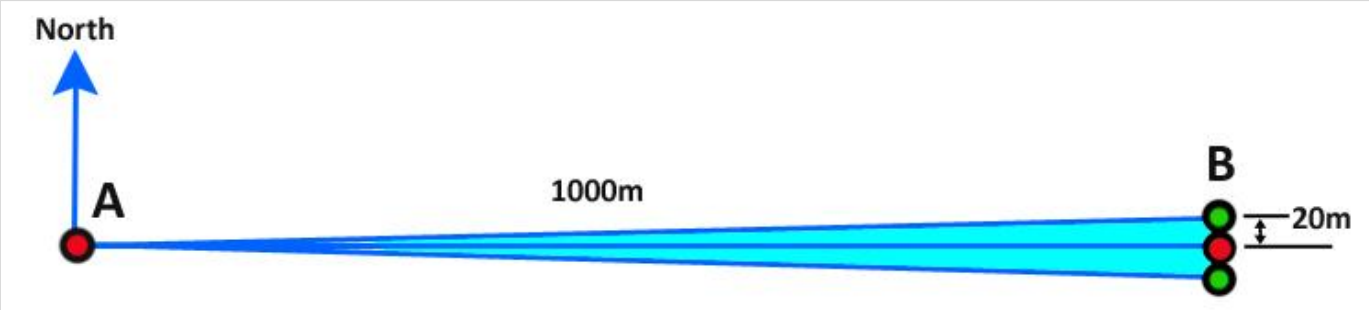

Figure 74: Trajectory error calculations.

The correct answer would be closer to 1000 sin (1o) = 17.45m but as a conservative estimate the 2% per 1° rule is easy to calculate.

It is not true that errors are proportional to measured depth. In surveying, systematic (i.e. unchanging) errors propagate in proportion to how far you are from your origin. A compass reference error for example may pull you to the right as you walk away from the origin but will still pull you to the right as you return effectively cancelling out the positional error. A scaling error may underestimate your distance from the origin but equally it will be proportional to the distance and will cancel out on the return. When estimating the likely positional error, we can use this simple fact and the assumption that the dominant errors are systematic. Clearly though, not all errors are.

Some errors like gyro drift are time dependent and therefore continue to get worse, the longer the route and others are random like the effects of inadequate survey intervals but we can still come up with a rough estimate that will allow us to assess the realism of any quoted error models and the likelihood of hitting a target.

In this example a target is to be drilled with MWD with the following typical accuracies: measured depth is good to 2m/1000m, inclination to +/- 0.3° and azimuth to +/- 1°. Let's try to work out the approximate ellipse of uncertainty by the time we reach the target.

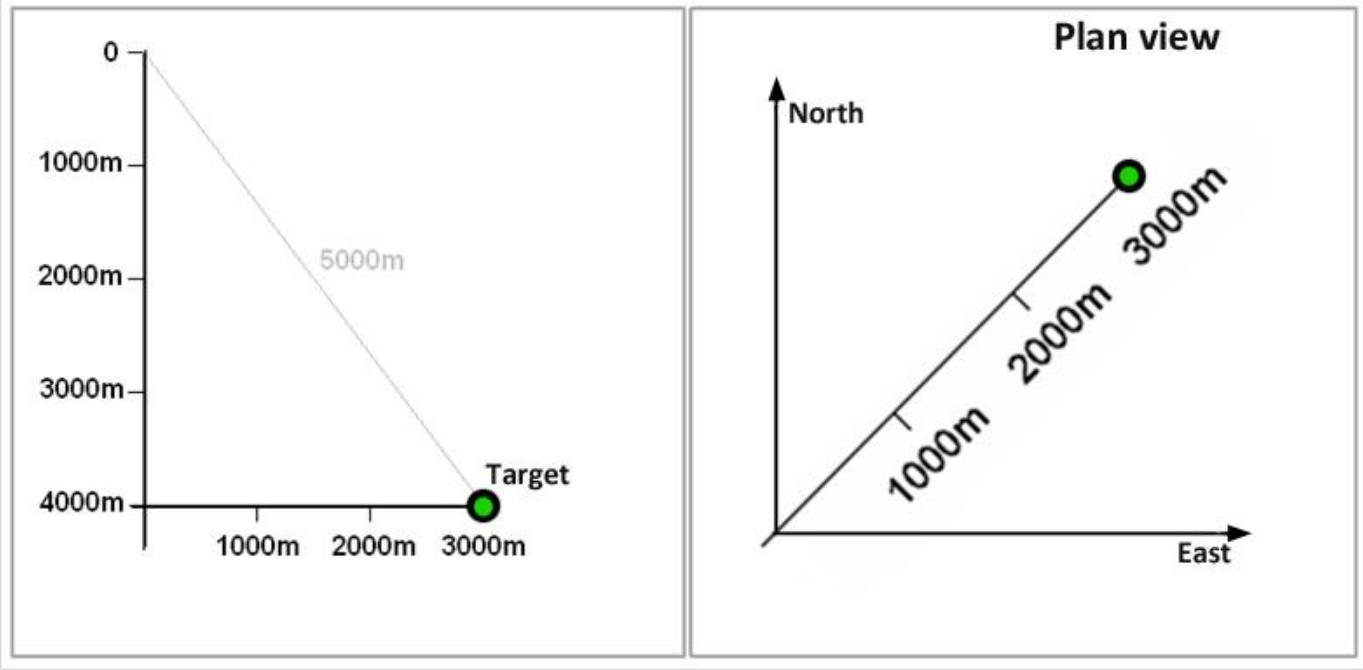

Figure 75: Plotting the uncertainty.

Firstly let's determine the effect of the measured depth error of 2 m/1000. In this simple example, this can be determined without knowing the planned trajectory. The accumulated error at the target will be the same no matter what path we take to get there. This is not necessarily obvious. Using the fact that survey error propagates with distance from origin we can draw the uncertainty axis created by depth error as a line of 10 m (2m/1000m x 5000m distance) towards and away from the origin.

By way of example, if the well was drilled as a horizontal well with 4000 m vertical drilling and 3000 m horizontal drilling after a sharp build to horizontal, the total MD would be 7000 m. Let's say that the depth was overshooting by 2 m/1000 m.

In this case, the depth error would be 2m/1000m x 7000m = +/-14m.

If this had been a straight vertical well our depth could actually be anywhere between 6986 m and 7014 m.

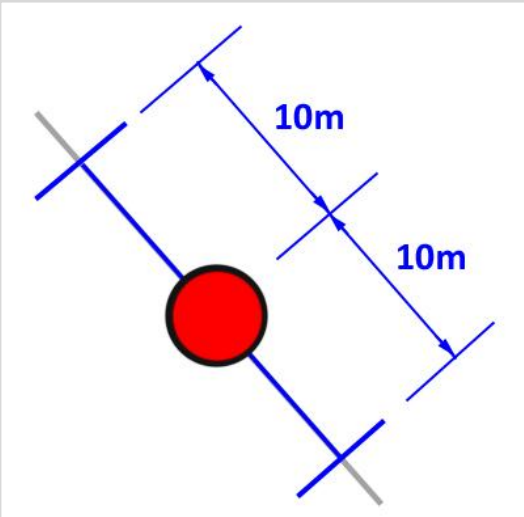

Figure 76a: Calculating positional error.

But in this case when we are only 5000 m from our origin our depth error at our presumed position is 2m/1000m x 5000m = +/-10m. Traveling to our target position would be to over/under shoot the vertical by 8 m and over/under shoot the horizontal by 6 m creating a positional error of 10 m on the axis shown above.

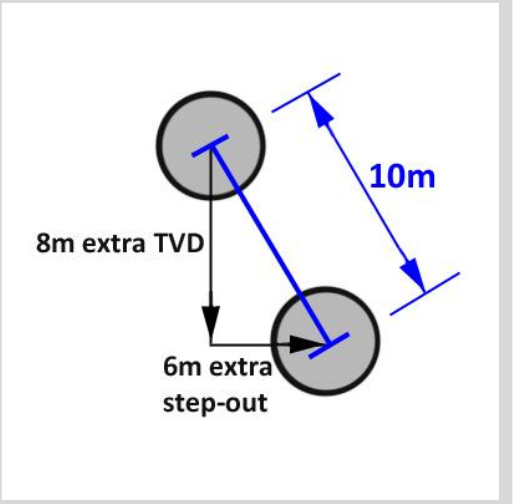

Figure 76b: Calculating positional error.

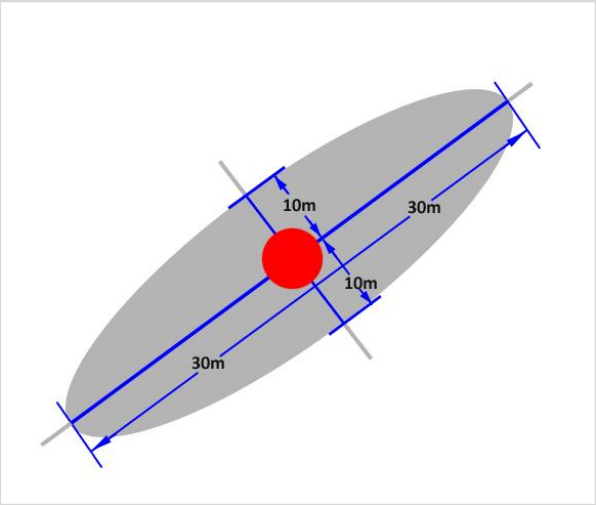

Figure 76c: Calculating positional error.

The effect of the inclination error can similarly be calculated using our simple rule. Inclination only affects the vertical plane and we are 5000 m from the origin in this plane so the positional error will be at right angles to our space vector and will have a magnitude of 0.6% of 5000 m or 30 m.

The third axis will be in the horizontal plane and is due to the azimuth error of 1°. This will produce an ellipse axis across the wellbore of approximately 2% of 3000 m which is 60 m. It is quite common for the azimuth error to be the dominant error in a 3D ellipse of uncertainty. These ellipses are not to scale but show the orientations and relative sizes.

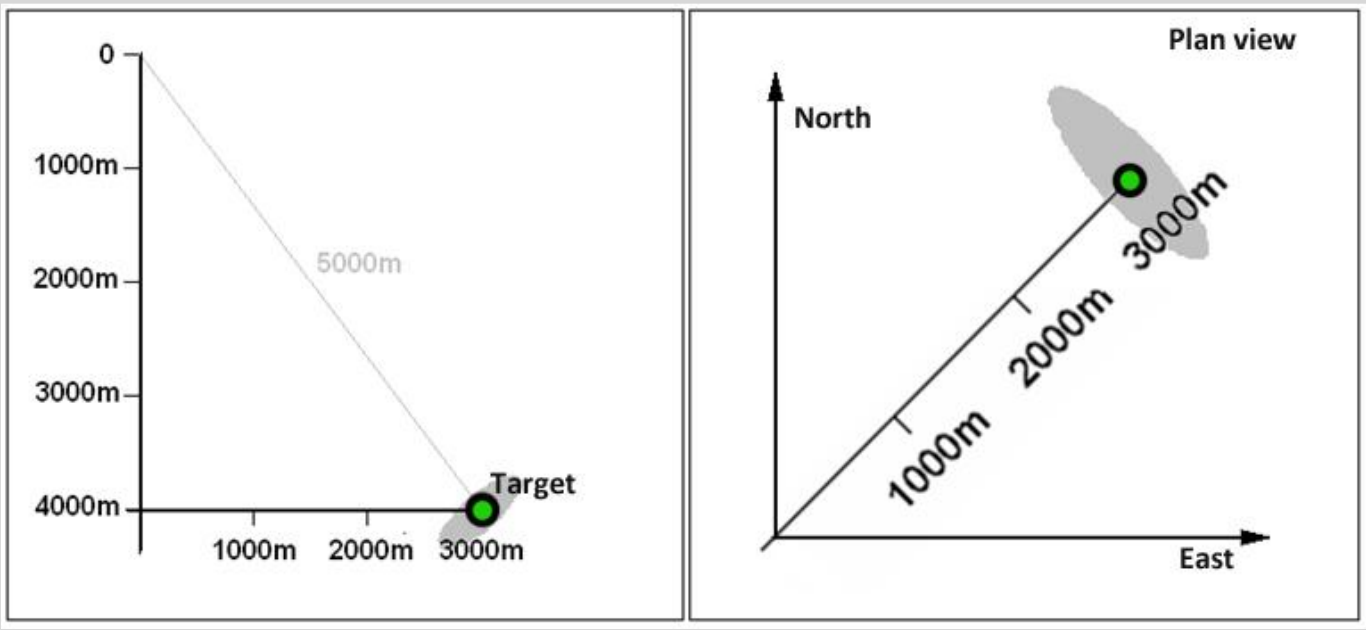

Figure 77: Plotting the ellipse uncertainty.

✧

CONTENTS

18. The ISCWSA Error Model: Introduction

For a detailed description of the ISCWSA error model, please see Chapter 19 by Dr Andrew McGregor.

18.1 Some background to ISCWSA

The Industry Steering Committee on Wellbore Survey Accuracy (ISCWSA) is seeking to dispel the confusion and secrecy currently associated with wellbore surveying and to enable the industry to produce consistent, reliable estimates of survey-tool performance in today's wells. They believe this will be achieved through the production and maintenance of standards covering the construction and validation of tool error models.

Work focused initially on MWD systems. They provide a large proportion of the total directional survey data world-wide and, because of their similarities between suppliers, are more amenable to specification standardisation than other types of survey tool. The results of the work on an error model for a basic directional MWD service has been presented in SPE 56702 'Accuracy Prediction for Directional MWD' by Hugh Williamson, at the 1999 SPE Annual Technical Conference and Exhibition in Houston, Texas, held from the 3-6 October 1999.

An updated version of this paper (SPE 67616) has been published in the December 2000 edition of SPE Drilling and Completion (Volume 15, Number 4, pages 221 to 233).

A gyro error model has been produced and published in paper SPE 90408 'Prediction of Wellbore Position Accuracy When Surveyed with Gyroscopic Tools' by Torgeir Torkildsen, Stein Havardstein, John Weston and Roger Ekseth.

Depth issues have been investigated and the results published as SPE 95611, "Quantification of Depth Accuracy", which was presented at the SPE Annual Technical Conference, Dallas, 9-12 October 2005.

Up till now, the process has been explained very simply to demonstrate how angular errors combine to produce elliptical uncertainty envelopes. In practice there are several sources of error all affecting the wellbore position in different ways and the ISCWSA error model provides a rigorous mathematical approach to combining these various sources into one 3D ellipse.

LINK ISCWSA website

18.2 Covariance

First we have to introduce the idea of "covariance".

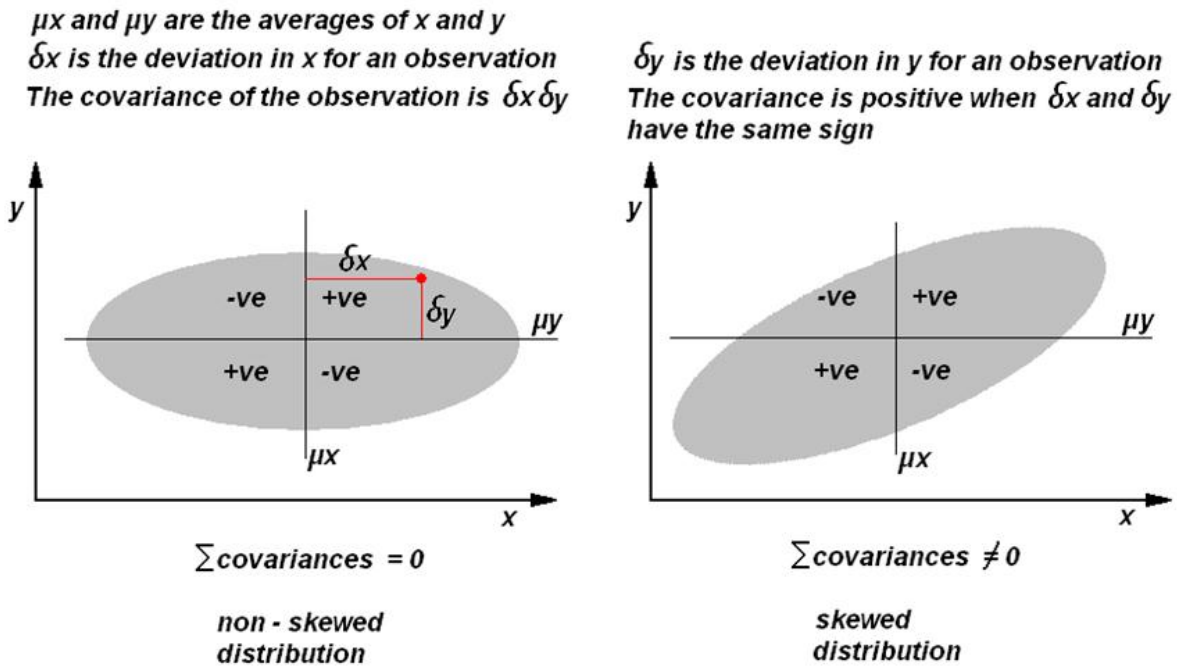

As the name suggests it is a measure of how parameters vary together. Recall that we discussed how height and weight might vary together (correlate) but height and intelligence do not. If we measure the variance of an observation it is simply the square of the deviation but the covariance is the product of the deviations of two parameters. The covariance helps us to measure the correlation which shows up as a "skew" in the ellipse.

Figure 78 above shows this, but it is also true in 3D and if we can build up a matrix of covariances in northings, eastings and TVD we can derive an ellipsoid, its dimensions and orientation in 3D space.

In order to build up this matrix we need to know how each error source affects the observations and how the observation error will move the wellpath in North, East and vertically in TVD.

18.1.1 How the errors affect the observations.

These error sources are multiple and varied. In the ISCWSA error model there are dozens of error sources. Each will affect a given survey station in different way. For example the accuracy with which we know our magnetic north would be a simple azimuth effect. This will not have any effect on either inclination or measured depth observations. "Weighting Functions" are used to determine the effect any error source will have on MD, inclination and azimuth respectively. We say that the weighting functions for a compass reference error are (0, 0, 1) i.e. they have no effect on MD, no effect on inclination and a full effect on azimuth.

However a tool misalignment due to a bent housing in the assembly might affect inclination or azimuth depending on the toolface. In this case the weighting function would be (0, cos(Toolface), sin(Toolface)). A drillpipe stretch error would have a weighting function of (1, 0, 0) as you might expect and a BHA sag correction error would have a weight function of (0, 1, 0). The ISCWSA error model SPE paper 67616 (from the ISCWSA website – iscwsa.org) details all the weighting functions for all the error sources.

The next step is to determine the effect of the observation error on the well path position. In this diagram you can see that a measured depth error could affect North East and TVD.

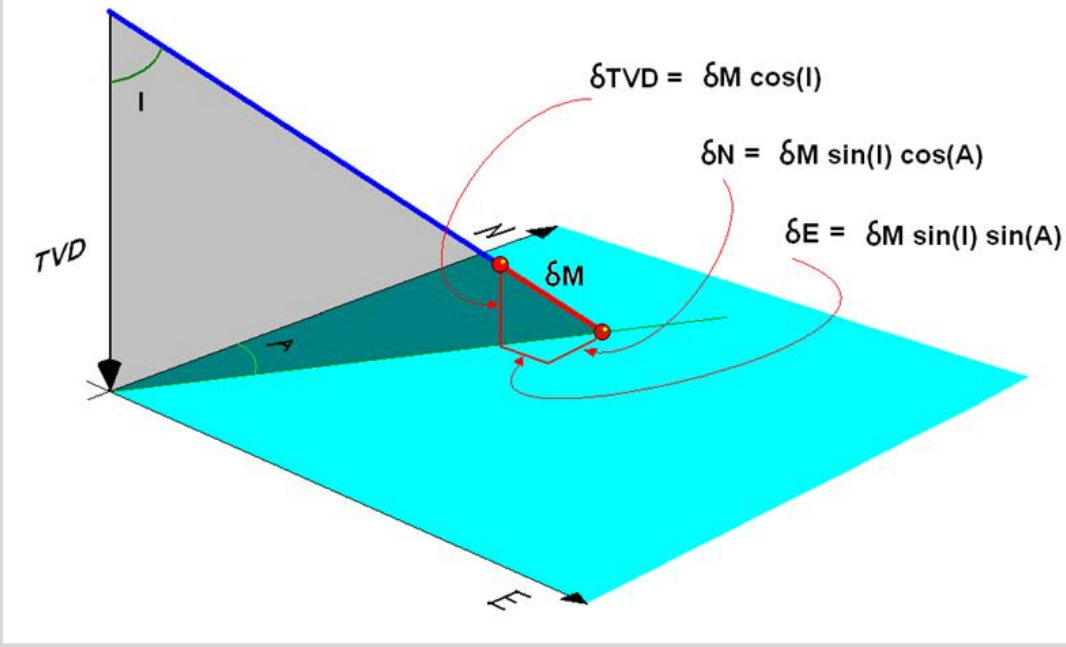

Figure 79: Showing that a measured depth error could affect North, East and TVD.

But an azimuth error only affects North and East, so we get the following:

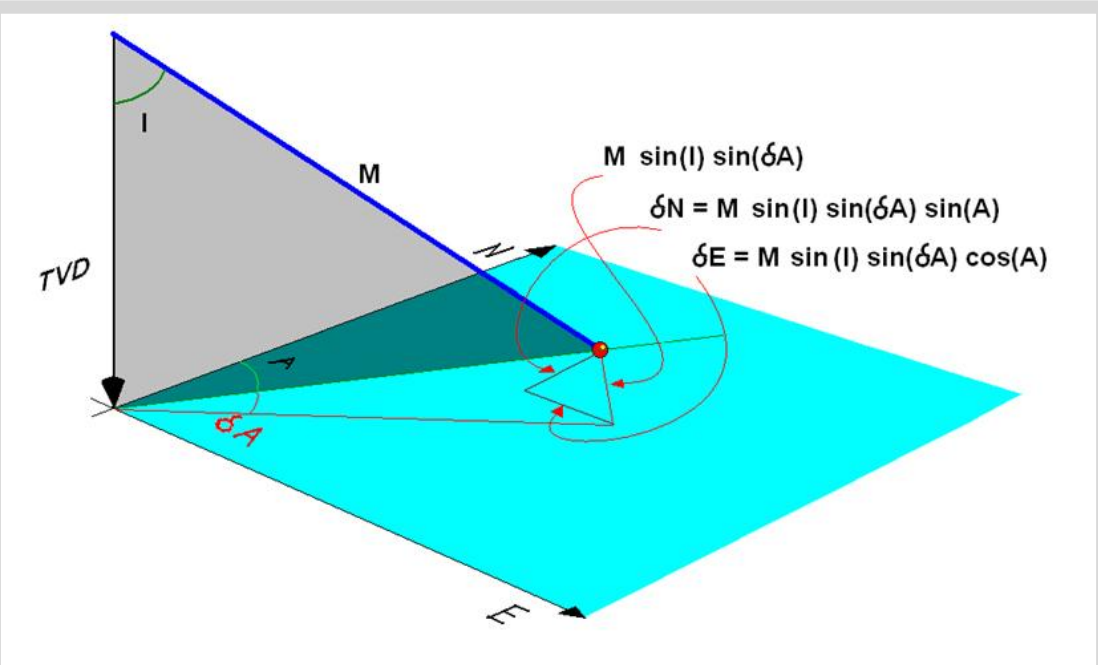

Figure 80: Effect of azimuth error on North and East elements.

18.3 The Variance Covariance Matrix

The Variance Covariance Matrix		
$\sum \delta N^2$	$\sum \delta N \delta E$	$\sum \delta N \delta V$
$\sum \delta E \delta N$	$\sum \delta E^2$	$\sum \delta E \delta V$
$\sum \delta V \delta N$	$\sum \delta V \delta E$	$\sum \delta V^2$

When accumulating the matrix, care has to be taken to ensure that errors that correlate from one survey station to the next are added to the delta values directly before summing but errors that can vary from one survey to the next are summed in their product form. This ensures that random and systematic effects are propagated correctly. Some errors also continue from one survey leg to another and some even from one well to another such as the error in magnetic north.

Once the matrix is complete a technique is required to derive the size and orientation of the three main axes.

18.4 Eigen Values and Eigen Vectors

Imagine looking at an almond which you are holding in your hand. You can choose to look at it from above, in front or any other direction in space. However, no matter how the almond is oriented there will always be three orthogonal viewing vectors that let you see the ellipses of the almond at their full size. In other words if you line up your eye on one axis, you will see the ellipse formed by the other two with no foreshortening effects.

Eigen vectors provide a way to derive the best viewing angles to see the 3 uncertainty ellipses. The Eigen vectors of the Covariance Matrix describe the "attitude vectors" of the three axes and the Eigen values tell us their length. The mathematics of converting a 3 x 3 Covariance Matrix to its Eigen vectors and Eigen values is very straightforward and provides us with the dimensions and orientation of our uncertainty ellipsoid. It is a matrix manipulation that finds the 'viewing' vectors that leave the main dimensions of the ellipse on the leading diagonal with zeros for all the covariances when seen from these axes.

By accumulating these ellipsoids along the wellbore, we create an "uncertainty envelope" like a funnel around the wellbore which we can then use to ensure a safe passage when drilling close to other wells.

18.5 Collision Risk

It would be wrong to think that if two uncertainty envelopes were touching there was always a high risk of collision. We often use between 2 and 3 standard deviations when determining the size of our ellipses which means that probability of being outside the ellipse is very small.

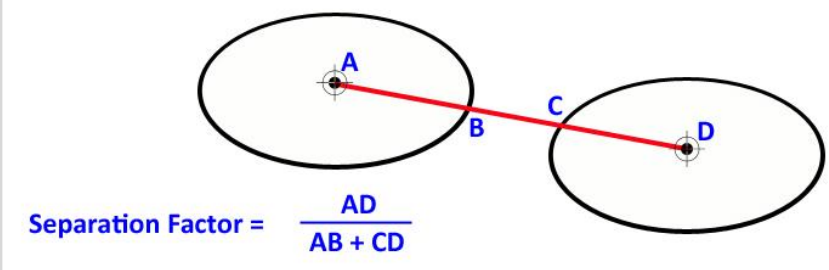

Figure 82: Calculating and plotting the collision risk.

When considering collision risk we often use the separation factor calculated in a plane at right angles to the offset well. This simple formula is one method of calculating separation factor. A separation factor of one would indicate that the ellipses were just touching. By way of example, if the hole size occupied one third of the ellipse and the ellipse was set at 3 standard deviations, the probability of these wells colliding would be less than 1 in 300,000 but the risk rises rapidly as the ellipses overlap. The separation factor is an excellent way of drawing attention to high risk areas quickly then more detailed analysis may be needed to determine the safety of continuing to drill.

18.6 Definition of Ellipse Axes

There is no recognized industry standard for defining the dimensions of the ellipse of uncertainty. The axes can be either the true 3D axes length or a projection usually in the horizontal plane or the perpendicular plane (looking down the wellbore). TVD Spread is always the vertical TVD occupied by the ellipse of uncertainty.

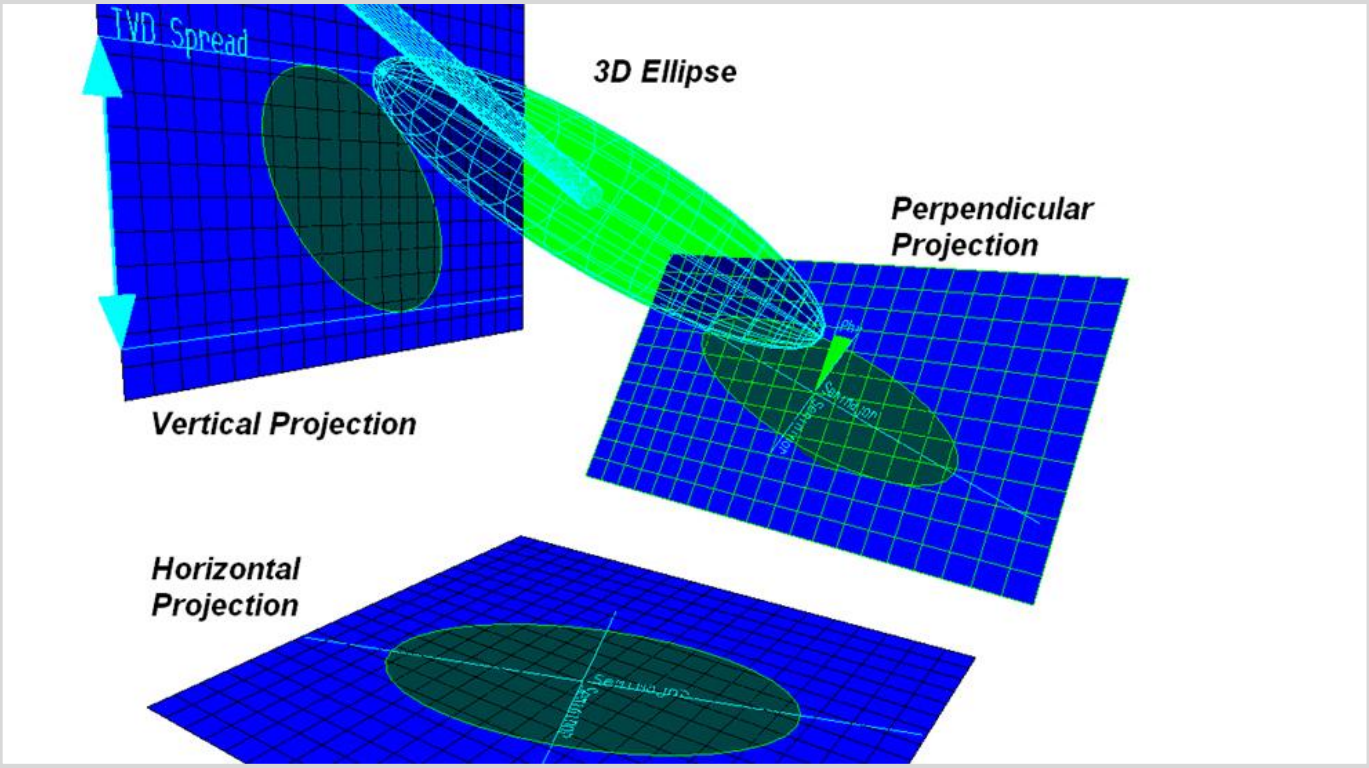

Figure 83: The ellipse of uncertainty mapped in 3D software.

Care should be taken when interpreting an ellipse of uncertainty report. Different companies report different definitions of the ellipse. The real uncertainty envelope is a 3 dimensional body and most software applications project this into a plane. In the graphic above, it can be seen that the plane may be vertical, horizontal or perpendicular to the wellpath. As a result the quoted semi major and semi minor axes (and possibly orientation) may mean any of the following;

- The 3D dimensions of the ellipse closest to the lateral and high side vectors.
- The horizontal projected ellipse major and minor axes and orientation from north.
- The perpendicular projected major and minor axes and orientation from high side

TVD Spread nearly always means the TVD occupied by the ellipse but can be quoted as a plus or minus number or an enclosing value.

Historically there has been no standardization of these terms but clearly they will produce different results for the same well path with the same error model.

18.7 How errors propagate

Errors in measurement systems can propagate randomly or systematically. The random errors tend to have a cancelling out effect over multiple observations as their effect can be positive or negative from observation to observation. The systematic errors are the ones that generally expand to dominate the error envelope since their effect is the same from observation to observation.

As an example of a systematic error, the azimuth error in MWD is largely created by the uncertainty of the magnetic field direction (declination). Clearly this does not change from one observation to another and can be taken as a systematic shift in azimuth. A misalignment error on the other hand would be considered random since its effect is toolface dependent and the surveys will have a scatter of tool faces throughout the survey.

Some errors, like declination, are referred to as 'global' in that they effect every survey in every well in the same field where the declination is uncertain. Others vary from one well to another such as vertical reference and others vary from one survey leg to another such as sensor errors. When we accumulate the uncertainties in a formal error model, the propagation effects of each error source are correctly accumulated so that global errors are always present and random errors are accumulated with RMS values across the boundaries where they become randomized. For a misalignment that is every survey station, for a sensor error, that is every survey leg, for a reference error that is for the whole well and for declination error that would be applied to every well in the field.

The next chapter describes the ISCWSA error models in more detail.

CONTENTS

19. The ISCWSA Error Models: Explanation and Synthesis

This chapter is included courtesy of Andrew McGregor of Tech21 Engineering Solutions, from a paper produced for ISCWSA. The text and associated appendices are taken from the paper:

The ISCWSA Error Models: An Explanation and Synthesis, version 11.

19.1 Introduction

Like all measurements, borehole surveys are subject to errors and uncertainties which mean that a downhole survey result is not 100% accurate. For many applications, such as anti-collision and target sizing, it is very important to be able to quantify the position uncertainty around a wellbore trajectory. However, since many different factors contribute to the final position uncertainty it is not a trivial matter to determine these bounds.

The Industry Steering Committee for Wellbore Survey Accuracy (ISCWSA) has produced an error model in an attempt to quantify the accuracy or uncertainly of downhole surveys. The error model is a body of mathematics for evaluating the uncertainty envelope around a particular survey.

Originally the error model dealt with only MWD surveys, but it has later been extended to also cover gyro surveys. This document sets out to provide an overview and understanding of these models. The full details can be found in two SPE papers; SPE-67616 and SPE-90408 (see references below). There have also been successive revisions to both models, details of which can be obtained from the ISCWSA website iscwsa.org

The error model identifies a number of physical phenomena which contribute to borehole survey errors and provides a mathematical framework for determining in numeric terms the uncertainty region around a particular survey. Typically this error model will be implemented in directional drilling software. The user will select the appropriate tool model for the survey tool that has been run and the error results will be used in anti-collision or target sizing calculations.

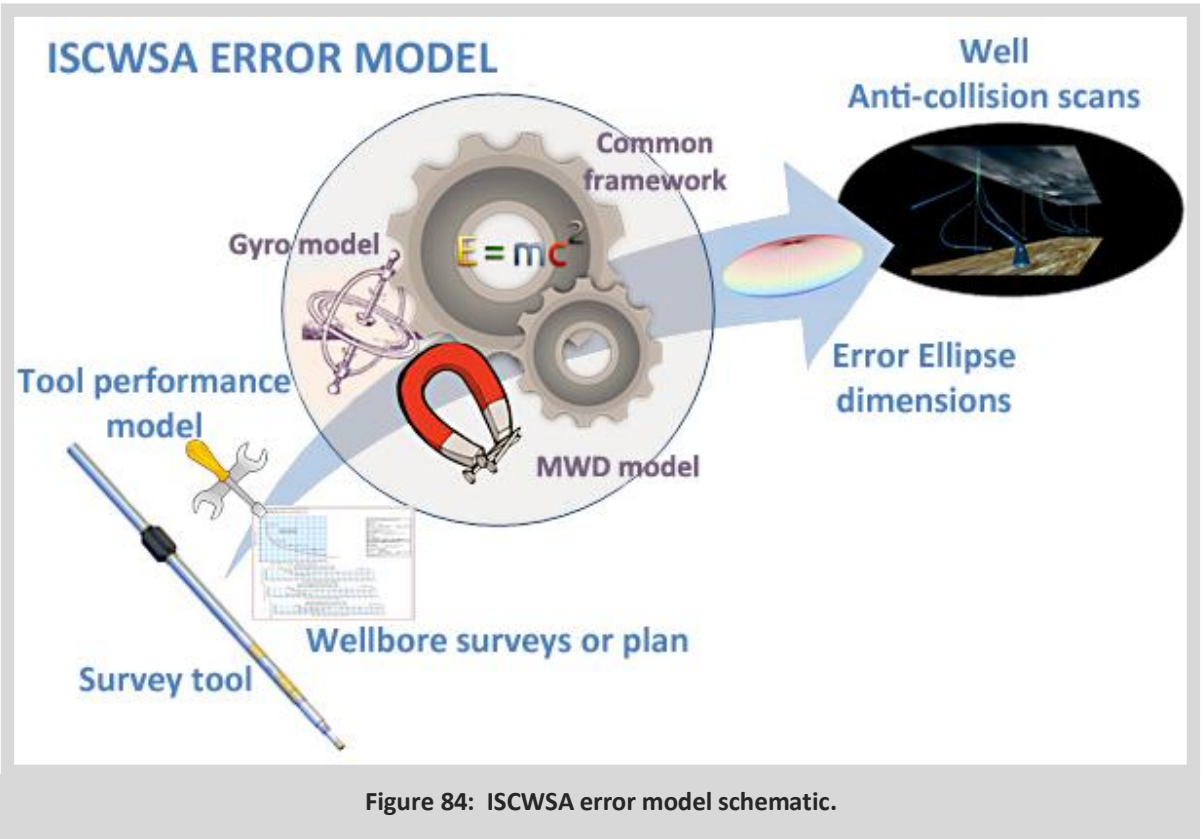

Figure 84: ISCWSA error model schematic.

In simple terms, the error model is a means to start from a gyro drift specification in deg/hr or a tool misalignment in degrees and evaluate how that error effects the borehole survey measurements of inclination, azimuth and measured depth at a particular survey station. The model then propagates and combines these error contributions, taking into account all of the important physical errors, at all of the survey stations from all of the survey runs within a well. The final results are error ellipse dimensions, in metres or feet, within which the actual wellbore is expected to be found to a specified level of confidence.

It is common to talk about the MWD model and the gyro model, but in fact these both of these models share a common framework for describing and propagating the errors. This document will present some of the background information on the ISCWSA models before presenting this basic mathematical framework on which they are based. The MWD model is described in some detail, followed by a discussion of the gyro error model. There follows a section which is concerned with implementation details, which will mainly be of interest to software developers. The last section discusses standardisation of the model.

There is some maths in these early sections but it should still be possible to follow the thread of the discussion without worrying too much about the details of the equations. For those with a thirst for more, three appendices present in detail the mathematics of the framework and all of the weighting function equations.

To follow the discussion, the reader should at least be familiar with the basic concepts of borehole surveying. A good starting point would be an understanding of chapters 5 and 10 of this book which describe the principles of MWD and gyro tools and also chapters 18 and 20 which present an introduction to error modelling and error propagation.

19.1.1 Assumptions and Limitations of the ISCWSA Model

The error model is designed to be a practical method that can be relatively easily implemented in software and then used by well planners and directional drillers. It is intended to be applied to a range of tools, used worldwide and accordingly attempts to give good representative survey uncertainties, without the need to model every single variation of tool or running conditions.

The model only applies to surveys run under normal industry best-practise procedures which include:

a. rigorous and regular tool calibration,
b. a maximum of 100ft survey intervals.
c. field QC checks, such as total magnetic field, gyro drifts , total gravity field and magnetic dip angle on each survey measurement,
d. the use of non-magnetic spacing for MWD surveys according to industry norms,
e. for MWD, surveys taken in a magnetically clean environment away from casing and adjacent wells.

It should be recognised that the model cannot cover all eventualities and works on a statistical basis and so does not say anything specifically about any individual survey. The results can be interpreted as meaning that if a well was properly surveyed a number of times by a variety of different tools with the same specification, then the results would be expected to be randomly distributed with a range of values corresponding to the error model uncertainty results.

The model cannot cover gross blunder errors such as user error in referencing gyros, defective tools or finger trouble entering surveys into a database. The model does not cover all variations and all possibilities in borehole surveying, For example survey data resolution is not modelled.

To qualify under the assumptions, the survey interval should be no more than 100ft. If the survey interval is greater than 100ft then strictly the model is not applicable. Hence, the error model does not include penalty terms for intervals greater than 100ft, nor does it model any improvements for shorter survey spacing.

MWD surveys which are subject to external magnetic interference will generally fail QC checks. The effect on survey accuracy of magnetic interference from adjacent wells or from casing, can vary enormously and in many instances are impossible to quantify. The error model does not attempt to determine the size of the error for any surveys which are subject to this kind of interference.
Finally, a major misconception is that the ISCWSA provides certified error models for specific survey tools. The published ISCWSA papers only define the process and equations to work from a set of error model parameters to an

estimate of position uncertainty. The ISCWSA committee does not define, approve or certify the tool codes containing the actual error model magnitudes which drive the error model. These should be obtained from the survey contractor who provides the tool, since they are the ones best placed to understand the specifications and limitations of their tools.

Only in the specific cases of a standard MWD tool, or a MWD tool with an axial (short-collar) interference correction applied does the ISCWSA specify any parameter values.

19.1.2 References in this chapter

1. Accuracy Prediction for Directional Measurement While Drilling
   Hugh Williamson, SPE-67616
2. Prediction of Wellbore Position Accuracy When Surveyed with Gyroscopic Tools
   Torgeir Torkildsen, Stein Harvardstein, John Weston, Roger Ekseth, SPE-90408
3. Quantification of Depth Accuracy
   A.Brooks, H Wilson, A.Jamieson, D.McRobbie, S.G.Holehouse SPE-95611
4. ISCWSA MWD Error Model Revisions
   S. Grindrod, rev6 8/10/09 available at www.iscwsa.org
5. MWD Toolface Independent Error Terms
   S. Grindrod CDR-SM-03 Rev4 November 2009 available at www.iscwsa.org
6. Confidence Limits Associated with Values of the Earth's Magnetic Field used for Directional Drilling
   Susan Macmillan, Allan McKay, Steve Grindrod SPE/IADC-119851
7. A Comparison of Collision Avoidance Calculations
   Shola Okewummi, Andrew Brooks SPE/IADC-140183
8. Borehole Position Uncertainty; Analysis of Measuring Methods and Derivation of Systematic Error Model Chris J.M. Wolff and John P. DeWardt SPE-9223

19.1.3 Abbreviations

BGGM	British Geological Survey Global Geomagnetic Model
HLA	Highside – Lateral – Alonghole Co-ordinate system
IFR	In Field Referencing
IPM	Instrument Performance Model
IGRF	International Geomagnetic Reference Field
ISCWSA	Industry Steering Committee for Wellbore Survey Accuracy
MWD	Measurement Whilst Drilling
NEV	North – East – Vertical Co-ordinate system
RSS	Root Sum Square
SPE	Society of Petroleum Engineers

19.1.4 Nomenclature

The following variables are used in the weighting functions:

A_m	magnetic azimuth
A	true azimuth
B	magnetic total field
B_H	horizontal component of magnetic field
D	along-hole depth
ΔD	along-hole depth between survey stations
G	Earth's gravity
I	inclination
α	toolface angle
Ω	Earth's rotation rate
ϕ	latitude
Θ	magnetic dip angle

γ	xy-accelerometer cant angle
f	noise reduction factor for initialisation of continuous surveys
k	logical operator for accelerometer switching
v_d	gyro drift
v_{rw}	gyro random walk
w_{12}	misalignment weighting term
w_{34}	misalignment weighting term

19.1.5 Definition of Axes

For clarity the following axes sets are used in the error model:

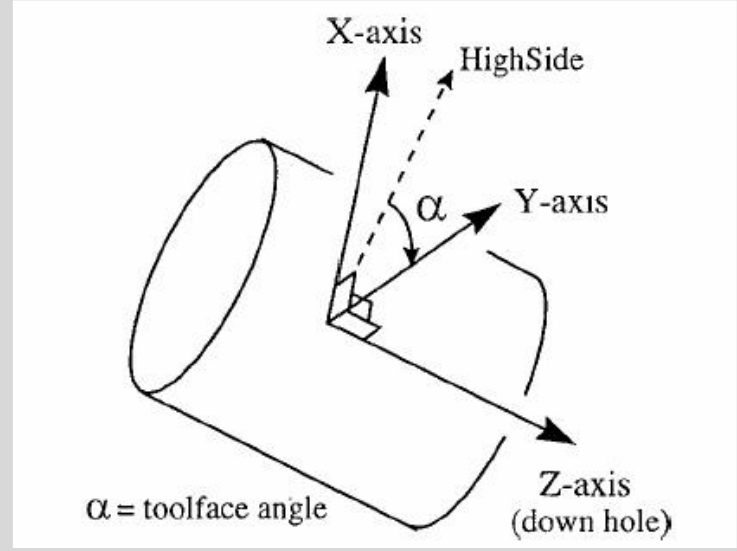

Figure 85: Error model axes definition.

Body Reference Frame (tool axes);

The z-axis is coincident with the along hole axis of the survey tool and the x and y-axes are perpendicular to z and to each other. This is axes set used to describe orientations of the various sensors.

Earth Centred Reference Frame (nev);

The x-axis is in the horizontal plane and points toward true north, the y-axis is also in the horizontal plane and points towards true east. The z-axis points downwards.

Borehole Reference Frame (hla);

The z-axis is aligned along the borehole axis. The x-axis is perpendicular to z and points toward the high side. The y-axis perpendicular to both of these and hence is laterally aligned across the borehole.

19.2 Framework of the Error Model

19.2.1 Overview of the Error Model

The basic purpose of the error model is to combine the effects of the various different physical factors which lead to survey errors in order to determine the 3-dimensional position error ellipse at any particular survey station. The same basic mathematical framework is used for both the MWD and gyro error models.
To do this,

i) the model identifies a number of **error sources** which effect downhole surveys. These are identifiable physical phenomena which will lead to an error in the final wellbore position; for example the residual sensor error after calibration.
ii) each error source has an **error code** string such as ABZ or MSZ. This is simply a shorthand identifier.
iii) each error source has a set of **weighting functions**, which are the equations which describe how the error source effects the actual survey measurements of measured depth, inclination and azimuth.
iv) Each error source also has a **propagation mode** which defines how it is correlated from survey to survey; this is used in summing up the errors.
v) for a particular survey tool, each error source has an **error magnitude**.

Before we discuss each of these items in detail, here is an example of how the error model works which should help to illustrate what these terms mean.

Example 1: Declination error
Downhole MWD tools measure magnetic azimuth and in order to calculate the true (or grid) north azimuth values, the declination term has to be added to the downhole data:

$$A_{true} = A_m + \delta$$

Usually, declination is determined from a global magnetic model like the BGGM or IGRF models. However, these work on a macro scale and may not be totally accurate in an oil field. So there is some uncertainty (or error bounds) on the declination value and this is clearly a possible source of survey error.

Therefore, the MWD model identifies an ***error source*** with the mnemonic ***code*** DEC which can be used to model declination uncertainty. From the above equation we can see that a declination error will lead directly to an error in the true azimuth, but it has no effect on inclination or depth measurements. Hence the DEC ***weighting functions*** are [0,0,1] (i.e. md=0, inc=0, az=1).

The standard MWD model gives the DEC error source a ***magnitude*** of 0.36˚. If an In-Field Reference survey was carried out in the field then the declination uncertainty would be smaller and there could be a different tool model for MWD+IFR with a smaller magnitude for this error source.

If we assume that, whatever the value, the declination is constant over the whole oil field then all MWD surveys, with all different survey tools and in all BHA used in all the wells in the field will be subject to the same error. Hence then DEC term has a global ***propagation mode***.

Declination error is a function of the Earth's magnetic field and has no influence on gyro survey tools, so the gyro model doesn't need to include a declination error term.

(N.B. In fact to model the variation in declination over the global the MWD model uses both the constant DEC term described here and also a second DBH term which is inversely proportional to the horizontal component of total field, but that complication can be ignored for the sake of this discussion.)

19.2.2 Error Sources

An error source is any physical phenomenon which contributes to the overall positional measurement error.

Examples of error sources include residual sensor errors after calibration, misalignment of the survey tool with the borehole axis, uncertainties in the Earth's magnetic field, which is the reference against which MWD measurements are made, deflection of the survey tool under gravity, stretch of drillpipe or wireline under the weight of the BHA or survey tool etc.

Between all versions of the MWD and gyro models, some ninety-eight individual error sources are identified. These are not all applicable to each survey tool, but are dependent on the type of tool in operation and how it works. A typical tool model (or IPM file) defines which of these error sources are invoked to model that tool.

19.2.3 Error Magnitudes

For a particular tool model, each error source has an error magnitude. The error magnitude is essentially the standard deviation of the range of values which the error source might be expected to take over a statistical sample of survey data under normal field operating procedures. For example, if you consider a large number of MWD runs, what are the statistics for the range of tool misalignments to the borehole?

The values may change depending on what survey techniques or corrections are being applied to the job in hand. So as previously mentioned, using an IFR survey to measure the declination value in the field reduces the magnitude of the declination error term. There is still a declination error source, and the weighting functions remain the same, but compared to the MWD tool model, the MWD+IFR tool model will have a smaller magnitude for the declination term. The MWD paper gives values for these for 'normal' MWD surveying. However beyond that initial set error magnitudes are not set by the ISCWSA.

For the gyro error model, it is expected that error magnitudes will be supplied by the gyro contractor. Test cases are defined in the gyro paper but these are not considered to model any particular survey tools.

The error magnitudes defined in the MWD paper are all at one standard deviation (1-sigma). If the user requires final error ellipses at two standard deviations (or three) then the 1-sigma ellipses can simply be multiplied up and typically drilling software has a user control to define at what level error ellipses are to be output. There are two provisos to this – some drilling software packages allow the user to enter error magnitudes at different defined confidence levels (e.g. 1-sigma or 2-sigma etc.) Also, changes to the MWD at revision 4 may require the user to define the required output confidence level first so that certain magnetic field reference terms can be correctly calculated (for further details see section 19.3.4 below.)

19.2.4 Weighting Functions

Each error source has a set of weighting functions which define how that error source effects the actual survey measurements of measured depth, inclination and azimuth. These weighting functions are simply the equations that link the error source to the survey measurements, e.g. the weighting functions enable us to take a z-magnetometer bias uncertainty in nano-Teslas and calculate a survey azimuth uncertainty in degrees at a particular survey station in a particular wellbore.

The actual survey inclination and azimuths are obtained from the sensor data via a set of survey equations. So for example for a standard MWD tool the inclination and azimuth are determined from the following equations:

$$\boldsymbol{I = cos^{-1}\left(\frac{G_z}{\sqrt{G_x^2 + G_y^2 + G_z^2}}\right)}$$

$$\boldsymbol{A_{true} = tan^{-1}\left(\frac{(G_xB_y - G_yB_x)\sqrt{G_x^2 + G_y^2 + G_z^2}}{B_z(G_x^2 + G_y^2) - G_z(G_xB_x - G_yB_y)}\right) + \delta}$$

Similar survey equations exist for gyros tools and these MWD equations change if axial interference corrections are made.

The weighting functions can be derived from these equations by taking the partial derivatives of the survey equations with respect to the error source. Examples of the derivations can be found in the SPE papers, whilst all of the error sources and weighting functions for both models are given in the appendices. We now consider another example to illustrate this point:

Example 2: Sensor error - Z-Accelerometer Bias
If we consider the effect of a z-accelerometer bias error; instead of reading the correct value of G_z^{true} the tool will actual give:

$$\boldsymbol{G_z^{measured} = (1 + G_z^{scalefactor})G_z^{true} + G_z^{bias}}$$

where G_z^{bias} and $G_z^{scalefactor}$ represent the residual errors of the survey tool after calibration.

This equation represents a fairly standard, first-order method for modelling the output of a sensor (almost any type of sensor), when we know that it will not give perfect output.

The MWD model has an error source, coded ABZ for the z-accelerometer bias which corresponds to this G_z^{bias} term. From the MWD survey equations above, we can see that the G_z term appears in both the inclination and azimuth equations.

However, the accelerometer readings don't have any effect on measured depth. So the MD weighting function is 0, but the inclination and azimuth ***weighting functions*** are determined by taking the partial derivates of these survey equations with respect to G_z i.e. for ABZ the weighting functions are:

$$\left[0, \frac{\sin I}{G}, \frac{tan\Theta\ sinI\ sinA_m}{G}\right]$$

Since we are assuming that this z-accelerometer bias is due to residual tools errors, this error source will have the same value for each survey taken with that tool. However, if we change tools, the error will change. Hence the ***propagation mode*** is systematic (the same at each survey station in a run, but different for different legs and wells).

The model gives ABZ a ***magnitude*** of 0.004 ms^{-2}, meaning that for a number of properly calibrated tools if we ran a number of tests, we'd expect to get a Gaussian distribution of results with a standard deviation of 0.004 ms^{-2}.

Gyro tools can be designed a little differently – some systems also have a cluster of three accelerometers and the inclination weighting function will be the same as the MWD case (this is the gyro AXYZ-ZB term). Other gyro tools only have x and y-accelerometers and use the assumed total gravity value, and therefore these tools would be modelled without a z-accelerometer bias term. We can see that the error sources which are included in any particular survey tool model depend on the design of that tool.

19.2.5 Error Propagation

The core equation for the propagation of the errors from the error source through to the survey position error is:

$$\boldsymbol{e_i = \sigma_i \frac{dr}{dp} \frac{\partial p}{\partial \varepsilon_i}}$$

Where:

e_i is the size of the error in NEV axis due to error source i at the current survey station (a 3x1 vector)

σ_i is the magnitude of the ith error source (a scalar)

$\frac{\partial p}{\partial \varepsilon_i}$ are the weightings functions, the effect of the ith error source on the survey measurements; md, inc and azimuth. (a 3x1 vector)

$\frac{dr}{dp}$ is the effect of the survey errors in md, inc and az on the wellbore position in the NEV axis, (i.e. a 3x3

$$\textbf{matrix}\begin{bmatrix} \frac{dN}{dMd} & \frac{dN}{dInc} & \frac{dN}{dAz} \\ \frac{dE}{dMd} & \frac{dE}{dInc} & \frac{dE}{dAz} \\ \frac{dV}{dMd} & \frac{dV}{dInc} & \frac{dV}{dAz} \end{bmatrix})$$

Wellbore positions are calculated using one of the standard methods such as minimum curvature or balanced tangential, so over an interval, the $\frac{dr}{dp}$ matrix depends on the surveys at either end of the interval. The derivation of the $\frac{dr}{dp}$ matrix equations is given more detail in Appendix A.

The tool model for any particular survey instrument will usually include a number of different error sources, and we must consider all survey legs in the well and all the survey stations in each leg. So for a well we must add the error contributions over all survey legs in the well; each survey station in each leg and the contributions from each error source.

19.2.6 Summing Error Terms and Propagation Modes

Once we have calculated the contribution to the error ellipse from each error source, at each survey station in each leg of our well we have to sum up all the contributions.

There are two basic cases:

1) The contributions are directly linked (correlated in mathematical terminology).

For example; the z-axis magnetometer bias error. If we are using the same tool and BHA, then we would expect this error source to have the same value from survey station to survey station and the effects of the error will build all the way down the wellbore.

In this case the error contributions are added in the usual arithmetic way:

$$\boldsymbol{e_{total} = e_1 + e_2}$$

2) The contributions are not linked at all (statistically independent).

For example; if we have two independent error sources, then they could both cause a positive inclination error and add together but it is also possible that one might create a positive inclination error and the other a negative error. In which case we are taking a random value from pot 1 and a random value from pot 2 and the error contributions must be root sum squared (RSS) together:

$$\boldsymbol{e_{total} = \sqrt{e_1^2 + e_2^2}}$$

In fact it is an assumption of the model that the statistics of the various different error sources are independent so they must be RSS'd together – for example, there is no reason why sag error would be connected to z-axis magnetometer bias or to declination error etc.

However, if we take the example from 1) above, although we can see that the z-axis magnetometer bias should

remain the same throughout a survey leg, if we go to another leg, using a different tool or to another well then we would expect that error source to be independent over that range.

So our the error sources are independent from each other, but a given error source might be independent at all times, or correlated from station to station within a survey leg or from survey leg to survey leg with a well or from well to well within a field.

Therefore the model defines four ***propagation modes*** for the errors:

Random	R	always independent
Systematic	S	correlated from survey station to survey station
Well by Well	W	correlated from leg to leg
Global	G	correlated over all wells

The propagation mode is a property of the error source and is defined in the tool model. In practise, most error sources are systematic or random and only a limited few well by well or global sources have been identified.

To combine all the error sources, we need to create a sum over all survey legs, survey stations and error sources which apply to a particular well. When doing this summation the propagation mode is used to define at what step in the summation arithmetic addition is used and at what stage RSS addition is required.

$$\boldsymbol{total\ error} = \sum_{\boldsymbol{l=}}^{\boldsymbol{Survey\ Legs}} \sum_{\boldsymbol{i=}}^{\boldsymbol{Survey\ Station}} \sum_{\boldsymbol{k=}}^{\boldsymbol{Error\ Source}} \boldsymbol{e_{l,i.k}}$$

The mathematical details of this process can be found in Appendix A. The final output of the summation is a 3x3 covariance matrix, which describes the error ellipse at a particular station. In the *nev*-axes, the covariance matrix is:

$$[\boldsymbol{C}]_{\boldsymbol{nev}} = \begin{bmatrix} \boldsymbol{\sigma_N^2} & \boldsymbol{\sigma_N\sigma_E} & \boldsymbol{\sigma_N\sigma_V} \\ \boldsymbol{\sigma_N\sigma_E} & \boldsymbol{\sigma_E^2} & \boldsymbol{\sigma_E\sigma_V} \\ \boldsymbol{\sigma_N\sigma_V} & \boldsymbol{\sigma_E\sigma_V} & \boldsymbol{\sigma_V^2} \end{bmatrix}$$

Here σ_N^2 is the variance in the north-axis and the uncertainty in north axis (at 1-standard deviation) is $\pm\sqrt{\boldsymbol{\sigma_N^2}}$.
In the same way, the other terms on the lead diagonal are uncertainties along the other principle axes. The $\sigma_N\sigma_E, \sigma_N\sigma_V$ and $\sigma_E\sigma_V$ terms are the covariances and give the skew or rotation of the ellipse with respect to the principle axes.

19.2.7 Transformation to Borehole Axes

The covariance matrix above is expressed in the earth-centred *nev*-axes, this can be transformed to the borehole reference frame, *hla* by pre- and post-multiplying the covariance matrix with the *nev*-to-*hla* direction cosine matrix, $[T]_{hla}^{nev}$.

$$[\boldsymbol{C}]_{\boldsymbol{hla}} = [\boldsymbol{T}]_{\boldsymbol{hla}}^{\boldsymbol{nev}\boldsymbol{T}} [\boldsymbol{C}]_{\boldsymbol{nev}} [\boldsymbol{T}]_{\boldsymbol{hla}}^{\boldsymbol{nev}}$$

The direction cosine matrix can be obtained a rotation in the horizontal place to the borehole azimuth, followed by a rotation in the vertical to the borehole inclination and is given by:

$$[\boldsymbol{T}]_{\boldsymbol{hla}}^{\boldsymbol{nev}} = \begin{bmatrix} \boldsymbol{cosIcosA} & \boldsymbol{-sinA} & \boldsymbol{sinIcosA} \\ \boldsymbol{cosIsinA} & \boldsymbol{cosA} & \boldsymbol{sinIsinA} \\ \boldsymbol{-sinI} & \boldsymbol{0} & \boldsymbol{cosI} \end{bmatrix}$$

19.2.8 Bringing It All Together

The effect of a particular ***error source*** on the survey results (md, inc or az) is found by multiplying the ***error magnitude*** by the appropriate ***weighting function***. It is an implicit assumption of the model that all the error statistics are Gaussian (see section 19.3.4 on the MWD error model revisions for the one exception to this rule).

Furthermore the error sources are assumed to be statistically independent of each other so the effects of the **different** error sources are summed by taking the square root of the sum of the squares (RSS). (N.B: this should not be confused with the effects of the **same** error source across different survey stations and survey legs.)
The effects of the error sources are all assumed to be linear (the weighting functions are all calculated to first order), so doubling the size of an error magnitude will in turn double the size of the error caused by that error source at any particular survey station. That error contribution will then be RSS'd with the other error sources, so that the effect on the final survey uncertainty will not be a simple doubling.

Then uncertainty in md, inc and az is converted to a positional uncertainty in the Earth-referenced co-ordinate frame. The equations for doing this are derived in [1] and are determined from the balanced tangential method of determining the borehole trajectory.

The positional values can then be converted to an uncertainty in the borehole referenced co-ordinate frame by multiplying by a direction cosine matrix dependant on the inclination and azimuth of the borehole.

The output of the error model is a covariance matrix describing the magnitude of the survey errors in the chosen co-ordinate frame. From this covariance matrix it is then possible to generate an error ellipse showing the estimated survey uncertainty in 3-d space. This error ellipse may be displayed in 3d or it may be sliced in a plane of interest, e.g. perpendicular to the well and displayed as an error ellipse. (Note to software implementers: this step is not given in the SPE paper but the axes of the error ellipsoid are the eigenvectors of the 3x3, real symmetric covariance matrix and the axes magnitudes are the eigenvalues of the covariance matrix.)

In the SPE paper the error sources are quoted at one standard deviation and hence the final error ellipse dimensions are the 1-sigma ellipse dimensions. There is then an probability that the actual well is contained with an ellipse of this size, centred on the obtained survey results. It is common practise in anti-collision calculations to use 2-sigma results – the 2-sigma ellipse is twice as large as the 1-sigma ellipse along each of the principle axes.

It is normal for directional drilling software such as 5D or Compass to be used to determine error values either for survey results for well planning or survey design. Usually the user can select whether results are reported at 1, 2 or 3 sigma. In some instances the magnitudes of the error sources are always quoted at 1-sigma, in others the software allows the 2 sigma values to be entered. You should check with company anti-collision policy, survey focal point or software vendor if you are uncertain how reporting is applied to the wells which you use.

19.2.9 Bias Terms

The error magnitudes discussed above are essentially the standard deviations of the range of values that error source can be expected to take. Many of these error sources will have zero mean and hence the standard deviation is all that is required.

However, the formulation of the model also allows for error sources which have a non-zero mean. These are known as bias terms and lead to error ellipses which not be centred on the survey point, but are offset in a particular direction.

The most obvious application for this would be for measured depth errors, where it is well known that drill pipe is measured on surface but when downhole expands with temperature and stretches under tension from the weight the drill-string. So the true measured depth will be longer than the sum of the drillpipe lengths on surface. However, after discussion at ISCWSA meetings, the committee took the view that biased models should are not encouraged. If biases are present these should be corrected where possible, and if not the error ellipses should be large enough to encompass the expected actual location of the wellbore.

19.3 MWD Error Model

19.3.1 MWD Tool Types

Most modern MWD tools are very similar and comprise six sensors - three orthogonal accelerometers to measure the inclination and toolface of the tool relative to the Earth's gravity vector and three orthogonal magnetometers to measure the azimuth of the tool.

19.3.2 MWD Error Sources

The MWD error sources were originally set out in reference [1]. Although there have been subsequent revisions to the details of modelling the same basic physical errors still apply.
The original paper identified 34 error sources and at the current state of the model (revision 3) 41 separate MWD error sources have been identified. These can be split into five groups:

1) Sensor errors (This gives a total of 26 MWD sensor error sources)

Bias and scalefactor terms are modelled for the accelerometer and magnetometers.
In the original derivation of the paper there was essentially one bias and on scalefactor term for each sensor, however that formulation of the mathematics required an estimate of the toolface angles which couldn't be reliably determined at the planning stage. The later revisions introduced toolface independent terms and now the effects of the x and y sensors are lumped together and are not explicitly separated out. For the biases there are still two terms for the x and y directions, however the scalefactors are now modelled using three error sources for these two axes.
So for standard MWD surveying there are 14 terms:

	Accelerometers	Magnetometers
Bias	2 xy-terms 1 z-term	2 xy-terms 1 z-term
Scalefactor	3 xy-terms 1 z-term	3 xy-terms 1 z-term

The model also covers the situation where an axial interference (or short-collar) correction is applied used to remove the axial effects of BHA magnetic interference. This changes the form of the MWD survey equations and hence the weighting functions and therefore needs to be modelled with a further set of sensor error sources. For axial interference corrections, the z-magnetometer reading is not used and hence a further 12 error sources are defined (14 – (z-mag-bias and z-mag-scalefactor).

2) Reference Field Errors (4 error sources)

All MWD survey results are measured relative to the Earth's magnetic field and uncertainty in this reference leads to survey errors. The magnitude and direction of the Earth's magnetic field is characterised by it total field strength, declination angle and dip angle and these values are normally obtained from a mathematical model, such as the IGRF or BGGM models, implemented in directional drilling software.

For standard MWD operations, only the declination is important. In order to give an accurate description of the declination uncertainty over the globe, the MWD paper models the declination error with a constant term and with a term which is inversely proportional to the horizontal component of the Earth's field.

When axial interference corrections are applied to MWD surveys, the reference total field and dip angle terms need to be considered and a further two error sources are identified for these.

3) Interference Errors (2 error sources)

The BHA itself will generally be steel and will have a magnetic field associated with it. Even when non-magnetic drillpipe is built into the BHA, according to industry standard spacing calculations, there will still be a residual effect on the survey results. This is modelled with two error terms, one for constant axial interference and one for direction dependent effects, since constant magnetic interference from the BHA will have an increasing effect on survey azimuth as the wellbore gets closer to a horizontal, magnetic east/west attitude.

4) Misalignment errors (5 error sources)

Following some work done for the gyro error model, the misalignment of the survey tool to the wellbore is now modelled with four misalignment terms. A further term is used to account for sag – the deflection of the BHA under gravity, which leads to an inclination error since the centreline of the survey tool will not be orientated parallel to the borehole axis

5) Depth errors (4 error sources)
A total of four error sources are used to model the errors in measured depth, due to both random and systematic errors, scale factor errors on the depths and drillpipe stretch under tension from the weight of the BHA.

In this modelling some physical error sources may be lumped together into one error source if in practise it is difficult or unnecessary to separate them. So for example, the misalignment error sources that are identified are for the misalignment of the tool itself to the borehole, not the sensors to the tool. The misalignment of the sensors themselves to the tool axes are accommodated within the sensor bias and scalefactors and are not explicitly separated out.

19.3.3 MWD Weighting Functions

As described in the example in section 19.2.4 the MWD weighting functions are determine by taking the partial derivatives of the survey equations with respect to the error sources. All of the MWD weighting functions are detailed in Appendix B.
Even a quick glance shows that many of the weighting functions are zero. Of the total list of error sources, only the four depth terms have any influence on measured depth. Some of the functions such as the effect of the declination errors on azimuth or sag error on inclination are relatively simple equations. However, other sources such as the accelerometer error sources may influence both the inclination and azimuth measurements and, particularly in the azimuth case, lead to relatively complex equations to be evaluated at each survey station.

19.3.4 MWD Error Magnitudes

The MWD model is the only case for which the ISCWSA defines error magnitudes and provides complete tool models, if only for a limited number of situations. This is because it is considered that the performance of most modern MWD tools is quite similar and a generic model is valid.

Much of the MWD paper [1] is given over to a justification of error magnitudes for the MWD error sources and a complete tool models are given both standard MWD surveys and for surveys which are corrected for axial-interference for the combinations situation where the tools are run from a fixed land rig with fixed depths and for an offshore floating platform.

So effectively there are four defined tool models:

i. MWD-Fixed Rig
ii. MWD-Floating Platform
iii. MWD + Axial Correction – Fixed Rig
iv. MWD + Axial Correction – Floating Platform

The application of survey correction techniques to improve the accuracy of MWD surveys will generally change the magnitudes of one or two error sources. So for example, running sag-correction software will reduce the magnitude of the sag error term; conducting an IFR survey will improve the knowledge of the Earth's magnetic field and lead to reduced magnitudes for the four reference field error terms. The use of the error model as implemented in directional-drilling software is the appropriate way to evaluate the effect of these techniques and to determine an appropriate survey program for a well. However, the ISCWSA has not defined or standardised values to be used to model these.

19.3.5 Relative Contribution of the Various Error Terms

For the ISCWSA#1 test well (typical North Sea Extended reach well), the plots below show the relative contribution of the various error sources to the overall ellipse dimensions. The values below have been calculated based upon revision 2 of the MWD model. All the values here are quoted in Earth referenced (NEV) frame and it must be remembered that being independent the terms are summed by the RSS method.

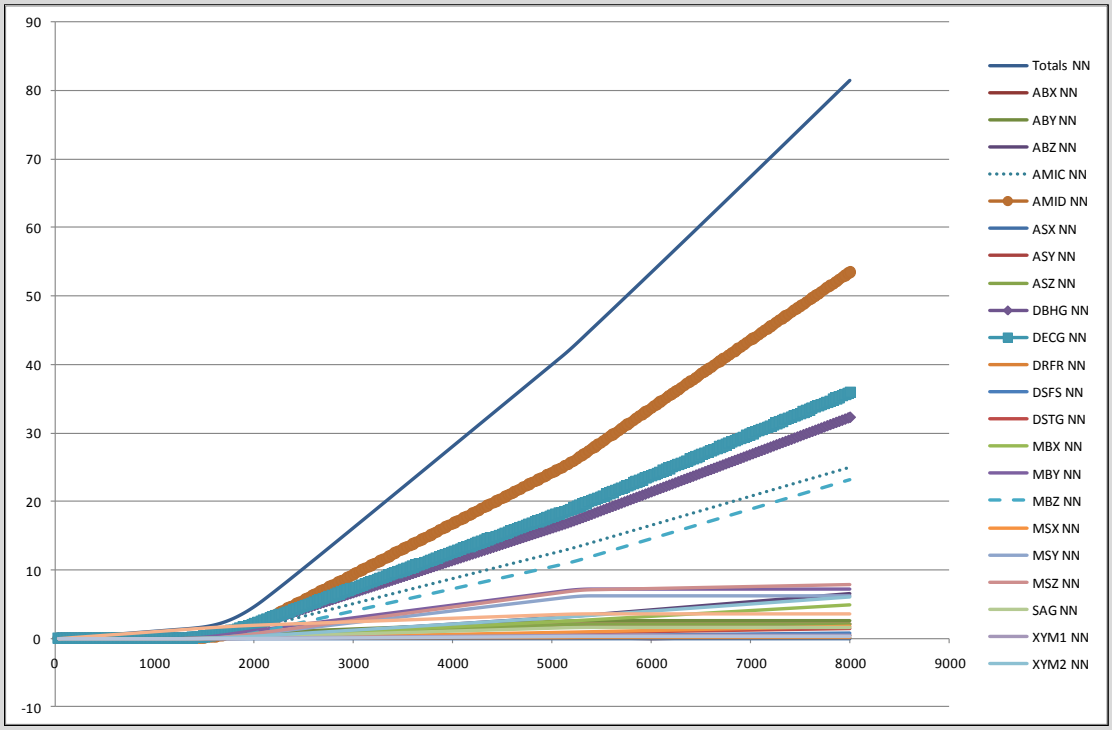

Figure 86a: North Axis Errors.

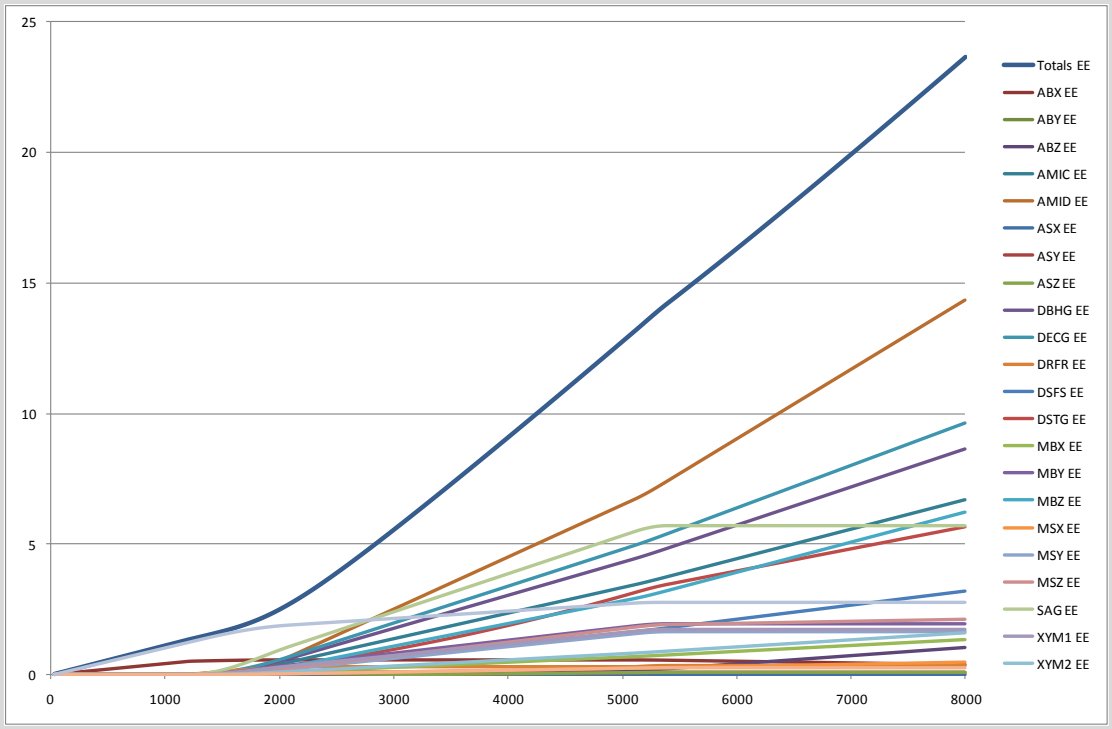

Figure 86b: East Axis Errors.

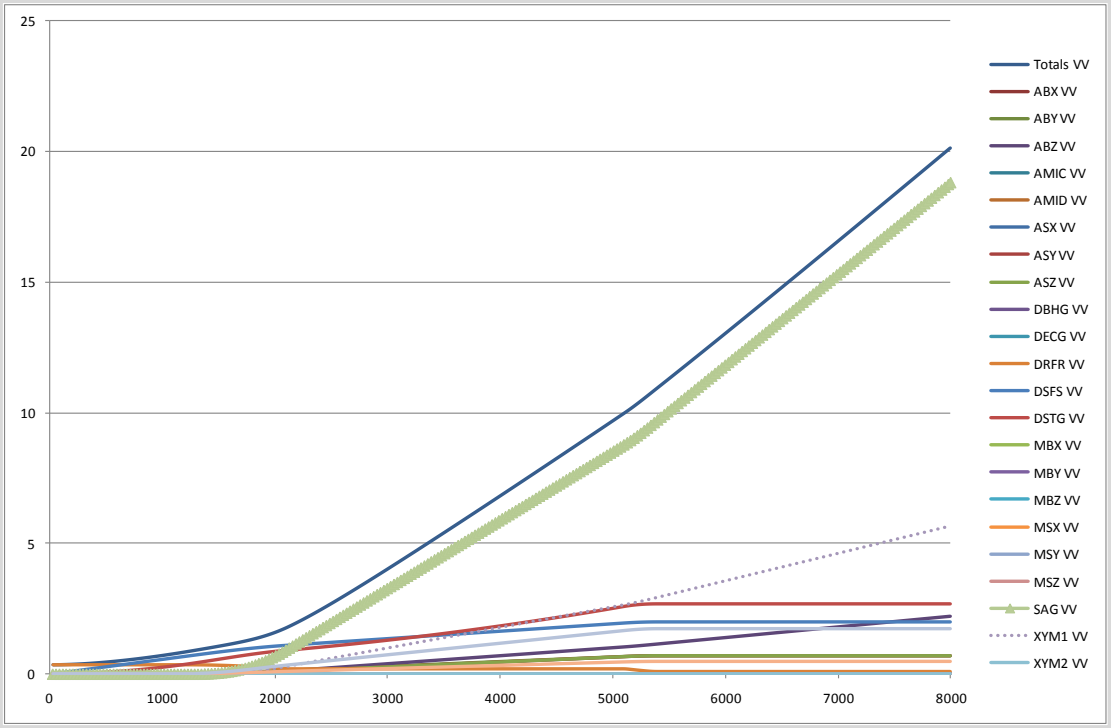

Figure 86c: Vertical Axis Errors.

From these graphs it is easy to see that as expected, the biggest error contribution in the vertical is from SAG. For this well the north and east errors are dominated by axial interference, followed by uncertainty in the magnetic model (i.e. declination uncertainty).

19.3.6 Revisions to the MWD Error Model

The reprinted MWD paper [1] by Hugh Williamson covers three distinct areas. It lays out the framework of the ISCWSA error model as discussed in the previous section, it defines the error sources applicable to MWD tools and it provides error magnitudes for these values, complete with a technical justification.
However, work on the ISCWSA error models is on-going and to date several revisions have been made to the basic model as defined in [1]. A summary of the revisions is presented here. More details can be found in [4,5,6].

The revisions to the MWD Error Model are:

Rev 0	As per SPE 67616 together with a number of typographical corrections [4]
Rev 1	Changed to the gyro style misalignment with 4 terms and calculation options [4]
Rev 2	Changes to the parameter values for the depth scale and stretch terms [4]
Rev 3	Replacement of all toolface dependant terms. [5]
Rev 4	Look up table for BGGM uncertainties. [6]

Revisions 0 and 2 make some relatively minor corrections and changes to the original paper. However, revisions 1 and 3 are more major and replace all if the toolface dependant terms misalignments. Combined these constitute a large change to the model. Between them these two revisions replace 18 of the original 33 weighting functions, including the misalignment terms, the x and y axis sensor biases and scalefactors. 24 new sources are added to model these.

Revision 0 consists of some relatively minor typographical and parameters corrections.

Revision 1 introduces a new method of calculating the effect of tool misalignment to the borehole axis. This avoids the complication of toolface dependency in the misalignments and is considered to handle certain geometries, such helix-shaped, vertical boreholes better than the original MWD terms. This replaces the two existing misalignment terms MX and MY and introduces four new terms and three possible calculation options which are handled via two weight parameters.

The calculation options are:

	W_{12}	W_{34}
Alternative 1	1	0
Alternative 2	0	1
Alternative 3	*sinI*	*cosI*

Alternatives 1 and 2 have their own strengths and weaknesses, whereas Alternative 3 is designed to combine the best of both options and is the preferred calculation option. This is discussed in detail in Appendix B of [2] and in [4].

Revision 2 makes some corrections to the depth error magnitudes.

Revision 3 replaced the remaining 16 toolface dependant weighting functions with 20 new ones, following a method developed for the gyro error model. This removes the need to either include survey toolfaces, or use methods to evaluate at the planning stage which toolfaces might be observed, a process which can give rise to unexpected results. The new terms replace all the existing x and y accelerometer and x and y magnetometer bias and scalefactor terms, for both the standard MWD and MWD with Axial correction cases. The new terms lump together the x and y effects, and the propagation mode varies from either random, where the toolface varies between survey stations and systematic for sliding between survey stations with constant toolface. In practise for MWD the random propagation would normally be considered at the planning stage. The details of revision 3 are dealt with in [5].
Revision 4 brings in lookup tables for the uncertainty in the BGGM model which will change how the error magnitudes are determined for the reference field terms. This revision does not may any changes to the weighting functions.

As discussed in section 19.2.3 above, the error model assumes that all the errors are Gaussian. However, as detailed in [6] it has come to light that the errors in the global geomagnetic models are in fact, non-Gaussian and are best modelled with a Laplacian distribution which has greater likelihood in the tails of the distribution. This presents some problems in the implementation, especially when varying the number of standard deviations at which to report the output results.

The current recommendation is to define in advance the number of standard deviations required for output and then determine the uncertainty in the magnetic model at that confidence level. Divide this value by the number of standard deviation required to get an 'equivalent Gaussian standard deviation' (valid only at the confidence level in question) and then use that value as normal in the subsequent calculations.

Although revision 4 has been approved by the ISCWSA, there is still on-going discussion on this point. The appearance of new global magnetic models may lead to further changes in this part of the model.

19.4 Gyro Error Model

19.4.1 Gyro Tool Types and Running Modes

Whereas we considered that all MWD tools were essentially the same and comprised three orthogonal accelerometers and three orthogonal accelerometers, there are many different types of gyro survey tool and main different ways of running them in a well.

The running modes can broadly be divided into tools which take measurements whilst stationary at regular survey stations and those which run into hole, whilst constantly moving and recording data. Furthermore a gyro tool may include three orthogonal accelerometers and three orthogonal gyros or might only use a subset of sensors. Tools with additional redundant sensors can be reflected in the error magnitudes assigned rather in than in the model mathematics.

So the gyro model covers tools which have:

1. x-y-z accelerometers - run in stationary or continuous mode
2. x-y only accelerometers – run in stationary or continuous mode
3. x-y-z gyros - run in stationary mode
4. x-y gyros only – run in stationary mode
5. x-y-z gyros - run in continuous mode
6. x-y gyros only – run in continuous mode
7. z gyro only – run in continuous mode

In addition the model considers these other running conditions:

8. initialisation to an external sighting reference
9. indexing in hole to remove gyro drifts
10. rotation in hole
11. the cant angle of the sensors in x-y accelerometers systems.

Furthermore the survey mode may vary within a survey run, as a function of inclination.

19.4.2 Gyro Error Sources

Due to the number of tool variations and running modes, the gyro error model is more complicated than the MWD model. However it is based on exactly the same framework for propagation, summation and transformation as the MWD model.

The gyro model contains 48 error sources. 39 of these are new and 9 are common to the latest revision of the MWD model. As before sensor errors are very prevalent.

Accelerometer biases and scalefactors and sensor misalignments are present, and these only effect inclination terms, but different error sources have been identified for tool configurations which have a full orthogonal tri-axial set of accelerometers and for tools with only x and y accelerometers, which may be canted relative to each other and not perpendicular.

For the gyros, bias, random noise, gravity dependant errors, scalefactor errors and sensor misalignment with the tool have all been identified. With suitable selection of error magnitudes it is considered that the model is sufficient to model the various types of mechanical spinning wheel gyros in use, both single and dual axes systems, ring-laser gyros and possible future gyro systems.

The gyro sensor error affect the azimuth measurements, but now different functions apply depending on whether the gyro operates in a stationary, gyro compassing mode at each survey station or is initialised and runs continuously in the hole. In addition the model accommodates xyz; xy and z-only gyro systems.
For the continuous gyro systems a new complication arises in that some of the errors will be dependent on elapsed time in the run (gyro drift errors) or the square root of elapsed time (random walk errors). These have been modelled by including a running speed in the tool model and including a term in the weighting functions which will accumulate over time. Terms for errors introduced with an external azimuth reference are also included.

From the outset, the gyro model excludes the need for toolface in any of the terms used. To do this the x and y effects are lumped together. For surveys where the tool is rotated between surveys these terms will propagate randomly, however when the tool slides between stations with fixed toolface, these same terms will propagate systematically.

The gyro error model introduced a new method of calculating the effect of tool misalignment to the borehole this was later incorporated in to the MWD model and is described in section 19.3.2.

19.4.3 Gyro Weighting Functions

The gyro model weighting functions are detailed in Appendix C. They are separated out more rigidly than the MWD model and aside from the misalignment terms, any given error source only effects one of the survey measurements. Hence two of the error function vector terms are zero for all expect the misalignments.

19.4.4 Gyro Error Magnitudes

The gyro paper defines error magnitudes for six example error models. However these are intended to be used only for testing and are not to be considered as representative of any given tool used in the industry.

19.4.5 Differences Between the Gyro and MWD Models

The gyro error model is essentially a superset of the MWD model. It uses the same framework for prorogation error sources, but naturally since the physics behind the tools are different, the error sources and weighting functions for the gyro error model are quite different to the MWD model.

The gyro error model uses the method of handling borehole misalignment, introduced into the MWD model as revision 1 and described in the MWD model section above.

But there are three main changes which introduced with the gyro model. Firstly, the tool running mode and hence the error sources in use, may change along the wellbore as a function of inclination. So the tool model must include inclination bounds, either for the possible running modes into which the error sources are grouped in [2] or simply for each individual error source and the software must accommodate these.

Secondly, in the MWD model the weighting functions remain fixed from survey station to station. However for the continuous gyro operating modes there are time dependent terms in the weighting functions, which are modelled as depth dependant and which will increment as the tool moves along the wellbore. So the software must initialise these and then implement the changes as it propagates the model. All six continuous gyro azimuth error sources have this property (gyro drift and random walk terms for the three continuous gyro sensor combinations, xyz, xy and z: GXYZ-GD, GXYZ-GRW, GXY-GD, GXY-GRW, GZ-GD, GZ-GRW).

Finally for MWD the tool model need only define which error sources are used to model a tool, the magnitudes of these error sources and their propagation modes. In the gyro model, some additional parameter values may be needed to define details of the running conditions;

a) a cant angle for x-y accelerometer systems
b) a logical operator indicating whether or not accelerometer switching is implemented.
c) a logical operator indicating whether or not the tool is indexed (z-rotated) at a survey station
d) a logical operator defining whether or not a stationary tool is rotated between stations, which will change the propagation mode for some bias terms

The latter two terms can also be accommodated either by correctly defining the error magnitude for the appropriate term to zero or by excluding these terms from the tool model, unless the values change with inclination.

19.5 Error Model Implementation

19.5.1 Algorithm Flow

The basic flow of the models is;

Initialise
Loop through error sources
Loop through survey legs
Handle tie -on
Loop through survey stations
Use inclination to define mode (for gyro)
Determine inc, az, depth error for each error source i.e. evaluate the weighting functions
Determine the NEV errors for each error source
Sum these according to propagation mode
Transform to HLA axis frame if required.

19.5.2 High Level Flow Chart

The chart below shows a high level overview of the dataflow for the model in general. Two other flow charts are provided in the gyro model paper [2] which give more specifics of detailed decision processes.

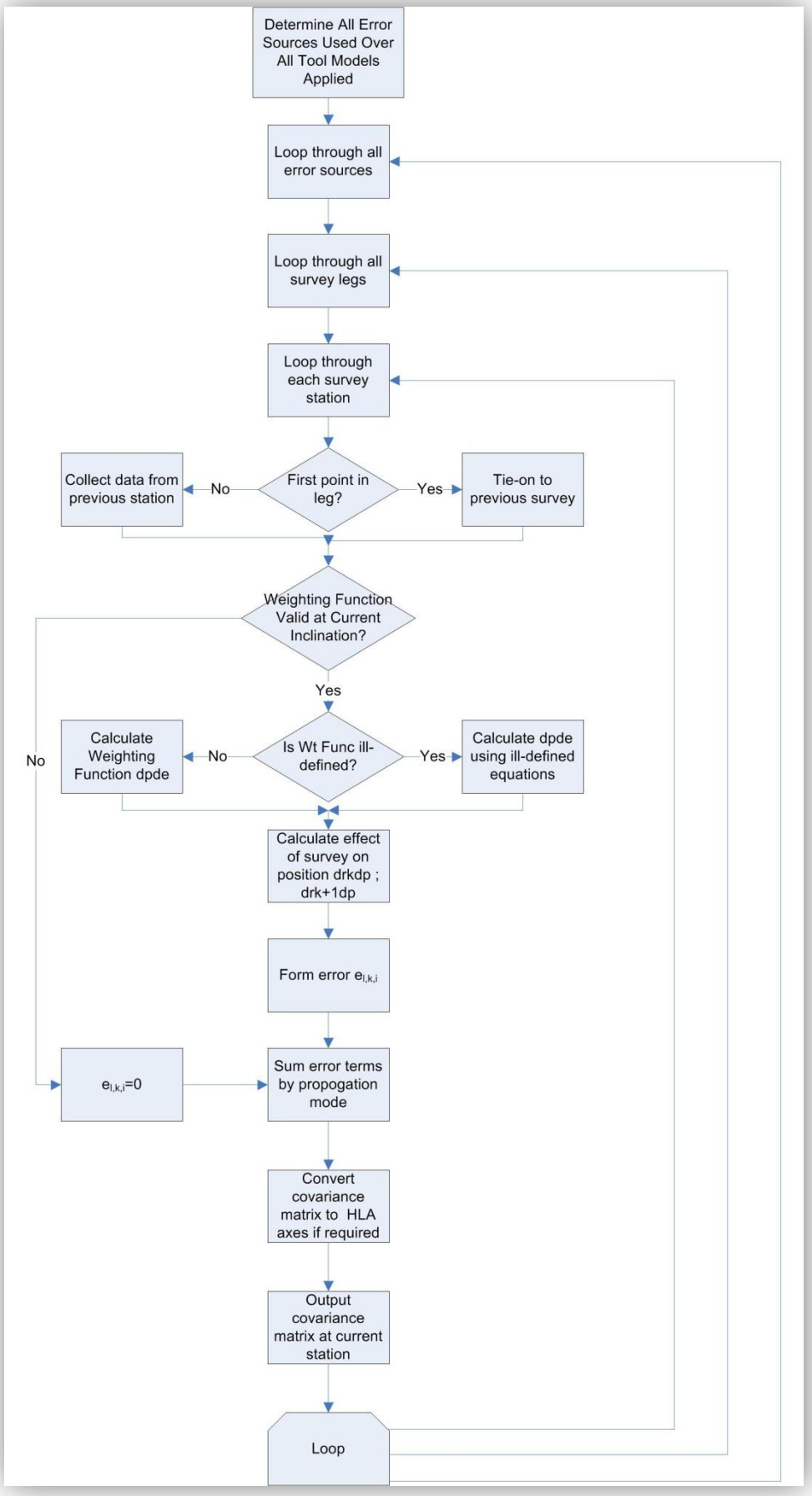

19.5.3 Inputs Required

Required input parameters for the weighting functions calculations:

Well site data:
Total gravity value
Total magnetic field value (MWD)
Magnetic Dip (MWD)
Horizontal magnetic field (function of total field and dip) (MWD)
Latitude (Gyro)

Survey data at each station:
Measured depth, Inclination, Azimuth, Toolface (early revisions)

Tool Model Terms:
Error sources included
Error magnitude for each source
Error propagation mode
Inclination bounds for change for mode or for each source (start , end)
Misalignment calculation method (ALT=1,2,3)
External reference method (gyro)
Running Speed (gyro)
Rotation of accelerometers between stations (R value, gyro))
Cant angle (gyro)
Running mode (sliding or rotating must be defined, either via IPM or as a parameter to control propagation modes.)
Noise reduction factor at initialisations
Minimum distance between initialisations

19.5.4 Poorly Defined Functions

The MWD model includes a set of equations for the cases where the weighting functions are mathematically ill-defined in vertical hole. The situation at 90 inclinations, 90 (or 270) azimuth is physically ill defined and a software implementation must handle these.

The following weighting functions are ill-defined in vertical hole:
ABX, ABIX, ABY,ABIY, MX,MY, XYM3, XYM4, ABXY-TI2 and ABIXY-TI2
References [1] and [5] include alternative calculation options that can be used to evaluate these functions.

19.5.5 Test Cases

The MWD paper [1] defines three standard test well profiles. These are for:

a. an example North Sea extended reach well,
b. a Gulf of Mexico fish-hook well,
c. a Bass Strait designer well.

For each test case the well profile, location, magnitude and direction of the Earth's magnetic field and the units (m or ft) are defined.

The MWD paper then defines seven test cases and error model results for each test case at Revision 0. The gyro paper defines six gyro models and applies each model to the same three test well profiles. The gyro paper also defines acceptance criteria as having numerical agreement to within ±1% of the results in the paper.

19.5.6 Consistent Naming of Error Sources

An attempt has been made to agree and utilise consistent naming conventions for error sources. Further details can be found in the Error Model Standardisation page of the ISCWSA website, www.iscwsa.org.

This naming convention has been used in this document, however it should be noted that same weighting functions should be preceded with the suffix, S, G, W or R depending on the associated propagation mode.

When designing a software implementation the decision as to be made whether or not the propagation mode is tied directly to the error codes, or whether the propagation mode is defined in with the specific tool model. The latter case allows more flexibility to the aware user when creating tool models.

19.5.7 Backward Compatibility

At each successive revision, the ISCWSA has generally advocated that the most current revision of the MWD model is promoted and should be used. In practise, software implementations have lagged behind updates of the model and also certain companies have made a conscious decision not to move to the latest versions. Therefore a range of versions of the ISCWSA model can be found in the industry.

If starting from scratch there is no reason why an implementer could not go directly to the most current version of the model and ignore the history that goes before. However, in practise of the basic framework of the model is incorporated then the overhead in adding the additional depreciated weighting functions is not too great. There may be an advantage in the flexibility to allow older versions of the model to evaluated or accommodate.

19.6 Standardisation

19.6.1 Why Do My Standard ISCWSA Results Not Agree with Yours?

A common concern voiced by users of the ISCWSA error model is that the results that when they compare error ellipse values from different directional drilling software packages, they get different answers. In general the immediate reaction is that one package must be wrong. However, the ISCWSA models leave a number of decisions up to either the user or software implementer and these should be taken into account when comparing results. See reference [7] for a fuller discussion on this topic.

What confidence limits are being reported?

The models make no comment on what confidence limit (number of standard deviations, sigma level) results should be given too. This is typically a user defined option in the software and values of 1, 2, 2.79 and 3 are all commonly used in the industry.

What co-ordinate system are ellipse dimensions reported in?

A error report may simply specify semi-major axes or semi-minor axis without detailing which co-ordinate system is being consider. Typically, the results can be in North-East-Vertical or Highside-Lateral-Alonghole axis. Some packages can output in only one or the other axis systems, other packages allow the user to select which ones are used.

What value is being reported?

Typically a package will output semi-major axis and semi-minor axis. In some cases (particularly TVD spread) it is 2 x semi-minor axis that is output (semi-diameter?).

What revision of the error model is implemented?

As detailed in the MWD section there have been a number of successive revisions of the MWD model and not all software packages will be at the same revision level.

What error magnitudes are being used in the tool model?

In general the ISCWSA does not standardise or define the tool models to be used. It is only the mathematics that is standardised and it is left up to the survey contractor to supply appropriate tool models. The only exception is the ISCWSA has standardised on tool models for standard MWD and MWD with Axial Interference corrections.

In other cases, the tool model comes supplied with directional package or can be edited by the user. Sadly, it is not uncommon to come across survey databases in use with tool models containing a very reduced set of error sources (or equivalently all the magnitudes set to zero.)

19.6.2 Non Standard Error Sources

All the error sources and weighting functions defined in the three ISCWSA error model papers and associated updates on the ISCWSA website have been listed in this document.

In addition, a number of other error sources are sometimes used within the framework of the ISCWSA model, such as Wolff and deWardt [8] terms and terms for other historic survey tools. Doing this is not exactly the same as implementing the Wolff and deWardt model as detailed in their paper, but is rather a halfway house between the two error models which may agree for some situations and may give very different answers in other circumstances.

No attempt has been made in this document to list any non-ISCWSA standard error sources. It has been recognised that a great deal of time can be lost when checking and migrating survey databases from one system to another and trying to map across historic survey tools. It is hoped in future that it may be possible to agree on some generic toolset to minimise these problems.

CONTENTS

20. Anti-collision Techniques

This section deals with the survey aspects of Anti-collision monitoring and does not venture into the various mitigation methods such as the use of jetting or non-aggressive bits to minimise the impact of collision. There are techniques available to monitor the proximity of adjacent wells by measuring the external magnetic interference from nearby casing but these are beyond the scope of this document.

20.1 Minimum Separation Methods and Limits

The point in an adjacent well at which minimum separation occurs is where the separation vector hits the well at right angles. This is determined by conducting a 3D closest approach scan from the planned well. Relics of early well planning software are scans that can be done either at right angles or in horizontal planes from the planned well. Both of these alternatives should be avoided as they do not represent the true geometrical separation between the wells. Figure 84 illustrates this fact. In particular, scanning at right angles to the well bore can completely miss a vertical appraisal well when drilling horizontally. Best policy is that only 3D closest approach will be used for the definitive anti-collision report. Clients may also require horizontal or perpendicular scans to use in matching against their checking software.

20.2 Definition of Separation Factor

There are three main methods of defining the separation factor and depending on how it is defined, the results change. Also, since the separation factor is always calculated in the plane determined by the scanning method, the scanning method also obviously can change the results. The older methods of scanning will calculate the separation factor along a plane either perpendicular or horizontal to the primary well path. Again, best policy is to use 3D closest approach scanning so that the shortest distance is seen.

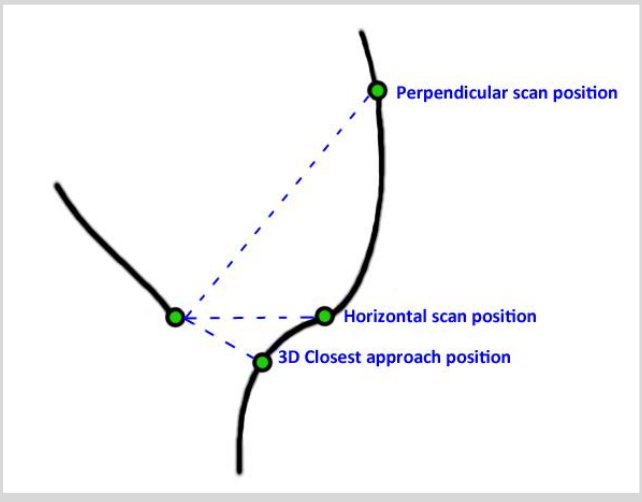

Figure 87: Separation Factor.

20.3 Separation Vector Method

The separation vector method of calculating separation factor is shown in figure 88a. (Note that in all these figures you are looking at the plane of the scan with the well bore centres and zones of uncertainty shown as they plot in that plane).

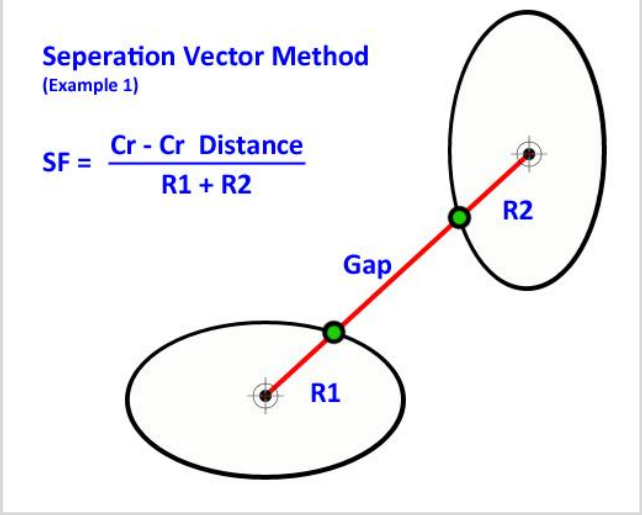

Figure 88a: Separation vector method

This has the disadvantage that it can be optimistic. In a worst case scenario it can even miss a potential collision situation as in figure 88b. This represents the same target and planned well as in the above example but the conditions have varied such that the lateral uncertainty is now much larger.

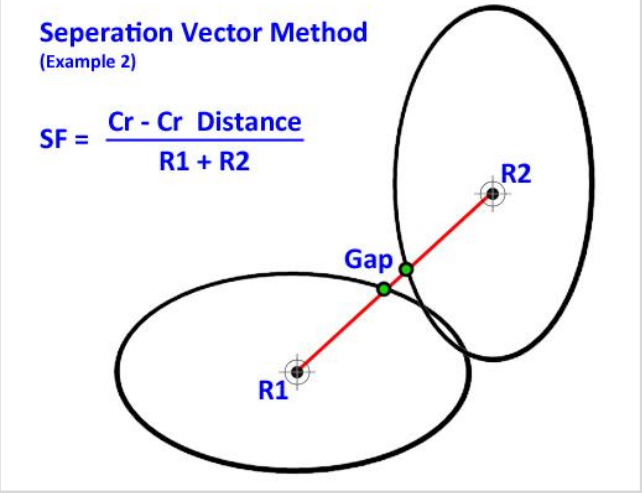

Figure 88b: Separation vector method

20.4 Pedal Curve Method

The second method for calculating separation factor is the pedal curve method. This overcomes the previous problem by projecting the extremities of the ellipses onto the separation vector.

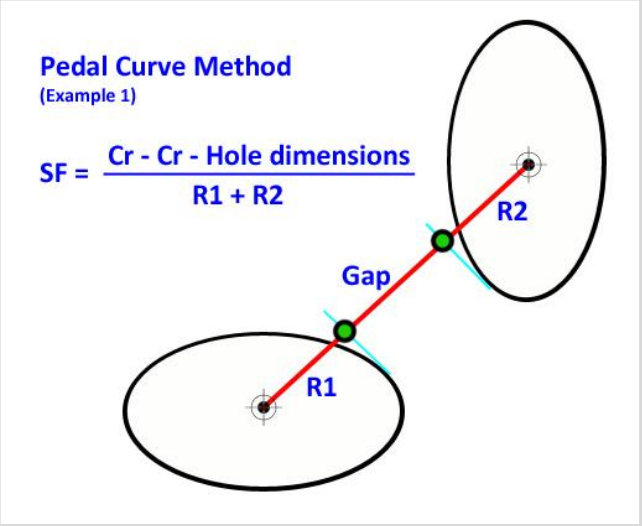

Figure 89a: Separation factor – pedal curve method

However, whereas the separation vector method can be too optimistic, this one has the opposite problem of sometimes being too pessimistic. In figure 86a the two wells are crossing safely in 3D space but using this method calculates a collision risk when in fact there is not one.

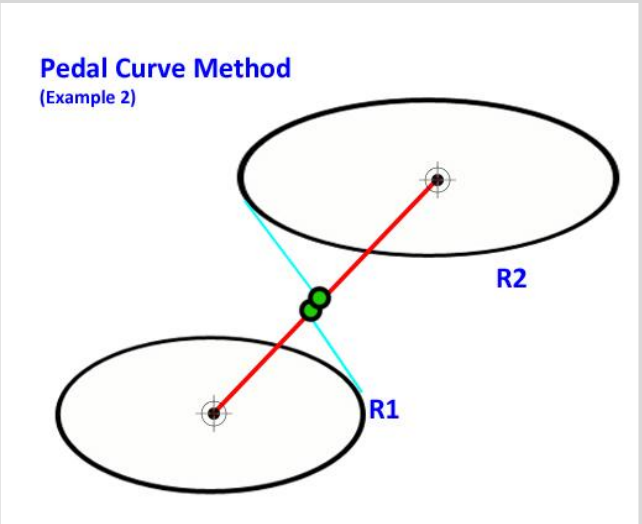

Figure 89b: Separation factor – pedal curve method

20.5 Scalar (Expansion) Method

A third method is the scalar or expansion method. This method calculates the amount the uncertainty ellipses must be expanded or contracted (in cases where the ellipses overlap) in order to just meet. The separation factor is simply the factor by which the ellipses are expanded or contracted. The calculations required to generate the separation factor using the scalar method are best left to the computer.

In the example the green ellipses are 40% bigger than the originals so the separation factor would be 1.4. When the geometries line up correctly this method produces the same number as the alternative methods. The same safety rules developed for use with the older methods can still be used. But the scalar method has the advantage of never calculating optimistic or pessimistic separation factors no matter what the 3D geometry.

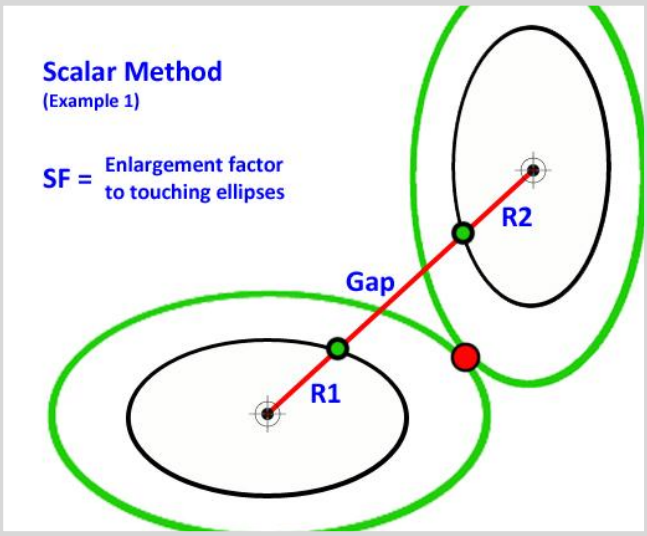

Figure 90: Scalar (expansion) method.

This method produces numbers which are very similar to the other two methods and can be used with the same safety rules but it is never optimistic or pessimistic in any geometry.

20.6 Probability of Collision

There is a movement in the industry towards more probability based anti-collision reporting. As of April, 2012 there is no final recommendation from the SPE technical section (ISCWSA) on this. At present this section will present information on collision probabilities and their calculation.

20.6.1 Difference between Separation Factor and Probability Based Rules

A separation factor based rule is purely geometric whereas a probability based rule relates to actual risk. For example, take two different uncertainty situations which both calculate a separation factor of 1.0. In the first case two 12-1/4" wellbores have uncertainty envelopes which are hundreds of feet across. In the second case the uncertainty envelopes only have a radius of one foot from each well centre. Clearly the second case has a much higher probability of being an actual collision than the former.

Rules merely using reported separation factor numbers will not distinguish between these two cases.

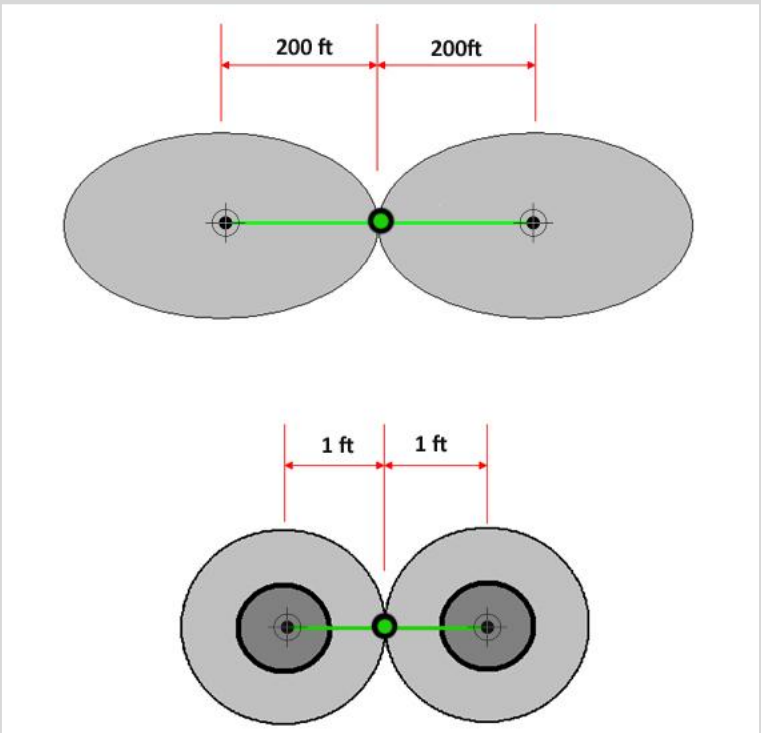

Figure 91: The uncertainty envelopes for two calculation methods.

20.7 Acceptable Risk of Collision

A key barrier to adopting probability based rules is defining what number represents an acceptable risk. Until industry standards are developed (currently under consideration in the ISCWSA) clients are unlikely to require reporting based on probability based rules.

20.8 A simplified Calculation of Probability of Collision

A second key barrier to adopting probability based rules is that calculating the actual probability of collision is a difficult problem that requires a huge 'Monte Carlo' analysis that would tax the capabilities of standard computing systems.

This is a further advantage of the scalar factor method for calculating separation factor. It can translate easily into a close approximation of the probability of intersection (actual collision) using the following process:

1. Calculate the Radius Factor for the two wells
   a. Rf1 = semi-major axis 1 x semi-minor axis 1 / hole 1 radius squared
   b. Rf2 = semi-major axis 2 x semi-minor axis 2 / hole 2 radius squared
   c. RF = square root of (RF1 x RF2)
2. Calculate the number of standard deviations at which the ellipses touch
   a. If the SF by expansion was based on 1 sigma then T = SF
   b. If the SF by Expansion was based on n sigma then T = n x SF
3. Calculate the following simple components
   a. S = T x 30 S is an angle in degrees that can be used in the following fit model
   b. Index = 7 x (1 + Cos (S))
   c. CR = e ^ Index E is the base for natural logarithms (2.718282)
   d. Collision Risk per million is CR / RF

Warning:
This formula only gives a good estimate of collision risk in the range from SF = 0 to SF = 3 at 2 sigma. Collisions are very rare indeed beyond this (6 standard deviations apart). Do not use this formula outside this range or collision risk will be over-estimated.

It should be noted that this calculation is the probability of the centre points of the ellipses colliding. It does not represent the complex probabilities of two curved well paths colliding in 3D space but serves as a useful guide.

The table on the following page gives an idea of what you could expect to see:

Separation Factor

Radius Factor

RF \ SF	0.25	0.5	0.75	1	1.25	1.5	1.75	2
10	94740	47079	15478	3632	671	110	18	3
20	47370	23540	7739	1816	336	55	9	2
30	31580	15693	5159	1211	224	37	6	1
40	23685	11770	3869	908	168	27	4	1
50	18948	9416	3096	726	134	22	4	1
60	15790	7847	2580	605	112	18	3	1
70	13534	6726	2211	519	96	16	3	0
80	11843	5885	1935	454	84	14	2	0
90	10527	5231	1720	404	75	12	2	0
100	9474	4708	1548	363	67	11	2	0
110	8613	4280	1407	330	61	10	2	0
120	7895	3923	1290	303	56	9	1	0
130	7288	3621	1191	279	52	8	1	0
140	6767	3363	1106	259	48	8	1	0
150	6316	3139	1032	242	45	7	1	0
160	5921	2942	967	227	42	7	1	0
170	5573	2769	910	214	39	6	1	0
180	5263	2616	860	202	37	6	1	0
190	4986	2478	815	191	35	6	1	0
200	4737	2354	774	182	34	5	1	0

Figure 92: Collision probability table.

20.9 Anti-collision Scanning and Reporting

Recommended practice is to observe the following rules when scanning wells for collision risk against a subject well;

1. On first pass, scan all wells in the field.
2. Be sure to pick up all the potential hazard wells.
3. Be sure to include plugged and abandoned wells, appraisal wells, wells drilled by other operators and wells drilled by other directional drilling companies.
4. Scan all wells to all depths at a close interval (30 ft or 10 m).
5. Document that you have checked with the client and they have verified that your database contains the same number of wells located in the same locations as their database.
6. Check that the hazard wells highlighted present no surprises to the client.
7. Thereafter scan reports may be done filtering on separation factor ≤ 4.0.

20.10 The Ellipse of Uncertainty Report

The ellipse of uncertainty report required can vary from customer to customer. Terms can vary in their usage from customer to customer and from software to software. There are certain terms that must be understood. Any ambiguity arising due to customer usage or from other software programs must be understood and dealt with so as to prevent poor well planning and accidents in execution.

Below is an example of a deep, close approach report. The table following the example presents definitions of terms commonly used in ellipse of uncertainty reporting.

Easting (m)	Northing (m)	TVD (m)	Inc	Az	MD (m)	Semi Major (m)	Semi Minor (m)	PHI	TVD Spread (m)	N'rest Well	Cr-Cr (m)	Sep Factor	Inter B'dary (m)	Hi-Side to Cr-Cr	Survey Tool
224258.31	9237705.59	1519.63	82.78	273.49	1920.00	6.46	2.57	5.16	4.86	Alpha 1 (s)	127.53	28.68	123.08	47.51	MWD
224228.61	9237707.40	1523.39	82.78	273.49	1950.00	6.82	2.68	7.59	5.06	Alpha 1 (s)	98.11	21.71	93.59	54.95	MWD
224198.90	9237709.21	1527.16	82.78	273.49	1980.00	7.19	2.78	9.75	5.25	Alpha 1 (s)	68.99	14.77	64.32	64.06	MWD
224169.19	9237711.02	1530.93	82.78	273.49	2010.00	7.56	2.88	11.67	5.44	Alpha 1 (s)	40.83	7.88	35.65	74.85	MWD
224139.48	9237712.84	1534.70	82.78	273.49	2040.00	7.93	2.99	13.38	5.64	Alpha 1 (s)	18.61	1.79	8.24	86.90	MWD
224109.78	9237714.65	1538.47	82.78	273.49	2070.00	8.30	3.09	14.89	5.84	Alpha 1 (s)	28.24	6.84	24.11	99.26	MWD
224080.07	9237716.46	1542.23	82.78	273.49	2100.00	8.67	3.19	16.23	6.05	Alpha 1 (s)	54.96	13.36	50.84	110.85	MWD

Figure 93: Example of a deep, close approach report.

Header Label-Expanded Header (Term)-Definition

Easting (m)	interpolated E-W map coordinate (in specified units) of the primary well
Northing (m)	interpolated N-S map coordinate (in specified units) of the primary well
TVD True Vertical Depth (m)	the true vertical depth (in specified units) of the centre of the primary well
Inc Inclination	the inclination vector direction of the centre of the primary well
Az Azimuth	the azimuth vector direction of the centre of the primary well
MD (m) Measured Depth (m)	the measured depth (in specified units) of the centre of the primary well
Semi Major (m)	the length (in specified units) of the longest uncertainty axis as seen looking along the centre of the primary well. (be aware that in other software it can mean the longest axis in 3D space or the longest axis in the horizontal plane. The differences are usually small.
Semi Minor (m)	the length (in specified units) of the axis at right angles to the semi major axis in whatever plane of projection is used.
PHI Phi Angle (Orientation)	the orientation of the semi minor axis from high side
TVD Spread (m)	the TVD (in specified units) occupied by the uncertainty envelope
N'rest Well Nearest Well	the name of the closest well at this point
Cr-Cr (m) Center-Center Distance	the distance (in specified units) from the centre of the primary well path to the centre of the nearest well's path
Sep Factor	Separation Factor - the separation factor calculated by the specified method
Inter b'dary (m) Inter Boundary Dist	the distance (in specified units) from the boundary of the uncertainty surface of the primary well to the boundary of the uncertainty surface of the nearest well measured along the direction of 3D closest approach
Hi-Side to Cr-Cr	the orientation of the nearest well to the primary well expressed as an angle from high side of the primary well
Survey Tool	the current survey tool being used in the primary well

20.11 Safe Scanning Intervals

It is normally not productive to scan and report an entire well plan on a very fine grained interval. A normal practice is to scan the entire well at a rather course level and then examine the report for areas that will require finer scanning intervals. For example, the report above was generated using 30 m intervals. Examining this report you should see the separation factor approaching an important value at 2040 m. When an approach is seen like this it is important to make sure that you also scan at finer resolution to make sure you catch the real closest point.

In the graphic example below a fine scanning interval has been selected and the 'tie lines' from a proposed horizontal well (blue) passing a vertical appraisal well (red) can be seen in the picture. Had a perpendicular plane scanning method been used on either well, the collision point may not have been picked up.

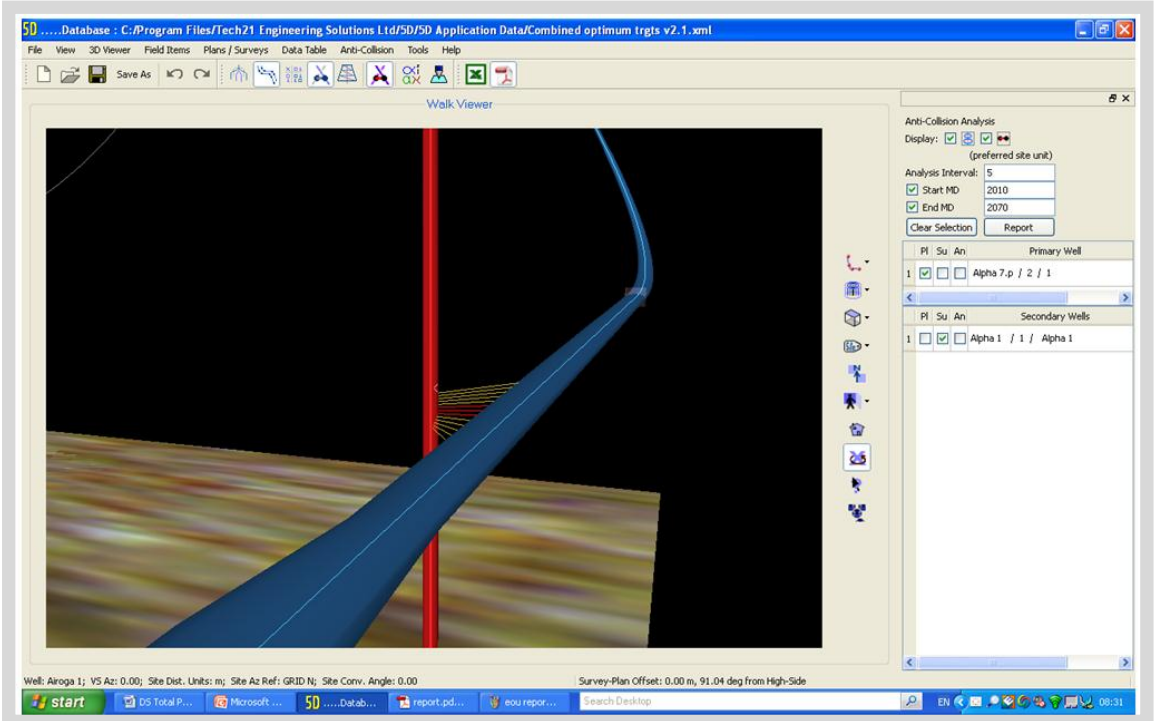

Figure 94: Fine scanning interval graphic.

This produces the report below (figure 95) and it can be seen that in this case the close approach point occurred between 2035 and 2045 meters.

Primary Well : alpha 7.p (p)

Easting (m)	Northing (m)	TVD (m)	Inc	Az	MD (m)	Semi Major (m)	Semi Minor (m)	PHI	TVD Spread (m)	N'rest Well	Cr-Cr (m)	Sep Factor	Inter B'dary (m)	Hi-Side to Cr-Cr	Survey Tool
224169.19	9237711.02	1530.93	82.78	273.49	2010.00	7.56	2.88	11.67	5.44	Alpha 1 (s)	40.83	7.88	35.65	74.85	MWD
224164.24	9237711.33	1531.56	82.78	273.49	2015.00	7.62	2.90	11.97	5.48	Alpha 1 (s)	36.38	6.74	30.99	76.79	MWD
224159.29	9237711.63	1532.19	82.78	273.49	2020.00	7.68	2.92	12.26	5.51	Alpha 1 (s)	32.09	5.61	26.37	78.77	MWD
224154.34	9237711.93	1532.81	82.78	273.49	2025.00	7.74	2.94	12.54	5.54	Alpha 1 (s)	28.02	4.47	21.76	80.77	MWD
224149.39	9237712.23	1533.44	82.78	273.49	2030.00	7.80	2.95	12.82	5.57	Alpha 1 (s)	24.28	3.35	17.03	82.79	MWD
224144.44	9237712.53	1534.07	82.78	273.49	2035.00	7.87	2.97	13.10	5.60	Alpha 1 (s)	21.05	2.31	11.93	84.84	MWD
224139.48	9237712.84	1534.70	82.78	273.49	2040.00	7.93	2.99	13.38	5.64	Alpha 1 (s)	18.61	1.79	8.24	86.90	MWD
224134.53	9237713.14	1535.33	82.78	273.49	2045.00	7.99	3.00	13.64	5.67	Alpha 1 (s)	17.27	2.30	9.77	88.97	MWD
224129.58	9237713.44	1535.95	82.78	273.49	2050.00	8.05	3.02	13.89	5.70	Alpha 1 (s)	17.31	3.13	11.78	91.04	MWD
224124.63	9237713.74	1536.58	82.78	273.49	2055.00	8.11	3.04	14.15	5.74	Alpha 1 (s)	18.72	3.98	14.01	93.11	MWD
224119.68	9237714.04	1537.21	82.78	273.49	2060.00	8.17	3.06	14.40	5.77	Alpha 1 (s)	21.21	4.87	16.86	95.17	MWD
224114.73	9237714.35	1537.84	82.78	273.49	2065.00	8.24	3.07	14.65	5.81	Alpha 1 (s)	24.48	5.83	20.28	97.22	MWD
224109.78	9237714.65	1538.47	82.78	273.49	2070.00	8.30	3.09	14.89	5.84	Alpha 1 (s)	28.24	6.84	24.11	99.26	MWD

Figure 95: Fine scanning interval report.

One good approach is to scan the entire deep well sections at a 30 m or 90 ft interval and then report close approaches at a finer 5 m or 15 ft interval. Top-hole sections with great well density may require other treatments.

20.12 Travelling Cylinder Plot

The travelling cylinder plot was invented by John Thorogood in the 1980s and is an excellent 2D representation of the proximity of other wells to planned trajectory.

20.12.1 Reading the Traveling Cylinder Plot

These plots were used regularly in the days before computers and 3D visualization software. They are still used on many rig sites where 3D visualization is unavailable. Following the examples and text below should enable you to read and understand traveling cylinder plots. Consider these screens like a radar scan when travelling down the planned trajectory.

This scan shows the basic radar screen out to a range of 250 ft. Our well passes to the left of the red well, beneath and to the right of the green well and over the top of the blue well.

At their closest points the red well comes within 120 ft., the green well comes within 70 ft. and the blue well within 30 ft.

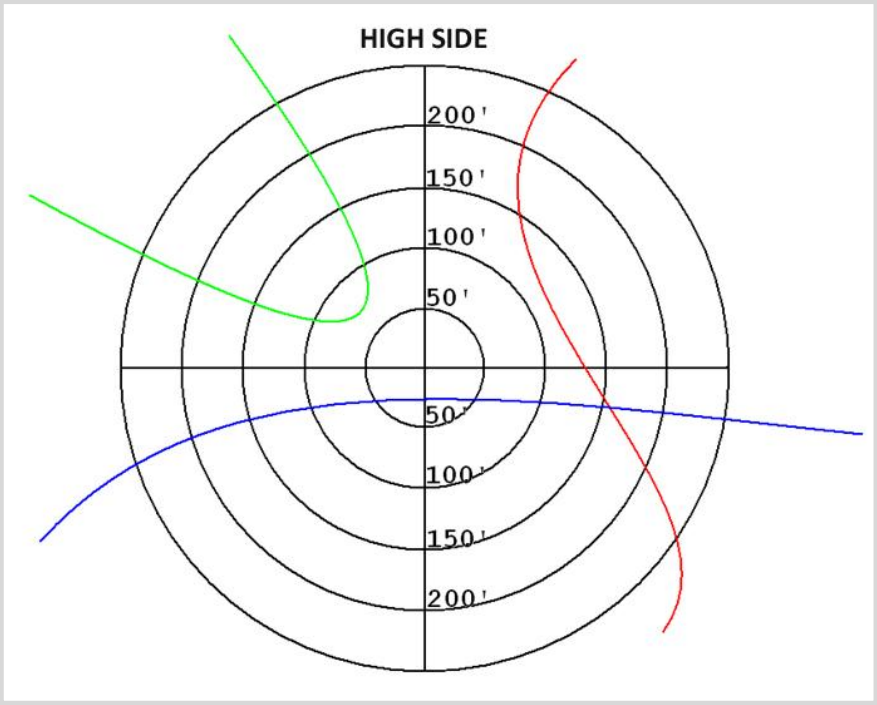

Figure 96: Traveling Cylinder Plot - basic.

It is useful then to include marker points on the object wells for each MD in our well at some reasonable interval. This shows us where that well will be relative to us when we reach that depth.

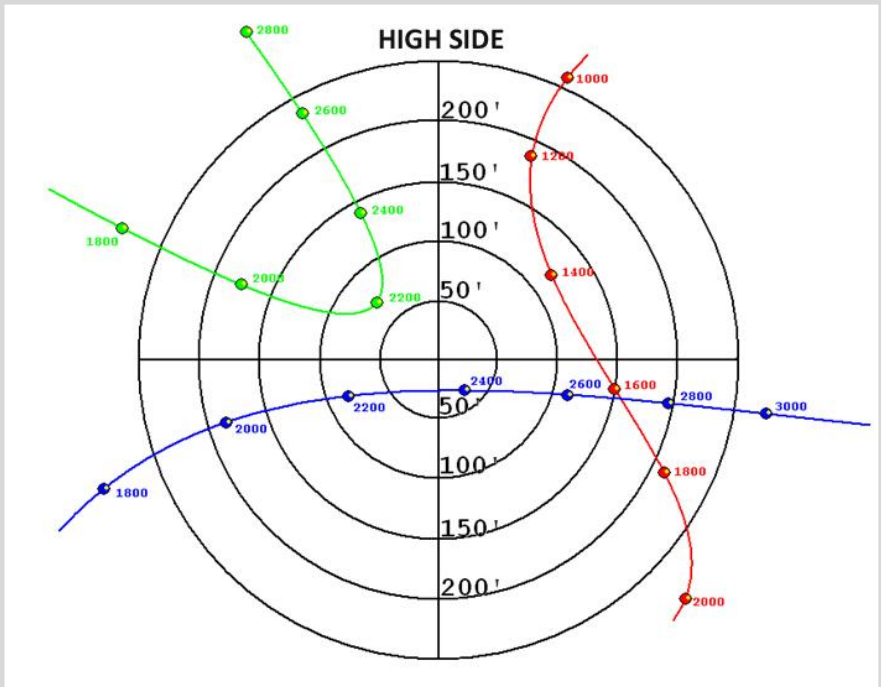

Figure 97: Traveling Cylinder Plot – with marker points.

Then it is also useful to include the uncertainty around the wells. This is best done by combining our uncertainty with the object well uncertainty and showing that as a simple offset towards us to create a 'no go' boundary for the other well.

Now we can see that the green and blue wells might be dangerously closer than we think. To avoid the blue well we would want to be above our current plan around 2300 ft. and to avoid the green we should perhaps be a little more to the right.

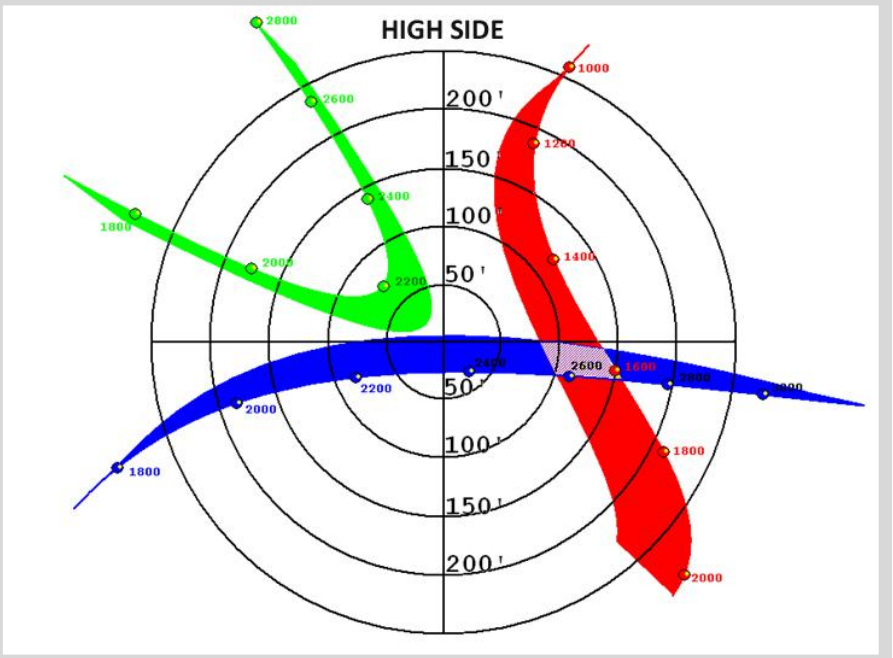

Figure 98: Traveling Cylinder Plot – marker points and uncertainty area.

20.13 Travelling Cylinder Options

There are two options for creating traveling cylinder plots, "High Side" referenced or "North" referenced.

The first example shown in this section is a "High Side" referenced traveling cylinder plot. This option has the advantage of being easier to understand but it suffers from a peculiarity in top hole as follows.

Consider how a vertical well would appear against a well drilled roughly towards and then away from it.

The red well is our well and from points A to C it would be plotted on our high side. However from points D to F it would be plotted on our low side since we have changed direction. This is the example "High Side" traveling cylinder plot shown on the right above. It appears that we will drill or have drilled straight through the blue well.

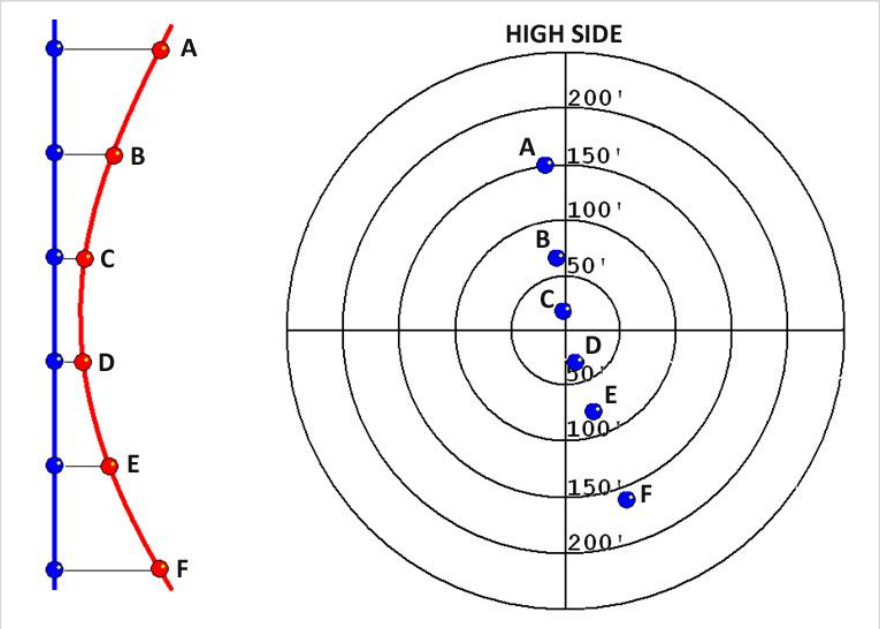

Figure 99: Traveling Cylinder Plot – marker points and uncertainty area.

One solution is always to plot your high side values along a line representing your current azimuth. This makes the traveling cylinder plot look a little different. Now North is at the top of the plot and for the first three points high side is plotted along my current azimuth e.g. 45°.

When the well is turned around before passing through points D, E, and F, the high side is now plotted along the new azimuth e.g. 225°. The points are correctly plotted to low side and appear to go out the same way they came in rather than causing unnecessary alarm with an apparent collision.

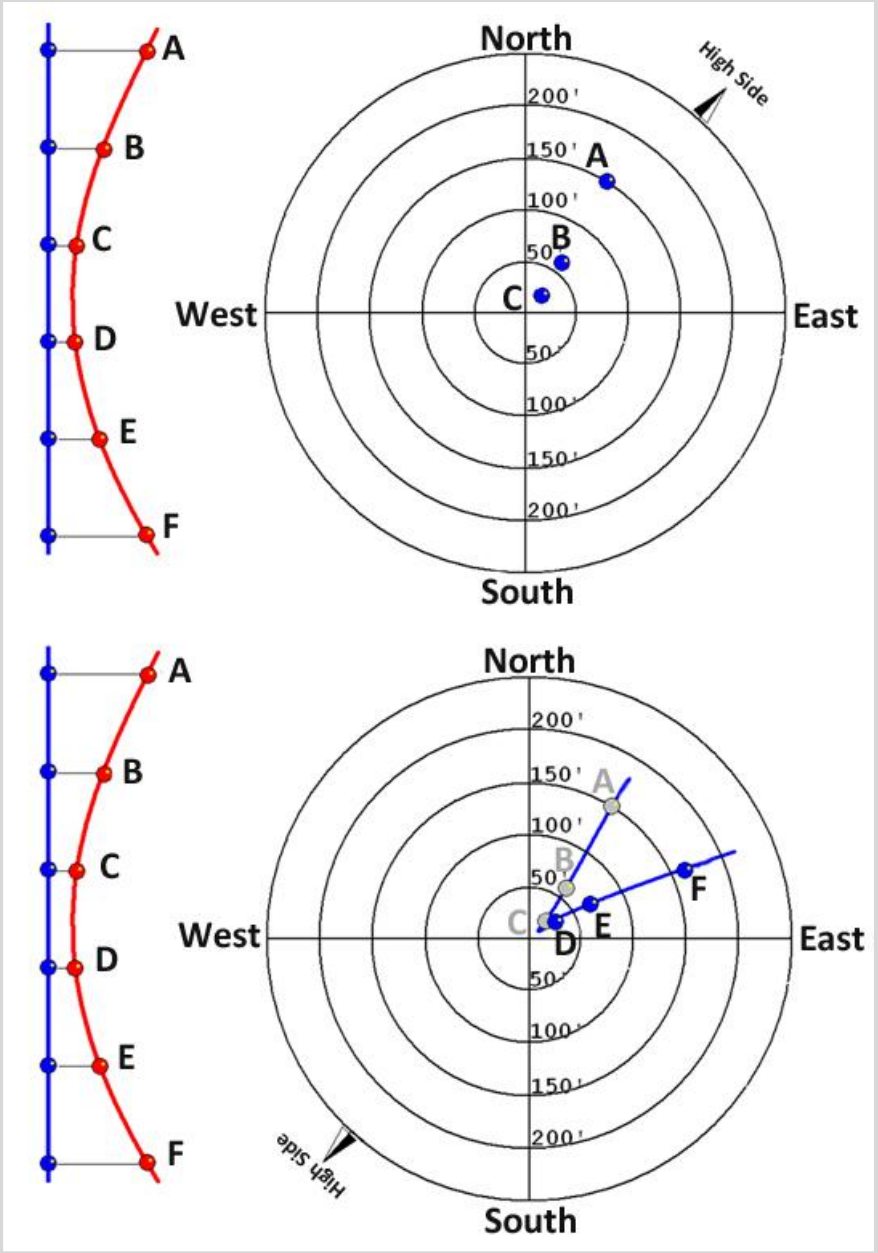

Figure 100: Azimuth referenced Traveling Cylinder Plot.

20.14 Using TVD “Crop” Diagrams

TVD “Crop” Diagrams are useful in determining the relative positions of wells when the inclinations of ALL the wells being viewed all have inclinations which are LESS THAN 60°. This diagram slices the wells along a TVD plane and presents a view of them from above. They are particularly useful in top-hole drilling to examine the trends and help visualize the clearances at each level. They are also a great aid when having collaborative discussions with either the office or client if all parties have a copy of the diagram to view.

This diagram represents a ‘slice’ through the wells at a given TVD which can be advanced and the relative positions of the wells are updated in real time. As you continue drilling down the actual well, the start of the slicing should be incremented to match the latest TVD achieved. The examples represent the well as the 0m, 50m and 100m TVDs are reached.

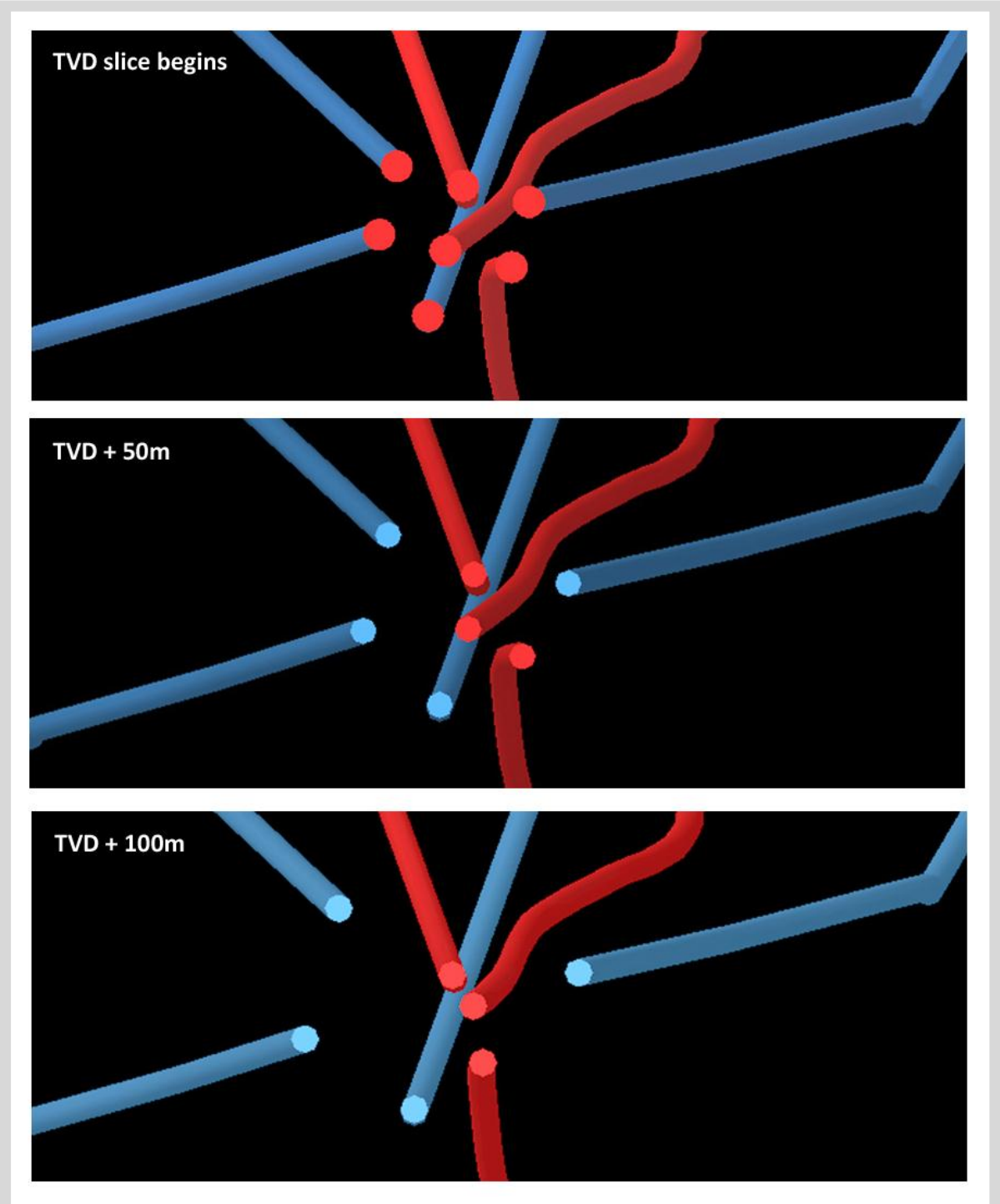

Figure 101: Slicing through the well models at a given TVD

20.15 Using Ladder Plots

The ladder plot is simply a graph of the separation to target wells against the measured depth of the planned well. They are very useful for determining which well to watch for at which depth.

The y-axis can either be the true centre to centre distance or more usefully, the inter-boundary distance of the zones of uncertainty to the object wells.

Be sure to understand the value on the y axis. The most common will be a simple centre to centre separation but ladder plots are more useful if they include uncertainty.

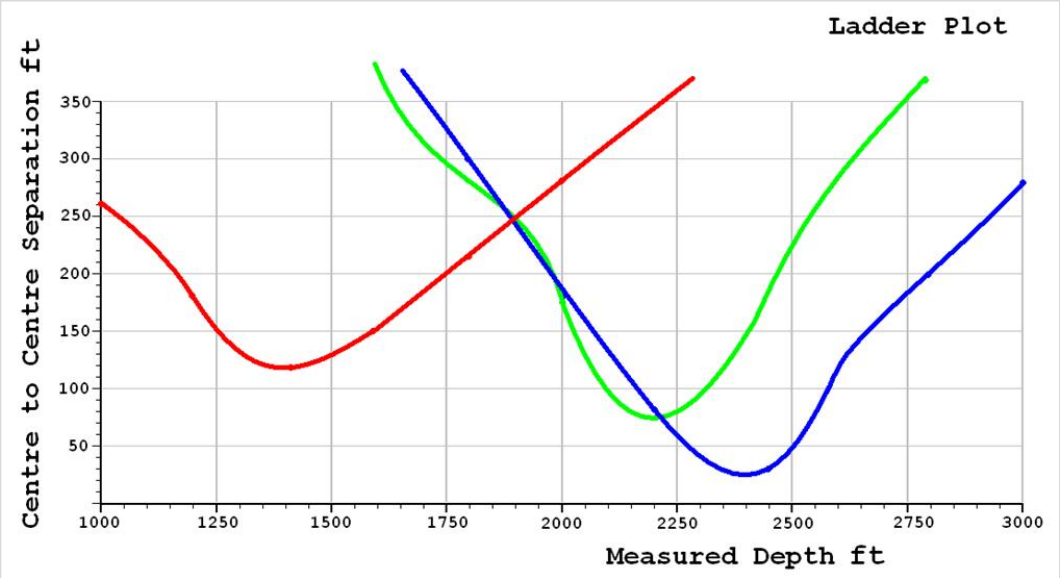

Figure 102: Basic ladder plot.

In this example the uncertainty is shown as a shaded area around the wellbores.

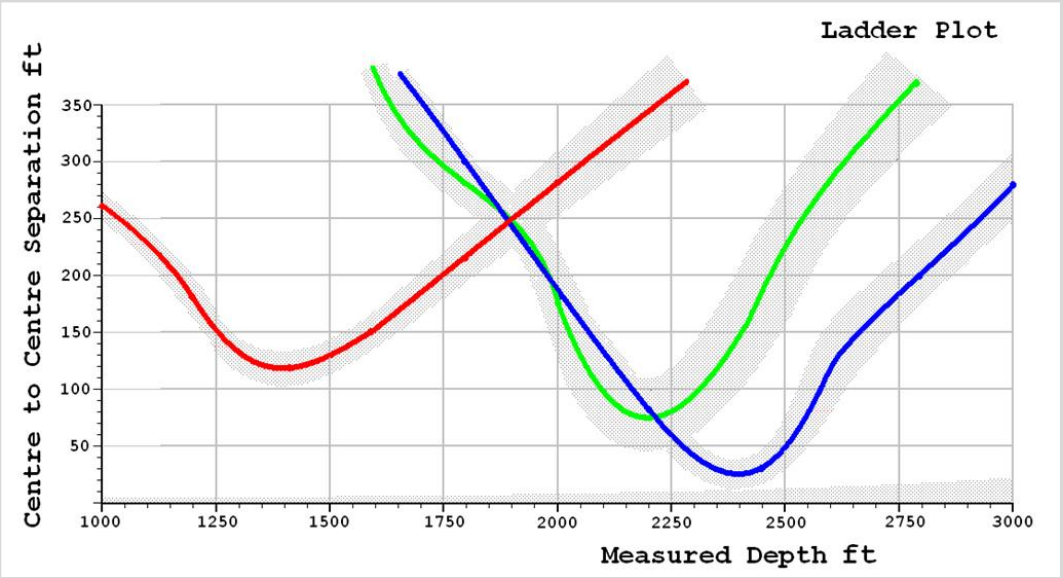

Figure 103: Ladder plot with uncertainty added.

Another example is to show the inter-boundary separation only on the y axis. In this example you can see that the blue well uncertainty combined with the planned well uncertainty uses up all the separation.

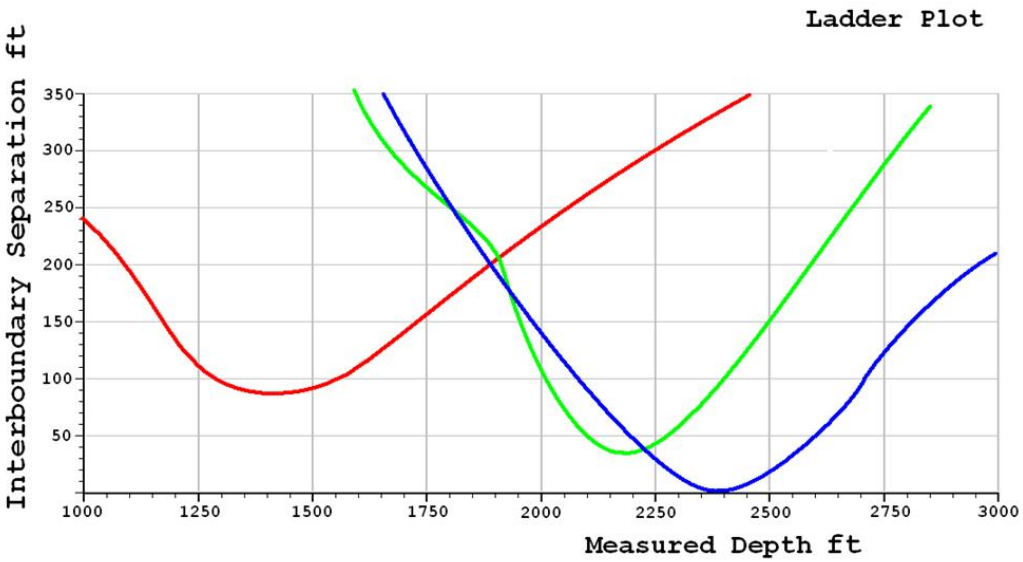

Figure 104: Ladder plot using inter-boundary separation only.

In these examples you can see that the most dangerous hazard is the blue well at the planned well's interval between 2350 ft. to 2450 ft.

✧

CONTENTS

21. Planning for Minimum Risk

21.1 Designing the wellpath

The well planner has to consider all of the following criteria when designing the original wellpath;

a) Is the design drillable in the formations it encounters?
b) Are the doglegs practical from a Torque and Drag standpoint, drillpipe fatigue, casing wear, formation damage, the potential for positioning ESPS or other dogleg dependent completion equipment?
c) Does the design hit the target with confidence?
d) Does the design avoid other wells safely and avoid geo hazards?

Once the well plan has been created the first time, it will only be a geometrical solution which may need reviewed in the light of experience.

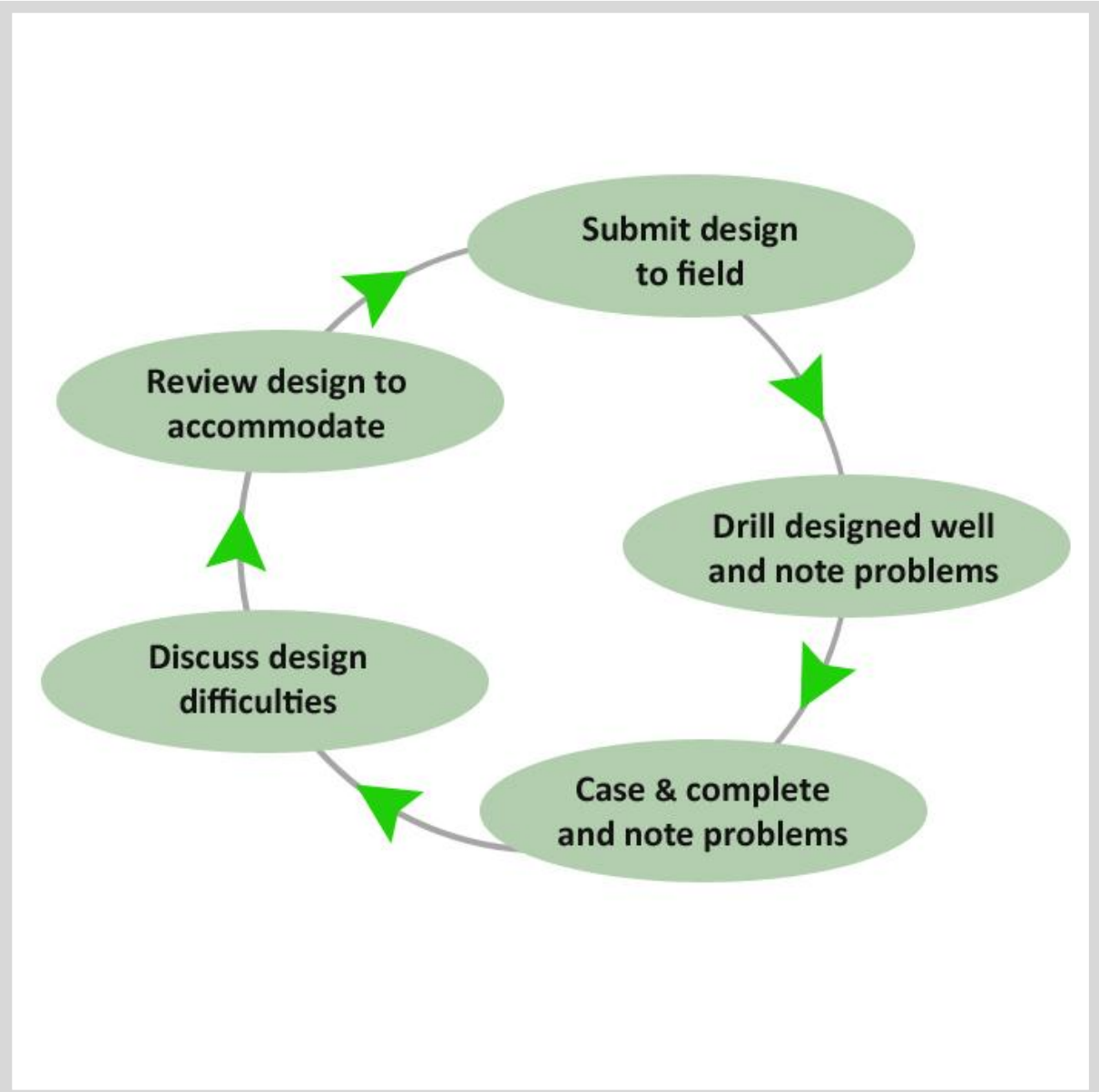

Figure 105: Minimum risk planning wheel.

The following shows some of the feedback from the field and some possible remedies that will ensure that the well plan is improved for the next iteration:

Problems

1. Shallow formation can't take the build rate.
2. Rotating the tangent drops 0.5 per 100.
3. Formation at 6700 to 6800 TVD is too soft.
4. Can't get RSS to go above 5.2 degs/100.
5. Formation tops are always early.

Remedies

1. Build at 1 then 1.5 then 2 in shorter sections.
2. Design the tangent as a 0.5 per 100 drop.
3. Either pass through at low inc or design a drop.
4. Use the RSS actual DLS value in the design.
5. Compensate to observed depths.

CONTENTS

22. Basic Data QC

22.1 Checking raw data

Raw data observed in the field can be checked for basic quality control. Any set of MWD raw sensor data can be used to calculate a field strength and dip angle using the following formulae.

The Dip Angle can be calculated from the following simple formula:

$$\text{DipAngle} = \sin^{-1}\left[\frac{(BxGx + ByGy + BzGz)}{(BtGt)}\right]$$

Where Bt = square root of (Bx2 + By2 + Bz2) ie the total Magnetic Field
And Gt = square root of (Gx2 + Gy2 + Gz2) i.e. the total Gravity Field

In general if the Field Strength calculated is within 300nT of the expected field and the dip angle to be within 0.25 of the expected dip, we would consider the MWD to be within acceptable tolerances.

CONTENTS

23. Advanced Data QC

23.1 Varying curvature method

Although Minimum Curvature is now considered the indisputable industry standard for survey calculation, another method was developed in the early 1990s known as Varying Curvature. It turns out that the VC method produces very similar results to Minimum Curvature but has the advantage that it can be used to perform QC on whole surveys to check for poor consistency in the data.

Consider again the effect of a small increase in MD along a particular inclination and direction.

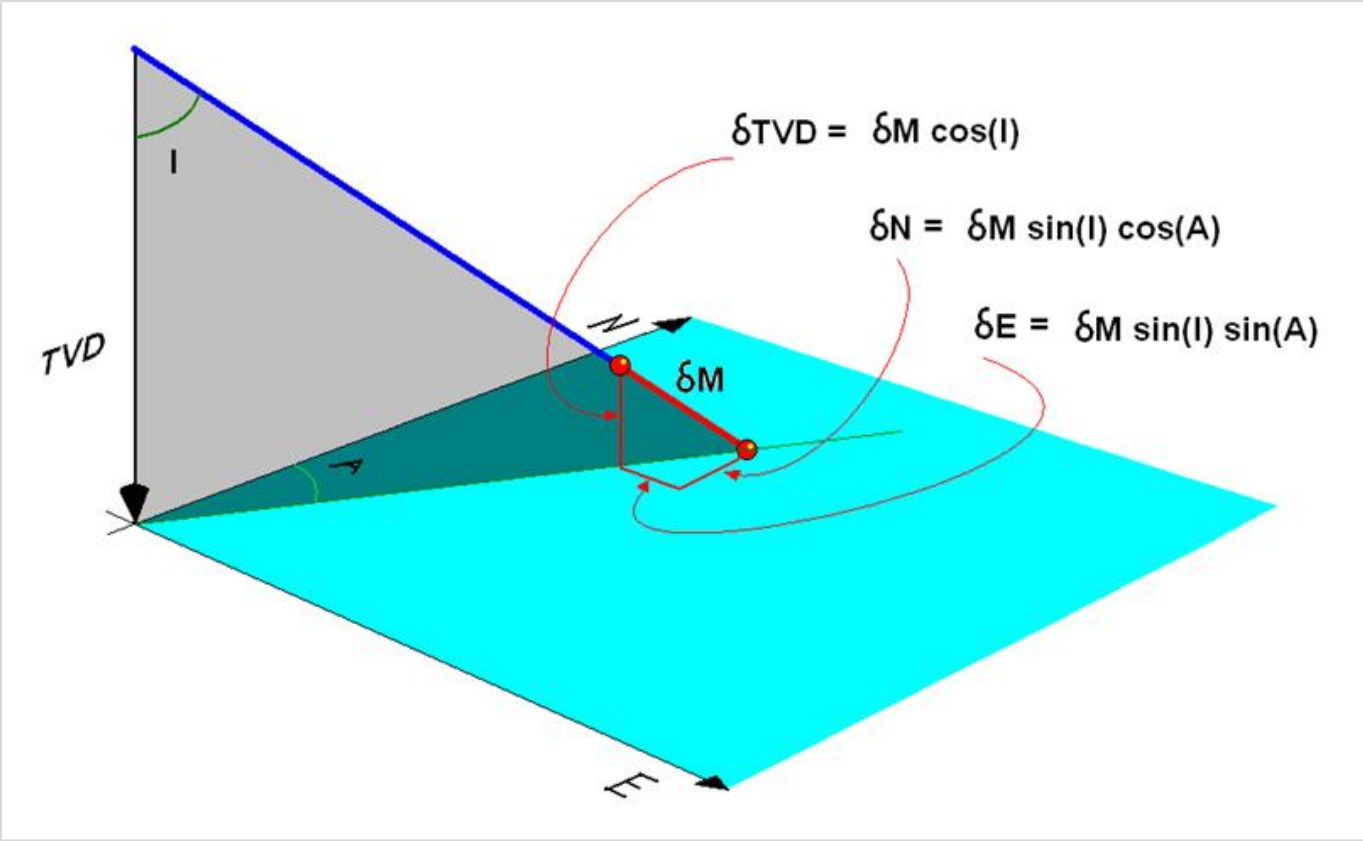

Figure 106: Measured depth error and the effect on North, East and TVD.

If we were to produce a set of graphs where the x axis is measured depth and the y axes were respectively cos(I), sin(I)cos(A) and sin(I)sin(A) then we can use the fact that the integrals of each would be the accumulated sums of TVD, Northing and Easting.

$$\begin{aligned} \delta TVD &= \delta M \cos(I) \\ \delta N &= \delta M \sin(I)\cos(A) \\ \delta E &= \delta M \sin(I)\sin(A) \end{aligned} \quad \Longrightarrow \quad \begin{aligned} \int \delta TVD &= \int \cos(I)\,\delta M = TVD \\ \int \delta N &= \int \sin(I)\cos(A)\,\delta M = N \\ \int \delta E &= \int \sin(I)\sin(A)\,\delta M = E \end{aligned}$$

In the graphs below, the y axis is used to plot the terms shown for each observation and if a smooth curve is drawn through the observed points, the TVD, Northing and Easting (from the start of the well to any MD) are simply the areas under the graphs.

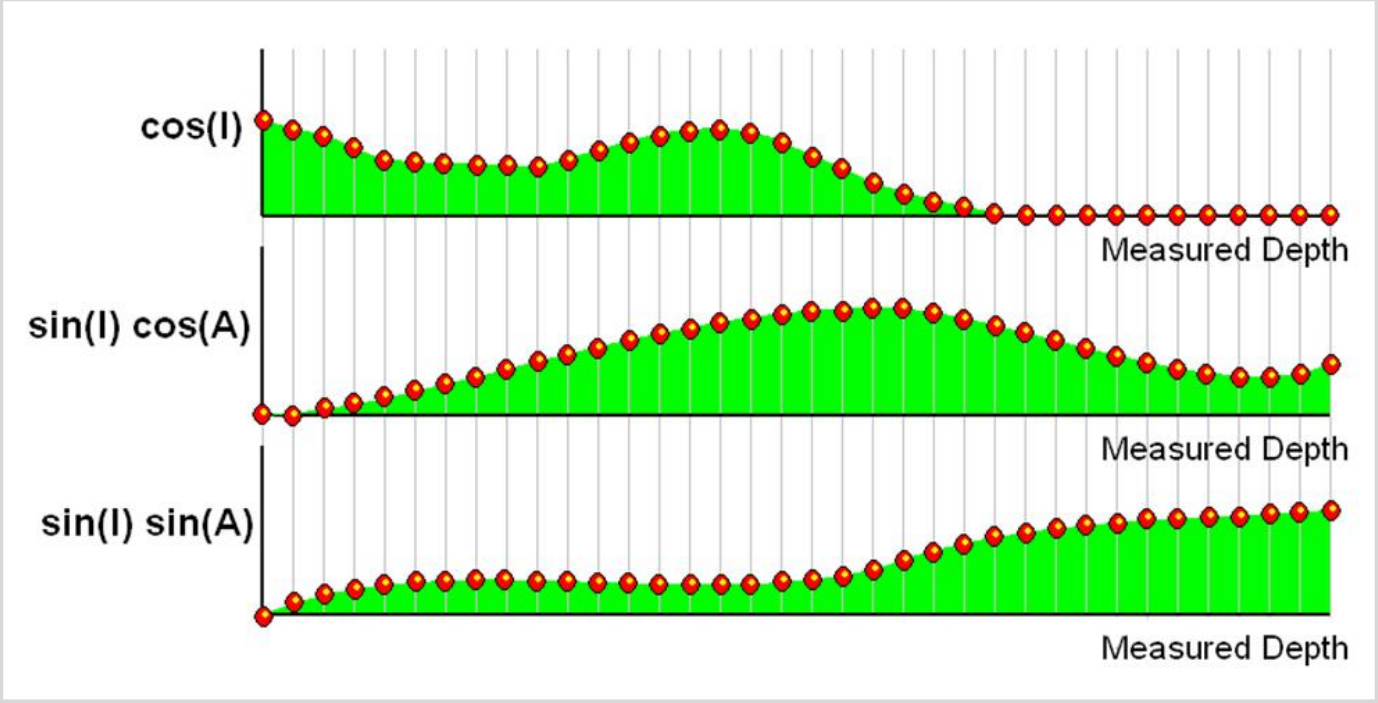

Figure 107: Using a smooth curve drawn through the observed points to show North, East and TVD.

The area of the cos(I) graph is the TVD, the area of the sin(I)cos(A) graph is the Northing and the area of the sin(I)sin(A) graph is the Easting. By fitting smooth curves through the points, the curvature of the wellpath effectively varies smoothly through the survey rather than being fixed to a given radius between observations. Now consider the effect of a poor survey on the above graphs.

The inconsistent survey will 'pull' the area towards itself and the difference it makes can be determined by the difference in the area (The blue region in figure 107). In other words, varying curvature can compare the area under any of the three graphs, with and without a given survey observation and determine the effect each observation has on the wellpath position. Surveys consistent with those on either side will have very little effect if they are removed. This produces a 3D vector 'shift' in TVD, Northing and Easting created by the rogue observation. This vector can be split into a high/low side component and a left/right component and plotted against measured depth for a very useful consistency 'signature' known as a varying curvature analysis. This provides the surveyor with a digital spellchecker on his data since any typing errors will show up as highly inconsistent with the surrounding surveys.

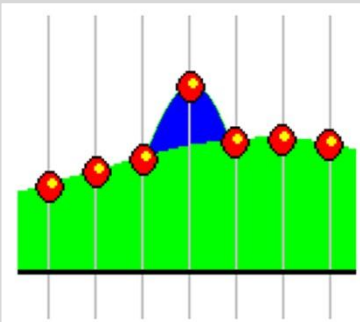

Figure 108: Spotting inconsistencies in the survey.

✧

CONTENTS

24. Tortuosity

24.1 Illustrating tortuosity

This has been variously defined as the variability in dogleg severity or the unnecessary undulations in the wellpath. Essentially tortuosity describes a lack of smoothness in the well trajectory and the greater the tortuosity the greater the likelihood of problems when running casing or excessive drillpipe stress when rotating in hole. One simple presentation of tortuosity is to plot the dogleg severity against measured depth.

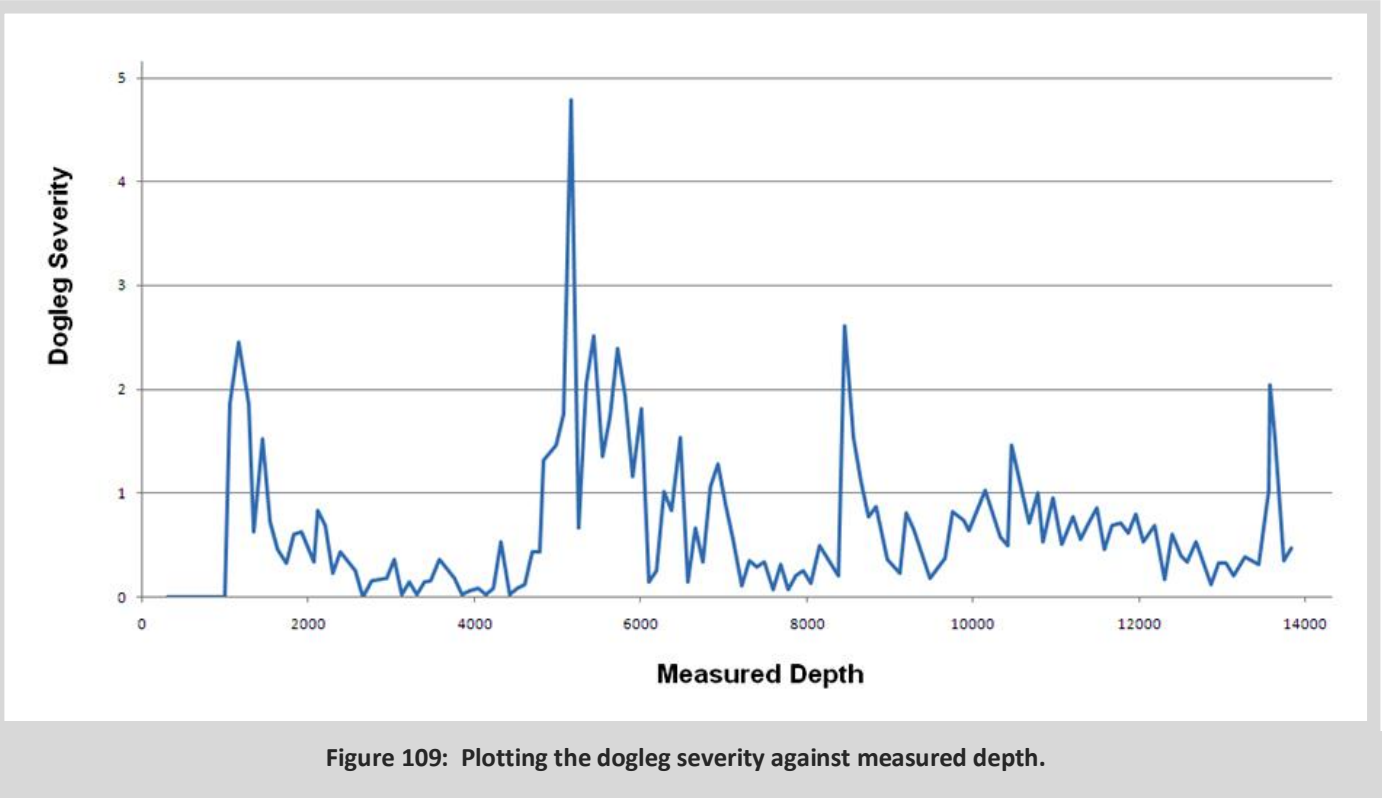

Figure 109: Plotting the dogleg severity against measured depth.

However, on its own, this is hard to interpret in a measurable way. Clearly, the well is tortuous but how can we define acceptable tortuosity? If the wellplan had prescribed a 4 deg/100 build rate, it would be inappropriate to penalise a dogleg severity of 4 deg/100. The real problem is when the dogleg severity varies too much and a 4 deg/100 build is constructed with dogleg severities of 0 to 12 varying wildly during the build section. A well which smoothly followed the wellplan would have very little variation in dogleg severity. Figure 109 is the well plan for the well above.

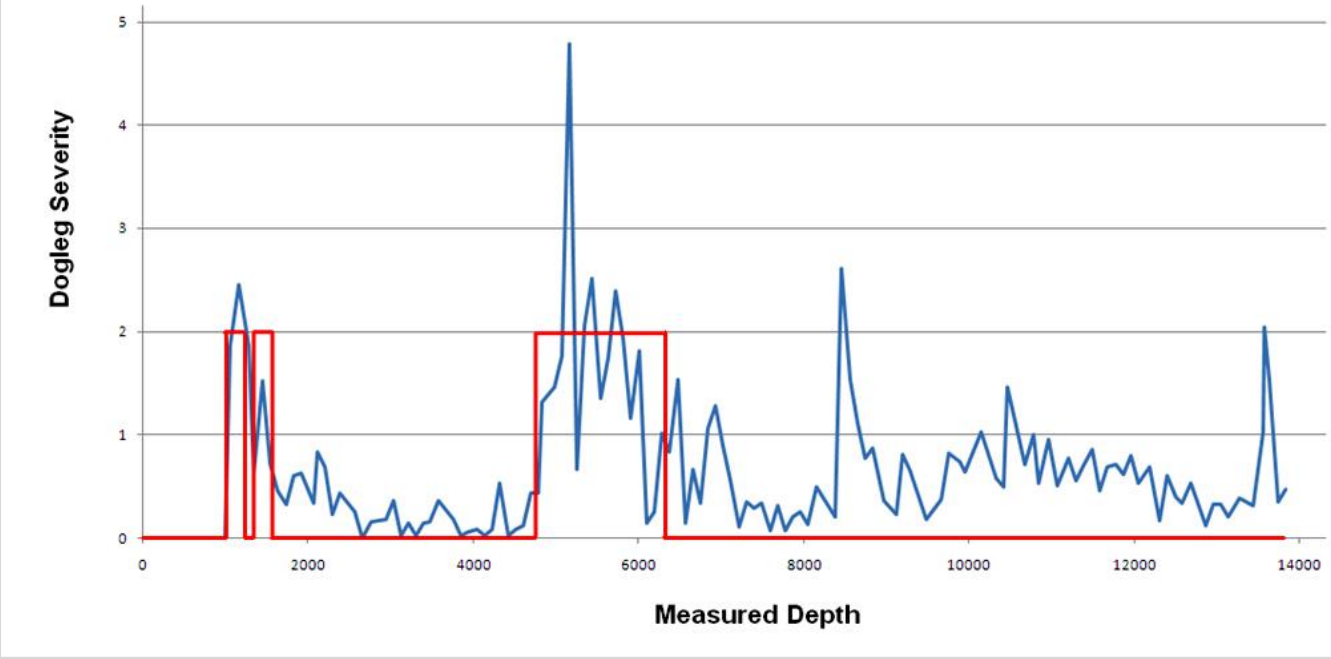

Figure 110: Example well plan graph.

The planned dogleg severity should have consisted of a short 2 deg/100 nudge and drop then a simple 2deg/100 build to 27 degrees inclination then a hold to TD. The actual inclination against md graph is plotted in figure 110:

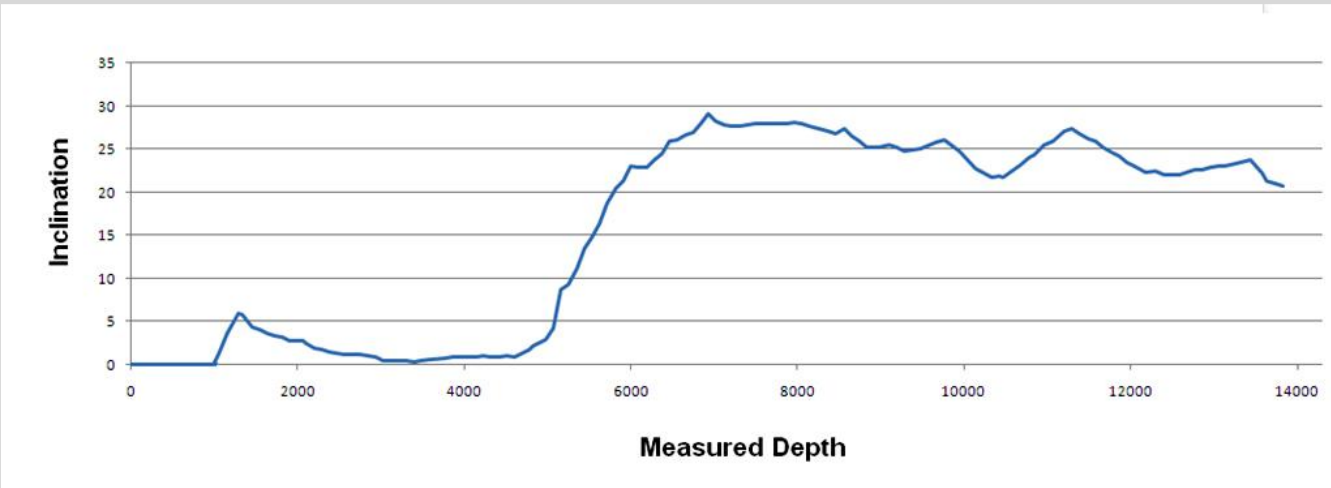

Figure 111: Actual inclination against measured depth graph.

Clearly things did not go according to plan. However, the directional driller used a standard technique for the drop section of the nudge by replacing a motor (smooth build) with a pendulum rotary assembly (slow natural drop) which is an acceptable and economic method of returning to vertical. On closer examination, the build section is rapid at first then slower later. This is likely to be an assembly with a bent sub above the motor which is less aggressive at higher inclinations but assembly was capable of over 5 degrees of dls when only 2 was needed, suggesting a slide ratio of less than 40%. This explains the rapid changes in dls in the build section but even that is not unusual. The main problems here lie in the hold section where the directional driller has great trouble holding inclination and tends to steer a great deal in an attempt to place the surveys 'on the line'. He is over correcting and creating unnecessary doglegs when a simple 'aim at the target from where you are' approach would have created a smoother well path.

24.2 Calculating Tortuosity

If we create an additional column in a spreadsheet to hold the changes in dls from one survey to the next, we can use that to calculate unwanted curvature induced in the wellbore. We do not need to know the well plan since any well plan will require constant curvature in each section and we are measuring the deviations from constant. By multiplying the change in dls (converted to degs/ft or degs/m) by the measured depth difference, we can simply add up the unwanted curvature in the wellpath. If the dls is unchanged, this process accumulates zero unwanted curvature.

Unwanted curvature is the sum of (dls change x md change). In the example above the unwanted curvature accumulation looks like this:

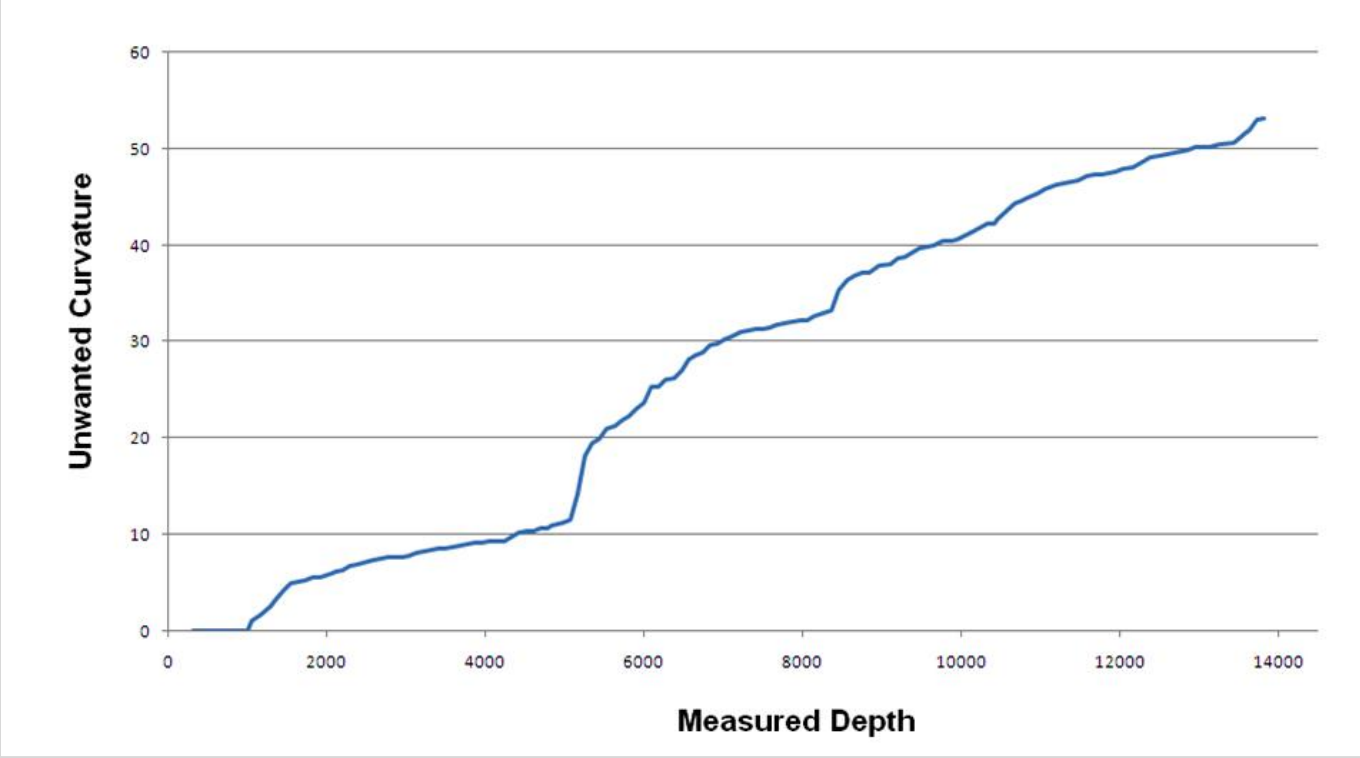

Figure 112: Unwanted curvature accumulation graph.

The design total curvature was only 27 degrees and the unwanted curvature is an additional 54 degrees or 200%. Anything over 100% would be considered tortuous and likely to cause casing and pipe problems.

✧

CONTENTS

25. Some Guidelines for Best Practice

25.1 Required Data

Experience has shown that the most common cause of an unexpected collision is lack of awareness of the very existence of the hazard well! It is essential that the following questions are asked before well planning commences;

1. What are the sources of the client survey data?
2. How can we be sure that the data set is complete?
3. How does the database compare with the data held by the geoscientists, in-house surveyors and the regulatory authorities?
4. Are we sure that all surveys are complete to TD?
5. Are all possible offset wells within reach of the current well included? (Be sure to include wells from other sites if necessary and exploration wells).
6. Does the reference data agree with those held in other in-house databases and is it what the site surveyors used when establishing site coordinates and directions?

The following information should be gathered and considered in detail prior to beginning the actual well planning design process.

25.2 Position and Referencing Data

Clearly it is essential that all data required to fully define the location of a well and its adjacent hazard wells must be available to the well planner. These must include;

Required Data:	**Example:**
The field or project name	Orkney West
The name of the well site	Alpha Platform
The units of measure used at this site	Ft
The geographic location of the Site Centre in Latitude and Longitude	56° 26’ 18.32” N 11° 32’ 56.78” W
The Geographic Datum on which Latitude and Longitude are defined	WGS 84
The map coordinates of the Site Centre	6257790.50 North 342842.46 East
The map units used	m
The coordinate system in which the Map Coordinates are defined	UTM Zone 29 North
The accuracy of this point (surface uncertainty)	+/- 5 m
The clients preferred North Reference True or Grid	Grid
The Grid Convergence	-2.12o
The height of the drill floor above Field Datum	120 ft
The Definition of Field Datum	Mean Sea Level
The Depth BDF to the Ref Point from which uncertainty accumulates	270ft
The Definition of the Reference Point	Mud Line

For each well including the new planned well:

The local slot coordinates relative to the site centre	15.56 ft N
(Note these must be in the clients preferred North Reference)	1.41 ft E
Any deviation of TVD origin above (or below) site drill floor	0 ft
Current Magnetic Vector at site (for inclusion in drawings only)	50017 nT @
	70.19° Dip Angle
	-7.76° Declination
Magnetic Field Date	27th July 2009
Magnetic Field Model	BGGM 2009

*If IFR data is to be used then the Magnetic Vector relevant to each hole section must be identified.

25.3 The Existing Well Data Including Survey Tools and Depth Ranges

Any missing data within the drilling range of the new well constitutes a serious safety hazard. Whilst the legal responsibility for the completeness and quality of a survey database rests with the asset owner, in practice, many operators do not have a formal survey focal point with responsibility for this. It is imperative that all steps be taken to ensure the quality and completeness of the data before the well is planned and this should be formally agreed in writing with the operator and included in any new proposals.

The required data includes the surveys and the detail of the individual tool runs in each survey leg, for example:

Survey Summary Form

*all depths in consistent units

Well Name	Surface Position				Survey Runs	Survey Tool	Date (dd/mm/yy)	Start Depth	End Depth	Corrections	Comments
	North	East	Defined	Accuracy							
Alpha 5	0	0	local		2	Gyrodata RGS	18/05/08	0	1567	None	13 3/8 Casing
						MWD	12/06/08	1620	7943	Sag + IFR	
Alpha 9	-15.56	-1.41	local		3	SDI Keeper	02/11/08	0	1638	None	13 3/8 Casing
						SDI Keeper	16/11/08	1640	2189	None	Drillpipe in 12 1/4 hole
						MWD	23/11/08	2240	8345	Sag + IFR + Mag Int	
22/17 a	6270163	341763.8	map	20m	1	TOTCO	09/04/83				

Then for each survey:
Alpha 5 Gyrodata RGS from 0-1567

Md	Inc	Dir	TVD	North	East
0	0	0	0	0	0
etc					
etc					

Notes on the treatment of vertical wells:

1. If any “inclination only” surveys are part of the database they are best entered with the inclinations set to 0.00 for the entire “inclination only” survey. A common error is to enter the actual inclination whilst leaving the azimuth set to 0.00. This erroneously enters a well that has been drilled due north and creates a false impression that a safe clearance exists passing to the south side of the “vertical” well.
2. If the vertical well has been surveyed by “inclination only” then well planners should assume the vertical well can deviate 50 feet per thousand in any direction as the safety envelope for planning around this “vertical” well.
3. When a ‘vertical’ well with “inclination only” surveys constitutes a high collision risk a recommended practice is to enter the “well” at least six times into the database. This should be done by entering the actual inclinations (in six successive wells) first with azimuths of 0°, then another with azimuths of 60°, and then additional wells at azimuths of 120°, 180°, 240° and 270° successively to create an ‘Eiffel Tower’ of possible locations of the vertical well. The well planners’ and directional drillers’ software can then conduct anti-collision scans against these dummy wellbores.

25.4 Existing Planned Well to be Avoided (Caging)

'Caging' can happen in the latter part of a site development program when collision risk with currently undrilled planned wells are given low priority. Eventually the planned wells cannot be drilled as the slot is 'caged' in by other wells. It is worth including the trajectories of currently undrilled but planned wells into the program so that their positions can be considered when assessing the impact of a non-conformity to plan. In such cases, the client should be apprised of the risk to future well plans and his agreement to proceed be obtained in writing. Clearly it is best if all anticipated future well plans are included at the earliest stage.

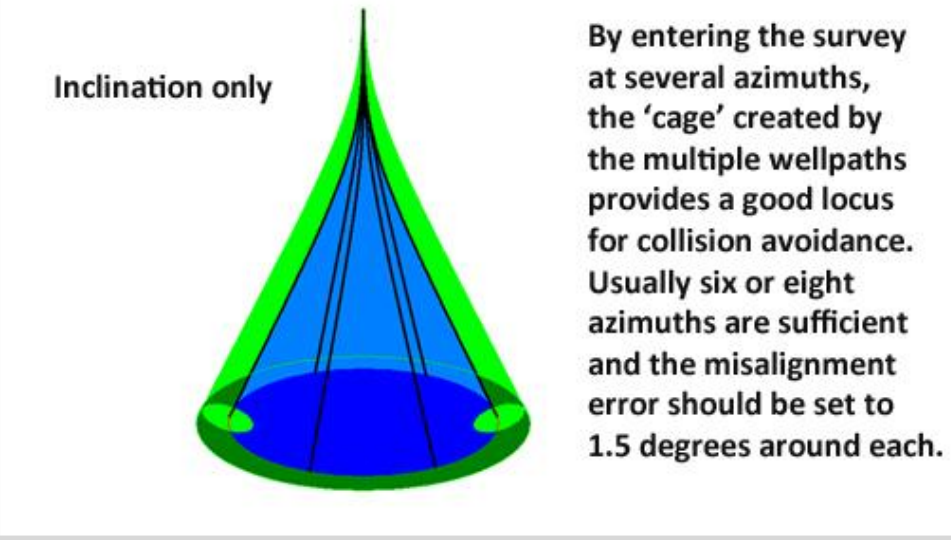

Figure 113: 'Caging' for collision avoidance planning.

25.5 Separation Rules

Most clients will adopt a safety rule based on separation factor. Separation factor is the ratio of the "as surveyed" or "as planned" centre to centre distance of the wells divided by the uncertainty as to their actual locations.

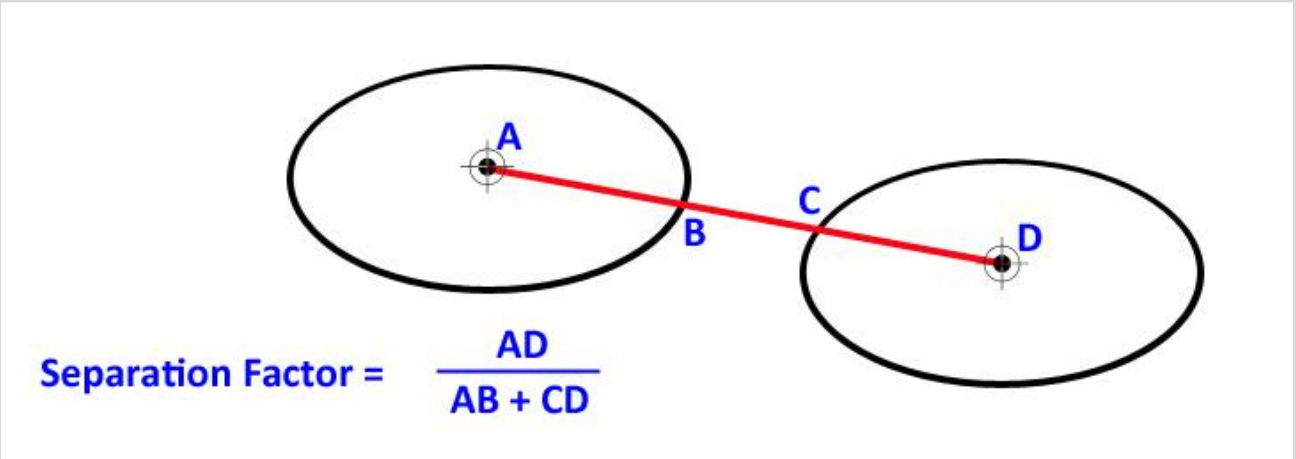

Figure 114: Graphic of separation factor calculation.

For most companies the rules will be similar to the following but in the absence of client guidelines the following should be adopted:

1. When the database is newly acquired or constructed, or when starting a new project a scan of all wells in the field must be conducted.
2. Review this scan with a local field expert to verify:
    a. All wells are present. (Be careful to verify plugged and abandoned exploration wells as well as wells drilled by other operators are included).
    b. All wells are located properly. (The catalogue of errors that can occur when transferring a database is numerous but just two examples are: 1) incorrect platform location and 2) transposing the inclination and azimuth values between the original data and the new database).
3. With a fully quality controlled database scan all wells that have even a remote possibility of being within the path of the planned well.
4. Report all sections where the separation factor falls to less than 4.0.
5. If the separation factor falls below 1.5 attempt to adjust the well plan. For many operators this is the approach limit that requires adjacent wells to be shut in whilst drilling the new well. This is not in itself a risk free strategy since the pressures rise bringing their own hazards.
6. If the separation factor falls below 1.25 attempt to adjust the well plan. This is leaving inadequate room for directional drilling adjustments during the execution phase.
7. In certain cases it will not be possible to plan the well without generating separation factors that transgress the limits in the two previous instructions. Most companies have a policy that in no cases should a well be planned with a separation factor less than 1.0. There may be some dispensation policy in place that if the risk is merely fiscal and other mitigating steps are taken, permission may be given to proceed but this should always be the last resort.
8. If it is impossible to plan the well without separation factors equal to or greater than 1.0 then a special dispensation to drill with a sub 1.0 separation factor must be granted by the client. The operator may grant this dispensation in special cases. Examples cases might be; if the hazard well is one that is planned but not yet drilled, or perhaps in a case where circumstances like the following apply: (These are only examples and by no means comprehensive).
    a. The hazard well is protected by at least two layers of casing.
    b. The angle of attack is less than 10 degrees.
    c. The wells are equally pressured or the pressure difference is safely manageable.
    d. The well cross sections make up less than 1% of the 1 sigma error ellipse.

CONTENTS

APPENDICES

Appendix A: Details of the Mathematical Derivations

A1 - Details of the Propagation Mathematics

Recall from section 19.2.5 that the core equation for the propagation of the errors from the error source through to the survey position error is:

$$\boldsymbol{e_i = \sigma_i \frac{dr}{dp} \frac{\partial p}{\partial \varepsilon_i}} \qquad \textbf{(A.1)}$$

Where:

e_i is the size of the error in NEV axis due to error source i at the current survey station (a 3x1 vector)

σ_i is the magnitude of the ith error source (a scalar)

$\frac{\partial p}{\partial \varepsilon_i}$ are the weightings functions, the effect of the ith error source on the survey measurements; md, inc and azimuth. (a 3x1 vector)

$\frac{dr}{dp}$ is the effect of the survey errors in md, inc and az on the wellbore position in the NEV axis, (i.e. a 3x3

$$\textbf{matrix} \begin{bmatrix} \frac{dN}{dMd} & \frac{dN}{dInc} & \frac{dN}{dAz} \\ \frac{dE}{dMd} & \frac{dE}{dInc} & \frac{dE}{dAz} \\ \frac{dV}{dMd} & \frac{dV}{dInc} & \frac{dV}{dAz} \end{bmatrix})$$

So we need to be able to calculate the $\frac{dr}{dp}$ matrix. Given that the survey measurements define the depth, inclination and azimuth at either end of an interval the position over an interval will depend on the survey measurements at two stations. If we write Δr_k for the displacement between survey station *k-1* and *k* and hence Δr_{k+1} for the displacement between stations *k* and *k+1,* then we can split $\frac{dr}{dp}$ in to the variation over the preceding and following survey intervals and write:

$$\boldsymbol{e_{i,l,k} = \sigma_{i,l} \left(\frac{d\Delta r_k}{dp_k} + \frac{d\Delta r_{k+1}}{dp_k} \right) \frac{\partial p_k}{\partial \varepsilon_i}}$$

Where:

$e_{i,l,k}$ is the error due to the *i*th error source at the *k*th survey station in the *l*th survey leg

$\frac{d\Delta r_k}{dp_k}$ is the effect of the errors in the survey measurements at station k, on the position vector from survey station k-1 to survey station k and similarly

$\frac{d\Delta r_{k+1}}{dp_k}$ is the effect of the errors in the survey measurements at station k, on the position vector from survey station k to survey station k+1

Although minimum curvature is the preferred method for calculating the wellbore positions, it is simpler to use the balanced tangential method to determine $\frac{d\Delta r_k}{dp_k}$ and there is no significant loss of accuracy.

The balanced tangential model gives us the following equation for the displacement between any two survey stations *j-1* and *j* in *nev*-axes:

$$\boldsymbol{\Delta r_j = \begin{bmatrix} \Delta N \\ \Delta E \\ \Delta V \end{bmatrix} = \frac{D_j - D_{j-1}}{2} \begin{bmatrix} sinI_{j-1} cosA_{j-1} + sinI_j cosA_j \\ sinI_{j-1} sinA_{j-1} + sinI_j sinA_j \\ cosI_{j-1} + cosI_j \end{bmatrix}} \qquad \textbf{(A.3)}$$

So for the interval between stations *k-1* and *k* we can write:

$$\frac{d\Delta r_k}{dp_k} = \begin{bmatrix} \frac{d\Delta r_k}{dD_k} & \frac{d\Delta r_k}{dI_k} & \frac{d\Delta r_k}{dA_k} \end{bmatrix}$$

Substituting *j=k* and differentiating equation (A.3) we get:

$$\frac{d\Delta r_k}{dD_k} = \frac{1}{2}\begin{bmatrix} sinI_{k-1}cosA_{k-1} + sinI_k cosA_k \\ sinI_{k-1}sinA_{k-1} + sinI_k sinA_k \\ cosI_{k-1} + cosI_k \end{bmatrix}$$

$$\frac{d\Delta r_k}{dI_k} = \frac{1}{2}\begin{bmatrix} (D_k - D_{k-1})cosI_k cosA_k \\ (D_k - D_{k-1})cosI_k sinA_k \\ -(D_k - D_{k-1})sinI_k \end{bmatrix}$$

$$\frac{d\Delta r_k}{dA_k} = \frac{1}{2}\begin{bmatrix} -(D_k - D_{k-1})sinI_k sinA_k \\ (D_k - D_{k-1})sinI_k cosA_k \\ 0 \end{bmatrix}$$

Putting it together:

$$\frac{d\Delta r_k}{dp_k} = \frac{1}{2}\begin{bmatrix} sinI_{k-1}cosA_{k-1} + sinI_k cosA_k & (D_k - D_{k-1})cosI_k cosA_k & -(D_k - D_{k-1})sinI_k sinA_k \\ sinI_{k-1}sinA_{k-1} + sinI_k sinA_k & (D_k - D_{k-1})cosI_k sinA_k & (D_k - D_{k-1})sinI_k cosA_k \\ cosI_{k-1} + cosI_k & -(D_k - D_{k-1})sinI_k & 0 \end{bmatrix}$$

Similarly, for the interval between stations *k* and *k+1* we can write:

$$\frac{d\Delta r_{k+1}}{dp_k} = \begin{bmatrix} \frac{d\Delta r_{k+1}}{dD_k} & \frac{d\Delta r_{k+1}}{dI_k} & \frac{d\Delta r_{k+1}}{dA_k} \end{bmatrix}$$

Substituting *j=k+1* and again differentiating equation (A.3) we get:

$$\frac{d\Delta r_{k+1}}{dD_k} = \frac{1}{2}\begin{bmatrix} -sinI_k cosA_k - sinI_{k+1}cosA_{k+1} \\ -sinI_k sinA_k - sinI_{k+1}sinA_{k+1} \\ -cosI_k - cosI_{k+1} \end{bmatrix}$$

$$\frac{d\Delta r_{k+1}}{dI_k} = \frac{1}{2}\begin{bmatrix} (D_{k+1} - D_k)cosI_{k+1}cosA_{k+1} \\ (D_{k+1} - D_k)cosI_{k+1}sinA_{k+1} \\ -(D_{k+1} - D_k)sinI_{k+1} \end{bmatrix}$$

$$\frac{d\Delta r_{k+1}}{dA_k} = \frac{1}{2}\begin{bmatrix} -(D_{k+1} - D_k)sinI_{k+1}sinA_{k+1} \\ (D_{k+1} - D_k)sinI_{k+1}cosA_{k+1} \\ 0 \end{bmatrix}$$

And so:

$$\frac{d\Delta r_{k+1}}{dp_k} = \frac{1}{2}\begin{bmatrix} -sinI_k cosA_k - sinI_{k+1} cosA_{k+1} & (D_{k+1} - D_k) cosI_{k+1} cosA_{k+1} & -(D_{k+1} - D_k) sinI_{k+1} sinA_{k+1} \\ -sinI_k sinA_k - sinI_{k+1} sinA_{k+1} & (D_{k+1} - D_k) cosI_{k+1} sinA_{k+1} & (D_{k+1} - D_k) sinI_{k+1} cosA_{k+1} \\ -cosI_k - cosI_{k+1} & -(D_{k+1} - D_k) sinI_{k+1} & 0 \end{bmatrix}$$

So in summary, we have now calculated the 3x3 matrix equations which describe the change in the wellbore position, in the nev-co-ordinate frame caused by changes to the survey measurement at any preceding given station, *k*.

For the last survey station of interest, only the preceding interval is applicable and equation (A.1) becomes:

$$e^*_{i,l,k} = \sigma_{i,l}\left(\frac{d\Delta r_k}{dp_k}\right)\frac{\partial p_k}{\partial \varepsilon_i}$$

A2 - Details of the Error Summation Method

Following on from the discussion in section 19.2.6, we have the example equations for adding error arithmetically or by root-sum-squaring:

$$\boldsymbol{e_{total} = e_1 + e_2}$$

$$\boldsymbol{e_{total} = \sqrt{e_1^2 + e_2^2}}$$

If we square both sides then we get:

$$\boldsymbol{e_{total}{}^2 = (e_1 + e_2)^2}$$

$$\boldsymbol{e_{total}{}^2 = e_1{}^2 + e_2{}^2}$$

So far we've only considered summing two error values. Generalising the sums to include more than two error sources, and remembering that for the error model at a particular point, the e variables will actually be 3x1 vectors and the squaring these would actually be $e_i \, . \, e_i{}^T$ then these equations become:

$$\boldsymbol{E_{total} = \left(\sum e_i\right)\left(\sum e_i\right)^T}$$

$$\boldsymbol{E_{total} = \sum e_i e_i^T}$$

Where now E_{total} is a 3x3 covariance matrix, whose lead diagonal terms are the $e_{total}{}^2$ values along the principle axes.

Returning to the error model, when we come to create the final error summations, we need consider three summations – over the error sources, the survey legs and the survey stations and use the propagation modes to determine at which steps arithmetic summation is appropriate and at which RSS summation is required.

The overall summation of random, systematic and global/well by well error sources is

$$\boldsymbol{[C]_K^{svy} = \sum_{i \in R} [C]_{i,K}^{rand} + \sum_{i \in S} [C]_{i,K}^{syst} + \sum_{i \in \{W,G\}} [C]_{i,K}^{well}}$$

The individual terms for the various groups of error sources are given below.

In these equations:

- $e_{i,l,k}$ is the vector contribution of *i*th error source, in the *i*th survey leg at the *k*th survey station (3x1 vector)
- $e^*_{i,l,K}$ is the vector contribution of *i*th error source, in the *i*th survey leg at the last survey point of interest i.e. the *K*th survey station (3x1 vector)
- i is the summation over error sources from 1…*I*
- k is the summation of survey stations from 1…*K*: the current survey station
- l is the summation over survey legs from 1..*L*: the current survey leg

The contribution of the random errors is given by:

$$[\boldsymbol{C}]_{i,K}^{\boldsymbol{rand}} = \sum_{l=1}^{L-1} [\boldsymbol{C}]_{i,l}^{\boldsymbol{rand}} + \sum_{k=1}^{K-1} (\boldsymbol{e}_{i,l,k}).(\boldsymbol{e}_{i,l,k})^{\boldsymbol{T}} + (\boldsymbol{e}_{i,L,K}^{*}).(\boldsymbol{e}_{i,L,K}^{*})^{\boldsymbol{T}}$$

and

$$[\boldsymbol{C}]_{i,l}^{\boldsymbol{rand}} = \sum_{k=1}^{K_l} (\boldsymbol{e}_{i,l,k}).(\boldsymbol{e}_{i,l,k})^{\boldsymbol{T}}$$

The systematic errors are:

$$[\boldsymbol{C}]_{i,K}^{\boldsymbol{syst}} = \sum_{l=1}^{L-1} [\boldsymbol{C}]_{i,l}^{\boldsymbol{syst}} + \left(\sum_{k=1}^{K_l} \boldsymbol{e}_{i,L,k} + \boldsymbol{e}_{i,L,K}^{*} \right).\left(\sum_{k=1}^{K_l} \boldsymbol{e}_{i,L,k} + \boldsymbol{e}_{i,L,K}^{*} \right)^{\boldsymbol{T}}$$

$$[\boldsymbol{C}]_{i,l}^{\boldsymbol{syst}} = \left(\sum_{k=1}^{K_l} \boldsymbol{e}_{i,l,k} \right)\left(\sum_{k=1}^{K_l} \boldsymbol{e}_{i,l,k} \right)^{\boldsymbol{T}}$$

And finally the well by well and global errors:

$$[\boldsymbol{C}]_{i,K}^{\boldsymbol{well}} = \boldsymbol{E}_{i,K}.\boldsymbol{E}_{i,K}^{\boldsymbol{T}}$$

$$\boldsymbol{E}_{i,K}^{\boldsymbol{well}} = \sum_{l=1}^{L-1} \left(\sum_{k=1}^{K_l} \boldsymbol{e}_{i,l,k} \right) + \sum_{k=1}^{K-1} \boldsymbol{e}_{i,L,k} + \boldsymbol{e}_{i,L,K}^{*}$$

Appendix B: List of MWD Model Error Sources and Weighting Functions

B1 - MWD Model Weighting Functions at Revision 3

Revisions 1 and 3 made changes to the MWD model weighting functions (see section 19.3.6 for a discussion of the revisions to the MWD model). This is the current list at revision 3. Revision 4 is a change to how certain error magnitude values are calculated and does not affect the weighting functions so this list is correct for both revisions 3 and 4. The next section lists the weighting functions which have been replaced.

	Error Code	Description	Propagation Mode	Weighting Function		
				MD	Inc	Azimuth
1	ABXY-TI1	Accelerometer bias – term1	S/R	0	$-\frac{\cos I}{G}$	$\frac{tan\theta.cosI.sinA_m}{G}$
2	ABXY-TI2	Accelerometer bias – term2	S/R	0	0	$\frac{cot\, I - tan\theta.cosA_m}{G}$
3	ABZ	Accelerometer bias z-axis	S	*0*	$\frac{-sinI}{G}$	$\frac{tan\Theta.sinI.sinA_m}{G}$
4	ASXY-TI1	Accelerometer scale factor – term1	S	0	$\frac{sinI.cosI}{\sqrt{2}}$	$-\frac{tan\theta\,.sinI.cos\,I\,.sinA_m}{\sqrt{2}}$
5	ASXY-TI2	Accelerometer scale factor – term2	S/R	0	$\frac{sinI.cosI}{\sqrt{2}}$	$-\frac{tan\theta\,.sinI.cos\,I\,.sinA_m}{2}$
6	ASXY-TI3	Accelerometer scale factor – term3	S/R	0	0	$\frac{tan\theta.sinI.cosA_m - cosI}{2}$
7	ASZ	Accelerometer scalefactor z-axis	S	*0*	$-sinI.cosI$	$tan\Theta.sinI.cosI.sinA_m$
8	MBXY-TI1	Magnetometer bias – term1	S/R	0	0	$\frac{-cos\,I\,.sinA_m}{B.cos\theta}$
9	MBXY-TI2	Magnetometer bias – term2	S/R	0	0	$\frac{cosA_m}{B.cos\theta}$
10	MBZ	Magnetometer bias z-axis	S	*0*	*0*	$\frac{-sinI.sinA_m}{B.cos\Theta}$
11	MSXY-TI1	Magnetometer scale factor – term1	S	0	0	$\frac{sinI.sinA_m.(tan\theta.cosI + sinI.cosA_m)}{\sqrt{2}}$
12	MSXY-TI2	Accelerometer scale factor – term2	S/R	0	0	$\frac{sinA_m.(tan\theta.sinI.cosI - cos^2I.cosA_m - cosA_m)}{2}$
13	MSXY-TI3	Magnetometer scale factor – term3	S/R	0	0	$\frac{(cosI.cos^2A_m - cosI.sin^2A_m - tan\theta.sinI.cosA_m)}{2}$
14	MSZ	Magnetometer scalefactor z-axis	S	*0*	*0*	$-(sinI.cosA_m + tan\Theta.cosI).sinI.sinA_m$
15	DEC	Constant declination error	G	*0*	*0*	*1*
16	DBH	Declination error dependant on the horizontal component of Earth's field	G	*0*	*0*	$\frac{1}{B.cos\Theta}$
17	SAG	BHA Sag	S	*0*	$sin\, I$	*0*
18	AMIC	Constant axial magnetic interference	S	*0*	*0*	*1*

19	AMID	Direction dependant axial magnetic interference	S	*0*	*0*	$sinI.sinA_m$
20	XYM1	xy misalignment 1	S/R	0	w_{12}	0
21	XYM2	xy misalignment 2	S/R	0	0	$-w_{12}/sinI$
22	XYM3	xy misalignment 3	S	0	$w_{34}cosA$	$-w_{34}sinA/sinI$
23	XYM4	xy misalignment 4	S	0	$w_{34}sinA$	$w_{34}cosA/sinI$
24	ABIXY-TI1	Accelerometer bias – axial interference correction – term1	S/R	0	$-\frac{\cos I}{G}$	$\frac{cos^2I.sinA_m(tan\theta.cosI+sinI.cosA_m)}{G(1-sin^2I.sin^2A_m)}$
25	ABIXY-TI2	Accelerometer bias – axial interference correction – term2	S/R	0	0	$\frac{-(tan\theta.cosA_m-cotI)}{G(1-sin^2I.sin^2A_m)}$
26	ABIZ	Accelerometer bias z-axis when axial interference correction applied.	S	*0*	$\frac{-sinI}{G}$	$\frac{sinI.cosI.sinA_m(tan\Theta.cosI+sinI.cosA_m)}{G.(1-sin^2I.sin^2A_m)}$
27	ASIXY-TI1	Accelerometer scale factor – axial interference correction – term1	S	0	$\frac{sinI.cosI}{\sqrt{2}}$	$-\frac{sinI.cos^2I.sinA_m.(tan\theta.cosI+sinI.cosA_m)}{\sqrt{2}(1-sin^2I.sin^2A_m)}$
28	ASIXY-TI2	Accelerometer scale factor – axial interference correction – term2	S/R	0	$\frac{sinI.cosI}{\sqrt{2}}$	$-\frac{sinI.cos^2I.sinA_m.(tan\theta.cosI+sinI.cosA_m)}{2(1-sin^2I.sin^2A_m)}$
29	ASIXY-TI3	Accelerometer scale factor – axial interference correction – term3	S/R	0	0	$-\frac{(tan\theta.sinI.cosA_m-cosI)}{2(1-sin^2I.sin^2\mathrm{A_m})}$
30	ASIZ	Accelerometer scalefactor z-axis when axial interference correction applied.	S	*0*	$-sinI.cosI$	$\frac{sinI.cos^2I.sinA_m(tan\Theta.cosI+sinI.cosA_m)}{G.(1-sin^2I.sin^2A_m)}$
31	MBIXY-TI1	Magnetometer bias – axial interference correction – term1	S/R	0	0	$-\frac{cosI.sinA_m}{B.cos\theta(1-sin^2I.sin^2A_m)}$
32	MBIXY-TI2	Magnetometer bias – axial interference correction – term2	S/R	0	0	$\frac{cosA_m}{B.cos\theta(1-sin^2I.sin^2A_m)}$
33	MSIXY-TI1	Magnetometer scale factor – axial interference correction – term1	S	0	0	$-\frac{sinI.sinA_m.(tan\theta.cosI+sinI.cosA_m)}{\sqrt{2}(1-sin^2I.sin^2A_m)}$
34	MSIXY-TI2	Magnetometer scale factor – axial interference correction – term2	S/R	0	0	$-\frac{sinA_m.(tan\theta.sinI.cosI-cos^2I.cosA_m-cosA_m)}{2(1-sin^2I.sin^2A_m)}$
35	MSIXY-TI3	Magnetometer scale factor – axial interference correction – term3	S/R	0	0	$\frac{(cosI.cos^2A_m-cosI.sin^2A_m-tan\theta.sinI.cosA_m)}{2(1-sin^2I.sin^2A_m)}$
36	MFI	Earth's total magnetic field when axial interference correction applied.	G	0	*0*	$-\frac{sinI.sinA_m(tan\Theta.cosI+sinI.cosA_m)}{B.(1-sin^2I.sin^2A_m)}$
37	MDI	Dip angle when axial interference correction applied.	G	0	*0*	$-\frac{sinI.sinA_m(cosI-tan\Theta.sinI.cosA_m)}{(1-sin^2I.sin^2A_m)}$
38	DREF-R	Depth reference random	R	*1*	*0*	*0*
39	DREF-S	Depth reference systematic	S	*1*	*0*	*0*
40	DSF-S	Depth Scale	S	*D*	*0*	*0*
41	DST-G	Depth Stretch	G	$D.D_V$	*0*	*0*

B2 - Historic Terms: No Longer Used in the MWD Model After Revisions 1 and 3

See section 19.3.4 for a discussion of the revisions to the MWD model. The following weighting functions have been replaced by new methods introduced in revision 1 (misalignment terms MX and MY replaced) and revision 3 (toolface dependant terms – i.e. all the remaining terms below).

	Error Code	Description		Weighting Function		
				MD	Inc	Azimuth
1	MX	Tool axial misalignment – x-axis	S	*0*	$sin\alpha$	$\frac{-cos\alpha}{sinI}$
2	MY	Tool axial misalignment – y-axis	S	*0*	$cos\alpha$	$\frac{sin\alpha}{sinI}$
3	ABX	Accelerometer bias x-axis	S	*0*	$\frac{-cosI.sin\alpha}{G}$	$\frac{(cosI.sinA_m.sin\alpha - cosA_m.cos\alpha).tan\Theta - cotI.cos\alpha}{G}$
4	ABY	Accelerometer bias y-axis	S	*0*	$-\frac{cosI.cos\alpha}{G}$	$\frac{(cosI.sinAm.cos\alpha + cosA_m.sin\alpha).tan\Theta - cotI.sin\alpha}{G}$
5	ASX	Accelerometer scalefactor x-axis	S	*0*	$sinI.cosI.sin^2\alpha$	$-\{tan\Theta.sinI(cosI.sinA_m.sin\alpha - cosA_m.cos\alpha) + cosI.cos\alpha\}.sin\alpha$
6	ASY	Accelerometer scalefactor y-axis	S	*0*	$sinI.cosI.cos^2\alpha$	$-\{tan\Theta.sinI(cosI.sinA_m.cos\alpha + cosA_m.sin\alpha) - cosI.sin\alpha\}.cos\alpha$
7	MBX	Magnetometer bias x-axis	S	*0*	*0*	$\frac{cosA_m.cos\alpha - cosI.sinA_m.sin\alpha}{B.cos\Theta}$
8	MBY	Magnetometer bias y-axis	S	*0*	*0*	$\frac{-cosA_m.sin\alpha + cosI.sinA_m cos\alpha}{B.cos\Theta}$
9	MSX	Magnetometer scalefactor x-axis	S	*0*	*0*	$(cosI.cosA_m sin\alpha - tan\Theta.sinI.sin\alpha + sinA_m.cos\alpha).(cosA_m.cos\alpha - cosI.sinA_m.sin\alpha)$
10	MSY	Magnetometer scalefactor y-axis	S	*0*	*0*	$-(cosI.cosA_m cos\alpha - tan\Theta.sinI.cos\alpha - sinA_m.sin\alpha).(cosA_m.sin\alpha + cosI.sinA_m.cos\alpha)$
11	ABIX	Accelerometer bias x-axis when axial interference correction applied.	S	*0*	$-cosI.sin\alpha$	$\frac{cos^2I.sinA_m.sin\alpha(tan\Theta.cosI + sinI.cosA_m) - cos\alpha(tan\Theta.cosA_m - cotI)}{G.(1 - sin^2I.sin^2A_m)}$
12	ABIY	Accelerometer bias y-axis when axial interference correction applied.	S	*0*	$-cosI.cos\alpha$	$\frac{cos^2I.sinA_m.cos\alpha(tan\Theta.cosI + sinI.cosA_m) + sin\alpha(tan\Theta.cosA_m - cotI)}{G.(1 - sin^2I.sin^2A_m)}$
13	ASIX	Accelerometer scalefactor x-axis when axial interference correction applied.	S	*0*	$sinI.cosI.sin^2\alpha$	$\frac{-sin\alpha[sinI.cos^2I.sinA_m.sin\alpha(tan\Theta.cosI + sinI.cosA_m) - cos\alpha(tan\Theta.sinI.cosA_m}{(1 - sin^2I.sin^2A_m)}$
14	ASIY	Accelerometer scalefactor y-axis when axial interference correction applied.	S	*0*	$sinI.cosI.cos^2\alpha$	$\frac{-cos\alpha[sinI.cos^2I.sinA_m.cos\alpha(tan\Theta.cosI + sinI.cosA_m) + sin\alpha(tan\Theta.sinI.cosA_m}{(1 - sin^2I.sin^2A_m)}$
15	MBIX	Magnetometer bias x-axis when axial interference correction applied.	S	0	*0*	$-\frac{cosI.sinA_m sin\alpha - cosA_m cos\alpha}{Bcos\Theta.(1 - sin^2I.sin^2A_m)}$

16	MBIY	Magnetometer bias y-axis when axial interference correction applied.	S	0	*0*	$-\frac{cosI.sinA_m cos\alpha + cosA_m sin\alpha}{Bcos\Theta.(1-sin^2 I.sin^2 A_m)}$
17	MSIX	Magnetometer scalefactor x-axis when axial interference correction applied.	S	0	*0*	$-\frac{(cosI.cosA_m sin\alpha - tan\Theta.sinI.sin\alpha + sinA_m cos\alpha)(cosI.sinA_m sin\alpha - cosA_m cos}{(1-sin^2 I.sin^2 A_m)}$
18	MSIY	Magnetometer scalefactor y-axis when axial interference correction applied.	S	0	*0*	$-\frac{(cosI.cosA_m cos\alpha - tan\Theta.sinI.cos\alpha + sinA_m sin\alpha)(cosI.sinA_m cos\alpha + cosA_m sin}{(1-sin^2 I.sin^2 A_m)}$

B3 - MWD Defined Error Magnitudes – Revision 3

The table below defines all MWD error magnitudes at revision 3. The revision 4 changes introduce look up tables for the reference magnitude field terms DEC-G and DBH-G. Some models may also include DEC-R and DBH-R to take into account random fluctuations in the reference field. These are not explicitly includes in the standard model.

	Error Code	Description	MWD	MWD with Axial Interference Correction
1	ABXY-TI1	Accelerometer bias xy – term1	0.004ms^{-2}	
2	ABXY-TI2	Accelerometer bias xy – term2	0.004ms^{-2}	
3	ABZ	Accelerometer bias z-axis	0.004ms^{-2}	
4	ASXY-TI1	Accelerometer scale factor xy – term1	0.0005	
5	ASXY-TI2	Accelerometer scale factor xy – term2	0.0005	
6	ASXY-TI3	Accelerometer scale factor xy – term3	0.0005	
7	ASZ	Accelerometer scalefactor z-axis	0.0005	
8	MBXY-TI1	Magnetometer bias xy – term1	70nT	
9	MBXY-TI2	Magnetometer bias xy – term2	70nT	
10	MBZ	Magnetometer bias z-axis	70nT	
11	MSXY-TI1	Magnetometer scale factor xy – term1	0.0016	
12	MSXY-TI2	Accelerometer scale factor xy – term2	0.0016	
13	MSXY-TI3	Magnetometer scale factor xy – term3	0.0016	
14	MSZ	Magnetometer scalefactor z-axis	0.0016	
15	DEC	Constant declination error	0.36˚	0.36˚
16	DBH	Declination error dependant on the horizontal component of Earth's field	5000nT	5000nT
17	SAG	BHA Sag	0.2˚	0.2˚
18	AZ	Constant axial magnetic interference	0.25˚	
19	AMID	Direction dependant axial magnetic interference	0.6˚	
20	XYM1	xy misalignment 1	0.06˚	0.06˚
21	XYM2	xy misalignment 2	0.06˚	0.06˚
22	XYM3	xy misalignment 3	0.06˚	0.06˚
23	XYM4	xy misalignment 4	0.06˚	0.06˚
24	ABIXY-TI1	Accelerometer bias xy – axial interference correction – term1		0.004ms^{-2}
25	ABIXY-TI2	Accelerometer bias xy – axial interference correction – term2		0.004ms^{-2}
26	ABIZ	Accelerometer bias z-axis when axial interference correction applied.		0.004ms^{-2}
27	ASIXY-TI1	Accelerometer scale factor xy – axial interference correction – term1		0.0005
28	ASIXY-TI2	Accelerometer scale factor xy – axial interference correction – term2		0.0005

`29	ASIXY-TI3	Accelerometer scale factor xy – axial interference correction – term3		0.0005
30	ASIZ	Accelerometer scalefactor z-axis when axial interference correction applied.		0.0005
31	MBIXY-TI1	Magnetometer bias xy – axial interference correction – term1		70nT
32	MBIXY-TI2	Magnetometer bias xy – axial interference correction – term2		70nT
33	MSIXY-TI1	Magnetometer scale factor xy – axial interference correction – term1		0.0016
34	MSIXY-TI2	Magnetometer scale factor xy – axial interference correction – term2		0.0016
35	MSIXY-TI3	Magnetometer scale factor xy – axial interference correction – term3		0.0016
36	MFI	Earth's total magnetic field when axial interference correction applied.		130nT
37	MDI	Dip angle when axial interference correction applied.		0.20˚

	Error Code	**Description**	**Drillpipe – Fixed Rig**	**Drillpipe – Floating Platform**
38	DREF-R	Random Depth Reference	0.35m	2.20m
39	DREF-S	Systematic Depth Reference	0.00m	1.00m
40	DSF-S	Depth Scalefactor	5.6×10^{-4}	5.6×10^{-4}
41	DST-G	Depth Stretch	$2.5 \times 10^{-7} m^{-1}$	$2.5 \times 10^{-7} m^{-1}$

B4 - MWD Defined Error Magnitudes – Revision 3

The table below defines all MWD error magnitudes at revision 3. The revision 4 changes introduce look up tables for the reference magnitude field terms DEC-G and DBH-G. Some models may also include DEC-R and DBH-R to take into account random fluctuations in the reference field. These are not explicitly includes in the standard model.

	Error Code	Description	MWD	MWD with Axial Interference Correction
1	ABXY-TI1	Accelerometer bias xy – term1	0.004ms^{-2}	
2	ABXY-TI2	Accelerometer bias xy – term2	0.004ms^{-2}	
3	ABZ	Accelerometer bias z-axis	0.004ms^{-2}	
4	ASXY-TI1	Accelerometer scale factor xy – term1	0.0005	
5	ASXY-TI2	Accelerometer scale factor xy – term2	0.0005	
6	ASXY-TI3	Accelerometer scale factor xy – term3	0.0005	
7	ASZ	Accelerometer scalefactor z-axis	0.0005	
8	MBXY-TI1	Magnetometer bias xy – term1	70nT	
9	MBXY-TI2	Magnetometer bias xy – term2	70nT	
10	MBZ	Magnetometer bias z-axis	70nT	
11	MSXY-TI1	Magnetometer scale factor xy – term1	0.0016	
12	MSXY-TI2	Accelerometer scale factor xy – term2	0.0016	
13	MSXY-TI3	Magnetometer scale factor xy – term3	0.0016	
14	MSZ	Magnetometer scalefactor z-axis	0.0016	
15	DEC	Constant declination error	0.36˚	0.36˚
16	DBH	Declination error dependant on the horizontal component of Earth's field	5000nT	5000nT
17	SAG	BHA Sag	0.2˚	0.2˚
18	AZ	Constant axial magnetic interference	0.25˚	
19	AMID	Direction dependant axial magnetic interference	0.6˚	
20	XYM1	xy misalignment 1	0.06˚	0.06˚
21	XYM2	xy misalignment 2	0.06˚	0.06˚
22	XYM3	xy misalignment 3	0.06˚	0.06˚
23	XYM4	xy misalignment 4	0.06˚	0.06˚
24	ABIXY-TI1	Accelerometer bias xy – axial interference correction – term1		0.004ms^{-2}
25	ABIXY-TI2	Accelerometer bias xy – axial interference correction – term2		0.004ms^{-2}
26	ABIZ	Accelerometer bias z-axis when axial interference correction applied.		0.004ms^{-2}
27	ASIXY-TI1	Accelerometer scale factor xy – axial interference correction – term1		0.0005
28	ASIXY-TI2	Accelerometer scale factor xy – axial interference correction – term2		0.0005
`29	ASIXY-TI3	Accelerometer scale factor xy – axial interference correction – term3		0.0005
30	ASIZ	Accelerometer scalefactor z-axis when axial interference correction applied.		0.0005
31	MBIXY-TI1	Magnetometer bias xy – axial interference correction – term1		70nT
32	MBIXY-TI2	Magnetometer bias xy – axial interference correction – term2		70nT
33	MSIXY-TI1	Magnetometer scale factor xy – axial interference correction – term1		0.0016
34	MSIXY-TI2	Magnetometer scale factor xy – axial interference correction – term2		0.0016

35	MSIXY-TI3	Magnetometer scale factor xy – axial interference correction – term3		0.0016
36	MFI	Earth's total magnetic field when axial interference correction applied.		130nT
37	MDI	Dip angle when axial interference correction applied.		0.20˚

	Error Code	**Description**	**Drillpipe – Fixed Rig**	**Drillpipe – Floating Platform**
38	DREF-R	Random Depth Reference	0.35m	2.20m
39	DREF-S	Systematic Depth Reference	0.00m	1.00m
40	DSF-S	Depth Scalefactor	$5.6x10^{-4}$	$5.6x10^{-4}$
41	DST-G	Depth Stretch	$2.5x10^{-7}m^{-1}$	$2.5x10^{-7}m^{-1}$

Appendix C: List of Gyro Model Error Sources and Weighting Functions

In addition to the above MWD weighting functions the gyro error model introduces a whole new set of error sources and associated weighting functions.
The weighting functions can be grouped into those which apply in **S**tationary survey mode, **C**ontinuous survey mode or either mode. During a single survey leg a tool made transition between these modes as a function of inclination.

	Error Code	Description	SurveyMode	Propagation Mode	Weighting Function		
					MD	Inc	Azimuth
1	AXYZ-XYB	3-axis: xy accelerometer bias	C/S	S/R	0	$\frac{\cos I}{G}$	0
2	AXYZ-ZB	3-axis: z accelerometer bias	C/S	S	0	$\frac{\sin I}{G}$	0
3	AXYZ-SF	3-axis: accelerometer scale factor error	C/S	S	0	1.3 sin*I* cos*I*	0
4	AXYZ-MS	3-axis: accelerometer misalignment	C/S	S	0	1	0
5	AXY-B	2-axis: xy accelerometer bias	C/S	S/R	0	$\frac{1}{Gcos(1-k.\gamma)}$	0
6	AXY-SF	2-axis: Accelerometer scale factor error	C/S	S	0	$\tan(I-k.\gamma)$	0
7	AXY-MS	2-axis: Accelerometer misalignment	C/S	S	0	1	0
8	AXY-GB	2-axis: Gravity Bias	C/S	S	0	$\frac{\tan(I-k.\gamma)}{G}$	0
9	GXYZ-XYB1	3-axis, stationary: xy gyro bias 1	S	S/R	0	0	$\frac{sinA\ cosI}{\Omega\cos\phi}$
10	GXYZ-XYB2	3-axis, stationary: xy gyro bias 2	S	S/R	0	0	$\frac{cosA}{\Omega\cos\phi}$
11	GXYZ-XYRN	3-axis, stationary: xy gyro random noise	S	R	0	0	$f.\frac{\sqrt{1-sin^2A.sin^2I}}{\Omega\cos\phi}$
12	GXYZ-XYG1	3-axis, stationary: xy gyro g-dependent error 1	S	S	0	0	$\frac{cosA\ sinI}{\Omega\cos\phi}$
13	GXYZ-XYG2	3-axis, stationary: xy gyro g-dependent error 2	S	S/R	0	0	$\frac{cosA\ cosI}{\Omega\cos\phi}$
14	GXYZ-XYG3	3-axis, stationary: xy gyro g-dependent error 3	S	S/R	0	0	$\frac{sinA\ cos^2I}{\Omega\cos\phi}$
15	GXYZ-XYG4	3-axis, stationary: xy gyro g-dependent error 4	S	S	0	0	$\frac{sinA\ sinI\ cosI}{\Omega\cos\phi}$
16	GXYZ-ZB	3-axis, stationary: z gyro bias	S	S	0	0	$\frac{sinA\ sinI}{\Omega\cos\phi}$
17	GXYZ-ZRN	3-axis, stationary: z gyro random noise	S	R	0	0	$\frac{sinA\ sinI}{\Omega\cos\phi}$
18	GXYZ-ZG1	3-axis, stationary: z gyro g-dependent error 1	S	S/R	0	0	$\frac{sinA\ sin^2I}{\Omega\cos\phi}$

19	GXYZ-ZG2	3-axis, stationary: z gyro g-dependent error 2	S	S	0	0	$\frac{sinA\ sinI\ cosI}{\Omega \cos\phi}$
20	GXYZ-SF	3-axis, stationary: Gyro scalefactor	S	S	0	0	$tan\phi\ sinA\ sinI\ cosI$
21	GXYZ-MIS	3-axis, stationary: Gyro misalignment	S	S	0	0	$\frac{1}{\cos\phi}$
22	GXY-B1	2-axis, stationary: xy gyro bias 1	S	S/R	0	0	$\frac{sinA}{\Omega\ \cos\phi\ \cos I}$
23	GXY-B2	2-axis, stationary: xy gyro bias 2	S	S/R	0	0	$\frac{cosA}{\Omega \cos\phi}$
24	GXY-RN	2-axis, stationary: xy gyro random noise	S	R	0	0	$f.\frac{\sqrt{1-cos^2A.sin^2I}}{\Omega \cos\phi\ \cos I}$
25	GXY-G1	2-axis, stationary: xy gyro g-dependent error 1	S	S	0	0	$\frac{cosA\ sinI}{\Omega \cos\phi}$
26	GXY-G2	2-axis, stationary: xy gyro g-dependent error 2	S	S/R	0	0	$\frac{cosA\ cosI}{\Omega \cos\phi}$
27	GXY-G3	2-axis, stationary: xy gyro g-dependent error 3	S	S/R	0	0	$\frac{sinA}{\Omega \cos\phi}$
28	GXY-G4	2-axis, stationary: xy gyro g-dependent error 4	S	S	0	0	$\frac{sinA\ tanI}{\Omega \cos\phi}$
29	GXY-SF	2-axis, stationary: Gyro scalefactor	S	S	0	0	$tan\phi\ sinA\ tanI$
30	GXY-MIS	2-axis, stationary: Gyro misalignment	S	S	0	0	$\frac{1}{\cos\phi\ \cos I}$
31	EXTREF	External reference error	S	S	0	0	1
32	EXTTIE	Un-modelled random azimuth error in tie-on tool	S	S	0	0	1
33	EXTMIS	Misalignment effect at tie-on	S	S	0	0	$\frac{1}{\sin I}$
34	GXYZ-GD	3-axis, continuous: xyz gyro drift	C	S	0	0	$h_i = h_{i-1} + \frac{\Delta D_i}{c}$
35	GXYZ-RW	3-axis, continuous: xyz gyro random walk	C	S	0	0	$h_i = \sqrt{h_{i-1}^2 + \frac{\Delta D_i}{c}}$
36	GXY-GD	2-axis, continuous: xy gyro drift	C	S	0	0	$h_i = h_{i-1} + \frac{1}{sin\left(\frac{I_{i-1}+I_i}{2}\right)}\frac{\Delta D_i}{c}$
37	GXY-RW	2-axis, continuous: xy gyro random walk	C	S	0	0	$h_i = \sqrt{h_{i-1}^2 + \frac{1}{sin\left(\frac{I_{i-1}+I_i}{2}\right)}.\frac{\Delta D_i}{c}}$
38	GZ-GD	z-axis, continuous: z gyro drift	C	S	0	0	$h_i = h_{i-1} + \frac{1}{sin\left(\frac{I_{i-1}+I_i}{2}\right)}\frac{\Delta D_i}{c}$

39	GZ-RW	z-axis, continuous: z gyro random walk	C	S	0	0	$h_i = \sqrt{h_{i-1}^2 + \frac{1}{sin\left(\frac{I_{i-1}+I_i}{2}\right)} \cdot \frac{\Delta D_i}{c}}$

The following terms are common to both the gyro and MWD models.

	Error Code	Description	Survey Mode	Propagation Mode	Weighting Function		
					MD	Inc	Azimuth
40	XYM1	xy misalignment 1	C/S	S	0	w_{12}	0
41	XYM2	xy misalignment 2	C/S	S	0	0	$-w_{12}/sinI$
42	XYM3	xy misalignment 3	C/S	S	0	$w_{34}cosA$	$-w_{34}sinA/sinI$
43	XYM4	xy misalignment 4	C/S	S	0	$w_{34}sinA$	$w_{34}cosA/sinI$
44	VSAG	Vertical sag (SAG in MWD model)	C/S	S	0	$sinI$	0
45	DRF-R	Depth random error	C/S	R	1	0	0
46	DRF-S	Depth systematic reference	C/S	S	-	0	0
47	DSF-W	Depth scale	C/S	S/W	ΔD	0	0
48	DST-G	Depth stretch type	C/S	G	$(D_v+DcosI).\Delta D$	0	0

VERSION & SUBMISSION INFORMATION

Submissions for assessment

The authors of this publication are fully aware the nature of the subject matter covered herein will develop over time as new techniques are arise or current practices and technologies are updated. It is, therefore, the intension of the author to regularly revise this eBook to reflect these changes and keep this publication current and as complete as possible.

Anyone who has expertise, techniques or updates they wish to submit to the author for assessment for inclusion in the next revision should email the data in the first instance to:

RO@uhi.ac.uk

This version is V01.7.12

This eBook and all subsequent revisions will be hosted at:
http://www.uhi.ac.uk/en/research-enterprise/energy/wellbore-positioning-download

✧

CONTENTS

INDEX

END